Deep Generative Models for Offline Policy Learning: Tutorial, Survey, and Perspectives on Future Directions

Anonymous authors
Paper under double-blind review

Abstract

Deep generative models (DGMs) have demonstrated great success across various domains, particularly in generating texts, images, and videos using models trained from offline data. Similarly, data-driven decision-making and robotic control also necessitate learning a generator function from the offline data to serve as the strategy or policy. In this case, applying deep generative models in offline policy learning exhibits great potential, and numerous studies have explored in this direction. However, this field still lacks a comprehensive review and so developments of different branches are relatively independent. Thus, we provide the first systematic review on the applications of deep generative models for offline policy learning. In particular, we cover five mainstream deep generative models, including Variational Auto-Encoders, Generative Adversarial Networks, Normalizing Flows, Transformers, and Diffusion Models, and their applications in both offline reinforcement learning (offline RL) and imitation learning (IL). Offline RL and IL are two main branches of offline policy learning and are widely-adopted techniques for sequential decision-making. Specifically, for each type of DGM-based offline policy learning, we distill its fundamental scheme, categorize related works based on the usage of the DGM, and sort out the development process of algorithms in that field. Subsequent to the main content, we provide in-depth discussions on deep generative models and offline policy learning as a summary, based on which we present our perspectives on future research directions. This work offers a hands-on reference for the research progress in deep generative models for offline policy learning, and aims to inspire improved DGM-based offline RL or IL algorithms.

Contents

1 Introduction **3**

2 Background on Deep Generative Models **4**

2.1 Variational Auto-Encoders 5

2.2 Generative Adversarial Networks 8

2.3 Normalizing Flows 10

2.4 Transformers 11

2.5 Diffusion Models 14

3 Variational Auto-Encoders in Offline Policy Learning **16**

3.1 Offline Reinforcement Learning 16

3.1.1 Background on Dynamic-Programming-based Offline Reinforcement Learning 16

3.1.2 An Overview of Applying VAEs in Offline Reinforcement Learning 18

3.1.3 Addressing the Issue of Out-of-Distribution Actions Using VAEs . . . 19
3.1.4 Data Augmentation and Transformation with VAEs . . . 20
3.1.5 Offline Multi-task/Hierarchical RL based on VAEs . . . 21
3.2 Imitation Learning . . . 23
3.2.1 Core Schemes of VAE-based Imitation Learning . . . 23
3.2.2 Improving Data Efficiency in Imitation Learning with VAEs . . . 25
3.2.3 Managing Multi-Modal Inputs in Imitation Learning via VAEs . . . 26
3.2.4 Skill Acquisition and Hierarchical Imitation Learning through VAEs . . . 27
3.2.5 Tackling Causal Confusion in Imitation Learning with VAEs . . . 28

4 Generative Adversarial Networks in Offline Policy Learning 30
4.1 Imitation Learning . . . 30
4.1.1 Fundamental GAN-Based Imitation Learning Algorithms: GAIL and AIRL . . . 30
4.1.2 Extensions of GAIL . . . 32
4.1.3 Extensions of AIRL . . . 32
4.1.4 Integrating VAEs and GANs for Imitation Learning: A Spotlight . . . 34
4.2 Offline Reinforcement Learning . . . 35
4.2.1 Background on Model-based Offline Reinforcement Learning . . . 35
4.2.2 Policy Approximation Using GANs . . . 36
4.2.3 World Model Representation through GANs . . . 37

5 Normalizing Flows in Offline Policy Learning 38
5.1 Imitation Learning . . . 38
5.1.1 Exact Density Estimation in Imitation Learning Using Normalizing Flows . . . 39
5.1.2 Policy Modeling in Imitation Learning with Normalizing Flows . . . 40
5.2 Reinforcement Learning with Offline Data . . . 41
5.2.1 Adopting Normalizing Flows in Offline Reinforcement Learning . . . 41
5.2.2 Adopting Normalizing Flows in Online Reinforcement Learning with Offline Data . . . 42

6 Transformers in Offline Policy Learning 44
6.1 Offline Reinforcement Learning . . . 44
6.1.1 Background on Trajectory-Optimization-based Offline Reinforcement Learning . . . 44
6.1.2 Balancing Model Capacity with Training Data . . . 45
6.1.3 Mitigating Impacts from Environmental Stochasticity . . . 47
6.1.4 Transformers in Extended Offline Reinforcement Learning Setups . . . 47
6.1.5 Reflections on Transformer-based Offline Reinforcement Learning . . . 50
6.2 Imitation Learning . . . 50

6.2.1 A Paradigm of Transformer-based Imitation Learning 50
6.2.2 Adopting Transformers as the Policy Backbone for Imitation Learning 51
6.2.3 Developing Generalist Imitation Learning Agents with Transformers 51

7 Diffusion Models in Offline Policy Learning 54
7.1 Imitation Learning 54
7.1.1 Improving Policy Expressiveness in Imitation Learning with Diffusion Models 54
7.1.2 Addressing Common Issues of Imitation Learning with Diffusion Models 55
7.2 Offline Reinforcement Learning 56
7.2.1 Diffusion Models as Policies 57
7.2.2 Diffusion Models as Planners 58
7.2.3 Diffusion Models as Data Synthesizers 59
7.2.4 Diffusion Models in Extended Offline Reinforcement Learning Setups 60

8 Discussions and Open Problems 62
8.1 Discussions on Deep Generative Models and Offline Policy Learning 62
8.2 Perspectives on Future Directions 66
8.2.1 Future Works on Data-centric Research 66
8.2.2 Future Works on Benchmarking 67
8.2.3 Future Works on Theories 68
8.2.4 Future Works on Algorithm Designs 68

9 Conclusion 70

1 Introduction

Offline Policy Learning is a machine learning discipline that leverages pre-existing, static datasets to learn effective policies for (robotic) control or decision-making. This paper delves into its two primary branches: Offline Reinforcement Learning (Offline RL) and Imitation Learning (IL). Offline RL utilizes a pre-compiled batch of experience data collected from other policies or human operators, typically comprising a series of state-action-reward-next state tuples. The principal objective of offline RL is to develop a policy that maximizes the cumulative rewards, which may necessitate deviating from the behavior patterns observed in the training data. On the other hand, IL trains a policy by mimicking an expert's behaviors. The data used for IL should be demonstrated trajectories from experts. These trajectories, highlighting the expert's responses to various scenarios, usually consist of a sequence of state-action pairs (Learning from Demonstrations, LfD) or state-next state pairs (Learning from Observations, LfO).

Generative Models are widely used in many subfields of AI and machine learning. Recent advances in parameterizing these models using deep neural networks, combined with progress in stochastic optimization methods, have enabled scalable modeling of complex, high-dimensional data including images, texts, and speech, with Deep Generative Models (DGMs). In particular, we notice the great success of applying DGMs to Computer Vision (CV) and Natural Language Processing (NLP). Examples include text-to-image generation using Diffusion Models (Stable Diffusion (Rombach et al. (2022))), text-to-video generation with Diffusion Models and Transformers (Sora (Brooks et al. (2024))), large language models based on Transformers (ChatGPT (OpenAI (2023))), and so on. Offline policy learning bears similarities to CV and NLP, as all

these domains involve learning from a set of offline data. While CV or NLP models generate images or texts based on given contexts, offline RL/IL models produce actions or trajectories conditioned on task scenarios. This similarity suggests that applying DGMs to offline policy learning could potentially replicate the success witnessed in CV and NLP, leveraging their capability to model and generate complex data patterns.

Great advances have been made in both DGMs and offline policy learning, and there are numerous works on applying the progress of DGMs to aid the development of offline policy learning. This paper provides a comprehensive review of DGMs in offline policy learning. Specifically, the main content is categorized by the type of DGMs, and we cover nearly all mainstream DGMs in this paper, including Variational Auto-Encoders, Generative Adversarial Networks, Normalizing Flows, Transformers, and Diffusion Models, where Transformers and Diffusion Models are representatives of autoregressive and score-based generative models, respectively. For each category, we present related works in both offline RL and IL as two subcategories. In each subcategory (e.g., VAE-based IL in Section 3.2), we abstract the core schemes of applying that DGM in IL or offline RL, categorize related works by how the DGM is utilized, and provide a summary table outlining the representative works with their key novelties and evaluation benchmarks. It is noteworthy that our paper is more than a survey. For the introduction of each work, we try to include its key insights and objective design, to help readers get the knowledge without referring to the original papers. Further, for each group of works (e.g., Section 3.1.5 and 7.2.2), algorithms are introduced in different levels of details, where the most representative ones are emphasized as a tutorial on that specific usage of DGMs for offline policy learning and then other extension works are presented for a thorough review. Specifically, research works in the same group are presented with unified notations, aiming to elucidate the relationships between their objectives and the evolution of their algorithm designs.

In the order of Variational Auto-Encoders, Generative Adversarial Networks, Normalizing Flows, Transformers, and Diffusion Models, we present the background on DGMs in Section 2 and the applications of DGMs for offline policy learning in Section 3 - 7. For the background of each DGM, we introduce its mathematical basics and model variants that are utilized in offline policy learning. Sections related to the same DGM (e.g., Section 2.2 and 4) share the same set of notations such that necessary background can be conveniently looked up. Regarding the background on offline RL and IL, we notice that different DGMs adopt distinct base offline RL/IL algorithms, so we distribute the background introductions to corresponding DGM sections. For instance, three main branches of offline RL: dynamic-programming-based, model-based, and trajectory-optimization-based offline RL, are adopted and they are respectively introduced in Section 3.1.1, 4.2.1, 6.1.1. Following the main content, in Section 8, we present in-depth discussions on the main topic of this paper and provide perspectives on future research directions. For the discussions (Section 8.1), we analyze both the common and unique usages of different DGMs in offline policy learning, summarize the seminal works in each category and the issues/extensions of offline policy learning that have been targeted by DGM-based algorithms. For the future works (Section 8.2), we offer our perspectives on potential research directions across four aspects: data, benchmarking, theories, and algorithm designs.

The main contributions of this paper are as follows: (1) This is the first review paper on Deep Generative Models for Offline Policy Learning. (2) This paper covers a wide array of topics, including five mainstream Deep Generative Models and their applications in both Offline Reinforcement Learning and Imitation Learning. (3) Throughout this paper, we distill key algorithmic schemes/paradigms and selectively highlight seminal research works, as tutorials on respective topics. (4) Our work showcases the evolution of DGM-based offline policy learning in parallel with the progress of generative models themselves. The summary provided at the end of this paper offers valuable insights and directions for future developments in this field.

2 Background on Deep Generative Models

In this section, we introduce five widely-adopted and cutting-edge deep generative models: Variational Auto-Encoders, Generative Adversarial Networks, Normalizing Flows, Transformers, and Diffusion Models, as the background of their applications in offline policy learning. For each of these generative models, we delve into their mathematical foundations and provide an overview of their significant variants, with a particular focus on those employed in offline policy learning.

Considering the extensive scope of content addressed in this work, notations utilized for different generative models are relatively independent. Within the context of the same generative model, including its background and applications in offline policy learning, notations are consistent and can be cross-referenced. However, notations used across different generative models may not be directly comparable or interchangeable, but consistently, we use $x \sim P_X(\cdot)$ to represent data points in the offline dataset and $z \sim P_Z(\cdot)$ to represent their latent representations or variations.

2.1 Variational Auto-Encoders

Variational Auto-Encoders (VAEs, Kingma & Welling (2014; 2019)) assume that the given data distribution $P_X(x)$ can be generated with a deep latent-variable model $P_{\theta^*}(x) = \int P_{\theta^*}(z)P_{\theta^*}(x|z)dz$, i.e., sampling a continuous latent variable z from the prior $P_{\theta^*}(z)$ and then generating x from the conditional (generative) model $P_{\theta^*}(x|z)$. It's also assumed that $P_{\theta^*}(z)$ ($P_{\theta^*}(x|z)$) comes from a parametric family of distributions $P_\theta(z)$ ($P_\theta(x|z)$). Intuitively, such $P_\theta(x)$ can be seen as an infinite mixture of some base probability distributions $P_\theta(x|z)$ (e.g., the Gaussian distribution) across a range of possible latent variables z, thus it can be quite flexible and powerful for modelling complex data distributions $P_X(x)$.

To learn the mapping from z to x, an extra model that can infer the latent variables z from the training data x is required, as z's are not provided with the offline data. However, according to the Bayes rule, the true posterior (inference) model $P_\theta(z|x) = P_\theta(z)P_\theta(x|z)/P_\theta(x)$ is intractable in most cases. For example, if $P_\theta(x|z)$ is implemented as a neural network, we do not have the analytical form for $P_\theta(x)$ and so not for $P_\theta(z|x)$. Therefore, in VAEs, a generative model $P_\theta(x|z)$ and corresponding inference model $P_\phi(z|x)$ (for approximating the true posterior) are jointly learned. The most notable contributions of VAEs are two-fold: firstly, they propose a variational lower bound as a practical learning objective, and secondly, they introduce the reparameterization trick, which facilitates end-to-end training of both the generative and inference models.

The objective function of VAEs is a variational lower bound (a.k.a., evidence lower bound (ELBO)) of the log likelihood $\log P_\theta(x)$, and its derivation process is widely adopted in algorithm designs related to latent-variable models, so we show the process here:

$$\begin{aligned}\log P_\theta(x) &= \mathbb{E}_{z\sim P_\phi(\cdot|x)}\left[\log P_\theta(x)\right] = \mathbb{E}_{z\sim P_\phi(\cdot|x)}\left[\log\left[\frac{P_\theta(x,z)}{P_\theta(z|x)}\right]\right] = \mathbb{E}_{z\sim P_\phi(\cdot|x)}\left[\log\left[\frac{P_\theta(x,z)}{P_\phi(z|x)}\frac{P_\phi(z|x)}{P_\theta(z|x)}\right]\right] \\ &= \mathbb{E}_{z\sim P_\phi(\cdot|x)}\left[\log\left[\frac{P_\theta(x,z)}{P_\phi(z|x)}\right] + \log\left[\frac{P_\phi(z|x)}{P_\theta(z|x)}\right]\right] = \mathcal{L}_{\theta,\phi}(x) + D_{KL}(P_\phi(z|x)||P_\theta(z|x)) \geq \mathcal{L}_{\theta,\phi}(x)\end{aligned} \tag{1}$$

$$\begin{aligned}\mathcal{L}_{\theta,\phi}(x) &= \mathbb{E}_{z\sim P_\phi(\cdot|x)}\left[\log P_\theta(x,z) - \log P_\phi(z|x)\right] = \mathbb{E}_{z\sim P_\phi(\cdot|x)}\left[\log P_\theta(x|z) - \log\left[\frac{P_\phi(z|x)}{P_\theta(z)}\right]\right] \\ &= \mathbb{E}_{z\sim P_\phi(\cdot|x)}\left[\log P_\theta(x|z)\right] - D_{KL}(P_\phi(z|x)||P_\theta(z))\end{aligned} \tag{2}$$

The inequality in Eq. (1) uses the fact that KL divergence (i.e., $D_{KL}(\cdot||\cdot)$) is non-negative (Csiszár & Shields (2004)). P_ϕ and P_θ are learned by maximizing $\mathbb{E}_{x\sim P_X(\cdot)}\mathcal{L}_{\theta,\phi}(x)$, which in turns maximizes $\mathbb{E}_{x\sim P_X(\cdot)}\log P_\theta(x)$. When using neural networks for both the inference model $P_\phi(z|x)$ and generative model $P_\theta(x|z)$, $\mathcal{L}_{\theta,\phi}(x)$ trains a specific type of auto-encoder, where $P_\phi(z|x)$ and $P_\theta(x|z)$ function as the encoder and decoder respectively. Intuitively, this auto-encoder is trained by maximizing the data reconstruction accuracy (i.e., the first term in $\mathcal{L}_{\theta,\phi}(x)$), while regularizing the distribution of z from the encoder to be close to the prior distribution of z. This regularization is necessary, since z is sampled from the encoder for data generation (i.e., $z \sim P_\phi(\cdot|x), \hat{x} \sim P_\theta(\cdot|z)$) when training but, during evaluation, z is sampled from the prior distribution (i.e., $z \sim P_\theta(\cdot), \hat{x} \sim P_\theta(\cdot|z)$).

Usually, VAEs assume that $P_\theta(z) = \mathcal{N}(z; 0, I)$ and $P_\phi(z|x) = \mathcal{N}(z; \mu(x;\phi), \text{diag}(\sigma^2(x;\phi)))$. Here, assuming $z \in \mathbb{R}^d$, I is a $d \times d$ identity matrix, $\mu(x;\phi) \in \mathbb{R}^d$ is a mean vector, and $\text{diag}(\sigma^2(x;\phi)) \in \mathbb{R}^{d\times d}$ is a diagonal covariance matrix with $\sigma^2_{1:d}(x;\phi)$ as the diagonal elements. In this case, the analytical form of $D_{KL}(P_\phi(z|x)||P_\theta(z))$ exists and we have:

$$\mathcal{L}_{\theta,\phi}(x) = \mathbb{E}_{z\sim P_\phi(\cdot|x)}\left[\log P_\theta(x|z)\right] + \frac{1}{2}\sum_{i=1}^{d}\left[1 + \log\sigma_i^2(x;\phi) - \mu_i^2(x;\phi) - \sigma_i^2(x;\phi)\right] = \mathcal{L}^1_{\theta,\phi}(x) + \mathcal{L}^2_\phi(x) \tag{3}$$

$\nabla_\phi \mathcal{L}^2_\phi(x)$ and $\nabla_\theta \mathcal{L}^1_{\theta,\phi}(x)$ can be easily estimated with gradient backpropagation. However, when calculating $\nabla_\phi \mathcal{L}^1_{\theta,\phi}(x)$, the gradient $\nabla_z \log P_\theta(x|z)$ cannot be backpropagated to ϕ, since z are samples from the encoder rather than a function of ϕ. One solution is the reparameterization trick. Specifically, z can be reparameterized as a deterministic function of ϕ by externalizing the randomness from the output to the input of the encoder, i.e., $z = P_\phi(x, \epsilon) = \mu(x;\phi) + \sigma(x;\phi) \odot \epsilon,\ \epsilon \sim \mathcal{N}(0, I)$. ($\epsilon \in \mathbb{R}^d$, and $\odot$ denotes the element-wise product.) In this way, the generative models and corresponding inference models can be jointly trained using straightforward learning techniques (e.g., stochastic gradient descent (Amari (1993))).

Next, we introduce some representative variants of VAEs, which are utilized in Section 3.

- **β-VAE:** Assuming that the data $x \sim P_X(\cdot)$ is generated by a groundtruth simulation process with a number of independent generative factors, β-VAE (Higgins et al. (2017)) is proposed to learn latent variables z that encode each generative factor in separate dimensions. For example, a simulator might sample independent factors corresponding to the object shape, colour, and size to generate an image of a small green apple; ideally, in the latent variable of the image, there should be separate dimensions for each of these factors. To learn such an encoder $P_\phi(z|x)$, the authors propose to constrain the KL divergence between $P_\phi(z|x)$ and an isotropic unit Gaussian distribution $P_\theta(z) = \mathcal{N}(z; 0, I)$ to encourage the dimensions of z to be conditionally independent, resulting in the objective:

$$\max_{\theta,\phi} \mathbb{E}_{z\sim P_\phi(\cdot|x)} \left[\log P_\theta(x|z)\right] \ \ s.t.\ D_{KL}(P_\phi(z|x)||P_\theta(z)) < \epsilon \tag{4}$$

  Introducing a Lagrangian multiplier $\beta > 0$, the equation above can be reformulated into an unconstrained optimization problem: $\max_{\theta,\phi,\beta} \mathbb{E}_{z\sim P_\phi(\cdot|x)} \left[\log P_\theta(x|z)\right] - \beta \left[D_{KL}(P_\phi(z|x)||P_\theta(z)) - \epsilon\right]$. They opt to fine-tune β as a hyperparameter instead of learning it, leading to the final objective:

$$\max_{\theta,\phi} \mathbb{E}_{z\sim P_\phi(\cdot|x)} \left[\log P_\theta(x|z)\right] - \beta D_{KL}(P_\phi(z|x)||P_\theta(z)) \tag{5}$$

  When $\beta = 1$, this recovers the original VAE formulation (i.e., Eq. (2)). β controls the tradeoff between limiting the latent channel capacity (via the second term) and preserving the information for reconstructing the data sample (via the first term). Empirically, they find that it's important to set $\beta > 1$ in order to learn the required disentangled latent variables.

- **Gated VAE:** As mentioned in β-VAE, disentangled latent variables can be viewed as data representations in which each element relates to an independent and semantically meaningful generator factor of the data. β-VAE provides an unsupervised manner to learn such disentangled representations (through constraining the KL divergence). However, consistent disentanglement has recently been demonstrated to be impossible without inductive bias or subjective validation (Locatello et al. (2019)). Thus, Gated VAE (Vowels et al. (2020)) is proposed to incorporate domain knowledge as weak supervision to encourage disentanglement. Specifically, as a form of weak supervision, data can be clustered such that each cluster comprises data sharing certain generative factors. Then, the latent variable z can be split into several partitions, each of which capture the generative factors of a specific cluster. Suppose that x_1 and x_2 are from the same cluster which is assigned to the i-th partition of the latent variable, i.e., z_i, the encoder and decoder can then be trained with a modified ELBO: (which is a lower bound of $\log P_\theta(x_2)$)

$$\mathcal{L}_{\theta,\phi}(x_1, x_2) = \mathbb{E}_{z\sim P_\phi(\cdot|x_1)} \left[\log P_\theta(x_2|z)\right] - D_{KL}(P_\phi(z|x_1)||P_\theta(z)) \tag{6}$$

  Note that the entire z is utilized to generate x_2 from x_1, but only gradients corresponding to z_i are backpropagated to the inference model P_ϕ. The rationale is that x_2 is intended to reconstruct only the shared generative factors with x_1, and these factors should exclusively be captured by z_i. Gated VAE requires domain knowledge as supervision, which may limit its general applicability.

- **CVAE:** Conditional VAE (CVAE, Sohn et al. (2015)) is a model for conditional generation. Given a set of data x and their corresponding conditional variables c (e.g., classification labels or desired attributes of the data), CVAE learns a conditional prior $P_\theta(z|c)$ and a conditional generative model $P_\theta(x|z, c)$, so that a data sample x that satisfies a certain condition c can be generated via $z \sim$

$P_\theta(\cdot|c), x \sim P_\theta(\cdot|z,c)$. CVAE is particularly useful in tasks requiring controlled data generation, like scenarios where manipulating specific attributes of the generated data is necessary. As in VAEs, an inference model $P_\phi(z|x,c)$ is introduced for the learning process, which gives the ELBO:

$$\mathcal{L}_{\theta,\phi}(x,c) = \mathbb{E}_{z\sim P_\phi(\cdot|x,c)}\left[\log P_\theta(x|z,c)\right] - D_{KL}(P_\phi(z|x,c)||P_\theta(z|c)) \tag{7}$$

Compared with the original VAE formulation, a conditional variable c is introduced to each function, i.e., the prior, inference, and generative model. Following a derivation process similar with Eq. (1), it can be shown that Eq. (7) is a variational lower bound for $\log P_\theta(x|c)$, i.e., the conditional generation likelihood. Further, they note that, during evaluation, latent variables are sampled from $P_\theta(z|c)$ rather than $P_\phi(z|x,c)$, as only the conditions c are available. Thus, to enhance consistency of the data generation process during training and evaluation, they introduce an additional objective term to Eq. (7):

$$\mathcal{L}^{\text{hybrid}}_{\theta,\phi}(x,c) = \alpha\mathcal{L}_{\theta,\phi}(x,c) + (1-\alpha)\mathbb{E}_{z\sim P_\theta(\cdot|c)}\left[\log P_\theta(x|z,c)\right] \tag{8}$$

- **VQ-VAE:** Unlike aforementioned VAE variants where z is continuous, VQ-VAE (van den Oord et al. (2017)) is an auto-encoder framework utilizing discrete latent variables. In particular, they assume the latent variable space is a codebook $[e_1^T, \cdots, e_k^T] \in \mathbb{R}^{k\times d}$, where k is number of categories and d is the dimension of the latent vector for each category (i.e., e_i). Such discrete representations are usually easier to model than continuous ones and can be particularly advantageous in some situations. For example, in a dataset of images with several categories, categorized latent representations are more appropriate, where each category is assigned a code from the codebook. In particular, the forward process of VQ-VAE is: $z_E = P_\phi(x), z_D = e_i$ $(i = \arg\min_j ||z_E - e_j||_2), \hat{x} \sim P_\theta(\cdot|z_D)$. Here, the latent variable from the encoder, i.e., z_E, is mapped to its nearest neighbour in the codebook, i.e., z_D, which is then input to the decoder for data generation. The learnable parameters of VQ-VAE include θ, ϕ, and $e_{1:k}$, for which the objective is as below: (z_D and e_i are defined as above; sg denotes the stop-gradient operator.)

$$\mathcal{L}_{\theta,\phi,e_{1:k}}(x) = \log P_\theta(x|z_D) - ||\text{sg}\left[P_\phi(x)\right] - e_i||_2^2 - \beta||P_\phi(x) - \text{sg}\left[e_i\right]||_2^2 \tag{9}$$

  The generative model is trained to reconstruct the data x, as in other VAE variants, via the first term of Eq. (9). The codebook parameters are trained to align with the encoded latent representations $z_E = P_\phi(x)$ through the second term. As for P_ϕ, it is trained by both the first and third terms. Specifically, they assume $\frac{\partial \log P_\theta(x|z_D)}{\partial z_E} = \frac{\partial \log P_\theta(x|z_D)}{\partial z_D}$, such that the gradient of the first term on z_D can be backpropagated to ϕ. The third term, on the other hand, is to make sure that the encoder commits to an embedding from the codebook. While empirical evidence demonstrates VQ-VAE's effectiveness, its objective design largely relies on intuition, so additional theoretical underpinning would be beneficial.

- **VRNN:** Chung et al. (2015) introduce a recurrent version of the VAE for the purpose of modeling sequences of data (i.e., $x_{\leq T} \triangleq [x_0, \cdots, x_T]$). At each time step t, the historical information $(x_{<t}, z_{<t})$ is involved for sequential decision making, where $z_{<t}$ are latent variables corresponding to $x_{<t}$. Instead of directly concatenating the sequence of variables, i.e., $(x_{<t}, z_{<t})$, as the history, a recurrent neural network (RNN) is adopted to embed the historical information recursively: $h_t = \text{RNN}_\omega(x_t, z_t, h_{t-1}),\ (t = 0, \cdots, T)$ [1]. To involve historical information in decision-making, the prior, generative, and inference model are conditioned on the history embedding as: $P_\theta(z_t|h_{t-1})$, $P_\theta(x_t|z_t, h_{t-1})$, and $P_\phi(z_t|x_t, h_{t-1})$, where h_{t-1} embeds the history $(x_{<t}, z_{<t})$. The overall objective (to maximize) for these three models and RNN_ω is as below:

$$\mathbb{E}_{P_{\phi,\omega}(z\leq T|x\leq T)}\left[\sum_{t=1}^{T}\left(\log P_\theta(x_t|z_t,h_{t-1}) - D_{KL}(P_\phi(z_t|x_t,h_{t-1})||P_\theta(z_t|h_{t-1}))\right)\right] \tag{10}$$

[1] According to (Chung et al. (2015)), additional embedding layers emb_X and emb_Z can be used to extract features from the data x_t and latent variables z_t, respectively.

where $P_{\phi,\omega}(z \leq T|x \leq T) = \prod_{t=0}^{T} P_\phi(z_t|x_t, h_{t-1})$ with h_t defined as above. This objective is a variational lower bound of the log likelihood of the data sequence, i.e., $\log P_\theta(x_{\leq T})$, as shown in Appendix A of (Chung et al. (2015)). The introduction of historical information and explicit use of the Hidden Markov Model (Rabiner & Juang (1986)) (e.g., for defining $P_{\phi,\omega}(z \leq T|x \leq T)$) significantly improve the representational capability of VRNN for sequential data.

2.2 Generative Adversarial Networks

The Generative Adversarial Network (GAN, Goodfellow et al. (2014a)) is a generative model based on the minimax optimization. It consists of a generator G and discriminator D that are trained simultaneously to compete against each other. The generator tries to capture the distribution of real data $P_X(x)$ and generate new data examples x from initial noise $z \sim P_Z(\cdot)$. The discriminator is usually a binary classifier used to discriminate generated examples from real data as accurately as possible. Formally, the generator can be modeled as a differentiable function that maps noise z following a certain prior distribution $P_Z(\cdot)$ to samples x in the data space X: $z \sim P_Z(\cdot), x = G(z) \sim P_G(\cdot)$. While, the discriminator's output $D(x)$ estimates the probability of a data point x being sampled from the true data distribution $P_X(\cdot)$ rather than generated by the generator. The training objective of GAN is formulated as a minimax game between G and D:

$$\min_G \max_D \mathbb{E}_{x\sim P_X(\cdot)}[\log D(x)] + \mathbb{E}_{z\sim P_Z(\cdot)}[\log(1 - D(G(z)))] \tag{11}$$

Here, D is trained to maximize the probability of assigning correct labels to both real data and fake ones from the generator: $D(x) \to 1, D(G(z)) \to 0$. For a certain G, the optimal discriminator is given by: $D^*_G(x) = \frac{P_X(x)}{P_X(x)+P_G(x)}$. Plugging this back in Eq. (11), the minimax problem can be converted to an optimization problem with regard to the generator G: $\min_G JS(P_X(\cdot)||P_G(\cdot))$, where $JS(\cdot)$ denotes the Jensen-Shannon divergence (Menéndez et al. (1997)). Please refer to (Goodfellow et al. (2014a)) for the detailed derivation. Thus, in essence, G is trained to generate samples that match the real data distribution.

Next, we introduce several representative variants of GAN, as the necessary background for Section 4:

- **Conditional GAN (CGAN) & InfoGAN:** CGAN (Mirza & Osindero (2014)) trains its generator and discriminator together with extra information y as conditions:

$$\min_G \max_D \mathbb{E}_{x\sim P_X(\cdot)}[\log D(x|y)] + \mathbb{E}_{z\sim P_Z(\cdot)}[\log(1 - D(G(z|y)))] \tag{12}$$

  Similarly, this objective can be converted to $\min_G JS(P_X(\cdot|y)||P_G(\cdot|y))$, i.e., matching the conditional distribution of the real data. With these conditional models, CGAN has the advantage of handling not only unimodal datasets but also multimodal ones like Flickr (Plummer et al. (2015)), which consists of diverse labeled image data. With the class label or text as the condition y, CGAN can be used for conditional generation. However, when the dataset contains multiple modalities but the labels y are not given, InfoGAN (Chen et al. (2016)) proposes to introduce a latent code c (following an assumed distribution $P_C(\cdot)$) to the generator. In this way, the data generation process is modified into $c \sim P_C(\cdot), z \sim P_Z(\cdot), x = G(z, c) \sim P_G(\cdot|c)$, where c is for capturing distinct modes in the dataset and z targets the unstructured noise shared across the modes. The generator G is trained not only with $V(D, G)$ (i.e., Eq. (11)) but also to maximize the mutual information between the mode variable C and the respective samples $X|_C = G(Z, C)$: $\min_G \max_D V(D, G) - \lambda I(C, X|_C))$, such that $G(Z, C)$ would not degenerate to a unimodal model. By replacing the mutual information with its practical lower bound, we have the objective for InfoGAN as below:

$$\min_{G,Q} \max_D V(D, G) - \lambda \left[\mathbb{E}_{c\sim P_C(\cdot), z\sim P_Z(\cdot), x=G(z,c)} [\log Q(c|x)] + H(C)\right] \tag{13}$$

  Here, $Q(x|c)$ is a variational posterior neural network trained to approximate the real but intractable posterior distribution $P(c|x)$, and $H(C)$ denotes the entropy of the mode variable C [2].

[2] $I(C, X|_C) = H(C) - H(C|X|_C) = -\int P_C(c) \log P_C(c)\, dc + \int P_C(c)P_G(x|c) \log P(c|x)\, dc\, dx \geq -\int P_C(c) \log P_C(c)\, dc + \int P_C(c)P_G(x|c) \log Q(c|x)\, dc\, dx$. The same trick as in Eq. (1) is adopted here to get this inequality.

- **f-GAN:** A large class of different divergences, including the KL divergence and JS divergence, are the so-called f-divergences (Csiszár & Shields (2004)). Specifically, given two continuous distributions $P(\cdot)$ and $G(\cdot)$, the f-divergence between them is defined as $D_f(P(\cdot)||Q(\cdot)) = \int Q(x) f\left(\frac{P(x)}{Q(x)}\right) dx$, where $f : \mathbb{R}^+ \rightarrow \mathbb{R}$ should be a convex, lower-semicontinuous function satisfying $f(1) = 0$ [3]. Given a data distribution $P_X(\cdot)$, a corresponding generative model G can be learned through minimizing $D_f(P_X(\cdot)||P_G(\cdot))$. As proposed in f-GAN (Nowozin et al. (2016)), this can be approximately solved via a minimax optimization problem:

$$\min_G \max_V \mathbb{E}_{x\sim P_X(\cdot)}\left[g_f(V(x))\right] + \mathbb{E}_{x\sim P_G(\cdot)}\left[-f^*(g_f(V(x)))\right] \tag{14}$$

  Here, V is a differentiable function without any range constraints on the output, g_f is an output activation function specific to the f-divergence used, and f^* is the convex conjugate function of f (Hiriart-Urruty & Lemaréchal (2004)). With specific choices of f, f^* and g_f, various types of f-GAN can be achieved (see Table 6 of (Nowozin et al. (2016))). For example, the original GAN can be recovered by setting $f^*(t) = -\log(1 - \exp(t))$ and $g_f(v) = -\log(1 + \exp(-v))$ [4]. In this way, f-GAN provides a generalization of multiple variants of GANs, including the original GAN, LSGAN, and WGAN.

- **Least Squares GAN (LSGAN):** During the early training stage, the generated examples would substantially differ from the real data, but the original GAN objective provides only very small penalties for updating G, as shown in Figure 16 of (Goodfellow (2017)). To overcome this vanishing gradient problem, LSGAN (Mao et al. (2017)) replaces the cross-entropy loss used in the original GAN objective with least-square losses:

$$\min_D \mathbb{E}_{x\sim P_X(\cdot)}\left[(D(x)-j)^2\right] + \mathbb{E}_{z\sim P_Z(\cdot)}\left[(D(G(z))-i)^2\right],\ \min_G \mathbb{E}_{z\sim P_Z(\cdot)}\left[(D(G(z))-k)^2\right] \tag{15}$$

  Here, i, j are the labels for the generated and real examples, respectively; k is the value that G hopes for D to believe for generated examples. As shown in (Mao et al. (2017)), when $j - i = 2$ and $j - k = 1$, Eq. (15) is equivalent to minimizing the Pearson χ^2 divergence, which is a type of f-divergence, between the real and generated data distribution, i.e., $P_X(x)$ and $P_G(x)$.

- **Wasserstein GAN (WGAN):** As mentioned earlier, for the original GAN, the optimization with respect to G is equivalent to minimizing the JS divergence $JS(P_X(\cdot)||P_G(\cdot))$. WGAN (Arjovsky et al. (2017)) proposes to minimize the Wasserstein distance instead, which is defined as $\sup_{||f||_L \leq K} \mathbb{E}_{x\sim P_X(\cdot)}[f(x)] - \mathbb{E}_{x\sim P_G(\cdot)}[f(x)]$. $||f||_L \leq K$ denotes the set of K-Lipschitz functions. In this case, the objective function of WGAN is as below:

$$\min_G \max_D \mathbb{E}_{x\sim P_X(\cdot)}\left[D(x)\right] - \mathbb{E}_{x\sim P_G(\cdot)}\left[D(x)\right] \tag{16}$$

  Here, D is used to estimate the Wasserstein distance, hence its output is not limited to $[0, 1]$ as in the original GAN. Also, the neural network D is applied with weight clipping, ensuring that D is K-Lipschitz. Compared with the original GAN, WGAN improves the learning stability and provides meaningful learning curves for parameter fine-tuning.

- **Triple-GAN:** To realize data classification and conditional generation in the meantime, Triple-GAN (Li et al. (2017a)) proposes to introduce a classifier $C(y|x)$ to the original GAN framework. Here, x and y denote the data and label, respectively. Given a dataset of (x, y), empirical joint and marginal distributions of the real data and labels can be acquired as $P_{X,Y}(x, y)$, $P_X(x)$, and $P_Y(y)$. $P_{X,Y}(x, y)$ can be approximated as either $P_X(x)P_C(y|x)$ or $P_Y(y)P_G(x|y)$, corresponding to the classification with C and conditional generation with G, respectively. Thus, C and G can be

[3] As an instance, when $f(a) = a \log a$, D_f recovers the KL divergence.

[4] The discriminator in the original GAN $D(x)$ would be a function of $V(x)$, i.e., $D(x) = 1/(1 + \exp(-V(x)))$. $V(x) \in \mathbb{R}$ and thus $D(x) \in (0, 1)$.

trained to match the joint distribution of (x, y). Here is the objective:

$$\begin{aligned}\min_{C,G}\max_{D}\ & \mathbb{E}_{(x,y)\sim P_{X,Y}(\cdot)}\left[\log D(x,y)\right] + \lambda_G \mathbb{E}_{y\sim P_Y(\cdot),x\sim P_G(\cdot|y)}\left[\log(1-D(x,y))\right] + \\ & (1-\lambda_G)\mathbb{E}_{x\sim P_X(\cdot),y\sim P_C(\cdot|x)}\left[\log(1-D(x,y))\right] + \mathbb{E}_{(x,y)\sim P_{X,Y}(\cdot)}\left[-\log P_C(y|x)\right] + \\ & \lambda_C \mathbb{E}_{y\sim P_Y(\cdot),x\sim P_G(\cdot|y)}\left[-\log P_C(y|x)\right]\end{aligned} \tag{17}$$

The first three terms resemble the GAN framework, where C and G are trained to fool the discriminator D by generating (x, y) close to the real data. The last two (cross entropy) terms provide extra supervision for C using samples from the real and generated distributions. Note that the last objective term is only utilized for training C. It is shown in (Li et al. (2017a)) that $P_{X,Y}(x, y) = P_X(x)P_C(y|x) = P_Y(y)P_G(x|y)$ if and only if the equilibrium among the three players (C, G, D) is achieved in Eq. (17).

2.3 Normalizing Flows

Normalizing Flows (NFs) represent a class of generative models that offer an elegant approach for density estimation and the generation of data samples from complex distributions (Kobyzev et al. (2021)). NFs allow for exact likelihood evaluation, which is crucial in many probabilistic modeling tasks. Formally, NFs transform a simple, known probability distribution on the latent variable (i.e., $z \sim P_Z(\cdot)$) into a complex, desired distribution on data (i.e., $x \sim P_X(\cdot)$) through a sequence of invertible and differentiable transformations. The mathematical representation of the transformation from x to z is given by a composition of a series of bijections as $F = F_N \circ F_{N-1} \circ \cdots \circ F_1$. The data flow $[x_0, x_1, \cdots, x_N]$ $(x_0 = x,\ x_N = z)$ within NFs adheres to the following: for all $1 \le i \le N,\ x_i = F_i(x_{i-1}),\ x_{i-1} = F_i^{-1}(x_i)$. The core principle behind the transformation is the change of variable formula. Specifically, the probability density functions of x and z are related as:

$$P_Z(z) = P_X(F^{-1}(z))|\det D(F^{-1}(z))|,\ P_X(x) = P_Z(F(x))|\det D(F(x))| \tag{18}$$

where $\det D(F(x))$ denotes the determinant of the Jacobian matrix of $F(x)$. Given the transformation function F and the basic distribution P_Z, the density of a data sample x can be exactly acquired as $P_X(x)$ defined in Eq. (18). Conversely, the data generation can be done by first sampling a latent $z \sim P_Z(\cdot)$ and then apply the generator function $G = F^{-1}$. As for training, it is usually through maximizing the log-likelihood of target data distribution (Dinh et al. (2017)):

$$\mathbb{E}_X[\log(P_X(x))],\ \log(P_X(x)) = \log(P_Z(F(x))) + \log(|\det D(F(x))|) \tag{19}$$

For NFs, the generator G should be sufficiently expressive to model the distribution of interest, while the transformation F should be invertible and the computation of the two directions mentioned above, especially regarding the determinant calculation, should be efficient. Based on these requirements, various types of flows have been developed. Here, we present a brief description of the representative categories. As mentioned above, G is composed of a series of generator modules $G_i = F_i^{-1}$. For each of the following categories, we introduce its specific design on G_i, and we use m and n to denote the input and output of G_i, respectively. Note that we will not delve into the complex mathematical details regarding calculations or objective designs of specific variants of NFs, as they are not essential for understanding the applications of NFs in offline policy learning, as introduced in Section 5.

- **Coupling Flows** enable highly expressive transformations via a coupling method. In particular, the input $m \in \mathbb{R}^D$ is partitioned into two subspaces: $(m^A, m^B) \in \mathbb{R}^d \times \mathbb{R}^{D-d}$, and the generator module G_i is defined in the format: $G_i(m) = (H(m^A; \Theta(m^B)), m^B)$. Here, $H(\cdot;\theta) : \mathbb{R}^d \to \mathbb{R}^d$ is a bijection, and Θ is the parameter function. H is also called the coupling function. In this case, the Jacobian of G_i is simply the Jacobian of H, and for efficient computation of determinants, H is usually designed to be an element-wise bijection, i.e., $H(m^A;\theta) = (H_1(m_1^A;\theta_1), \cdots, H_d(m_d^A;\theta_d))$ where each $H_i(\cdot;\theta_i) : \mathbb{R} \to \mathbb{R}$ is a scalar bijection. The expressiveness of a coupling flow lies in the complexity of its parameter function Θ, which, in practical applications, is typically modeled using

neural networks. Algorithms in this category include NICE (Dinh et al. (2015)), RealNVP (Dinh et al. (2017)), Glow (Kingma & Dhariwal (2018)), NSF (Durkan et al. (2019)), Flow++ (Ho et al. (2019)), etc.

- **Autoregressive Flows** utilize autoregressive models for generation. To be specific, each entry of $n = G_i(m)$ conditions on the previous entries of the input: $n_t = H(m_t; \Theta_t(m_{1:t-1}))$, where $H(\cdot;\theta) : \mathbb{R} \to \mathbb{R}$ is a scalar bijection and Θ_t is a parameter function. Thus, each n_t relies solely on $m_{1:t}$, resulting in a triangular Jacobian maxtrix of G. This structure allows for efficient computation of the determinant and parallel computation of each entry in n. However, the inverse process, represented as $m_t = H^{-1}(n_t; \Theta_t(m_{1:t-1}))$, must be performed sequentially, since the parameter for the subsequent step (i.e., $\Theta_{t+1}(m_{1:t})$) uses the output of the current step, i.e., m_t, as input. Algorithms like IAF (Kingma et al. (2016)), MAF (Papamakarios et al. (2017)), and NAF (Huang et al. (2018)), fall in this category.

- **Residual Flows** employ residual networks (He et al. (2016)) as the generator component, characterized by $G_i(m) = m + R(m)$. Here, $R(\cdot)$ symbolizes the residual block, which can be implemented as any variant of neural network that is invertible. Several studies (Gomez et al. (2017); Chang et al. (2018); Jacobsen et al. (2018)) have aimed to develop invertible network architectures suitable for use as residual blocks. Nonetheless, these architectures present a significant challenge in efficiently calculating their Jacobian determinants. Research works such as iResNet (Behrmann et al. (2019)) and Residual Flow (Chen et al. (2019)) propose an invertible G_i by limiting the Lipschitz constant of the residual block to be less than 1 and compute its inverse through fixed-point iterations. However, controlling the Lipschitz constant of a neural network is also quite challenging.

- **ODE-based Flows** aim to learn a continuous dynamic system shown as a first-order ordinary differential equation (ODE): $\frac{d}{dt}m(t) = R(m(t); \theta(t)),\ t \in [0, 1]$. It's worthy noting that the residual flows mentioned above can be interpreted as a discretization of this ODE. Assuming the uniform Lipschitz continuity in m and setting the initial condition $m(0) = z$, the solution of that ODE at each time point $\Phi^t(z)$ exists and is unique (Arnold (1992)). As proposed in NODE (Chen et al. (2018b)), the map at time one $\Phi^1(z)$ can work as the generator, i.e., $x = \Phi^1(z)$, which can be considered as an "infinitely deep" neural network with stacked weights $\theta(t), t \in [0, 1]$. Thus, typically, continuous ODE-type flows require fewer parameters to match the performance of discrete ones (Grathwohl et al. (2018)). As for the invertibility of Φ^1, it is naturally ensured by the theorem of existence and uniqueness pertaining to the solution of the ODE. However, Φ^1 must be orientation preserving - that is, its Jacobian determinant must be positive, which may constrain its representational capacity. In order to give freedom for the Jacobian determinant to remain positive, the authors of ANODE (Dupont et al. (2019)) propose augmenting the original ODE with supplementary variables $\hat{m}(t)$, resulting in $\frac{d}{dt}[m(t)||\hat{m}(t)] = \hat{R}(m(t)||\hat{m}(t); \theta(t)),\ t \in [0, 1]$, with $||$ signifying concatenation.

There are other types of flows which are not widely used in practice and so not introduced here, such as Planar and Radial Flows (Rezende & Mohamed (2015); van den Berg et al. (2018)) and Langevin Flows (continuous and SDE-based) (Welling & Teh (2011); Chen et al. (2018a)). Coupling Flows and Autoregressive Flows facilitate straightforward invertible transformations and efficient determinant computation, yet lag in expressiveness compared to Residual Flows which are computationally costly. ODE-based Flows provide a potentially elegant and parsimonious representation with fewer parameters. However, they necessitate the resolution of ODEs during training, a process that can be computationally demanding and sensitive to the choice of numerical solver settings. Compared with VAEs and GANs, NFs allow for exact density estimation of a generated sample and can avoid training issues like mode collapse, vanishing gradients, etc (Salimans et al. (2016)). However, its requirements for bijection functions and determinant calculations can restrict its capacity to effectively model complex data distributions (Cornish et al. (2020)).

2.4 Transformers

Transformer (Vaswani et al. (2017)) is an important foundation model that has shown exceptional capability across various areas, such as natural language processing (Kalyan et al. (2021)), computer vision (Han et al.

(2022)), time series analysis (Wen et al. (2023)), and so on. Recently, there has been a growing trend in developing IL and offline RL algorithms based on transformers, with the hope to achieve sequential decision-making based on next-token predictions as in natural language processing. As shown in Figure 1, the transformer follows the widely-adopted encoder-decoder structure. The encoder maps the input $(x_1, \cdots, x_n)$ to a sequence of embeddings $(z_1, \cdots, z_n)$, and the decoder generates the output sequence auto-regressively. That is, the decoder predicts one token y_{m+1} at a time, based on the input embeddings $(z_1, \cdots, z_n)$ and previously-generated outputs $(y_1, \cdots, y_m)$. Both the encoder and decoder are composed of a stack of L identical modules. For clarity, we present each layer in the module sequentially following the data flow.

- **Positional Encoding:** After the token embedding layer, which is shared by $(x_1, \cdots, x_n)$ and $(y_1, \cdots, y_m)$, each element is converted to a d-dim vector. To enable the model to make use of the order of tokens, information about the relative or absolute positions of tokens within the sequence is injected through a positional encoding. For the i-th token, its positional encoding is also a d-dim vector, of which the j-th dimension is $\sin(\frac{i}{10000^{j/d}})$ if j is even and $\cos(\frac{i}{10000^{(j-1)/d}})$ otherwise. The positional encoding and token embedding are then combined through summation. Per Vaswani et al. (2017), this (periodic function) positional encoding design embeds relative position information and helps the model to manage sequences longer than those experienced in training.

- **Self Multi-Head Attention (MHA):** This component utilizes the attention mechanism. Given s queries and t key-value pairs, the attention function maps each query to a weighted-sum of the values, where the weight assigned to each value is computed as the compatibility of the query with the key paired with that value. The queries, keys, and values can be represented as $Q \in \mathbb{R}^{s \times d_q}$, $K \in \mathbb{R}^{t \times d_k}$, and $V \in \mathbb{R}^{t \times d_v}$, respectively, and the outputs for all queries (i.e., O) can be computed in parallel as: (For conformability of matrix multiplication, $d_k = d_q$.)

$$O = \text{Attention}(Q, K, V) = \text{SoftMax}\left(\frac{QK^T}{\sqrt{d_k}}\right)V, \; O_i = \text{SoftMax}\left(\frac{\langle Q_i, K_1\rangle}{\sqrt{d_k}}, \cdots, \frac{\langle Q_i, K_t\rangle}{\sqrt{d_k}}\right)V \quad (20)$$

  Here, SoftMax is a row operator, and the output for query i, i.e., O_i, is a weighted sum of the rows of V, where the weight for row j is propotional to the similarity of Q_i (i.e., the i-th row of Q) and K_j measured by their inner product $\langle Q_i, K_j\rangle$. The dot products grow large with d_k, which would push the SoftMax function to regions with vanished gradients, so the factor $1/\sqrt{d_k}$ is introduced. The input embeddings H_x (in Figure 1) can potentially be used as the matrices Q, K, and V for self attention. However, to enable the model to jointly attend to information from different representation subspaces, a multi-head attention mechanism is adopted:

$$\text{MHA}(Q, K, V) = \text{Concat}(\text{head}_1, \cdots, \text{head}_h)W^O, \; \text{head}_i = \text{Attention}(QW_i^Q, KW_i^K, VW_i^V) \quad (21)$$

  where $Q = K = V = H_x \in \mathbb{R}^{n \times d}$, $W_i^Q \in \mathbb{R}^{d \times d'}$, $W_i^K \in \mathbb{R}^{d \times d'}$, $W_i^V \in \mathbb{R}^{d \times d'}$, $W_i^O \in \mathbb{R}^{d \times d}$, $d' = d/h$, and Concat represents the concatenation operation. W_i^Q, W_i^K, W_i^V convert H_x to matrices in the i-th attention head, providing a distict representation subspace. It's worthy noting that the output of MHA belongs to $\mathbb{R}^{n \times d}$, that is, the same in shape as its input.

- **Add & Normalize:** A residual connection (He et al. (2016)) is employed around each attention layer, followed by a layer normalization (Ba et al. (2016)). As common practice, these two operations are adopted to stabilize training of (very) deep networks (e.g., by alleviating ill-posed gradients and model degeneration). Suppose the previous layer is F, which can be an MHA or Feed-forward Network as shown in Figure 1, and its input is X, then the calculation of this Add & Normalize layer can be denoted as $\text{LayerNorm}(F(X) + X)$.

- **Point-wise Feed-forward Network (FFN):** FFN layers are important for a Transformer to achieve good performance. Dong et al. (2021) observe that simply stacking MHA modules causes a rank collapse problem (e.g., leading to token-uniformity), and that the FFN is one of the important building blocks to mitigate this issue. Specifically, a two-layer fully-connected network with a ReLU activation function in the middle is applied to each of the n token embeddings separately, leading to n new d-dim embeddings as output.

- **Masked Self MHA & Cross MHA:** For the decoder, H_x is replaced by $H_y \in \mathbb{R}^{m \times d}$, i.e., embeddings of previously-generated outputs. For rationality, the query (of the Masked Self MHA) at each position is only allowed to attend to positions up to and including that position, as the other queries correspond to outputs yet to generate. This is realized within the Masked Self MHA by masking out corresponding compatibility values, i.e., $\langle Q_i, K_j \rangle = -\infty, \ \forall j > i$ (in Eq. (20)). As for the Cross MHA, its queries come from the previous decoder layer and key-value pairs are from the output of the encoder, i.e., $H_z \in \mathbb{R}^{n \times d}$ in Figure 1. Note that these matrices will be embedded with W_i^Q, W_i^K, W_i^V to get multiple representation subspaces, as Eq. (21). In this way, every query for predicting the next token can attend over all positions in the input sequence (via the Cross MHA) and all previously-generated tokens (via the Masked Self MHA).

Each encoder module outputs an $n \times d$ matrix, and each decoder module outputs an $m \times d$ matrix. Here, n and m denote the counts of elements in the input and output sequences, respectively, while d represents the embedding dimension. This uniformity in the input and output dimensions enables the stacking of multiple encoder (or decoder) modules to create a deep model. Each encoder (or decoder) module will take the output from the previous encoder (or decoder) module. Generally, the transformer architecture can be used in three different ways: **encoder-only**, **decoder-only**, or **encoder-decoder**. When using only the encoder, its output serves as a representation of the input sequence, suitable for natural language understanding tasks such as text classification. While, if only the decoder is employed, the Cross MHA modules are removed and this architecture is suitable for sequence generation tasks like language modeling. Applications of transformers in IL or offline RL usually adopt this decoder-only way. The overall encoder–decoder architecture is equipped with the ability to perform both natural language understanding and generation, typically used in sequence-to-sequence modeling (e.g., neural machine translation).

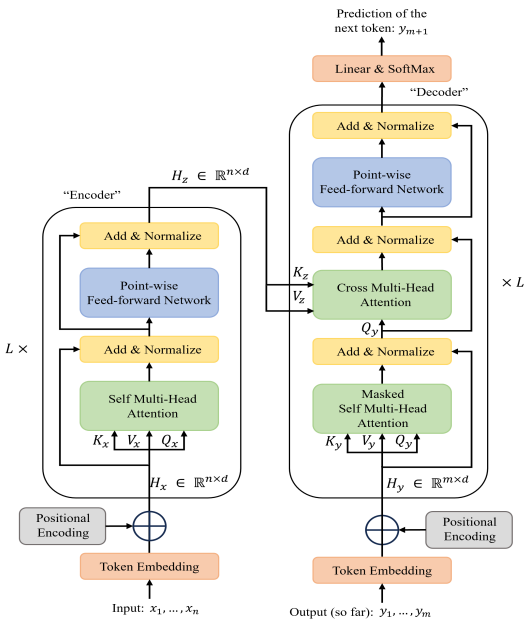

Figure 1: The Transformer Architecture

Compared with other types of neural networks, the transformer architecture has significant advantages. Compared with **fully-connected layers**, the transformer is more flexible in handling variable-length inputs (i.e., with different n) and more parameter-efficient, since the amount of network parameters in a transformer is irrelevant to the sequence length n [5]. **The convolutional layer** uses a convolution kernel of size $k < n$ to connect pairs of tokens, so, to link distant token pairs, a stack of convolutional layers is required. However, with the attention mechanism, each pair of tokens can be connected in one MHA layer and the time complexity for matching their corresponding query and key is constant (i.e., irrelevant to n). This makes the transformer excel at capturing long-range dependencies within a sequence. **Recurrent layers** produce a sequence of hidden states h_i, each dependent on the previous hidden state h_{i-1} and the input at position i. This sequential nature prevents parallel computation. However, in transformers, computations at each position are independent, allowing for parallel execution that are essential for processing long sequences. Last, both convolutional and recurrent models make structural assumptions over the inputs, suitable for image-like and time series data, respectively. However, the transformer has few prior assumptions on the data structure and thus is a more universal model. Empirical results have shown that the transformer has superior performance on a wide-range of tasks and a larger capacity than CNNs and RNNs to handle a huge amount of training data.

[5] The FFN layers are applied to each position rather than the whole sequence, and the MHA layers only require updating the weights: W_i^Q, W_i^K, W_i^V, W^O, the sizes of which are irrelevant with n.

As listed above, the transformer contains multiple types of layers. Numerous studies have explored modifications or replacements of layers in the standard transformer for improvements. For a comprehensive review, please refer to (Lin et al. (2022c)). On the other hand, the computation and memory complexity of MHA modules are quadratic to the length of the input sequence (i.e., n), leading to inefficiency at processing extremely long sequences. Various extensions have been developed to enhance either the computational or memory efficiency. Additionally, due to the minimal structural assumptions made by the transformer about the input data, transformers are prone to overfitting when trained on small-scale datasets. Attempts like pretraining the transformer on large-scale unlabeled data (Brown et al. (2020)), introducing sparsity assumptions (Child et al. (2019)) such as limiting the number and positions of key-value pairs that each query can attend to, have been made to solve these issues. Finally, extensions to adapt the transformer for particular downstream applications are possible. Studies detailed in Section 6 can be viewed as examples of this type of extensions.

2.5 Diffusion Models

Diffusion models have demonstrated superior performance across multiple domains, such as computer vision (Amit et al., 2021; Baranchuk et al., 2021), natural language processing (Austin et al., 2021b; Hoogeboom et al., 2021), and multi-modal learning (Avrahami et al., 2022; Ramesh et al., 2022), showcasing their impressive capabilities of generating detailed and diverse instances. Diffusion models contain two interconnected processes: the forward diffusion process and the backward denoising process (Yang et al. (2022a)). Specifically, the forward process is predefined and transforms the data with a certain (but unknown) distribution, i.e., $x \sim P_X(\cdot)$, into a (standard Gaussian) random noise z. This process progressively corrupts the input data by adding a varying scale of noise at each diffusion step. Correspondingly, the reverse process uses a neural network as the denoising function to gradually undo the forward transformation to reconstruct the data from the random noise. There exist three main formulations of diffusion models: Score-based Generative Models (SGM) (Song & Ermon, 2019; 2020), Denoised Diffusion Probabilistic Models (DDPM) (Sohl-Dickstein et al., 2015; Ho et al., 2020; Nichol & Dhariwal, 2021), and Stochastic Differential Equations (Score SDE) (Song et al., 2020; 2021). Next, we introduce these formulations by illustrating their forward/backward processes and learning objectives, while discussing their connections with each other.

- **SGM** learns (Stein) score functions (Hyvärinen (2005)) for samples at each diffusion step, i.e., $S_\theta(x_t, t),\ t \in [1, \cdots, T]$. As defined, the Stein score function of x is the gradient of its log likelihood $\nabla_x \log P(x)$, with which data samples $x \sim P(\cdot)$ can be generated via various efficient score-based sampling schemes such as (Song & Ermon (2019); Jolicoeur-Martineau et al. (2021)). Specifically, the forward process of SGM starts from $x_0 \sim P_X(\cdot)$ and injects intensifying Gaussian noise to generate $x_{1:T}$: ($\beta_{1:T}$ is a predefined schedule of variance levels.)

$$x_t \sim F(\cdot|x_0) = \mathcal{N}(x_0, \beta_t I),\ 0 < \beta_1 < \beta_2 < \cdots < \beta_T \tag{22}$$

  The score functions for each step $S_\theta(x_t, t)$ are trained to approximate $\nabla_{x_t} \log P(x_t)$, where $P(x_t) = \int F(x_t|x_0)P_X(x_0)dx_0$. In particular, the training objective is as below:

$$\min_\theta \mathbb{E}_{t\sim\mathcal{U}[1,T], x_0\sim P_X(\cdot), \epsilon\sim\mathcal{N}(0,I)} \left[\lambda(t)||\epsilon + \sqrt{\beta_t} S_\theta(x_t, t)||^2\right] \tag{23}$$

  Here, $\mathcal{U}[1, T]$ is a uniform distribution on $[1, \cdots, T]$, $\lambda(t)$'s are positive weighting functions. This objective is derived based on the definition of the forward process, i.e., $x_t = x_0 + \sqrt{\beta_t}\epsilon,\ \epsilon \sim \mathcal{N}(0, I)$. For detailed derivations and the definition of $\lambda(t)$, please refer to (Song & Ermon (2019)). Regarding the backward generation process, the score functions $S_\theta(x_t, t),\ t \in [T, \cdots, 1]$, are sequentially used as denoising functions to generate x_{t-1} from x_t. Finally, the required data samples $x_0 \sim P_X(\cdot)$ can be acquired. As mentioned, multiple score-based sampling schemes can be adopted in this process. We take the annealed Langevin dynamics sampling scheme (Song & Ermon (2019)) as an example: $(x_T = x_T^0,\ x_0 = x_0^0)$

$$x_t^{i+1} = x_t^i + \frac{1}{2} s_t S_\theta(x_t^i, t) + \sqrt{s_t}\epsilon,\ (i = 0, \cdots, N-1),\ x_{t-1}^0 = x_t^N \tag{24}$$

N and s_t are hyperparameters, denoting the number of iterations and step size for denoising x_t^0 to x_{t-1}^0 $(t = T \to 1)$.

- **DDPM** gradually adds random noise to the data over a series of time steps $(x_0, \cdots, x_T)$ in the forward process, where $x_0 = x,\ x_T = z$. In particular, the sample at each time step is drawn from a Gaussian distribution conditioned on the sample from the previous time step: ($\beta_{1:T}$ are predefined.)

$$x_t \sim F(\cdot|x_{t-1}) = \mathcal{N}(\sqrt{1-\beta_t}x_{t-1}, \beta_t I) \tag{25}$$

With Eq. (25), the sample at each step t can be expressed as a function of x_0: $x_t = \sqrt{\alpha_t}x_0 + \sqrt{1-\alpha_t}\epsilon$, where $\alpha_t = \prod_{s=0}^{t}(1-\beta_s),\ \epsilon \sim \mathcal{N}(0, I)$ (Sohl-Dickstein et al. (2015)). α_T is designed to be close to 0, so that $z = x_T$ approximately follows $\mathcal{N}(0, I)$. Conversely, through the reverse denoising process, x_T is converted back to x_0 step by step: $(t = T \to 1)$

$$x_{t-1} \sim G_\theta(\cdot|x_t) = \mathcal{N}(\mu_\theta(x_t, t), \Sigma_\theta(x_t, t)) \tag{26}$$

where μ_θ and Σ_θ can be implemented as neural networks. The objective for learning this denoising function is to match the joint distributions of $x_{0:T}$ in the forward and backward processes, i.e., $\min_\theta D_{KL}(F(x_0, \cdots, x_T)||G_\theta(x_0, \cdots, x_T))$, which is equivalent to: (Sohl-Dickstein et al., 2015)

$$\min_\theta \mathbb{E}_{x_0 \sim P_X(\cdot), x_{1:T} \sim F(\cdot|x_0)} \left[-\log P(x_T) - \sum_{t=1}^{T} \log \frac{G_\theta(x_{t-1}|x_t)}{F(x_t|x_{t-1})} \right] \tag{27}$$

Note that $P(x_T)$ and $F(x_t|x_{t-1})$ have analytical forms and this objective is an upper bound for the negative log-likelihood $\mathbb{E}_{x_0 \sim P_X(\cdot)}[-\log P_\theta(x_0)]$. Although this objective can be directly optimized through Monte Carlo sampling, Ho et al. (2020) propose a reformulation of it for variance reduction. Since all (forward or backward) transformations are based on Gaussian distributions, by specifying the variance schedule $\beta_{1:T}$ and fixing the backward variance $\Sigma_\theta(x_t, t)$ to be $\beta_t I$, Eq. (27) can be converted to: (Ho et al. (2020))

$$\min_\theta \mathbb{E}_{t \sim \mathcal{U}[1,T], x_0 \sim P_X(\cdot), \epsilon \sim \mathcal{N}(0,I)} \left[\lambda(t)||\epsilon - \epsilon_\theta(\sqrt{\alpha_t}x_0 + \sqrt{1-\alpha_t}\epsilon, t)||^2 \right] \tag{28}$$

Here, $\lambda(t)$ is a positive weighting function which has a closed-form, but in practice, $\lambda(t)$ is set as 1 for all t to improve sample quality. Intuitively, the denoising function ϵ_θ is trained to predict the noise injected to samples at each step. Also, by setting $\epsilon_\theta(x, t) = -\sqrt{\beta_t}S_\theta(x, t)$, the objective forms of SGM (Eq. (23)) and DDPM (Eq. (28)) can be unified. Finally, with the learned ϵ_θ, the sampling process $x_{t-1} \sim G_\theta(\cdot|x_t)$ is equivalent to: $x_{t-1} = \frac{1}{\sqrt{1-\beta_t}}(x_t - \frac{\beta_t}{\sqrt{1-\alpha_t}}\epsilon_\theta(x_t, t)) + \sqrt{\beta_t}\epsilon,\ \epsilon \sim \mathcal{N}(0, I)$.

- **Score SDE** extends the discrete-time schemes of the previous two methods to a unified continuous-time framework, building upon stochastic differential equations (SDE). In the forward process, it perturbs data to noise with a diffusion process governed by the following differential equation:

$$dx = f(x, t)\, dt + g(t)\, dw,\ t \in [0, T] \tag{29}$$

where w is the standard Wiener process (Ricciardi (1976)), $f(x, t),\ g(t)$ are the diffusion and drift functions, respectively. In particular, the forward process of DDPM and SGM can be described by the following two equations (Song et al. (2020)), respectively, with specified $f(x, t)$ and $g(t)$:

$$dx = -\frac{1}{2}\beta(t)x\, dt + \sqrt{\beta(t)}\, dw,\ dx = \sqrt{\frac{d\beta(t)}{dt}}\, dw \tag{30}$$

The reverse process can be realized via solving the reverse-time SDE (Anderson, 1982):

$$dx = [f(x, t) - g^2(t)\nabla_x \log P_t(x)]\, dt + g(t)\, d\bar{w} \tag{31}$$

where $\bar{w}$ denotes the standard Wiener process when time flows backwards, $P_t(x)$ denotes the distribution of x at time t in the forward process. Similarly with SGM, the score function at each time

$\nabla_{x_t} \log P_t(x_t)$ can be estimated with an NN-based function $S_\theta(x_t, t)$ through various score matching techniques (Vincent (2011); Song et al. (2019)). Further, in (Song et al. (2020)), they propose to get rid of the random noise injection $g(t)\, d\bar{w}$ and prove that the resulting equation is a probability flow ordinary differential equation (ODE) which shares the same marginal densities as those of the reverse-time SDE, and both equations allow sampling from the required data distribution, i.e., $P_X(x)$.

3 Variational Auto-Encoders in Offline Policy Learning

In this section, we present a comprehensive overview of the applications of VAEs in offline policy learning, encompassing both offline RL (Section 3.1) and IL (Section 3.2). Within each subsection, we categorize related research works based on how VAEs are utilized. Additionally, we provide necessary background and a summary on the algorithm design paradigm as a brief tutorial. At the end of each subsection, we provide a table to summarize the representative algorithms with their key novelties and evaluation tasks, serving as a reference for future research in algorithm design and evaluation.

The sections focusing on other generative models, i.e., Sections 4 - 7, follow a structure similar to this section. As mentioned in the beginning of Section 2, notations of functions or variables are not shared across different generative models. However, all content is grounded in the fundamental Markov Decision Process (Puterman (2014)), denoted as $\mathcal{M} = (\mathcal{S}, \mathcal{A}, \mathcal{T}, r, \rho_0(s), \gamma)$. $\mathcal{S}$ is the state space, $\mathcal{A}$ is the action space, $\mathcal{T} : \mathcal{S} \times \mathcal{A} \times \mathcal{S} \to [0, 1]$ is the transition function, $\rho_0 : \mathcal{S} \to [0, 1]$ is the distribution of the initial state, $r : \mathcal{S} \times \mathcal{A} \to \mathbb{R}$ is the reward function, and $\gamma \in (0, 1]$ is the discount factor.

3.1 Offline Reinforcement Learning

Interestingly, our findings indicate that VAEs, Normalizing Flows, and Diffusion Models are typically integrated with dynamic-programming-based offline RL, whereas GANs are employed to enhance model-based offline RL, and Transformers are utilized in trajectory-optimization-based offline RL. Therefore, we split the background introduction on offline RL into three parts, categorized under the corresponding generative models: Section 3.1, Section 4.2, and Section 6.1. Based on the background on model-free offline RL (Section 3.1.1), we delve into the specific applications of VAEs for offline RL in Sections 3.1.3 -3.1.5, preceded by an overview in Section 3.1.2.

3.1.1 Background on Dynamic-Programming-based Offline Reinforcement Learning

Dynamic-programming-based offline RL is a main branch of model-free offline RL, as detailed in (Levine et al. (2020)). Given an offline dataset D_μ collected by the behavior policy $\mu(a|s)$, dynamic-programming-based offline RL usually would adopt a constrained policy iteration process as below: (k denotes the index of the learning iteration.)

$$\begin{aligned} Q^\pi_{k+1} &= \arg\min_Q \mathbb{E}_{(s,a,r,s')\sim D_\mu} \left[Q(s,a) - \left(r + \gamma \mathbb{E}_{a'\sim\pi_k(\cdot|s')} Q^\pi_k(s',a') \right) \right]^2; \\ \pi_{k+1} &= \arg\max_\pi \mathbb{E}_{s\sim D_\mu} \left[\mathbb{E}_{a\sim\pi(\cdot|s)} Q^\pi_{k+1}(s,a) \right] \;\; s.t.\; \mathbb{E}_{s\in D_\mu} \left[D(\pi(\cdot|s), \mu(\cdot|s)) \right] \le \epsilon. \end{aligned} \tag{32}$$

Here, the first and second equations are referred to as the policy evaluation and policy improvement steps, respectively. When updating the Q function, (s, a, r, s') are sampled from D_μ but the target action a' is sampled by the being-learned policy π_k. If $\pi_k(a'|s')$ differs substantially from $\mu(a'|s')$, out-of-distribution (OOD) actions, which have not been explored by μ, can be sampled. Further, the Q-function trained on D_μ, i.e., Q^π_{k+1}, may erroneously produce over-optimistic values for these OOD actions, leading the policy π_{k+1} to generate unpredictable OOD behaviors. In online RL, such issues are naturally corrected when the agent interacts with the environment, attempting the actions it (erroneously) believes to be good and observing that in fact they are not. In offline RL, interactions with the environment are not accessible, but, alternatively, the over-optimism can be controlled by limiting the discrepancy between π and μ, as shown in Eq. (32). The discrepancy measure $D(\cdot||\cdot)$ has multiple candidates. For a comprehensive review, please refer to (Levine et al. (2020)). Built upon this basic paradigm (i.e., Eq. (32)), we introduce some practical and representative offline RL algorithms that focus on addressing the issue of OOD actions.

Policy constraint methods, such as AWR (Peng et al. (2019b)) and AWAC (Nair et al. (2020)), choose the KL-divergence as the discrepancy measure, for which the policy improvement step in Eq. (32) has a closed-form solution:

$$\begin{aligned} \pi_{k+1} &= \arg\max_{\pi} \mathbb{E}_{s\sim D_\mu}\left[\mathbb{E}_{a\sim\pi(\cdot|s)} Q^\pi_{k+1}(s,a) - \lambda(D_{KL}(\pi(\cdot|s)||\mu(\cdot|s)) - \epsilon)\right] \\ \Rightarrow \pi_{k+1}(a|s) &= \mu(a|s)\exp\left(Q^\pi_{k+1}(s,a)/\lambda\right)/Z(s) \end{aligned} \tag{33}$$

In this expression, $1/Z(s)$ serves as the normalization factor across all possible action choices at state s; λ is the Lagrangian multiplier to convert the original constrained optimization problem to an unconstrained one, typically set as a constant rather than being optimized. In practice, such an policy can be acquired through weighted supervised learning from D_μ, where $\exp\left(Q^\pi_{k+1}(s,a)\right)$ serves as the weight for (s,a). Offline RL algorithms based on diffusion models typically adhere to policy constraint methods. Therefore, we will provide further details on policy constraint methods in Section 7.2.

Policy penalty methods, such as BRAC (Wu et al. (2019)), utilize approximated KL-divergence $\widehat{D}_{KL}(\pi(\cdot|s)||\mu(\cdot|s)) = \widehat{\mathbb{E}}_{a\sim\pi(\cdot|s)}\left[\log\pi(a|s) - \log\hat{\mu}(a|s)\right]$, where $\hat{\mu}$ is learned via Behavioral Cloning from D_μ to estimate μ and $\widehat{\mathbb{E}}$ denotes the estimated expectation via Monte Carlo sampling, and modify the reward function as $\tilde{r}(s,a) = r(s,a) - \lambda\widehat{D}_{KL}(\pi(\cdot|s)||\mu(\cdot|s))$ ($\lambda > 0$). In this way, the deviation from μ is implemented as a penalty term in the reward function for the policy learning to avoid deviating from μ not just in the current step but also in future steps. This method is usually implemented in its equivalent form (Wu et al. (2019)) as below:

$$\begin{aligned} Q^\pi_{k+1} &= \arg\min_{Q} \mathbb{E}_{(s,a,r,s')\sim D_\mu}\left[Q(s,a) - \left[r + \gamma\left(\mathbb{E}_{a'\sim\pi_k(\cdot|s')} Q^\pi_k(s',a') - \lambda\widehat{D}_{KL}(\pi(\cdot|s')||\mu(\cdot|s'))\right)\right]\right]^2; \\ \pi_{k+1} &= \arg\max_{\pi} \mathbb{E}_{s\sim D_\mu}\left[\mathbb{E}_{a\sim\pi(\cdot|s)} Q^\pi_{k+1}(s,a) - \lambda\widehat{D}_{KL}(\pi(\cdot|s)||\mu(\cdot|s))\right]. \end{aligned} \tag{34}$$

One significant disadvantage of this approach is that it requires explicit estimation of the behavior policy, i.e., $\hat{\mu}$ and the estimation error could hurt the overall performance of this approach.

Support constraint methods, such as BCQ (Fujimoto et al. (2019)) and BEAR (Kumar et al. (2019)), propose to confine the support of the learned policy within that of the behavior policy to avoid OOD actions, because constraining the learned policy to remain close in distribution to the behavior policy, as in the previous two methods, can negatively impact the policy performance, especially when the behavior policy is substantially suboptimal. As an example, BEAR proposes to replace the discrepancy constraint in Eq. (32) with a support constraint: $\pi \in \{\pi' : \mathcal{S}\times\mathcal{A} \to [0,1] \mid \pi'(a|s) = 0 \text{ whenever } \mu(a|s) < \epsilon\}$ [6]. With such a support constraint, the target actions a' used in policy evaluation (i.e., the first equation in Eq. (32)), would all satisfy $\mu(a|s) \geq \epsilon$ and so are in-distribution actions, that is:

$$Q^\pi_{k+1} = \arg\min_{Q} \mathbb{E}_{(s,a,r,s')\sim D_\mu}\left[Q(s,a) - \left(r + \gamma\mathbb{E}_{a'\sim\pi_k(\cdot|s')\ s.t.\ \mu(a|s)\geq\epsilon} Q^\pi_k(s',a')\right)\right]^2 \tag{35}$$

Pessimistic value methods regularize Q-function directly to avoid overly optimistic values for OOD actions, as an alternative to imposing (support or distributional) constraints on the policy. As a representative, CQL (Kumar et al. (2020)) removes the policy constraint in Eq. (32) and modifies the policy evaluation process as below:

$$\begin{aligned} Q^\pi_{k+1} = \arg\min_{Q}\ & \mathbb{E}_{(s,a,r,s')\sim D_\mu}\left[Q(s,a) - \left(r + \gamma\mathbb{E}_{a'\sim\pi_k(\cdot|s')} Q^\pi_k(s',a')\right)\right]^2 + \\ & \lambda\left[\mathbb{E}_{s\sim D_\mu, a\sim\pi_k(\cdot|s)} Q(s,a) - \mathbb{E}_{(s,a)\sim D_\mu} Q(s,a)\right] \end{aligned} \tag{36}$$

Here, the second term (with $\lambda > 0$) can be viewed as a regularizer for the policy evaluation process, which minimizes Q-values under the being-learned policy distribution, i.e., $\pi_k(\cdot|s)$, and maximizes the Q-values for (s,a) within D_μ. Intuitively, this ensures that high Q-values are only assigned to in-distribution

[6] In practice, they use a sampled maximum mean discrepancy (MMD, Gretton et al. (2012)) between the being-learned policy and behavior policy to implement such a support constraint, of which the effectiveness is empirically justified.

actions. Suppose $\widehat{Q}^\pi = \lim_{k\to\infty} Q_k^\pi$ and define Q^π as the true Q-function for π, they theoretically prove that $\mathbb{E}_{a\sim\pi(\cdot|s)}\left[\widehat{Q}^\pi(s,a)\right] \leq \mathbb{E}_{a\sim\pi(\cdot|s)}\left[Q^\pi(s,a)\right],\ \forall s \in D_\mu$, with a high probability, when λ is large enough. Thus, this algorithm mitigates the overestimation issue with a theoretical guarantee. However, it tends to learn an overly conservative Q function [7].

3.1.2 An Overview of Applying VAEs in Offline Reinforcement Learning

A major use of VAEs for offline RL is to estimate the behavior policy from the offline data D_μ. Specifically, a CVAE (see Eq. (7) in Section 2.1) is adopted for this estimation:

$$\max_{\theta,\phi} \mathbb{E}_{(s,a)\sim D_\mu}\left[\mathbb{E}_{z\sim P_\phi(\cdot|a,s)}\left[\log P_\theta(a|z,s)\right] - D_{KL}(P_\phi(z|a,s)||P_\theta(z|s))\right] \tag{37}$$

Corresponding to Eq. (7), s and a here work as the condition variable c and data sample x, respectively. As introduced in Section 2.1, the objective above constitutes a lower bound for $\mathbb{E}_{(s,a)\sim D_\mu}\left[\log P_\theta(a|s)\right]$, i.e., the typical supervised learning objective. After training, actions at state s can be sampled from the estimated behavior policy $\hat{\mu}(\cdot|s)$ as: $z \sim P_\theta(\cdot|s), \hat{a} \sim P_\theta(\cdot|s,z)$. In practice, the reconstruction term $\log P_\theta(a|z,s)$ can be replaced with $-||a-\hat{a}||_2^2$ for continuous action spaces, and the prior $P_\theta(z|s)$ can simply be chosen as $\mathcal{N}(z|0,I)$. Following the β-VAE (i.e., Eq. (5)), a factor $\beta > 0$ is usually introduced as the weight of the KL term in Eq. (37) to balance the two objective terms.

With the estimated behavior policy $\hat{\mu}$, the policy penalty and support constraint offline RL methods introduced in Section 3.1.1 can be naturally applied. As a representative of support constraint methods, **BCQ** (Fujimoto et al. (2019)) trains such $\hat{\mu}$ and defines the policy to learn based on $\hat{\mu}$ as $\pi(\cdot|s) = \hat{a} + \xi(\cdot|s,\hat{a})$, where $\hat{a}$ is a sample from $\hat{\mu}(\cdot|s)$ and $\xi(\cdot|s,\hat{a})$ is a **bounded** and learnable residual term. π is trained to maximize the approximated Q-values as in standard RL [8]. In this way, the action support of π is constrained to be close to the behavior policy's. Furthermore, inspired by (Shamir (2018)), **AQL** (Wei et al. (2021)) proposes to improve the estimation for the behavior policy μ using a residual generative model $W_1(W_2 G(s) + \hat{a})$, where $W_{1,2}$ and $G(\cdot)$ constitute a residual network and $\hat{a} \sim \hat{\mu}(\cdot|s)$ is used as a residul term. They claim that such a residual structure could effectively reduce the estimation error (compared with using $\hat{a}$) for the behavior policy μ.

Regarding the benefits of using a VAE as the policy network, compared to feedforward networks composed solely of fully-connected layers, VAEs excel at capturing the multiple modalities present in D_μ, which could be collected by a diverse set of policies, by utilizing the latent variable z. Also, the action generation process, $z \sim \mathcal{N}(0,I)$ and $a \sim P_\theta(\cdot|s,z)$, allows for stochastic action sampling. Compared to other deep generative models, VAEs may be less expressive but are more lightweight than normalizing flows and diffusion models and can provide more stable training than GANs.

Based on these background knowledge, we provide a review of VAE-based offline RL algorithms in the following subsections, with a particular focus on works whose primary novelty lies in the use of VAEs. One category of such algorithms seeks to enhance aforementioned offline RL algorithms via the use of VAEs. They either modify the learning objective to further mitigate the issue of OOD actions, or apply augmentation/conversion to the offline data for improved learning. The other category concentrates on extended offline RL setups, such as hierarchical or multi-task offline RL, leveraging the fact that the latent variable z can be learned as embeddings for tasks or subgoals/subtasks within a task. Consequently, $P_\theta(a|s,z)$ can be interpreted as a task-conditioned policy (for multi-task RL) or a subtask-conditioned policy within a hierarchical policy structure (for hierarchical RL).

[7] According to Theorem 3.2 in (Kumar et al. (2020)), the minimum value of λ is linked to $\max_{s\in D_\mu} \frac{1}{\sqrt{|D_\mu(s)|}}$, where $|D_\mu(s)|$ denotes the frequency of state s in D_μ. Given that D_μ's coverage could be limited and certain states would have low visitation frequencies, this can result in a high value of λ. However, as shown in Eq. (36), this same λ value is used in the Q-update for every state, potentially leading to underestimation for other states in D_μ.

[8] For BCQ, multiple Q functions are learned simultaneously, and the target value for policy evaluation is specifically designed based on these Q functions, which is though not our focus. Please refer to (Fujimoto et al. (2019)) for the details.

3.1.3 Addressing the Issue of Out-of-Distribution Actions Using VAEs

As introduced in Section 3.1.1, there are four categories of algorithms for mitigating the issue of OOD actions. VAEs have been used to improve three categories among them, which are detailed as follows.

Applying support constraints: PLAS (Zhou et al. (2020)) proposes that the support constraint can be simply applied to the latent space of a VAE. In particular, they first estimate the behavior policy as a CVAE $\hat{\mu}$ with Eq. (37). Ideally, after training, for latent variables z which have high probabilities under $P_\theta(z|s)$, the corresponding decoder $P_\theta(a|s,z)$ should output high-probability actions under the behavior policy distribution (i.e., in-distribution actions), since $\mu(a|s)$ is estimated as $\int P_\theta(z|s)P_\theta(a|s,z)\ dz$. In this case, they learn a latent space policy $\pi(z|s)$ and use it in conjunction with the pretrained (and fixed) decoder $P_\theta(a|s,z)$ as the mapping from s to a. The output of π is constrained to $[-\sigma,\sigma]$, i.e., the high probability area of the prior distribution $\mathcal{N}(z;0,I)$, to ensure that $(P_\theta \circ \pi)(a|s)$ outputs in-distribution actions. As introduced in Section 5.2, NF-based offline RL algorithms adopt the same algorithm idea. **SPOT** (Wu et al. (2022)) suggests that the constraint in BEAR (equivalently for a deterministic policy, $\log \mu(\pi(s)|s) \geq \epsilon, \forall s \in D_\mu$) can be relaxed to $\mathbb{E}_{s\sim D_\mu}\left[\log \mu(\pi(s)|s)\right] \geq \epsilon'$ for practicality. Then, the constrained policy improvement step (i.e., the second equation in Eq. (32)) can be converted to: (We use π and Q to represent the policy and Q function from now on, for simplicity.)

$$\max_\pi \mathbb{E}_{s\sim D_\mu}\left[Q(s,\pi(s)) + \lambda(\log \mu(\pi(s)|s) - \epsilon')\right] \tag{38}$$

Here, $\lambda > 0$ is the Lagrangian multiplier. Again, they explicitly model μ as a CVAE $\hat{\mu} = (P_\phi, P_\theta)$ and propose to approximate $\log \mu(a|s)$ as below: $(z^{(l)} \sim P_\phi(\cdot|s,a),\ l = 1,\cdots,L.)$

$$\log \mu(a|s) \approx \log P_\theta(a|s) = \log \mathbb{E}_{z\sim P_\phi(\cdot|s,a)}\left[\frac{P_\theta(a|s,z)P_\theta(z|s)}{P_\phi(z|s,a)}\right] \approx \log\left[\frac{1}{L}\sum_{l=1}^{L}\frac{P_\theta(a|s,z^{(l)})P_\theta(z^{(l)}|s)}{P_\phi(z^{(l)}|s,a)}\right] \tag{39}$$

As introduced in Section 2.3, normalizing flows enable exact density estimation, which can potentially eliminate the need for sample-based approximations as in Eq. (39).

Applying policy penalty: TD3-CVAE (Rezaeifar et al. (2022)) proposes to replace the penalty term in Eq. (34) (i.e, $\widehat{D}_{KL}(\pi(\cdot|s)||\mu(\cdot|s))$) with a prediction error $b(s,a) = ||a - P_\theta \circ P_\phi(s,a)||$, where $\hat{\mu} = (P_\phi, P_\theta)$ is the pretrained CVAE for estimating μ. Intuitively, if an action a from the being-learned policy $\pi(\cdot|s)$ corresponds to a high prediction error under $\hat{\mu}(\cdot|s)$, a is probably an OOD action and so (s,a) should be assigned with a high penalty. Further, they theoretically show the equivalence (under certain conditions) of $b(s,a)$ and a KL-divergence penalty term $D_{KL}(\pi(\cdot|s)||\pi_b(\cdot|s))$, where $\pi_b(\cdot|s) = \text{SoftMax}(-b(s,\cdot)/\tau)$ and $\tau > 0$ is a temperature parameter. Compared with $\widehat{D}_{KL}(\pi(\cdot|s)||\mu(\cdot|s))$, $b(s,a)$ is easier to approximate and brings superior empirical performance. **BRAC+** (Zhang et al. (2021a)) points out that estimating the penalty term $D_{KL}(\pi(\cdot|s)||\mu(\cdot|s))$ as $\widehat{D}_{KL}(\pi(\cdot|s)||\mu(\cdot|s))$ in BRAC requires generating a large number of samples to reduce the estimation variance. Therefore, they propose an upper bound for $D_{KL}(\pi(\cdot|s)||\mu(\cdot|s))$, which has an analytical form:

$$\begin{aligned}
&D_{KL}(\pi(\cdot|s)||\mu(\cdot|s)) \approx \mathbb{E}_{a\sim\pi(\cdot|s)}\left[\log \pi(a|s) - \log \hat{\mu}(a|s)\right] \\
&\leq \mathbb{E}_{a\sim\pi(\cdot|s)}\left[\log \pi(a|s)\right] - \mathbb{E}_{a\sim\pi(\cdot|s)}\left[\mathbb{E}_{z\sim P_\phi(\cdot|s,a)}\left[\log P_\theta(a|s,z)\right] - D_{KL}(P_\phi(z|s,a)||P_\theta(z|s))\right] \\
&= \mathbb{E}_{a\sim\pi(\cdot|s),z\sim P_\phi(\cdot|s,a)}\left[\log \pi(a|s) - \log P_\theta(a|s,z)\right] - \mathbb{E}_{a\sim\pi(\cdot|s)}\left[D_{KL}(P_\phi(z|s,a)||P_\theta(z|s))\right]
\end{aligned} \tag{40}$$

Here, the inequality is based on the fact that a CVAE $\hat{\mu} = (P_\phi, P_\theta)$ is used to estimate μ and $\mathbb{E}_{z\in P_\phi(\cdot|s,a)}\left[\log P_\theta(a|s,z)\right] - D_{KL}(P_\phi(z|s,a)||P_\theta(z|s))$ constitutes a variational lower bound for $\log \hat{\mu}(a|s)$, as shown in Eq. (7). Given that $P_\theta(a|s,z)$, $P_\theta(z|s)$, and $P_\phi(z|s,a)$ all have Gaussian outputs and suppose that the policy $\pi(a|s)$ is also Gaussian, then both $\log \pi(a|s) - \log P_\theta(a|s,z)$ and $D_{KL}(P_\phi(z|s,a)||P_\theta(z|s))$ have analytical forms, which can reduce the sample variance. However, sampling for a and z is still required.

Applying pessimistic values: CPQ (Xu et al. (2022a)) extends the idea of CQL to safe RL, where the policy is trained to maximize its Q-values while minimizing the accumulative cost $Q_c(s,a) = c(s,a) + \mathbb{E}_{s',a'\sim\pi(\cdot|s')}[Q_c(s',a')]$. In particular, they train the cost Q-function Q_c to assign high costs to OOD actions,

such that, by constraining Q_c as in standard safe RL algorithms, OOD actions can be avoided at the same time. To realize this, the objective for Q_c is designed as below, which is similar in form with Eq. (36):

$$\min_{Q_c} \mathbb{E}_{(s,a,c,s')\sim D_\mu} \left[Q_c(s,a) - \left(c + \gamma \mathbb{E}_{a'\sim\pi(\cdot|s')} Q_c(s',a')\right)\right]^2 - \lambda \mathbb{E}_{s\sim D_\mu, a\sim\tilde{\mu}(\cdot|s)} Q_c(s,a) \tag{41}$$

Here, $\tilde{\mu}$ is defined based on $\hat{\mu} = (P_\phi, P_\theta)$. In particular, $\forall a \sim \tilde{\mu}(\cdot|s),\ D_{KL}(P_\phi(z|s,a)||P_\theta(z|s)) \geq d$, where $P_\theta(z|s) = \mathcal{N}(z; 0, I)$ and d is a predefined threshold. Intuitively, $\tilde{\mu}(\cdot|s)$ produces OOD actions a of which the corresponding posterior distribution $P_\phi(z|s,a)$ deviates significantly with its training target $P_\theta(z|s)$. **MCQ** (Lyu et al. (2022)) explores mild but enough conservatism for offline RL to mitigate the underestimation issue of CQL. Their algorithm's design does not hinge on VAEs; instead, the VAE is employed solely for estimating μ as in previous works, so we do not provide details here. For similar reasons, we skip introductions of **UAC** (Guan et al. (2023)) and **O-RAAC** (Urpí et al. (2021)), both of which can be considered as extensions of BCQ, a support constraint method.

3.1.4 Data Augmentation and Transformation with VAEs

Data augmentation: The provided offline data D_μ may have limited coverage of the state-action space or lack diversity in behavioral patterns. Consequently, constraint- or pessimism-based algorithms may learn sub-optimal policies with limited generalization capabilities in the entire environment. In this case, VAEs have been used for data augmentation, aiming at improving the coverage or diversity of the offline data. (1) **ROMI** (Wang et al. (2021)) is a model-based data augmentation strategy utilizing reverse rollouts. They first learn the backward dynamic model $\widehat{\mathcal{T}}_{\text{rev}}(s|s',a)$, reward model $\hat{r}(s,a)$, and reverse policy $\hat{\mu}_{\text{rev}}(a|s')$ from D_μ via simple supervised learning, where s' denotes the next state. Specifically, $\hat{\mu}_{\text{rev}}(a|s')$ is modeled with a CVAE (P_ϕ, P_θ), and its training objective is the same as Eq. (37) but to replace s with s'. With a random sample s_{t+1} from D_μ, a reverse rollout (of length h) can be generated as below:

$$\left[(s_{t-i}, a_{t-i}, r_{t-i}, s_{t+1-i}) \mid a_{t-i} \sim \hat{\mu}_{\text{rev}}(\cdot|s_{t+1-i}), s_{t-i} \sim \widehat{\mathcal{T}}_{\text{rev}}(\cdot|s_{t+1-i}, a_{t-i}), r_{t-i} \sim \hat{r}(s_{t-i}, a_{t-i})\right]_{i=0}^{h-1} \tag{42}$$

Unlike the forward generation process, such a reverse manner prevents rollout trajectories that end in OOD states. Also, the CVAE makes it possible for stochastic inference: $z \sim \mathcal{N}(0, I), a \sim P_\theta(\cdot|s', z)$, which improves the diversity. These generated rollouts are then combined with D_μ for the use of offline RL. This work is closely related to offline model-based RL, which is another important branch of offline RL and mainly introduced in Section 4.2. (2) To enable the learned policy to generalize to OOD states, **SDC** (Zhang et al. (2022)) suggests training the policy on perturbed states and motivating it to revert to in-distribution states from any state deviations. In particular, a forward dynamic model $\widehat{\mathcal{T}}(s'|s,a)$ and a CVAE-based state transition model $\widehat{U}(s'|s)$ is learned from D_μ through supervised learning. At a state $\tilde{s}$ perturbed from s, the policy π is trained to minimize MMD $\left(\widehat{\mathcal{T}}(\cdot|\tilde{s}, \pi(\cdot|\tilde{s}))||\widehat{U}(\cdot|s)\right)$, i.e., to produce actions that can lead it back to the next state s' in the original trajectory from the perturbation $\tilde{s}$. MMD denotes the maximum mean discrepancy. (3) Han & Kim (2022) point out that the latent space of a VAE pretrained on D_μ can capture the data distribution in D_μ. Based on that, they suggest selectively augmenting the data region that is sparse in the original dataset through data generation with the VAE. However, that paper does not provide details on training the VAE or measuring sparsity through the latent space. (4) **KFC** (Weissenbacher et al. (2022)) suggests inferring symmetries (Hambidge (1967)) of the underlying dynamics of an environment using a VAE forward prediction model, and applying such symmetry transformations to generate new data points as data augmentation. This work requires extensive knowledge of control theory, so it will not be discussed in depth here.

Data conversion: VAEs have been used to transform the states or actions in the offline dataset to simplify the learning task. Here, we present two notable works in this direction. When the state space is very high-dimensional (e.g., images), directly applying offline RL to the raw data may be challenging. Thus, Rafailov et al. (2021) propose using VAEs to get compact representations z of high-dimensional states s to improve the learning efficiency. z effectively represents s, since the VAE is trained to reconstruct s from z while adhering to variational regulations (i.e., the KL term in Eq. (2)). However, this data conversion manner is not specific to VAEs, and other generative models with an encoder-decoder structure, such as

the normalizing flows and transformers, could potentially be employed for this purpose. On the other hand, **SAQ** (Luo et al. (2023)) proposes to convert continuous actions to discrete ones, to make it significantly simpler to implement constraint/regulation-based offline RL methods. To realize this, they train a VQ-VAE (introduced in Section 2.1) on D_μ, which can map a continuous action a at a given state s to a discrete variable $\tilde{a}$ (through its encoder) for training and map a given discrete variable back to the original action space (with its decoder) for evaluation. This state-conditioned action discretization scheme is learned by:

$$\max_{\theta,\phi,e_{1:k}} \mathbb{E}_{(s,a)\sim D_\mu} \left[\log P_\theta(a|e_i) - ||\text{sg}\left[P_\phi(s,a)\right] - e_i||_2^2 - \beta||P_\phi(s,a) - \text{sg}\left[e_i\right]||_2^2\right] \tag{43}$$

Here, $e_{1:k}$ is the codebook and represents the k discretized actions; $i = \arg\min_j ||P_\phi(s,a) - e_j||_2$ is the index of the nearest action latent for the embedding $P_\phi(s,a)$. Applying the pretrained VQ-VAE encoder P_ϕ on D_μ leads to discretized actions, i.e., $(s,a) \to (s, e_i)$. For discrete action spaces, the estimation of the constraint terms in offline RL, such as the approximated behavior policy $\hat{\mu}(\tilde{a}|s)$ and KL divergence $\widehat{D}_{KL}(\pi(\tilde{a}|s)||\mu(\tilde{a}|s))$, could be easier and more accurate.

3.1.5 Offline Multi-task/Hierarchical RL based on VAEs

Multi-task RL and hierarchical RL extend the basic RL setting. In particular, multi-task RL (Sodhani et al. (2021)) aims at learning a policy that can be directly applied to or quickly adapted to a distribution of tasks. Hierarchical RL, on the other hand, learns a hierarchical (two-level) policy for complex, long-horizon tasks which can usually be decomposed into a sequence of subtasks. In this case, low-level policies can be used to accomplish each subtask, while the high-level policy coordinates the subtasks and the use of low-level policies. For example, in goal-achieving tasks, a goal-conditioned policy can be considered a multi-task policy, as it can reach multiple goals in an environment by changing the goal condition. However, if the goal is distant, the entire path might be divided into several subgoals by the high-level policy, and to reach each subgoal, a corresponding low-level (subgoal-conditioned) policy can be employed.

Next, we formally introduce these two setups — multi-task RL and hierarchical RL — and explore how VAEs can be utilized to enhance them. By providing detailed introductions of the most notable research in each category, such as BOReL for multi-task RL and OPAL & HiGoC for hierarchical RL, our aim is to present the fundamental paradigms as a brief tutorial for these specific research directions.

Multi-task RL: Given a multi-task offline dataset $D_\mu^M = [[\tau^{i,j} = (s_0^{i,j}, a_0^{i,j}, r_0^{i,j}, \cdots, s_T^{i,j})]_{i=1}^N]_{j=1}^M$, where i and j are the indexes for the trajectory and task respectively, offline multi-task RL aims at learning a multi-task policy that can be adapted to unseen tasks with zero- or few-shot training. The testing tasks are required to be in the same distribution as the training ones. As a representative, **BOReL** (Dorfman et al. (2021)) is proposed for the case where the reward and dynamic function $(r_j, \mathcal{T}_j)$ vary with the task. To train a multi-task policy, a straightforward manner is to condition that policy on the task information $(r_j, \mathcal{T}_j)$. In particular, they adopt the latent variable z [9] of a CVAE as a representation of the reward and dynamic function, and learns a latent-conditioned policy $\pi(a|s,z)$ as the multi-task policy. To this end, the CVAE is trained as follows:

$$\begin{aligned}
&\max_{\theta,\phi} \sum_{t=0}^{T-1} \text{ELBO}_t,\ \text{ELBO}_t = \mathbb{E}_{z\sim P_\phi(\cdot|\tau_{0:t})}\left[\log P_\theta(s_{0:T}, r_{0:T-1}|z, a_{0:T-1}) - D_{KL}(P_\phi(z|\tau_{0:t})||P_\theta(z))\right], \\
&\log P_\theta(s_{0:T}, r_{0:T-1}|z, a_{0:T-1}) = \log P_\theta(s_0|z) + \sum_{t=0}^{T-1}\left[\log P_\theta(s_{t+1}|s_t, a_t, z) + \log P_\theta(r_t|s_t, a_t, s_{t+1}, z)\right]
\end{aligned} \tag{44}$$

In this context, $\tau_{0:T} = (s_{0:T}, r_{0:T-1}, a_{0:T-1})$; $a_{0:T-1}$ and $(s_{0:T}, r_{0:T-1})$ can be viewed as c and x in the CVAE framework. As shown in (Zintgraf et al. (2020)), ELBO_t constitutes a variational lower bound for $\log P_\theta(s_{0:T}, r_{0:T-1}|a_{0:T-1})$. The second equation in Eq. (44) is derived based on the Markov assumption (Puterman (2014)), and it can be observed from this equation that z is trained to embed information regarding the initial state distribution, reward and dynamic functions, so as to reconstruct the whole task-specific trajectory $\tau_{0:T}$. Subsequently, the pretrained $P_\phi(z|\tau_{0:t})$, which is implemented as a recurrent neural

[9] Actually, they adopt the mean and variance of the latent variable (i.e., the output of the encoder) as the policy conditioner.

Algorithm	VAE Type	VAE Usage	Evaluation Task
BCQ	CVAE	Estimating μ (Support Constraint)	MuJoCo
AQL	CVAE	Estimating μ (Improved Estimation for μ)	D4RL (L)
PLAS	CVAE	Estimating μ (Support Constraint)	D4RL (L, A, K), Real Robot
SPOT	CVAE	Estimating μ (Support Constraint)	D4RL (L, M)
TD3-CVAE	CVAE	Providing prediction errors (Policy Penalty)	D4RL (L, A)
BRAC+	CVAE	Estimating μ and $D_{KL}(\pi(a\|s)\|\|\mu(a\|s))$ (Policy Penalty)	D4RL (L)
CPQ	β-CVAE	Estimating μ and using the latent space for OOD detection (Pessimistic Value)	MuJoCo
MCQ	CVAE	Estimating μ (Pessimistic Value)	D4RL (L)
UAC	CVAE	Estimating μ (Support Constraint)	D4RL (L, M, A)
O-RAAC	β-CVAE	Estimating μ (Support Constraint)	D4RL (L)
ROMI	CVAE	Estimating the reverse behavior policy $\mu_{\text{rev}}(a\|s')$ (Data Augmentation)	D4RL (L, M, M2d)
SDC	CVAE	Estimating the state transition model $U(s'\|s)$ of D_μ (Data Augmentation)	GridWorld, D4RL (L)
KFC	VAE	Modelling $U(s'\|s)$ for inference of dynamic symmetries (Data Transformation)	D4RL (L, M, A, K), MetaWorld, RoboSuite
SAQ	VQ-VAE	Discretizing the action space to simplify the learning (Data Conversation)	D4RL (L, M, A, K), Robomimic
BOReL	CVAE (T)	Embedding MDPs for Multi-task RL	GridWorld, Meta-MuJoCo
OPAL	β-CVAE (T)	Embedding skills for Hierarchical RL	D4RL (M, K)
TACO-RL	CVAE (T)	Embedding skills for Hierarchical RL	CALVIN, Real Robot
HiGoC	CVAE	Generating subgoals (Hierarchical RL)	D4RL (M), CARLA
FLAP	CVAE	Generating subgoals (Hierarchical RL)	Real Robot

Table 1: Summary of VAE-based offline RL algorithms. In Column 1, we list representative (but not all) algorithms in this section. These algorithms are grouped by their categories. Regarding the VAE types, β-CVAE refers to an integration of CVAE and β-VAE, where a weight β is added to the KL term in CVAE. The annotation (T) means that the VAE is implemented on trajectories rather than individual state transitions. The evaluation tasks are listed in Column 4. Most works are evaluated on D4RL (Fu et al. (2020)), which provides offline datasets for various tasks, including Locomotion (L), AntMaze (M), Adroit (A), Kitchen (K), Maze2d (M2d), etc. MuJoCo (Todorov et al. (2012)) and CARLA (Dosovitskiy et al. (2017)) are commonly-used simulators for robotic and self-driving tasks, respectively. Meta-MuJoCo (Dorfman et al. (2021)) is a multi-task version of MuJoCo. By Real Robot, we mean evaluations on real robotic platforms, which vary from one study to another. For other benchmarks, we provide their references here: GridWorld (Zintgraf et al. (2020)), MetaWorld (Yu et al. (2019c)), RoboSuite (Zhu et al. (2020)), Robomimic (Mandlekar et al. (2021a)), CALVIN (Mees et al. (2022b)).

network as in VRNN (see Section 2.1), can be applied to D_μ to infer the task embedding z_t at each time step, leading to a dataset of transitions in the form $((s_t, z_t), a_t, r_t)$. Note that (s_t, z_t) can be viewed as an extended state $\tilde{s}_t$, and thus standard offline RL algorithms can then be directly applied to this dataset to learn a latent-conditioned policy $\pi(a_t|(s_t, z_t))$.

Hierarchical RL: This category of algorithms try to learn a hierarchical policy $(\pi_{\text{high}}(z|s), \pi_{\text{low}}(a|s, z))$ from the offline dataset. Intuitively, the agent would segment the whole task into a sequence of subtasks or subgoals, each of which is denoted by a (continuous or discrete) variable z and accomplished by a corresponding subpolicy/skill $\pi_{\text{low}}(a|s, z)$. This hierarchical scheme is especially beneficial for complex tasks with long horizons. **OPAL** (Ajay et al. (2021)) is a representive algorithm in this direction. They define the horizon of each skill to be h and organize the offline data as a set of trajectory segments $D_\mu = [\tau^i = [s^i_{0:h-1}, a^i_{0:h-1}]]_{i=1}^N$.

Then, they learn the low-level policy π_{low} for different subtasks z as the decoder of a CVAE:

$$\max_{\theta,\phi} \mathbb{E}_{\tau\sim D_\mu}\left[\mathbb{E}_{z\sim P_\phi(\cdot|\tau)}\left[\sum_{t=0}^{h-1}\log\pi_\theta(a_t|s_t,z)\right]-\beta D_{KL}(P_\phi(z|\tau)||P_\theta(z|s_0))\right],\ \pi_{\text{low}}\triangleq\pi_\theta \tag{45}$$

This objective is equivalent to a (β-)CVAE ELBO, where s_0 and τ work as the conditioner c and data x respectively [10]. However, unlike Eq. (37), here π_θ is trained on sets of trajectory segments rather than single-step transitions. This is because, as a skill, π_θ is expected to extend temporally, for example, lasting for h time steps after being selected. Also, the prior $P_\theta(z|s)$ is not fixed but implemented as a neural network that takes s_0 as input, to make sure the skill choice z is predictable (by the high-level policy $\pi_{\text{high}}(z|s)$) given only the initial state s_0. Applying the pretrained $P_\phi(z|\tau)$ on D_μ and introducing the reward signals, a new dataset $D_\mu^{\text{high}}=(s_0^i,z^i\sim P_\phi(\cdot|\tau^i),\sum_{t=0}^{h-2}r_t^i,s_{h-1}^i)_{i=1}^N$ can be obtained for training $\pi_{\text{high}}(z|s)$ with any offline RL methods. With this hierarchical policy $(\pi_{\text{high}},\pi_{\text{low}})$, the decision horizon of offline RL is effectively shorten (by a factor of h) and so OOD actions caused by the accumulated distribution shift can be mitigated. Rosete-Beas et al. (2022) propose **TACO-RL**, which is a very similar algorithm with OPAL but specifically tailored for goal-achieving tasks. **HiGoC** (Li et al. (2022)) is also a hierarchical framework for goal-achieving tasks, where the high-level part is a model-based planner [11] for generating the subgoal list and the low-level part is a goal-conditioned policy trained by offline RL to reach each subgoal sequentially. The subgoals are not labeled in the dataset, so the low-level policy is trained in an unsupervised manner. Specifically, for $\pi_{\text{low}}(a_{t_1}|s_{t_1},s_{t_2})$, s_{t_2} $(t_2>t_1)$ is the subgoal and randomly sampled from states after s_{t_1} in the same trajectory. To be robust to possible OOD subgoals during evaluation, a CVAE $m(s_t|s_{t-h})=(P_\phi(z|s_t,s_{t-h}),P_\theta(s_t|z,s_{t-h}))$ is pretrained on D_μ for generating the subgoal s_t conditioned on the previous subgoal s_{t-h}, where h is a predefined time interval for subgoal selections. With this CVAE, a perturbed subgoal can be generated based on the sampled one (i.e., s_{t_2}) as $P_\theta(P_\phi(s_{t_2},s_{t_2-h})+\epsilon,s_{t_2-h})$ (ϵ is a noise vector), which can replace s_{t_2} as the subgoal of π_{low} for robustness. In cases of high-dimensional states, such as images, adding noise to a well-defined low-dimensional embedding space (from VAEs) is a more effective and reasonable approach. Further, it's noteworthy that the pretrained decoder $P_\theta(s_t|z,s_{t-h})$ can also be used for high-level planning. Specifically, a subgoal list can be generated from the initial state s_0 by specifying a list of latent variables $z_{1:k}$: $s_{t_i}\sim P_\theta(\cdot|z_i,s_{t_i-h}),\ i\in[1,\cdots,k]$. Such a list can then be evaluated by task-relevant objectives. In this case, searching for an optimal list $z_{1:k}$ is literally a model predictive planning problem and is more efficient than directly searching on the high-dimensional state space, i.e., the list of subgoals. **FLAP** (Fang et al. (2022)) adopts a quite similar protocol with HiGoC, where the CAVE m is referred to as the affordance model.

3.2 Imitation Learning

In this section, we offer an overview of VAE-based IL algorithms. First, we provide a tutorial-like overview of the four schemes of VAE-based IL. Based on this, we introduce a categorization of all related works based on how VAEs are utilized. The use of VAEs focuses on enhancing Behavioral Cloning, either from a data or algorithmic perspective. To conclude, we include a table summarizing the representative algorithms.

3.2.1 Core Schemes of VAE-based Imitation Learning

Imitation Learning (IL) aims at recovering the expert policy $\pi(a|s)$ from a set of demonstrations D_E. Behavioral Cloning (BC) is a straightforward and widely-used IL framework (Pomerleau (1991)), which implements imitation by supervised learning: $\max_\pi \mathbb{E}_{(s,a)\sim D_E}\log\pi(a|s)$. With its special encoder-decoder structure, the VAE has been utilized to improve BC from multiple perspectives. As a summary, here we provide the four schemes of VAE-based IL.

[10] For a standard CVAE, the reconstruction term should be $\log P_\theta(\tau|s_0,z)=\sum_{t=0}^{h-1}\log\pi_\theta(a_t|s_t,z)+\sum_{t=0}^{h-2}\log\mathcal{T}(s_{t+1}|s_t,a_t)$. However, the transition function $\mathcal{T}$ is not trainable and so would not influence the gradient calculation.

[11] Please refer to (Li et al. (2022)) for further details.

Scheme (1): Similar with the major use of VAE for offline RL (as introduced in Section 3.1.1), a CVAE conditioned on the state can be directly used to model the expert policy:

$$\max_{\theta,\phi} \mathbb{E}_{(s,a)\sim D_E} \left[\mathbb{E}_{z\sim P_\phi(\cdot|s,a)} \log P_\theta(a|s,z) - D_{KL}(P_\phi(z|s,a)||P_\theta(z|s))\right] \tag{46}$$

As introduced in Section 2.1, this objective constitutes a variational lower bound for $\mathbb{E}_{(s,a)\sim D_E} \log \pi(a|s)$, i.e., the BC objective. After training, $z \sim P_\theta(\cdot|s), a \sim P_\theta(\cdot|s,z)$, where $P_\theta(z|s)$ is a predefined prior and usually set as $\mathcal{N}(z;0,I)$, can be used as the policy $a \sim \pi(\cdot|s)$. With the latent variable, the VAE-based policy can model stochastic behaviors with diverse modes. Theoretically, $\pi(a|s) = \int P_\theta(a|s,z)P_\theta(z|s)dz$. Rather than using a fixed prior distribution $P_\theta(z|s)$, Ren et al. (2020) propose an algorithm to fine-tune the prior online for specific tasks by optimizing a generalization bound from the PAC-Bayes theory.

Scheme (2): The second scheme is based on representation learning (RepL), where the latent variable z is adopted as a representation of the state s and usually can be learned via state reconstructions:

$$\max_{\theta,\phi} \mathbb{E}_{s\sim D_E} \left[\mathbb{E}_{z\sim P_\phi(\cdot|s)} \mathrm{Rec}_\theta(s,z) - D_{KL}(P_\phi(z|s)||P_\theta(z))\right], \ \max_{\pi} \mathbb{E}_{(s,a)\sim D_E, z\sim P_\phi(\cdot|s)} \log \pi(a|z) \tag{47}$$

where the reconstruction objective $\mathrm{Rec}_\theta(s,z) = \log P_\theta(s|z)$ or $-||s - P_\theta(z)||_2^2$. Note that the first objective in Eq. (47) is usually coupled with extra regularization terms to encourage the disentanglement of the learned representation, or enable the fusion of state inputs s from multiple modalities, etc. Based on the representation learning, a policy $\pi(a|z)$ conditioned on the compact representation z can be learned with any IL algorithm. Compared with s, z is in a lower dimension and is less noisy for decision making. As a result, RepL can effectively reduce the need of IL for large amounts of training data. In Eq. (47), there are in total three functions (besides $P_\theta(z)$ which may not be learnable): $P_\phi(z|s)$, $P_\theta(s|z)$, and $\pi(a|z)$. One manner is to pretrain $P_\phi(z|s)$ and $P_\theta(s|z)$ within the VAE framework and then train $\pi(a|z)$ with IL as shown in the second term of Eq. (47). When training π, the parameters of P_ϕ can either be frozen or not. The other manner is to jointly train the three functions through an integrated objective, i.e., adding the two objectives in Eq. (47) together with an adjustable weight λ. In this case, the state reconstruction with a VAE can be viewed as an auxiliary task for IL. **EIRLI** (Chen et al. (2021a)) provides a systematic empirical investigation of representation learning for imitation. They find that RepL using VAEs can effectively improve the performance of vision-based IL. However, they also mention that the relative impact of adding representation learning tends to be lower than the impact of adding or removing data augmentations. This may be because usual RepL techniques (for images) tend to capture the most visually salient axes of variation (e.g., the color, background, or objects) but the action choices are often determined by more fine-grained, local cues in the environment, which calls for RepL that is more specific to decision making. Additional examples in this category include (Lee et al. (2019); Rahmatizadeh et al. (2018)).

Scheme (3): VAEs can also be directly applied to expert trajectories $\tau = (s_0, a_0, \cdots, s_T)$ with the following objective:

$$\begin{gathered}\max_{\theta,\phi} \mathbb{E}_{\tau\sim D_E} \left[\mathbb{E}_{z\sim P_\phi(\cdot|\tau)} \left[\log P_\theta(\tau|z)\right] - D_{KL}(P_\phi(z|\tau)||P_\theta(z))\right], \\ \log P_\theta(\tau|z) = \log P_\theta(s_0|z) + \sum_{t=0}^{T-1} \left[\log P_\theta(a_t|s_t,z) + \log P_\theta(s_{t+1}|s_t,a_t,z)\right]\end{gathered} \tag{48}$$

The decomposition of $P_\theta(\tau|z)$ makes use of the MDP model, where the three terms correspond to the initial state distribution, policy distribution, and transition dynamic, respectively. $P_\theta(s_0|z)$ and $P_\theta(s_{t+1}|s_t,a_t,z)$, which may be independent of z, are usually defined within the simulator and not required to model, so $\log P_\theta(\tau|z)$ can be replaced with $\sum_{t=0}^{T-1} \log P_\theta(a_t|s_t,z)$ in the original objective. It's worthy noting that $P_\theta(\tau|z)$ has multiple alternative decomposition forms. For example, **T-VAE** (Lu et al. (2019)) proposes to model it as $\log P_\theta(s_{0:T}|z) + \log P_\theta(a_{0:T-1}|z, s_{0:T})$. Specifically, two RNNs are adopted to generate the state and action sequences respectively, leading to a new definition of $\log P_\theta(\tau|z)$: (The state sequence $\hat{s}_{0:T}$ is generated before the action sequence $\hat{a}_{0:T-1}$; the generation of $\hat{s}_t/\hat{a}_t$ is conditioned on $h_{t-1}^{\hat{s}}/h_{t-1}^{\hat{s},\hat{a}}$ which embeds the history $\hat{s}_{1:t-1}/(\hat{s}_{1:t-1}, \hat{a}_{1:t-1})$.)

$$\log P_\theta(\tau|z) = \sum_{t=0}^{T} \log P_\theta(s_t|z, h_{t-1}^{\hat{s}}) + \sum_{t=0}^{T-1} \log P_\theta(a_t|z, h_{t-1}^{\hat{s},\hat{a}}) \tag{49}$$

In this way, the whole trajectory can be predicted without interacting with the environment/simulator, which is necessary in certain scenarios. In this scheme, the embedding z is inferred from the entire trajectory τ, necessitating that the encoder P_ϕ be implemented with specialized architectures, such as encoder-only transformers (see Section 2.4) or RNNs (like VRNN in Section 2.1). Different from aforementioned two schemes, such a trajectory-conditioned encoder can output embeddings z that encapsulate information at the task or subtask level. Thus, the learned $P_\theta(a_t|s_t, z)$ can be viewed as a multi-task policy which varies with the task embedding z. As a side note, if replacing the decoder $P_\theta(\tau|z)$ with $P_\theta(\tau'|z)$, where $(\tau, \tau') \sim D_E$ are (state-only) expert trajectories and τ' is a future trajectory segment of τ, Eq. (48) can be used for training a trajectory forecasting model, as detailed in **RC-VAE** (Qi et al. (2020)). By using such a temporal target, i.e, the future segment, the representation z is forced to contain predictive information.

Scheme (4): The last scheme is based on the Variational Information Bottleneck (VIB) framework (Alemi et al. (2017)), of which the original objective function is as below:

$$\max_{f:X\to Y} I(Z, Y; f) \ s.t. \ I(X, Z; f) \leq I_c \Rightarrow \max_{f:X\to Y} I(Z, Y; f) - \beta I(X, Z; f) \tag{50}$$

where $I(\cdot)$ denotes the mutual information, I_c is the information constraint, and $\beta > 0$ is the Lagrangian multiplier. The goal of this framework is to learn an encoding Z that is maximally expressive about the target Y while being maximally compressive about the input X. Substituting X, Y with s, a, the function to learn, i.e., f, is then the expert policy $\pi(a|s)$. VIB-based IL can be practically solved by the following objective, which is a lower bound of Eq. (50) (see (Alemi et al. (2017))):

$$\max_{\phi,\theta,\omega} \mathbb{E}_{(s,a)\sim D_E} \left[\mathbb{E}_{z\sim P_\phi(\cdot|s)} \log P_\theta(a|z) - \beta D_{KL}(P_\phi(z|s)||P_\omega(z))\right] \tag{51}$$

This objective is similar with the VAE ELBO (i.e., Eq. (2)) in form but with two main differences. First, the decoder P_θ here can predict variables different from the input of the encoder, whereas in VAEs, it is typically trained to reconstruct the input variable. Second, $P_\omega(z)$ is not an assumed prior distribution of z as in VAEs but a variational approximation of the marginal distribution of z, i.e., $P_Z(z) = \int P_X(x)P_\phi(z|x)dx$, and it is usually learned as a neural network. Both Scheme (2) and Scheme (4) can be regarded as forms of imitation learning that incorporate effective representation learning. After the training, to sample an action $a \sim \pi(\cdot|s)$, the policy encoder first compresses the state to a representation, i.e., $z \sim P_\phi(\cdot|s)$, and then its decoder predicts the action based on z, i.e., $a \sim P_\theta(\cdot|z)$. When dealing with high-dimensional and noisy observations s, using an information bottleneck can filter out redundant information while retaining essential knowledge for action predictions in z. A higher compression rate on the input often results in better generalization of the learned policy across tasks.

Next, we provide an overview of the applications of VAEs in IL. Most works in this direction focus on extending BC. From a data perspective, VAEs can increase BC's data efficiency in scenarios where original, task-specific data is limited, or enable the use of multi-modal input data (e.g., from various sensor types). Regarding algorithmic advancements, VAEs have been utilized for skill discovery to enable hierarchical IL, and to address the causal misidentification issue inherent in BC.

3.2.2 Improving Data Efficiency in Imitation Learning with VAEs

IL, especially BC, requires a large amount of training data to cover possible task scenarios for robust performance. However, expert-level demonstrations for a specific task, i.e., D_E, are usually costly to acquire. Therefore, efficient data usage in IL is crucial. This can be achieved by leveraging the inherent structures within the data, or by gathering and processing task-related data from alternative sources for training. The capability of VAEs to extract latent representations plays a key role in facilitating these processes. Here, we present several notable works in this direction.

Behavior Retrieval (Du et al. (2023)) is proposed for the case where vast task-unlabelled demonstrations are available, i.e., D_{prior}. Specifically, D_{prior} may contain demonstrations for a range of different but related tasks (following the same task distribution) or suboptimal behaviors for the current task. To this end, they propose to adopt a β-VAE (i.e., (P_ϕ, P_θ) in Eq. (5)) to learn the latent representations of $(s, a) \sim D_{\text{prior}}$. Then, new training data that is similar with the ones in D_E can be retrieved from D_{prior} as the augmentation

D_{ret}. The similarity between data points can be simply measured based on their latents from the pretrained encoder P_ϕ:

$$f((s_1, a_1), (s_2, a_2)) = -\|z_1 - z_2\|_2,\ (s_1, a_1) \in D_{\text{prior}},\ (s_2, a_2) \in D_E,\ z_i \sim P_\phi(\cdot|(s_i, a_i)). \tag{52}$$

They claim that this method would effectively filter out sub-optimal or task-irrelevant data. As a final step, a policy $\pi(a|s)$ can be learned on $D_E \cup D_{\text{ret}}$ through BC. This whole protocol resembles aforementioned Scheme (2).

For robotic control tasks, state-only demonstrations from a third-person view (e.g., videos from a demonstrator) are usually more available than the ones in the first-person view. State observations from the first- and third-person views, i.e., s^F and s^T, correspond to the same true environment state s. Given a set of demonstrations synchronized across different viewpoints $[(s_i^F, s_i^{T_1}, \cdots, s_i^{T_k})]_{i=1}^N$, where $T_{1:k}$ denotes k different third-person viewpoints, a common viewpoint-agnostic representation is required to make full use of these data. To realize this, **VAE-TPIL** (Shang & Ryoo (2021)) proposes to learn two VAEs for the first- and third-person view data respectively, i.e., $(P_{\phi^F}, P_{\theta^F})$ and $(P_{\phi^T}, P_{\theta^T})$, and to disentangle the latent variable to a viewpoint embedding v and a viewpoint-agnostic state embedding h. To realize this, besides usual reconstruction objective terms, auxiliary objectives are involved: $(i \neq j,\ (h, v) \sim P_\phi(s))$

$$\mathcal{L}_v = \mathbb{E}_{s_i^T}\left[||P_\theta(h_i^T, v_j^T) - s_i^T||_2\right],\ \mathcal{L}_h = \mathbb{E}_{s^{T_i}}\left[||P_\theta(h^{T_j}, v^{T_i}) - s^{T_i}||_2\right],\ \mathcal{L}_F = \mathbb{E}_{s^T, s^F}\left[||h^T - \text{sg}(h^F)||_2\right] \tag{53}$$

The intuition behind these terms are: (a) The view embeddings v_i^T and v_j^T of states in the same view s_i^T and s_j^T should be semantically equivalent and so $P_\theta(h_i^T, v_j^T)$ should still recover s_i^T. (b) The embeddings h^{T_i} and h^{T_j} corresponding to the same state from different views T_i and T_j should be interchangeable for reconstructing s^{T_i}, since h is expected to be view-agnostic. (c) For the same reason, h^T and h^F should be similar as they correspond to the same true environment state. With the pretrained P_{ϕ^F} and P_{ϕ^T}, demonstrations across various viewpoints can be converted to viewpoint-agnostic latent representations (i.e., h). Then, a representation-based policy $\pi(a|h)$ can be learned with any IL method.

GIRIL (Yu et al. (2020b)) suggests modelling the underlying transition from (s_t, a_t) to s_{t+1} in D_E using a CVAE, where (s_t, a_t) and s_{t+1} work as the condition c and data sample x respectively, besides imitating the policy $\pi(a_t|s_t)$. Then, an intrinsic reward can be defined as $r_t = ||\hat{s}_{t+1} - s_{t+1}||_2^2$, where $\hat{s}_{t+1} \sim P_\theta(\cdot|s_t, a_t)$. (Offline) RL can be applied to the extended demonstrations $[(s_t, a_t, r_t, s_{t+1})]$ to further improve the imitator learned via BC, i.e., $\pi(a_t|s_t)$. Intuitively, this process encourages the agent to explore states with high prediction errors more to reduce the state uncertainty, making it possible to achieve better-than-expert performance.

3.2.3 Managing Multi-Modal Inputs in Imitation Learning via VAEs

In real-world scenarios, decision-making inputs often come from multiple modalities, including RGB images, depth images, 3D point clouds, language instructions, and more. As a motivating example, consider the task of navigating a drone in an outdoor environment, where multiple modalities emerge due to visual information captured by various sensors and factors like the drone's current pose and location. Coherently managing the multi-modal input is essential for the real-life applications of IL. In this context, VAEs have proven effective for fusing or unifying inputs from multiple modalities based on the use of latent embeddings.

RGBD-VIB (Du et al. (2022)) proposes to fuse multi-modal inputs based on their uncertainty for evaluation, ensuring that inputs with higher certainty are given more weight in decision-making. To this end, a VAE $(P_{\phi^i}(z|s), P_{\theta^i}(a|z), P_{\omega^i}(z))$ is trained for each modality $i \in [1, \cdots, N]$ using the VIB framework (i.e., Eq. (50)). Note that these VAEs share the same action space but vary in their state spaces. The uncertainty measure can then be acquired based on the pretrained VAEs as $u^i(s) = D_{KL}(P_{\phi^i}(z|s)||P_{\omega^i}(z))$. Intuitively, a large uncertainty $u^i(s)$ indicates that the current state in modality i may be out of the distribution of the training dataset. Finally, the action is a weighted sum of the output from each VAE, where the weight assigned to each modality is proportional to $\sum_{j=1}^N u^j(s) - u^i(s)$, inversely related to the uncertainty.

Demonstrations may come with contexts c, such as the task id, language instructions, goal images, etc. In this case, a conditional policy $\pi(a|s, c)$ can be learned for specific task goals or instructions. **MCIL**

(Lynch & Sermanet (2021)) is proposed for the scenario where multiple related contexts $c_i, i \in [1, \cdots, N]$ are provided for a task. For a coherent use of these contexts, MCIL learns an encoder for each context, i.e., $(P_{\phi^1}(z|c_1), \cdots, P_{\phi^N}(z|c_N))$, to embed different contexts into a unified latent space, and a decoder $P_\theta(a|s,z)$ as the latent-conditioned policy. The decoder and encoders can be trained end-to-end by $\max_{\theta,\phi^{1:N}} \mathbb{E}_{(s,a,c_i)\sim D_E, z\sim P_{\phi^i}(\cdot|c_i)} [\log P_\theta(a|s,z)]$ [12]. This leads to a policy that generalizes over multi-modal contexts: $z \sim P_{\phi^i}(\cdot|c_i), a \sim P_\theta(\cdot|s,z), i \in [1, \cdots, N]$. As an example, language instructions are usually costly to annotate, but other contexts like the goal images are relatively easy to obtain (from sensors). Through such a unified latent space, MCIL enables the use of (large-amount) demonstrations from easier sources to aid the learning of a language-conditioned policy.

Similarly with MCIL, **CM-VAE-BC** (Bonatti et al. (2020)) aims at learning a joint low-dimensional embedding for multiple data modalities. It utilizes CM-VAE (Spurr et al. (2018)), where a pair of encoder-decoder $(P_{\phi^i}(z|s), P_{\theta^i}(s|z))$ is trained for each modality $i \in [1, \cdots, N]$ via cross-modality reconstructions of which the objective is:

$$\max_{\phi^i,\theta^j} \mathbb{E}_{z\sim P_{\phi^i}(\cdot|s^i)} \left[\log P_{\theta^j}(s^j|z)\right] - D_{KL}(P_{\phi^i}(z|s^i)||P_{\theta^i}(z)) \tag{54}$$

Suppose $N = 2$, then (i,j) in the equation above is an enumeration over the set $\{(1,1),(1,2),(2,1),(2,2)\}$. Note that the equation above is a variational lower bound of $\log P_{\theta^j}(s^j)$ and s^i & s^j corresponds to the same true environment state. This cross-modal training regime results in a single latent space that allows embedding and reconstructing multiple data modalities. After the representation learning, a policy conditioned on the latent variable $\pi(a|z)$ can be learned with any IL method (e.g., BC), following aforementioned Scheme (2), i.e., Eq. (47).

3.2.4 Skill Acquisition and Hierarchical Imitation Learning through VAEs

In the context of IL, skills are meaningful subsequences/patterns within the expert trajectories, which can be potentially utilized in multiple tasks. As an example, consider IL for cooking tasks, where the tasks can be diverse but often have overlapping patterns, such as, slicing, chopping, etc. As introduced in OPAL (see Section 3.1.5), VAEs can be used to extract such patterns via learnt latent embeddings (i.e., using Eq. (45) which is a special case of aforementioned Scheme (3)). As in OPAL, after training, the decoder $P_\theta(a|s,z)$ can be viewed as the policy for skill z (i.e., $\pi_{\text{low}}(a|s,z)$), and the encoder $P_\phi(z|\tau)$ can be used to parse the expert data into trajectories of (s,z) pairs for training the high-level policy $\pi_{\text{high}}(z|s)$ with any IL method. Then, the hierarchical policy can be executed in a call-and-return manner: sampling a skill $z \sim \pi_{\text{high}}(\cdot|s)$, executing the corresponding policy $a \sim \pi_{\text{low}}(\cdot|s,z)$ for h time steps, sampling the next skill, and so on. This whole process can be considered as a hierarchical extension of BC. Beyond this straightforward use of VAEs, some works have proposed to impose additional structures or properties, such as disentanglement, to the latent space for improved skill acquisition (e.g., in interpretability). As mentioned in Section 2.1, being disentangled means that each dimension/partition of the latent variable is independent and semantically meaningful. One way to realize this is to directly incorporate an auxiliary loss term to the standard VAE ELBO as regularization:

$$\max_{\phi,\theta,\omega} \mathcal{L}^{\text{ELBO}}_{\theta,\phi}(D_E) - \lambda \mathcal{L}^{\text{reg}}_{\omega,\theta,\phi}(D_E), \tag{55}$$

where $\mathcal{L}^{\text{ELBO}}_{\theta,\phi}(D_E)$ usually takes the form of Eq. (45); ω is the parameter of an auxiliary network; $\lambda > 0$ controls the tradeoff between the two loss terms.

SAILOR (Nasiriany et al. (2022)) defines $\mathcal{L}^{\text{reg}}_{\omega,\theta,\phi}(D_E) = \mathbb{E}_{(\tau_1,\tau_2)\sim D_E} \left[f_\omega\left(\mu(P_\phi(\cdot|\tau_1), \mu(P_\phi(\cdot|\tau_2)))\right) - t\right]^2$, where τ_1 and τ_2 belong to the same trajectory and are separated by t time steps, $\mu(P_\phi(\cdot|\tau_1))$ denotes the mean of the encoder output. Such a term can encourage the learned embedding to be predictable (for the temporal difference between skills) and consistent, which is important for downstream policy learning with these skills. Note that the gradient from $\mathcal{L}^{\text{reg}}_{\omega,\theta,\phi}(D_E)$ can be backpropagated to the encoder, allowing this term to shape the learned skill embeddings.

[12] This objective ensembles the VIB framework, i.e., Eq. (50), but overlooks the regulation on z. Also, training a separate encoder for each context is necessary, since dealing with different modalities requires different foundation models.

Both OPAL and SAILOR would partition trajectories into segments of length h (i.e., the assumed skill horizon) and then train a CVAE on these independent segments for skill acquisition (i.e., with Eq. (45)). **CKA** (Pasula (2020)), on the other hand, proposes a regularization term on the entire trajectory. In particular, if a trajectory τ can be decomposed into m skills in a sequence, the learned skill embeddings $z_{1:m}$ can be regularized by a mutual information term $\mathcal{L}^{\text{reg}}_{\omega,\theta,\phi}(D_E) = -\mathbb{E}_{\tau\sim D_E, z_i\sim P_\phi(\cdot|\tau_i)} I\left(\sum_{i=1}^m z_i; \tau\right)$, where τ_i is the i-th segment of τ. The intuition is that, as a complex behavior, τ should be a combination of these skills. By maximizing the mutual information, the interpretability of the learned embeddings for the behavior τ can be enhanced. The reason to assume a summation structure $\sum_{i=1}^m z_i$ as the combination form is to enable a practical estimation of the mutual information term (see (Pasula (2020))). Aforementioned methods either assume a fixed skill horizon of h or require that the skill segmentation of the trajectory is readily available, thus only learning skill embeddings for each segment. **CompILE** (Kipf et al. (2019)) suggests a method to concurrently infer both the skill boundaries and skill embeddings directly from the trajectory.

A major benefit of skill acquisition lies in the potential for skills to be transferred across multiple related tasks. This transfer can facilitate the learning of a multi-task policy, $\pi(a|s, z, c)$, where z and c represent the skill and task, respectively. In this case, (z, c) constitutes the policy condition and disentanglement between z and c are required for interpretable and controlled behavior generation. To this end, **TC-VAE** (Noseworthy et al. (2019)) is proposed for the scenario where the task variables c are provided and task-irrelevant skill embeddings z need to be learned. A regularization term $\max_\phi \min_\omega \mathcal{L}^{\text{reg}}_{\omega,\theta,\phi}(D_E) = \max_\phi \min_\omega \mathbb{E}_{(\tau,c)\sim D_E} ||f_\omega(\mu(P_\phi(\cdot|\tau))) - c||_1$ is adopted, where f_ω is trained to predict the task from the mean of the encoder $\mu(P_\phi(\cdot|\tau))$. Intuitively, maximizing this objective over ϕ will encourage the learned latent space z to be non-informative about the task c. **SKILL-IL** (Bian et al. (2022)), on the other hand, learns z and c in the meantime as the latent variable of a VAE encoded from a set of multi-task demonstrations. To encourage the disentanglement, a Gated VAE (see Section 2.1) is adopted, where the latent variable is partitioned into two subdomains for z and c respectively. Parameters related to subdomain z are updated on data comprising different skills but within the same task. Similarly, parameters related to subdomain c are trained with data corresponding to the same skill but from different tasks.

3.2.5 Tackling Causal Confusion in Imitation Learning with VAEs

Causal confusion/misidentification happens when learnt imitator policies become strongly correlated on certain nuisance variables present in the task environment, rather than identifying the causal variables that expert demonstrators actually exploited in decision-making. Thus, more information in the environment could yield worse IL performance as there would be more nuisance factors. For instance, in a driving task, the driver must brake when encountering obstacles or pedestrians. If the demonstration images include brake light indicators on the dashboard, imitators might incorrectly associate the braking behavior with these indicators. However, evaluation scenarios may not always feature these indicators, leading to potentially catastrophic outcomes (such as hitting a pedestrian). Therefore, to be maximally robust to distribution shifts (between the training and evaluation scenarios), a policy must rely solely on true causes of expert actions, thereby avoiding causal misidentification.

As a seminal work, **RCM-IL** (De Haan et al. (2019)) resolves causal misidentification in IL by learning a disentangled representation $z \in \mathbb{R}^d$ of the state s, each dimension of which represents a disentangled factor of variation, and then differentiating between nuisance and actual causal factors in z. In particular, a β-VAE is adopted to learn such a disentangled representation z following Eq. (5) (with x replaced by s). After pretraining the β-VAE on D_E, states s in D_E can be replaced by their corresponding latent embeddings z. Each of the d dimensions of z could represent either a causal or nuisance factor, and it is necessary to mask out the nuisance factors. The problem is then to find the correct mask vector $m \in \{0, 1\}^d$. With m, the policy can be defined on the masked representations as $\pi(a|m \odot z)$, where $\odot$ denotes element-wise multiplication and $m \odot z$ keeps only actual causal factors. De Haan et al. (2019) propose methods for finding the correct m by querying experts or interacting with the environment, which does not rely on the use of VAEs and so is not detailed here. **Masked** (Pfrommer et al. (2023)) adopts the same protocol as RCM-IL but improves the algorithm for finding the mask vector. Specifically, it uses a carefully-designed statistical hypothesis testing algorithm to efficiently mask out nuisance variables among the latent dimensions produced by the β-VAE, which does not require expensive queries to the expert or environment for intervention. Under

Algorithm	VAE Type	VAE Usage	Evaluation Task
EIRLI	VAE	Representation Learning (2)	dm_control, Procgen, MAGICAL
T-VAE	VAE	Trajectory modeling (3)	2D Navigation, 2D Circle, Minecraft
RC-VAE	VRNN	Trajectory forecasting (3)	Basketball Tracking, PEMS-SF Traffic, Billiard Ball Trajectory
Behavior Retrieval	β-VAE	Data augmentation (2)	RoboSuite, PyBullet, Real Robot
VAE-TPIL	VAE	Data augmentation (2)	Minecraft, PyBullet
GIRIL	CVAE	Data augmentation	OpenAI Atari, Pybullet
RGBD-VIB	VIB	Handling multi-modal input (4)	Real Robot
MCIL	VAE	Handling multi-modal input (1)	3D Playroom
CM-VAE-BC	CM-VAE	Handling multi-modal input (2)	AirSim, Real Robot
SAILOR	β-VAE	Skill acquisition (3)	Franka Kitchen, CALVIN
CKA	VAE	Skill acquisition (3)	PyBullet
CompILE	VAE	Skill acquisition (3)	GridWorld, dm_control
TC-VAE	β-VAE	Skill acquisition (3)	Synthetic Arcs, MIME Pouring
SKILL-IL	Gated VAE	Skill acquisition (2)(3)	Craftworld, Real-world Navigation
RCM-IL	β-VAE	Addressing causal confusion (2)	OpenAI Gym/MuJoCo/Atari
Masked	β-VAE	Addressing causal confusion (2)	OpenAI Gym/MuJoCo
OREO	VQ-VAE	Addressing causal confusion (2)	OpenAI Atari, CARLA

Table 2: Summary of representative VAE-based IL algorithms. For each algorithm, we detail the type of VAE used, how the VAE is applied, and the tasks on which it was evaluated. In Column 3, (1)-(4) refer to the 4 schemes of VAE-based IL introduced in Section 3.2.1. As for the evaluation tasks, IL algorithms has relatively more diverse choices than offline RL algorithms (as shown in Table 1). By Real Robot or Real-world Navigation, we mean evaluations on real-world platforms, which vary from one study to another. We provide the references of these benchmarks here: dm_control (Tassa et al. (2018)), Procgen (Cobbe et al. (2020)), MAGICAL (Toyer et al. (2020)), 2D Navigation/Circle (Lu et al. (2019)), Minecraft (Guss et al. (2019)), Basketball Tracking (Felsen et al. (2018)), PEMS-SF Traffic (Dua et al. (2019)), Billiard Ball Trajectory (Fragkiadaki et al. (2016)), RoboSuite (Zhu et al. (2020)), PyBullet (Coumans & Bai (2016–2021)), OpenAI Gym/Atari/MuJoCo (Brockman et al. (2016)), 3D Playroom (Lynch et al. (2019)), AirSim (Shah et al. (2017)), Franka Kitchen (Gupta et al. (2019a)), CALVIN (Mees et al. (2022b)), GridWorld (Zintgraf et al. (2020)), Synthetic Arcs (Noseworthy et al. (2019)), MIME Pouring (Sharma et al. (2018)), Craftworld (Devin (2024)), CARLA (Dosovitskiy et al. (2017)).

certain assumptions, this algorithm is guaranteed not to incorrectly mask factors that causally influence the expert. Please see (Pfrommer et al. (2023)) for details.

Alternatively, Park et al. (2021) present **OREO** to ameliorate causal misidentification in IL, of which the main idea is to encourage the policy to uniformly attend to all semantic factors in the state to prevent it from strongly exploiting certain nuisance factors. In particular, a VQ-VAE is trained on states from demonstrations using Eq. (9), where x is replaced with $s \sim D_E$. Since there could be multiple (say n) semantic factors within s, the latent representations from the VQ-VAE, i.e., z_E and z_D, are set to be 2D matrices in $\mathbb{R}^{n\times d}$, where d is the dimension of the representation for each single factor. After pretraining, given a state s, its multi-factor representation z_D can be acquired by querying the closet code for each row of z_E: ($e_{1:k}$ is the codebook, $e_j \in \mathbb{R}^d$, and $z_{E,i} \in \mathbb{R}^d$ is the i-th row of z_E.)

$$z_E \sim P_\phi(\cdot|s),\ z_D = [e^T_{q(1)}, \cdots, e^T_{q(n)}],\ q(i) = \underset{j\in[1,\cdots,k]}{\arg\min}\ \|z_{E,i} - e_j\|_2. \tag{56}$$

The next step is to learn a policy through BC based on the multi-factor representation while reducing the influence of nuisance factors. Specifically, at each state s, a sample of k binary random variables $M_i \in \{0,1\}, i \in [1,\cdots,k]$ are iid sampled from a Bernoulli distribution, and then a mask vector m corresponding to s can be created as: $m = [M_{q(1)}, \cdots, M_{q(n)}]$, where $q(1), \cdots, q(n)$ are defined as above. Finally, the IL objective is: $\max_{\pi,f} \mathbb{E}_{(s,a)\sim D_E, m} \log \pi(a|m \odot f(s))$, where f is initialized with the pretrained encoder P_ϕ

and updated during the policy training. Suppose the $q(i)$-th factor is a nuisance factor that is strongly correlated with decision-making, then it would occur frequently in the latent representations, i.e., $e^T_{q(i)}$ in z_D. By randomly setting the corresponding mask $M_{q(i)}$ to 0, this nuisance factor can be effectively dropped out, thereby mitigating the issue of causal misidentification. Randomized dropping provides a simple yet effective way to regularize the uniform treatment of each generative factor, i.e., either a causal variable that explains expert actions or a nuisance variable that just shows strong correlation with the demonstrations.

The representative VAE-based offline RL and IL algorithms are summarized in Table 1 and 2, respectively. We notice that most applications of VAEs in offline policy learning are based on the learned embedding z. For example, it can be used to identify OOD actions (Section 3.1.3), transform high-dimensional states or continuous actions for improved learning efficiency (Section 3.1.4), represent tasks or skills for multi-task or hierarchical learning (Section 3.1.5), fuse input from multiple modalities (Section 3.2.3), provide disentangled representations of the states for tackling causal confusion (Section 3.2.5), and so on. On the other hand, we note that some directions of VAE-based offline policy learning can be further explored. For instance, as introduced in Scheme (2) of Section 3.2.1, the VAE can be used to extract compact representations of the states, which can then be used for learning a representation-based policy $\pi(a|z)$. However, EIRLI (Chen et al. (2021a)) suggests that reward- and value-prediction would benefit more (than policy learning) from a representation that captures mostly coarse-grained visual differences. Thus, it's worth investigating whether VAE-based representation learning would improve offline RL/IL that requires reward- or value-predictions. Moreover, RCM-IL and Masked in Section 3.2.5 assume that β-VAEs can extract well-disentangled representations of the states as the basis of mitigating causal confusion. However, as noted in Gated VAE (Section 2.1), consistent disentanglement with β-VAEs, such an unsupervised manner, has been demonstrated to be impossible. Thus, further improvements can be made regarding tackling causal confusion.

4 Generative Adversarial Networks in Offline Policy Learning

Similar to the previous section, we divide the content here into two parts: the applications of GANs in IL (Section 4.1) and offline RL (Section 4.2). There are relatively more GAN-based IL algorithms compared to GAN-based offline RL algorithms. Interestingly, GAN-based IL primarily extends two fundamental algorithms: GAIL and AIRL, while GAN-based offline RL focuses on expanding the model-based offline RL.

4.1 Imitation Learning

In this section, we starts with a detailed introduction of the fundamental algorithms in this direction: GAIL and AIRL, as a tutorial, and then present extensions for each of them. Finally, we provide a spotlight on the integrated use of GANs and VAEs for IL, as examples of synthesizing the use of different generative models for offline policy learning.

4.1.1 Fundamental GAN-Based Imitation Learning Algorithms: GAIL and AIRL

Nearly all works regarding applying GANs for IL can be viewed as extensions of two fundamental works in this area: GAIL (Ho & Ermon (2016)) and AIRL (Fu et al. (2017)). Both works are based on the maximum causal entropy inverse RL (MaxEntIRL) framework (Ziebart et al. (2010)), of which the objective is as below:

$$\max_c \left[\min_\pi -H(\pi) + \mathbb{E}_{(s,a)\sim\rho_\pi(\cdot)}[c(s,a)]\right] - \mathbb{E}_{(s,a)\sim\rho_{\pi_E}(\cdot)}[c(s,a)] \tag{57}$$

Here, $\rho_\pi(s,a) = \pi(a|s)\sum_{t=0}^{\infty}\gamma^t P(s_t = s|\pi)$ is the discounted occupancy measure (i.e., visit frequency) of (s,a) when taking π, and $H(\pi) = \mathbb{E}_{(s,a)\sim\rho_\pi(\cdot)}[-\log\pi(a|s)]$ denotes the policy entropy. Intuitively, this framework looks for a cost function c that assigns low costs to the expert policy π_E and high costs to any other policy, thereby allowing the expert policy to be learned via minimizing the expected cost, i.e., through the inner RL process shown in Eq. (57). π_E is not directly accessible and usually represented as a set of expert demonstrations.

GAIL proposes that, to ensure the expressiveness of c while avoiding overfit on the set of demonstrations, c can be any real function (i.e., $\mathbb{R}^{\mathcal{S}\times\mathcal{A}}$) but an extra regularizer $\psi : \mathbb{R}^{\mathcal{S}\times\mathcal{A}} \to \mathbb{R}$ on c should be introduced to

Eq. (57). This ψ-regularized MaxEntIRL problem is equivalent to an occupancy measure matching problem:

$$\min_{\pi} -H(\pi) + \psi^*(\rho_\pi - \rho_{\pi_E}),\ \psi^*(\rho_\pi - \rho_{\pi_E}) = \sup_{c \in \mathbb{R}^{\mathcal{S}\times\mathcal{A}}} (\rho_\pi - \rho_{\pi_E})^T c - \psi(c) \tag{58}$$

That is, ψ-regularized MaxEntIRL implicitly seeks a policy, whose occupancy measure is close to the expert's, as measured by the convex conjugate of the regularizer, i.e., ψ^*. As introduced in Section 2.2, GANs provide a scalable manner for distribution matching. GAIL proposes that, with a certain design of ψ (i.e., Eq. (13) in (Ho & Ermon (2016))), Eq. (58) can be converted to a GAN objective:

$$\min_{\pi} \max_{D \in (0,1)^{\mathcal{S}\times\mathcal{A}}} -H(\pi) + \mathbb{E}_{(s,a)\sim\rho_\pi(\cdot)}[\log(1 - D(s,a))] + \mathbb{E}_{(s,a)\sim\rho_{\pi_E}(\cdot)}[\log D(s,a)] \tag{59}$$

Compared with Eq. (57), we can see that $c(s,a)$ is defined with the discriminator as $\log(1-D(s,a))$ [13]. Also, the policy π works as the generator G, so D and π can be alternatively trained as in GANs to optimize Eq. (59). Specifically, in each training episode, π is trained for several iterations to maximize the expected return $Q(s_0,a_0) = \sum_{t=0}^{\infty} \gamma^t(-\log(1 - D(s_t,a_t)) - \lambda \log \pi(a_t|s_t)),\ \forall(s_0,a_0)$, with a widely-adopted RL algorithm – TRPO (Schulman et al. (2015)) [14], and then D is trained for iterations to correctly classify samples from π or π_E with Eq. (59). Compared with the original MaxEntIRL, which requires solving a complete RL problem as the inner loop for each update of c, GAIL ensures both expressiveness and scalability, especially useful for tasks in high-dimensional state/action spaces. Further, GAIL provides solid theoretical results on the connection between IRL and GANs. As for the global optimality and convergence rate of GAIL, Zhang et al. (2020b) provide an analysis under the condition of using two-layer neural networks (with ReLU between the two layers) as function estimators and applying natural policy gradient for policy updates, when the underlying MDP belongs to the class of linear MDPs.

AIRL also adopts a GAN-like framework as follows:

$$\begin{aligned} &\max_{D} \mathbb{E}_{(s,a)\sim\rho_\pi(\cdot)}[\log(1 - D(s,a))] + \mathbb{E}_{(s,a)\sim\rho_{\pi_E}(\cdot)}[\log D(s,a)], \\ &\min_{\pi} \mathbb{E}_{(s,a)\sim\rho_\pi(\cdot)}[\log(1 - D(s,a)) - \log D(s,a)] \end{aligned} \tag{60}$$

However, instead of applying a sigmoid function (i.e., $D(s,a) = \frac{\exp(f(s,a))}{\exp(f(s,a))+1}$) as the activation function on the last layer output of the discriminator, i.e., $f(s,a)$, as in GAN and GAIL, AIRL adopts $D(s,a) = \frac{\exp(f(s,a))}{\exp(f(s,a))+\pi(a|s)}$. They claim that, with this design, AIRL is equivalent to MaxEntIRL, under the assumption that trajectories $\tau = \{s_0, a_0, \cdots, s_T, a_T, s_{T+1}\}$ follow the Boltzmann distribution (i.e., $P(\tau) \propto \rho_0(s_0) \prod_{t=0}^{T-1} \mathcal{T}(s_{t+1}|s_t,a_t) \exp(\gamma^t r(s_t,a_t))$). However, the derivation provided in (Fu et al. (2017)) is not rigorous [15]. Further, they propose to replace $D(s,a)$ with $D(s,a,s') = \frac{\exp(f(s,a,s'))}{\exp(f(s,a,s'))+\pi(a|s)}$, where $f(s,a,s') = g(s) + \gamma h(s') - h(s)$. They state that, at optimality, $g(s)$ and $h(s)$ can recover the reward and value function, respectively, if the real reward function is a function of s only and the environment is deterministic [16]. While its theoretical foundation is not robust, AIRL can be considered as a GAN-based IL algorithm, drawing inspiration from MaxEntIRL and well substantiated by empirical results.

There is an extensive amount of works developed based on GAIL or AIRL. Instead of providing details on each of them, we put an emphasis on the representative ones by presenting their objective designs and key novelties in tables, and briefly enumerate other works for comprehensiveness.

[13] We equivalently substitute all $D(s,a)$ in (Ho & Ermon (2016)) as $1 - D(s,a)$ to be in line with GAN, where the true and fake data should be labeled as 1 and 0, respectively, by the discriminator D.

[14] $\max_\pi Q(s_0,a_0) = \sum_{t=0}^{\infty} \gamma^t(-\log(1-D(s_t,a_t)) - \lambda \log \pi(a_t|s_t))$ is equivalent to $\min_\pi -\lambda H(\pi) + \mathbb{E}_{(s,a)\sim\rho_\pi(\cdot)}[\log(1-D(s,a))]$. $\lambda > 0$ is introduced here to balance the two objective terms.

[15] In Appendix A.1 of (Fu et al. (2017)), the step $\frac{\partial}{\partial\theta} \log Z_\theta = \mathbb{E}_{p_\theta}\left[\sum_{t=0}^{T} \frac{\partial}{\partial\theta} r_\theta(s_t,a_t)\right]$ is questionable. Also, in its Appendix A.2, they erroneously mix up the use of μ_t and $\hat{\mu}_t$.

[16] In Appendix A.4 of (Fu et al. (2017)), they claim that the global minimum of the discriminator objective is reached when $\pi = \pi_E$, which is backed up by the original GAN paper (Goodfellow et al. (2014b)). However, the objective design of AIRL is significantly distinct from the original GAN. Moreover, this claim forms the basis of the proof presented in its Appendix C on $g(s)$ and $h(s)$ recovering the reward and value functions respectively.

4.1.2 Extensions of GAIL

In Table 3, we provide an overview of representative works that extend GAIL. They either substitute the original GAN framework with more advanced GAN variants (as introduced in Section 2.2) or expand the use of GAIL to other IL settings, including the multi-agent, multi-task, hierarchical, and model-based scenarios. Moreover, to provide a thorough review, we briefly enumerate other related research works as follows, which are further categorized by their topics.

GAIL: Extensions of GAIL concentrate on enhancing its learning efficiency, tackling key challenges such as increasing the sample efficiency for policy learning, ensuring balanced training of the discriminator and policy, etc. (1) **DGAIL** (Zuo et al. (2020)) and **SAM** (Blondé & Kalousis (2019)) replace the stochastic policy $a \sim \pi(\cdot|s)$ in GAIL with a deterministic one $a = \pi(s)$ and, correspondingly, proposes a DDPG-based (Lillicrap et al. (2016)) updating rule for π. As an off-policy algorithm, DDPG is more sample efficient than TRPO (used in the original GAN). **BGAIL** (Jeon et al. (2018)) improves the sample efficiency by approximating the discriminator parameters' posterior distribution in the ideal case where correct labels are assigned to both demonstrated and generated behaviors. A more accurate estimation of the cost function can then be acquired through sampling from that distribution, consequently improving the policy training. (2) **VAIL** (Peng et al. (2019a)) suggests limiting information flow in the discriminator of GAIL (or AIRL) using the Variational Information Bottleneck framework (Tishby & Zaslavsky (2015)), to prevent the discriminator from converging too quickly and supplying uninformative gradients to the generator. **TRAIL** (Zolna et al. (2020)) proposes a different manner to regularize the discriminator (through an auxiliary task), with the aim to discourage the agent to exploit spurious patterns in observations which are associated with the expert label but task-irrelevant. (3) For applications demanding reliability and robustness, **RS-GAIL** (Lacotte et al. (2019)) presents a risk-sensitive version of GAIL by introducing a constraint to the original GAIL objective, such that the conditional value-at-risk (Duffie & Pan (1997)) of the learned policy is at least as well as that of the expert. This algorithm is supported by rigorous theoretical validation.

Multi-agent/Hierarchical GAIL: IGASIL (Hao et al. (2019)) extends GAIL to fully-collaborative multi-agent scenarios. It adopts a similar objective design with MAGAIL's (listed in Table 3) but suggests two major improvements for learning efficiency: training the policy with DDPG for enhanced sample efficiency and adopting high-return trajectories from the policy as demonstrations for self-imitation learning. Like Option-GAIL introduced in Table 3, **OptionGAN** and **Directed-Info GAIL** extend GAIL to the hierarchical learning setting, taking advantage of the Mixture-of-Experts framework (Masoudnia & Ebrahimpour (2014)) and directed information maximization (Massey et al. (1990)), respectively. However, these two algorithms are not suitable for learning from demonstrations segmented by sub-tasks. Also, Directed-Info GAIL trains π_H and π_L in two separate stages, leading to suboptimality of the hierarchical policy $\pi = (\pi_H, \pi_L)$.

InfoGAIL: Hausman et al. (2017) and Peng et al. (2022) address the same challenge as InfoGAIL, i.e., IL from multi-modal but unstructured demonstrations. Hausman et al. (2017) achieve the same objective function as InfoGAIL but through a distinct perspective; Peng et al. (2022) proposes an alternative manner to update Q (in InfoGAIL) through a VAE framework, where Q and π serve as the encoder and decoder, respectively. **Ess-InfoGAIL** (Fu et al. (2023)) extends InfoGAIL to manage demonstrations from a mix of experts, wherein the quantity of demonstrations from each expert is imbalanced. **Burn-InfoGAIL** (Kuefler & Kochenderfer (2018)) improves InfoGAIL to reproduce expert behaviors over extended time horizons.

4.1.3 Extensions of AIRL

Extensions of AIRL are fewer than those of GAIL, but we follow the content structure in Section 4.1.2, providing a summarization table as Table 4 and offering a comprehensive review as below.

AIRL adopts the function design $f(s, a, s') = g(s) + \gamma h(s') - h(s)$, where $g(s)$ is assumed to recover the environment reward function and $h(s)$ can be viewed as the potential function for reward shaping (Ng et al. (1999)). **EAIRL** (Qureshi et al. (2019)) proposes to implement $h(s)$ as the empowerment function (Mohamed & Rezende (2015)), maximizing which would induce an intrinsic motivation for the agent to seek the states that have the highest number of future reachable states. However, as claimed in AIRL, $h(s)$ is designed to recover the value function at optimality, which is different from the empowerment function in definition. AIRL has been extended to various IL setups, including model-based, off-policy, multi-task, and hierarchical

Algo (GAN Type)	Objective	Key Novelty
CGAIL (CGAN) (Zhang et al. (2019))	$\min_\pi \max_D -\lambda H(\pi(\cdot\|c)) + \mathbb{E}_{\rho_{\pi_E}(\cdot\|c)}[\log D(s,a\|c)]+$ $\mathbb{E}_{\rho_\pi(\cdot\|c)}[\log(1-D(s,a\|c))]+$ $\mathbb{E}_{\rho_{\pi_E}(\cdot\|c)}[\log(1-D(s,a\|c')]$	Recovering a policy $\pi(a\|s,c)$ for each condition c; Demonstrations are shareable among similar task conditions, so the data efficiency can be high; $\max_D \mathbb{E}_{\rho_{\pi_E}(\cdot\|c)}[\log(1-D(s,a\|c')]$ discourages the mismatch between c' and (s,a) for consistency.
InfoGAIL (InfoGAN) (Li et al. (2017b))	$\min_{\pi,Q} \max_D -\lambda_1 H(\pi) + \mathbb{E}_{\rho_\pi}[\log(1-D(s,a))]+$ $\mathbb{E}_{\rho_{\pi_E}}[\log D(s,a)] - \lambda_2 L_I(\pi,Q)$, $L_I(\pi,Q) = \mathbb{E}_{c\sim P_C(\cdot),a\sim\pi(\cdot\|s,c)}[\log Q(c\|s,a)] + H(C)$, $P_C(\cdot)$ is an assumed prior distribution.	Demonstrations are multi-modal but labels c are not provided, unlike CGAIL; $L_I(\pi,Q)$ is a lower bound of the mutual information $I(c;(s,a))$, by maximizing which we can disentangle trajectories corresponding to different c; Policies for each latent modality $\pi(a\|s,c)$ can then be recovered.
f-GAIL (f-GAN) (Zhang et al. (2020a))	$\min_\pi \max_{f^*\in\mathcal{F}^*,T} \mathbb{E}_{\rho_{\pi_E}}[T(s,a)] - \mathbb{E}_{\rho_\pi}[f^*(T(s,a))]$ $-H(\pi)$, f^* is the convex conjugate of f (which defines a certain f-divergence) and satisfies: convexity and $\inf_{u\in\mathrm{dom}_{f^*}}\{f^*(u)-u\}=0$. Like π and T, f^* is modeled as a neural network but specially designed to fulfill its two constraints.	GAIL is a special case of f-GAIL, when $T(x)=\log D(x)$, $f^*(x)=-\log(1-e^x)$; Maximizing over $f^*\in\mathcal{F}^*$ aims to find the largest f-divergence between ρ_π and ρ_{π_E}, which can better guide π to π_E.
Triple-GAIL (Triple-GAN) (Fei et al. (2020))	$\min_{\pi,C} \max_D -\lambda_1 H(\pi) + \mathbb{E}_{\rho_{\pi_E}}[\log D(s,a,c)]+$ $\lambda_2\mathbb{E}_{\rho_\pi}[\log(1-D(s,a,c))]+$ $(1-\lambda_2)\mathbb{E}_{\rho_C}[\log(1-D(s,a,c))]+$ $\lambda_4\mathbb{E}_{\rho_{\pi_E}}[-\log C(c\|s,a)] + \lambda_5\mathbb{E}_{\rho_\pi}[-\log C(c\|s,a)]$; c can be viewed as labels for (s,a), provided in demonstrations; $C(c\|s,a)$ is utilized to classify (s,a), while $\pi(a\|s,c)$ is the policy for the class c.	The development and theoretical validation of Triple-GAIL exactly follow Triple-GAN (see Section 2.2). C and π are trained by matching the approximated joint occupancy measures of (s,a,c): $\rho_\pi(\cdot)$ and $\rho_C(\cdot)$, with $\rho_{\pi_E}(\cdot)$. The last two objective terms serve as extra supervision for C. Viewing c as options/skills, C and π then constitute a hierarchical policy.
MGAIL (GAN) (Baram et al. (2017))	The objective of D is the same as the one of GAIL. $\pi(a\|s;\theta)$ is trained by maximizing the return $J(s_0,a_0;\theta)$, where the policy gradient, i.e., J^0_θ, can be approximated recursively as: $(t=T\to 0)$ $J^t_\theta = R_a\pi_\theta + \gamma(J^{t+1}_\theta + J^{t+1}_{s'} f_a\pi_\theta)$, $J^t_s = R_s + R_a\pi_s + \gamma J^{t+1}_{s'}(f_s + f_a\pi_s)$; f is the learned dynamics: $s'=f(s,a)$, $R(s,a)$ is the reward defined with D, $R_s \triangleq \frac{\partial R}{\partial s}$ and so on.	This is a model-based version of GAIL. A dynamic model f is learned, such that the agent can look one-step ahead to additionally adopt the gradient from f, i.e., $\gamma J^{t+1}_{s'} f_a\pi_\theta$, as part of J^t_θ. (Typically, $J^t_\theta = R_a\pi_\theta + \gamma J^{t+1}_\theta$.) Thus, fewer expert data and policy samples would be required, compared with GAIL.
MAGAIL (GAN) (Song et al. (2018))	$\min_\pi \max_D \mathbb{E}_{\rho_\pi}\left[\sum_{i=1}^N \log(1-D_i(s,a_i))\right] +$ $\mathbb{E}_{\rho_{\pi_E}}\left[\sum_{i=1}^N \log D_i(s,a_i)\right]$, $\pi=(\pi_1,\cdots,\pi_N)$, $\pi_E=(\pi^1_E,\cdots,\pi^N_E)$. All agents share the state s but choose their own action $a_i\sim\pi_i(\cdot\|s)$. The other agents $-i$ can be viewed as part of the environment for agent i. However, if π_{-i} is unknown, the training environment would be non-stationary for i, as π_{-i} are also being updated.	A multi-agent extension of GAIL, which learns a D_i and π_i for each agent. As agents interact with each other, D_i and π_i are not learned independently. The paper's theoretical results assume π^{-i}_E is known, enabling the learning for each agent i to be treated separately. Yet, in practice, better management for the non-stationarity than MAGAIL is required.
Option-GAIL (GAN) (Jing et al. (2021))	$\min_\pi \max_D -\lambda H(\pi) + \mathbb{E}_{\rho_\pi}[\log(1-D(o',s,o,a))]$ $+\mathbb{E}_{\rho_{\pi_E}}[\log D(o',s,o,a)]$, $\pi=(\pi_H,\pi_L)$, $o\sim\pi_H(\cdot\|s,o')$, $a\sim\pi_L(\cdot\|s,o)$. The agent decides on its current option (a.k.a., skill) o with π_H based on s and o' (i.e., the previous option), and then samples actions a with π_L subject to o.	A hierarchical learning version of GAIL. Long-horizon tasks can be segmented to a sequence of sub-tasks, each of which can be done with an option o (i.e., sub-policy). This algorithm can recover a hierarchical policy, useful for long-horizon tasks, from the expert data through matching the occupancy measure of (o',s,o,a) between π and π_E, which follows GAIL. An EM version of Option-GAIL is proposed, in case the expert's options are not labeled.

Table 3: Summary of representative works following GAIL. In Column 1, we list the algorithms and the type of GANs they utilize. Their key objectives and novelties are listed in Column 2 and 3, respectively.

Algo (GAN Type)	Objective	Key Novelty
f-IRL (GAN) (Ni et al. (2020))	$\max_D \mathbb{E}_{s\sim\rho_{\pi_E}(\cdot)}[\log D(s)] + \mathbb{E}_{s\sim\rho_\theta(\cdot)}[\log(1-D(s))]$, $\min_\theta L_f(\theta)$, $L_f(\theta) = D_f(\rho_{\pi_E}(s)\|\rho_\theta(s))$, $\rho_\theta(s) \propto \int \rho_0(s_0)\prod_{t=0}^{T-1}\mathcal{T}(s_{t+1}\|s_t,a_t)\exp(\frac{r_\theta(s_{t+1})}{\alpha})\eta_\tau(s)d\tau$, $\eta_\tau(s) = \sum_{t=1}^{T}\mathbb{1}(s_t = s)$; The training alternates between $\max_D$ and $\min_\theta$; With the learned reward function r_θ, π is trained by RL. $\min_\theta L_f(\theta)$ is realized by gradient descents: $\nabla_\theta L_f(\theta) = \frac{1}{\alpha T}\mathrm{cov}_{\tau\sim\rho_\theta(\cdot)}\left(\sum_{t=1}^{T} f(u_t) - f'(u_t)u_t, \sum_{t=1}^{T}\nabla_\theta r_\theta(s_t)\right)$, $u_t = \frac{\rho_{\pi_E}(s_t)}{\rho_\theta(s_t)} \approx \frac{D(s_t)}{1-D(s_t)}$, $\mathrm{cov}(\cdot)$ denotes covariance.	This work provides a generalization of AIRL by applying the the general f-divergence. The reward $r_\theta(s)$ is trained by state marginal matching, i.e., $\min_\theta D_f(\rho_{\pi_E}(s)\|\rho_\theta(s))$. D is used to estimate u_t in $\nabla_\theta L_f(\theta)$, based on the fact: $D^*(s) = \rho_{\pi_E}(s)/(\rho_{\pi_E}(s) + \rho_\theta(s))$. So, each update of θ requires a near-optimal D^*, which is time-consuming.
MA-AIRL (GAN) (Yu et al. (2019a))	$\max_D \sum_{i=1}^{N}\mathbb{E}_{\rho_{\pi_E}}[\log D_i(s,a)] + \mathbb{E}_{\rho_\pi}[\log(1-D_i(s,a))]$, $\min_{\pi_i}\mathbb{E}_{\rho_\pi}[\log(1-D_i(s,a)) - \log D_i(s,a)], i = 1,\cdots,N$; $D_i(s,a) = \exp(f(s,a))/(\exp(f(s,a)) + \pi_i(a_i\|s))$, $a = (a_1,\cdots,a_N)$, $\pi = (\pi_1,\cdots,\pi_N)$. All agents share a state s and have access to action decisions from the other agents, i.e., a_{-i}, during the training process.	This is a multi-agent version of AIRL, which trains D_i, π_i and applies AIRL to each agent. States and joint actions are shared among agents. Theoretical results are based on Markov games and logistic stochastic best response equilibirum. However, viewing a_{-i} as part of the environment, the problem and derivations degenerate to the single-agent AIRL case.
MH-AIRL (GAN) (Chen et al. (2023d))	$\max_D \mathbb{E}_{\pi_E}\sum_{t=0}^{T-1}\log D(\tilde{s}_t,\tilde{a}_t\|c) + \mathbb{E}_\pi\sum_{t=0}^{T-1}\log(1-D(\tilde{s}_t,\tilde{a}_t\|c))$, $(\tilde{s}_t,\tilde{a}_t) = ((o_{t-1},s_t),(o_t,a_t))$; $\min_\pi \mathbb{E}_\pi\left[\sum_{t=0}^{T-1}\log(1-D_t^c) - \log D_t^c\right] - \lambda_1 I(\tau_\pi;C) - \lambda_2 I(\tau_\pi \to O_{0:T}\|C)$, $\tau_\pi = \{(s_t,a_t)\}_{t=0:T-1}$, $D_t^c = \frac{\exp(f(\tilde{s}_t,\tilde{a}_t\|c))}{\exp(f(\tilde{s}_t,\tilde{a}_t\|c))+\pi(\tilde{a}_t\|\tilde{s}_t,c)}$, $\pi = (\pi_H,\pi_L)$ and $\pi(\tilde{a}_t\|\tilde{s}_t,c) = \pi_H(o_t\|s_t,o_{t-1})\pi_L(a_t\|s_t,o_t)$. c and o denote the task and option variable, respectively. MH-AIRL can also be adopted, when c and o are not labeled in demonstartions, via an Expectation–Maximization (EM) design.	This algorithm integrates multi-task learning, hierarchical learning, and AIRL. π is a hierarchical policy that can be applied to multiple tasks by conditioning on corresponding c. The objective design can be viewed as AIRL on the extended state-action space $(\tilde{s}_t,\tilde{a}_t)$. As regularization, π is trained to maximize the mutual /directed information $I(\tau_\pi;C)$ $/I(\tau_\pi \to O_{0:T}\|C)$ to build the causal relationship between π and the task /option variables.

Table 4: Summary of representative works following AIRL.

IL. **MAIRL** (Sun et al. (2021)) simply replaces the GAIL objective in MGAIL (introduced in Table 3) with the AIRL's and gets a model-based version of AIRL. Following the same intuition as DGAIL and SAM (introduced in Section 4.1.2), **Off-policy-AIRL** suggests adopting off-policy RL algorithms (specially, SAC (Haarnoja et al. (2018))) to train the generator π in AIRL for improved sample efficiency. Table 4 introduces MH-AIRL, which extends AIRL to support both multi-task and hierarchical learning. As related works, **PEMIRL** (Yu et al. (2019b)) and **SMILe** (Ghasemipour et al. (2019a)) are proposed for multi-task AIRL, while **oIRL** (Venuto et al. (2020)) and **H-AIRL** (Chen et al. (2023c)) focus on hierarchical AIRL.

4.1.4 Integrating VAEs and GANs for Imitation Learning: A Spotlight

Lastly, we spotlight some papers that utilize VAEs to enhance GAIL, serving as examples of integrating different generative models for advanced imitation learning. GANs are recognized for their capacity to generate sharp image samples, as opposed to the blurrier samples from VAE models. However, GANs, unlike VAEs, are susceptible to the mode collapse problem, meaning that they may only capture partial modes in a multi-modal dataset. Therefore, the capabilities of GANs and VAEs are highly complementary. As mentioned in Table 3, one approach, such as CGAIL and InfoGAIL, for solving the mode collapse issue is to train a discriminator and policy for each mode by conditioning them on the mode embedding. Such embeddings could be acquired from a pretrained VAE. In particular, a VAE (P_ϕ, P_θ) can be trained to imitate expert trajectories $\tau = (s_0, a_0, \cdots, s_T) \sim D_E$ through an ELBO objective:

$$\max_{\theta,\phi}\mathbb{E}_{\tau\sim D_E}\left[\mathbb{E}_{c\sim P_\phi(\cdot\|\tau)}[\log P_\theta(\tau\|c)] - D_{KL}(P_\phi(c\|\tau)\|P_C(c))\right] \tag{61}$$

where $P_C(c)$ is the predefined prior distribution, $P_\phi(c|\tau)$ and $P_\theta(\tau|c)$ work as the encoder and decoder of the VAE. $\log P_\theta(\tau|c)$ can be decomposed as $\log\rho_\theta(s_0|c) + \sum_{t=0}^{T-1}[\log\pi_\theta(a_t|s_t,c) + \log\mathcal{T}_\theta(s_{t+1}|s_t,a_t,c)]$ based on

the MDP model. Through this unsupervised training process, the VAE is expected to capture the multiple modes in the dataset and its encoder $P_\phi(c|\tau)$ can be employed to provide mode embeddings for demonstration trajectories. Then, the mode-conditioned discriminator and policy can be trained via an objective similar with CGAIL:

$$\min_\pi \max_D \mathbb{E}_{\tau\sim D_E, c\sim P_\phi(\cdot|\tau)} \left[\frac{1}{T} \sum_{t=0}^{T-1} \log D(s_t, a_t|c)] + \mathbb{E}_{\rho_\pi(\cdot|c)}[\log(1 - D(s, a|c))] - \lambda H(\pi(\cdot|c)) \right] \tag{62}$$

The pretrained VAE policy $\pi_\theta(a|s, c)$ can be used to initialize the GAIL policy $\pi(a|s, c)$. Through further training with GAIL (i.e., Eq. (62)), the VAE policy can be refined by addressing the tendency to produce blurry imitations. **Diverse GAIL** (Wang et al. (2017)) and **VAE-ADAIL** (Lu & Tompson (2020)) are notable examples of this paradigm. A more straightforward manner to integrate the VAE and GAN for IL is to add a regularizer $\min_\pi \mathbb{E}_{s\sim\rho_\phi(\cdot)} D_{KL}(\pi(a|s)||\pi_{\text{VAE}}(a|s))$ to the GAIL objective, where $\pi_{\text{VAE}}(a|s)$ is the VAE-based policy pretrained on D_E (see Section 3.2.1). In this way, the GAIL policy π is encouraged to be close to the potentially multi-modal VAE policy. **SAIL** (Liu et al. (2020)) explores in this direction. Another significant advantage of VAEs over GANs is that they can provide semantically meaningful latent embeddings for the input data. As mentioned in Section 3.1.4, such embeddings can be used as transformed training data to lower the difficulty of GAIL training. As an example, **LAPAL** (Wang et al. (2022b)) proposes to adopt a CVAE to transform high-dimensional actions into low-dimensional latent vectors and apply GAIL on the latent space instead, in order to stabilize and accelerate the learning process.

4.2 Offline Reinforcement Learning

In this section, we starts with an introduction on model-based offline RL, for which both a world model of the environment and policy need to be learned from the offline dataset. GANs have been used to improve both aspects, as detailed in Section 4.2.2 and 4.2.3.

4.2.1 Background on Model-based Offline Reinforcement Learning

Most research works in this category are based on Offline Model-based RL (Janner et al. (2019); Yu et al. (2020a)). Different from the model-free case, a parametric dynamic model $\widehat{\mathcal{T}}(s'|s, a)$ and reward model $\hat{r}(s, a)$ need to be learned through supervised learning: (D_μ: offline data collected by the behavior policy μ.)

$$\max_{\widehat{\mathcal{T}}} \mathbb{E}_{(s,a,s')\sim D_\mu} \left[\log \widehat{\mathcal{T}}(s'|s, a) \right], \ \min_{\hat{r}} \mathbb{E}_{(s,a,r)\sim D_\mu} \left[(\hat{r}(s, a) - r)^2 \right] \tag{63}$$

The approximated MDP $\widehat{\mathcal{M}} = (\mathcal{S}, \mathcal{A}, \widehat{\mathcal{T}}, \hat{r}, \hat{\rho}_0(s), \gamma)$, where $\hat{\rho}_0(s)$ is the empirical distribution of initial states in D_μ, can be used as proxies of the real environment, and (short-horizon) trajectories can be collected by interacting with $\widehat{\mathcal{M}}$ using the being-learned policy π_θ, forming another dataset D_π. Note that, to mitigate the impact from the model bias of $\widehat{\mathcal{M}}$, an estimation of the uncertainty in dynamics, i.e., $u(s, a)$, is utilized as a penalty reward term to discourage the agent to visit uncertain regions in the state-action space, so the reward at (s, a) is calculated as $\tilde{r}(s, a) = \hat{r}(s, a) - \lambda_r u(s, a)$, where $\lambda_r > 0$ is a hyperparameter. This conservative way to avoid OOD behaviors resemble the policy penalty method in dynamic-programming-based offline RL, as introduced in Section 3.1. Typical choices of the uncertainty measure include variance or disagreement of estimations from an ensemble of Q-functions or approximated world models (Prudencio et al. (2023)). Specifically, D_π is generated as follows: $s_0 \sim \hat{\rho}_0(\cdot), a_0 \sim \pi_\theta(\cdot|s_0), \tilde{r}_0 = \hat{r}(s_0, a_0) - \lambda_r u(s_0, a_0), s_1 \sim \mathcal{T}(\cdot|s_0, a_0)$, and so on. As a final step, offline/off-policy RL algorithms can be applied to train the policy π_θ on an augmented dataset $D_{\text{aug}} = \lambda_D D_\mu + (1 - \lambda_D) D_\pi$. Here, $\lambda_D \in [0, 1]$ is another hyperparameter. A typical (off-policy) actor-critic framework for this process is as below (Levine et al. (2020)): ($Q_{\bar{\phi}}$ is the target Q-function.)

$$\max_\theta \mathbb{E}_{s\sim D_{\text{aug}}, a\sim\pi_\theta(\cdot|s)} \left[Q_\phi(s, a) \right], \ \min_\phi \mathbb{E}_{(s,a,\tilde{r},s')\sim D_{\text{aug}}} \left[(Q_\phi(s, a) - (\tilde{r}(s, a) + \gamma \mathbb{E}_{a'\sim\pi_\theta(\cdot|s')} Q_{\bar{\phi}}(s', a')) \right] \tag{64}$$

As introduced in Section 2.2, the GAN framework consists of a generator G and discriminator D that are trained simultaneously to compete against each other. For offline model-based RL, the generator G can

be trained to approximate the policy or environment models, which is further discussed in the following subsections.

4.2.2 Policy Approximation Using GANs

As mentioned in Section 3.1, to avoid OOD states and actions, the learned policy π_θ should be close to the underlying behavior policy μ, which is typically realized through introducing a regularization term to the objective for training π_θ. Thus, the first objective in Eq. (64) can be improved as:

$$\max_\theta \lambda_Q \mathbb{E}_{s\sim D_{\text{aug}}, a\sim\pi_\theta(\cdot|s)} \left[Q_\phi(s,a)\right] - f(\pi_\theta, \mu) \tag{65}$$

where $\lambda_Q > 0$ is the regularization coefficient. **SGBCQ** (Dong et al. (2023)) proposes to directly constrain the action distribution of π_θ at each state to be close to the one of μ by implementing $f(\pi_\theta, \mu)$ as $\mathbb{E}_{s\sim D_\mu}\left[d(\pi_\theta(\cdot|s)||\mu(\cdot|s))\right]$, where $d(\cdot)$ denotes a statistical divergence, resembling the policy constraint methods (i.e., Eq. (33)). As introduced in Section 2.2, GANs are be used to model and minimize the JS divergence between two data distributions. Thus, SGBCQ gives out a practical framework to solve Eq. (65) based on a CGAN as below:

$$\begin{aligned} &\max_D \mathbb{E}_{(s,a)\sim D_\mu}[\log D(a|s) + \mathbb{E}_{z\sim P_Z(\cdot)} \log(1 - D(G(z|s)))], \\ &\min_G -\lambda_Q \mathbb{E}_{s\sim D_{\text{aug}}, z\sim P_Z(\cdot)} \left[Q_\phi(s, G(z|s))\right] + \mathbb{E}_{s\sim D_\mu, z\sim P_Z(\cdot)}[\log(1 - D(G(z|s))] \end{aligned} \tag{66}$$

Compared with the CGAN objective (i.e., Eq. (12)), s and a here work as the conditional information y and data point x, respectively. Intuitively, the stochastic policy $a \sim \pi_\theta(\cdot|s)$ is implemented as a generator $a = G(z|s), z \sim P_Z(\cdot)$ and the generator is trained to maximize the expected Q-values and fool the discriminator D at the same time. Involving such a GAN training process encourages the policy to generate behaviors close to the demonstrated ones in distribution.

SDM-GAN (Yang et al. (2022b)) follows a similar protocol but chooses to regularize the stationary (s, a) distribution of π_θ towards the offline dataset to avoid OOD cases. Specifically, they define $f(\pi_\theta, \mu)$ in Eq. (66) as $d(\rho^{\mathcal{T}}_\mu(\cdot)||\rho^{\mathcal{T}}_{\pi_\theta}(\cdot))$, where $\rho^{\mathcal{T}}_\mu(s,a)$ can be approximated as the empirical distribution of (s, a) in D_μ, $\rho^{\mathcal{T}}_{\pi_\theta}(s,a) = \lim_{T\to\infty} \frac{1}{T+1}\sum_{t=0}^{T} P(s_t = s, a_t = a|s_0 \sim \rho_0(\cdot), a_t \sim \pi_\theta(\cdot|s_t), s_{t+1} \sim \mathcal{T}(\cdot|s_t, a_t))$ is the stationary (s, a) distribution of π_θ under the real dynamic $\mathcal{T}$. Assuming the dynamic function $\widehat{\mathcal{T}}$ is well-fitted, $d(\rho^{\mathcal{T}}_\mu(\cdot)||\rho^{\mathcal{T}}_{\pi_\theta}(\cdot))$ is upper bounded by: (Please refer to (Yang et al. (2022b)) for the derivations and definitions of the function classes $\mathcal{G}_{1,2}$.)

$$\sup_{g\sim\mathcal{G}_1} |\mathbb{E}_{(s,a)\sim\rho^{\mathcal{T}}_\mu(\cdot)}[g(s,a) - \mathbb{E}_{s'\sim\widehat{\mathcal{T}}(\cdot|s,a), a'\sim\pi_\theta(\cdot|s')} g(s',a')]| + \sup_{g\sim\mathcal{G}_2} |\mathbb{E}_{(s,a)\sim\rho^{\mathcal{T}}_\mu(\cdot)}[g(s,a)] - \mathbb{E}_{s\sim\rho^{\mathcal{T}}_\mu(\cdot), a\sim\pi_\theta(\cdot|s)} g(s,a)]| \tag{67}$$

The equation above is in a similar form with the Wasserstein distance (defined in Section 2.2) between samples stored in D_μ and generated by π_θ, which inspires the use of GANs for the estimation. In particular, the objective is as below:

$$\begin{aligned} &\max_D \mathbb{E}_{(s,a)\sim D_\mu}[\log D(s,a)] + \mathbb{E}_{(s,a)\sim D_G}[\log(1 - D(s,a))], \\ &\min_G -\lambda_Q \mathbb{E}_{s\sim D_{\text{aug}}, z\sim P_Z(\cdot)} \left[Q_\phi(s, G(z|s))\right] + \mathbb{E}_{(s,a)\sim D_G}[\log(1 - D(s,a)] \end{aligned} \tag{68}$$

Here, inspired by Eq. (67), D_G contains $(s, a)/(s', a')$ pairs collected in this way: $s \sim D_\mu, a \sim \pi_\theta(\cdot|s), s' \sim \widehat{\mathcal{T}}(\cdot|s, a), a' \sim \pi_\theta(\cdot|s')$, where $a \sim \pi_\theta(\cdot|s)$ is implemented as $a = G(z|s), z \sim P_Z(\cdot)$. The only difference between Eq. (66) and (68) is thus the way to generate samples. For Eq. (66), the (s, a) pairs are simply generated by $s \sim D_\mu, a \sim \pi_\theta(\cdot|s)$. The same authors have also proposed a model-free variant of this algorithm (Yang et al. (2022c)), sharing similar motivations and algorithm designs.

AMPL (Yang et al. (2022d)) adopts the same objective (i.e., Eq. (68)) for training π_θ, but proposes that the environment models $\widehat{\mathcal{T}}$ and $\hat{r}$ can be periodically updated with π_θ by collecting new data with π_θ and applying supervised learning (e.g., with Eq. (63)) to update $\widehat{\mathcal{T}}$ and $\hat{r}$. Interestingly, they theoretically show that the objective for π_θ, which combines the Q-function and distribution discrepancy, approximates

an upper bound for $-J(\pi_\theta, \mathcal{M})$, i.e, the negative expected return of the policy on the real MDP. On the other hand, **DASCO** (Vuong et al. (2022)) proposes that the two terms in the objective of π_θ may conflict with each other, since fooling the discriminator requires mimicking all in-distribution actions, which can be suboptimal, but maximizing the Q function would mean avoiding low-return behaviors. Thus, they propose to introduce an auxiliary generator G_{aux} to generate low-return samples and modify the objective as follows:

$$\min_{G, G_{\text{aux}}} \max_D \mathbb{E}_{(s,a)\sim D_\mu}[\log D(s,a)] + \mathbb{E}_{(s,a)\sim D_{G,G_{\text{aux}}}}[\log(1 - D(s,a))] - \lambda_Q \mathbb{E}_{s\sim D_{\text{aug}}, z\sim P_Z(\cdot)}\left[Q_\phi(s, G(z|s))\right] \quad (69)$$

Here, samples in $D_{G,G_{\text{aux}}}$ are generated as: $s \sim D_\mu, z \sim P_Z(\cdot), a = (G(z|s) + G_{\text{aux}}(z|s))/2$. Both G and G_{aux} are adopted to mimic the demonstrations, but only the primary generator G is trained to maximize the Q-values. Theoretically, they prove that the optimal solution for the primary generator G will maximize the probability mass of in-support samples that maximize the Q-function.

All aforementioned algorithms utilize a very similar objective design, which can be viewed as **a paradigm of using GANs for policy approximations in offline RL**. **GOPlan** (Wang et al. (2023a)) proposes an advantage-weighted CGAN objective, which is different in form from previous ones, for capturing the multi-modal action distribution in goal-conditioned offline planning:

$$\min_G \max_D \mathbb{E}_{g\sim D_\mu}\left[\mathbb{E}_{(s,a)\sim D_\mu^g}[w(s,a,g)\log D(s,a|g)] + \mathbb{E}_{s\sim D_\mu^g, z\sim P_Z(\cdot)}[\log(1 - D(s, G(z|s)|g))]\right] \quad (70)$$

Here, D_μ^g denotes the partition of D_μ that takes g as the goal; $w(s,a,g) = \exp(A^\mu(s,a,g))$ denotes the weight function, where $A^\mu(s,a,g)$ is a separately trained advantage function. This mechanism encourages the policy to produce actions that closely resemble high-quality (i.e., high-advantage) actions from the offline dataset, but no theoretical guarantee is provided.

4.2.3 World Model Representation through GANs

Beyond policy generation, GANs can also be used to approximate the environment models $\widehat{\mathcal{M}}$, as illustrated in MOAN (Yang et al. (2023a)), TS (Hepburn & Montana (2022)), S2P (Cho et al. (2022)), which is expected to outperform traditional supervised learning methods (i.e., using Eq. (63)). To be specific, **MOAN** proposes the following objective:

$$\begin{aligned} &\max_D \mathbb{E}_{(s,a,r,s')\sim D_\mu}[\log D(s,a,r,s')] + \mathbb{E}_{(s,a)\sim D_\mu, (\hat{r},\hat{s}')\sim G(\cdot|s,a)}[\log(1 - D(s,a,\hat{r},\hat{s}'))], \\ &\min_G -\lambda_N \mathbb{E}_{(s,a,r,s')\sim D_\mu}\left[-\log G(r,s'|s,a)\right] + \mathbb{E}_{(s,a)\sim D_\mu, (\hat{r},\hat{s}')\sim G(\cdot|s,a)}[\log(1 - D(s,a,\hat{r},\hat{s}'))] \end{aligned} \quad (71)$$

This objective design is similar with Eq. (68) in form, but replaces the Q-function term with a negative log-likelihood (i.e., $-\log G(r,s'|s,a)$) that is commonly used for environment model learning. In this CGAN framework, the conditional generator $G(\cdot|s,a)$ is learned to predict s' and r, working as the approximated reward $\hat{r}(s,a)$ and transition function $\mathcal{T}(s'|s,a)$. In particular, the generator $G(\cdot|s,a) = \mathcal{N}(\text{mean}(s,a), \text{std}(s,a))$ is implemented as a stochastic Gaussian model, and the standard deviation of the predictions, i.e., $\text{std}(s,a)$, can be used as uncertainty measure (i.e., $u(s,a)$ in Section 4.2.1). MOAN proposes to further include the confidence level given by the discriminator, i.e., $u(s,a) = \text{std}(s,a) + \sqrt{2(1 - D_{(\hat{r},\hat{s}')\sim G(\cdot|s,a)}(s,a,\hat{r},\hat{s}'))}$. Intuitively, if the variance of the estimation is high or the discriminator classifies the prediction as generated data, i.e., $D \to 0$, the uncertainty level at this point (s,a) should also be high. However, this objective design is not backed up by theoretical analysis.

Different from MOAN, TS and S2P are not limited to model-based offline RL. **TS** proposes to stitch high-value segments from different trajectories together to form higher-quality trajectories for offline RL. To realize this, they model the distribution $P(a,r,s'|s) = P(s'|s)P(a|s',s)P(r|a,s',s)$, that is, searching for a potential next state s' from the neighbourhood of s, which has a higher probability $P(s'|s)$ and value $V(s')$ than its original next state, and then identifying the most probable intermidiate a, r. In particular, they learn $P(s'|s)$, $P(a|s',s)$, $P(r|a,s',s)$ with the traditional supervised learning, CVAE, and WGAN (see Section 2.2), respectively. The WGAN objective is: ($G(z|s,a,s')$ works as the approximation of $P(r|a,s',s)$.)

$$\min_G \max_D \mathbb{E}_{(s,a,s',r)\sim D_\mu}[D(s,a,s',r)] - \mathbb{E}_{(s,a,s')\sim D_\mu, z\sim P_Z(\cdot)}[D(s,a,s',G(z|s,a,s'))] \quad (72)$$

Algorithm	GAN Type	GAN Usage	Evaluation Task
SGBCQ	CGAN	Policy	D4RL (L)
SDM-GAN	GAN	Policy	D4RL (L, M, A)
AMPL	GAN	Policy	D4RL (L, M, A)
DASCO	GAN (auxiliary generator)	Policy	D4RL (L, M)
GOPlan	CGAN (advantage-weighted)	Policy	MuJoCo Robotic Manipulation
MOAN	GAN	Environment Model	D4RL (L)
TS	WGAN	Environment Model	D4RL (L)
S2P	WGAN	Environment Model	dm_control
IOM	LSGAN	Representation Function	Design-Bench

Table 5: Summary of GAN-based offline RL algorithms. Most algorithms in this category have been evaluated on D4RL (Fu et al. (2020)), which provides multiple datasets for data-driven RL tasks, including Locomotion (L), AntMaze (M), Adroit (A), etc. MuJoCo Robotic Manipulation (Yang et al. (2023b)) provides offline datasets for a series of goal-conditioned robotic manipulation tasks, several of which can be utilized to assess the OOD generalization capabilities of the policy. dm_control (Tassa et al. (2018)) includes 6 environments, which are typically used for vision-based RL benchmarks. Design-Bench (Trabucco et al. (2022)) includes tasks specific for data-driven offline model-based optimization.

This algorithm can be viewed as a model-based data augmentation method for offline RL using generative models. **S2P** is a model learning approach for vision-based offline RL, where they first learn the approximated transition and reward model (i.e., $\widehat{T}(s'|s,a)$, $\hat{r}(s,a)$) for the underlying states through traditional supervised learning and then a generator to synthesize the image I/I' that perfectly represents the corresponding state s/s'. The generator is conditioned on both the current state and previous image, i.e., $I' = G(z|s, I)$, and trained within a WGAN framework. Finally, we briefly introduce an interesting work, i.e., **IOM** (Qi et al. (2022)), on offline model-based optimization, which cannot be categorized as either policy or world model approximation. They propose to address the distributional shift in offline decision-making by enforcing invariance between the learned representations in the source and target domains. Specially, they adopt an LSGAN (introduced in Section 2.2), where the generator works as the representation function of the data and the discriminator tries to discriminate between representations from the source and target domains. In this way, the discrepancy between distributions of representations under the source and target domains can be minimized.

As shown in Table 5, we provide a summary of GAN-based offline RL algorithms. GANs can be employed for both policy and world model approximations in model-based offline RL, primarily due to its use in minimizing distributional discrepancy.

5 Normalizing Flows in Offline Policy Learning

The applications of Normalizing Flows (NFs) in offline policy learning are less frequent compared to other deep generative models, particularly for NF-based offline RL methods. Thus, we slightly broaden the scope of the RL part to include online RL methods that utilize offline datasets in Section 5.2.

5.1 Imitation Learning

As mentioned in Section 2.3, NFs can convert a simple prior distribution $P_Z(z)$ on the latent space into a potentially intricate target distribution $P_X(x)$ through a sequence of bijections. NFs allow efficient sampling (i.e., via the generation direction $z \to x$) and exact density estimation (i.e., via the normalizing direction $x \to z$). In particular, for data generation, a sample $z \sim P_Z(\cdot)$ is drawn from the latent space, and then the data sample can be generated as $x = F^{-1}(z) = G(z)$. For the other direction, computing the density of a point x is accomplished by computing the density of its corresponding latent variable $z = F(x)$ and multiplying the associated Jacobian determinant $|\det D(F(x))|$, i.e., $P_X(x) = P_Z(F(x))|\det D(F(x))|$ where $P_Z(\cdot)$ is known.

NF-based IL works either employ NFs for exact density estimation or leverage their proficiency in modelling complex policies to manage challenging task scenarios. Next, we present a comprehensive review of works from both categories.

5.1.1 Exact Density Estimation in Imitation Learning Using Normalizing Flows

As a paradigm, NF-based IL methods that adopt NFs as density estimators usually start with standard IL objectives, and optimize them as RL problems wherein the rewards necessitate estimation of specific distributions. In this case, NFs are introduced to model those distributions and provide exact density inference for reward calculation, which greatly enhance the training stability and performance. To be specific, we present some representative works here:

As proposed in Ghasemipour et al. (2019b), most IL methods can be viewed as matching the agent's state-action distribution with the expert's, by minimizing some f-divergence D_f. **CFIL** (Freund et al. (2023)) realizes IL by minimizing the KL divergence between the agent's and expert's state-action occupancy measure (as defined in Section 4.1.1):

$$\arg\min_{\pi} D_{KL}(\rho_\pi(s,a)||\rho_E(s,a)) = \arg\max_{\pi} \mathbb{E}_{(s,a)\sim\rho_\pi(\cdot)}\left[\log\frac{\rho_E(s,a)}{\rho_\pi(s,a)}\right] = \arg\max_{\pi} J(\pi, r = \log\frac{\rho_E}{\rho_\pi}) \tag{73}$$

where $J(\pi, r)$ denotes the expected return (Sutton & Barto (2018)) of the policy π under the reward function r. MAF (Papamakarios et al. (2017)) is used to model the distributions $\rho_E(s,a)$ and $\rho_\pi(s,a)$ based on which the rewards can be acquired. Specifically, (s,a) can be viewed as x in the NF framework and the densities at (s,a), i.e., $\rho_E(s,a)$ and $\rho_\pi(s,a)$, can be estimated using Eq. (18). However, rather than optimizing these two NFs independently with corresponding MLE objectives (i.e., Eq. (19)), they couple the modelling of these two distributions based on the optimality point of the Donsker-Varadhan form of the KL divergence Donsker & Varadhan (1976):

$$D_{KL}(\rho_\pi(s,a)||\rho_E(s,a)) = \sup_{f:S\times A\to\mathbb{R}} \mathbb{E}_{(s,a)\sim\rho_\pi(\cdot)}\left[f(s,a)\right] - \log\mathbb{E}_{(s,a)\sim\rho_E(\cdot)}\left[e^{f(s,a)}\right] \tag{74}$$

In the equation above, optimality occurs with $f^*(s,a) = \log\frac{\rho_\pi(s,a)}{\rho_E(s,a)} + C$ where $C \in \mathbb{R}$. Thus, through maximizing the right-hand side of the equation above, the log ratio used as the reward function can be recovered. Specifically, they model f as $f_{\psi,\phi}(s,a) = \log\rho_\pi^\psi(s,a) - \log\rho_E^\phi(s,a)$ with the two flows ρ_π^ψ and ρ_E^ϕ. Given this improved estimator, the overall IL objective can be written as:

$$\arg\max_{\pi}\min_{\rho_\pi^\psi,\rho_E^\phi} \log\mathbb{E}_{(s,a)\sim D_E(\cdot)}\left[\frac{\rho_\pi^\psi(s,a)}{\rho_E^\phi(s,a)}\right] - \mathbb{E}_{(s,a)\sim\rho_\pi(\cdot)}\left[\log\frac{\rho_\pi^\psi(s,a)}{\rho_E^\phi(s,a)}\right] \tag{75}$$

In this case, the learning alternates between $\max_\pi$ and $\min_{\rho_\pi^\phi,\rho_E^\psi}$. $\max_\pi$ is realized with an RL process using $\log\frac{\rho_E^\psi(s,a)}{\rho_\pi^\phi(s,a)}$ as the reward function. While, $\rho_E^\psi(s,a)$ and $\rho_\pi^\phi(s,a)$ are updated with expert data (i.e., $(s,a)\sim D_E$) and rollout data collected by π (i.e., $(s,a)\sim\rho_\pi(\cdot)$).

IL-flOw (Chang et al. (2022)) focuses on Learning from Observations (LfO), where the agent only gets access to a dataset of state sequences. This work also starts with the KL divergence but processes to decouple the policy optimization from the reward learning to improve the training stability. In particular, the learning objective for the policy π is to maximize $-D_{KL}(P_\pi(s'|s)||P_E(s'|s))$:

$$\mathbb{E}_{s_{0:T}\sim P_\pi}\left[\sum_{t=0}^{T-1}\left(\log P_E(s_{t+1}|s_t) - \log P_\pi(s_{t+1}|s_t)\right)\right] = \mathbb{E}_{s_{0:T}\sim P_\pi}\left[\sum_{t=0}^{T-1}(\log P_E(s_{t+1}|s_t) + H(\pi(\cdot|s_t)))\right] \tag{76}$$

The equality holds when environment dynamics are deterministic and invertible. This can be optimized with RL by setting the reward as $r_t = \log P_E(s_{t+1}|s_t)$ while maximizing the entropy of the policy, i.e., $H(\pi(\cdot|s_t))$. As a separate stage, before the RL training, $P_E(s'|s)$ is modeled with a conditional NF (i.e., conditioning the transformation function F on a fixed state variable s: $s' = F(z|s),\ z\sim P_Z(\cdot)$) based on a dataset of demonstrations D_E. Specifically, they select NSF (Durkan et al. (2019)) as the density estimator.

SOIL-TDM (Boborzi et al. (2022; 2021b)) also focuses on LfO and starts with the same objective as IL-flOw. However, SOIL-TDM gets rid of the requirements for deterministic and invertible dynamics by estimating $P_\pi(s_{t+1}|s_t)$ as $\mathcal{T}_\pi(s_{t+1}|s_t, a_t)\pi(a_t|s_t)/\pi'(a_t|s_{t+1}, s_t)$, based on the Bayes Theorem. With this new definition, the objective for π is converted into:

$$\max_\pi \mathbb{E}_{(s_{0:T}, a_{0:T})\sim P_\pi} \sum_{t=0}^{T-1} [r(s_t, a_t) + H(\pi(\cdot|s_t))] \tag{77}$$

where $r(s_t, a_t) = \mathbb{E}_{s_{t+1}\sim\mathcal{T}_\pi(\cdot|s_t,a_t)} \Big[-\log \mathcal{T}_\pi(s_{t+1}|s_t, a_t) + \log \pi^{'}(a_t|s_{t+1}, s_t) + \log P_E(s_{t+1}|s_t)\Big]$. Still, they separate the reward learning from the policy optimization. In this case, besides the expert state transition model $P_E(s_{t+1}|s_t)$, they adopt conditional NFs to model the agent's transition dynamics $\mathcal{T}_\pi(s_{t+1}|s_t, a_t)$ and the posterior distribution associated with π, i.e., $\pi'(a_t|s_{t+1}, s_t)$, for which they choose Real NVP (Dinh et al. (2017)). Note that the approximation of $P_E(s_{t+1}|s_t)$ is trained on D_E, while approximations of $\mathcal{T}_\pi(s_{t+1}|s_t, a_t)$ and $\pi'(a_t|s_{t+1}, s_t)$ are trained on rollout data collected by π during the RL process.

SLIL (Zhang et al. (2021b)) is based on the Likelihood-based Imitation Learning (LIL) framework:

$$\max_\pi \mathbb{E}_{(s,a)\sim D_E} [\log P_\pi(s, a)] \;\; s.t. \; P_\pi = \arg\max_P \mathbb{E}_{(s,a)\sim\rho_\pi} [\log P(s, a)] \tag{78}$$

Intuitively, $P_\pi(s, a)$ represents the probability of observing an expert state-action pair $(s, a) \in D_E$ when executing the learner policy π. Directly solving this bilevel optimization problem requires jointly learning π and P_π, which brings training instability. Thus, they propose to maximize its tight lower bound:

$$\max_\pi \mathbb{E}_{(s,a)\sim D_E} [\log \pi(a|s)] + \mathbb{E}_{s\sim\rho_\pi} [\log P_E(s)] \;\; s.t. \; P_E = \arg\max_P \mathbb{E}_{s\sim D_E} [\log P(s)] \tag{79}$$

where $\rho_\pi(s)$ denotes the occupancy measure of s using π. The training process can then be divided into two stages for stability. At stage 1, they train an NF to model the expert state distribution $P_E(s)$ based on the demonstration set D_E, which is, at stage 2, adopted to optimize the policy $\pi(a|s)$ using Eq. (79). This objective combines Behavioral Cloning (i.e., $\max_\pi \mathbb{E}_{(s,a)\sim D_E} [\log \pi(a|s)]$) and RL with $\log P_E(s)$ as the reward (i.e., $\max_\pi \mathbb{E}_{s\sim\rho_\pi} [\log P_E(s)]$). It is worthy noting that they utilize a Continuous Normalizing Flow – DCNF (Zhang et al. (2021b)), rather than discrete ones like other works, as density estimators. This choice is due to the enhanced modeling capabilities and fewer model restrictions that Continuous Normalizing Flows offer Grathwohl et al. (2018).

GPRIL (Schroecker et al. (2019)) also utilizes the LIL framework but optimizes it in a different manner:

$$\max_{\pi_\theta} \mathbb{E}_{(s,a)\sim D_E} [\log P_{\pi_\theta}(s, a)] = \max_{\pi_\theta} \mathbb{E}_{(s,a)\sim D_E} [\log \pi_\theta(a|s) + \log P_{\pi_\theta}(s)] \tag{80}$$

Here, the first term of the right-hand side is simply Behavioral Cloning. While, for the second term, according to (Ross & Bagnell (2010)), the gradient from it can be estimated as $\nabla_\theta \log P_{\pi_\theta}(s) \propto \mathbb{E}_{(s'',a'')\sim\mathcal{B}_{\pi_\theta}(\cdot|s)} [\nabla_\theta \log \pi_\theta(a''|s'')]$, where $\mathcal{B}_{\pi_\theta}$ corresponds to the long-term predecessor distribution modelling the distribution of states and actions that, under the current policy π_θ, will eventually lead to the given target state s: $\mathcal{B}_{\pi_\theta}(s'', a''|s) = (1-\gamma)\sum_{j=0}^{\infty} \gamma^j P_{\pi_\theta}(s_t = s'', a_t = a''|s_{t+j+1} = s)$. In GPRIL, $\mathcal{B}_{\pi_\theta}(s'', a''|s)$ is modeled as $\mathcal{B}^{\omega_1}_{\pi_\theta}(s''|s) \cdot \mathcal{B}^{\omega_2}_{\pi_\theta}(a''|s, s'')$, i.e., the product of two density functions modelled by conditional MAF (Papamakarios et al. (2017)). To train these models, they collect training data using self-supervised roll-outs. In particular, they sample states, actions and target-states (i.e., (s'', a'', s)) where the separation in time between the s'' and s is selected randomly from a geometric distribution parameterized by γ. In this way, the triplets collected theoretically obey: $(s'', a'') \sim \mathcal{B}_{\pi_\theta}(\cdot|s)$. As a subsequent research, the work Schroecker & Jr. (2020) utilizes the same objective function, but introduces an alternative method for estimating $\nabla_\theta \log P_{\pi_\theta}(s)$ from a goal-conditioned RL perspective.

5.1.2 Policy Modeling in Imitation Learning with Normalizing Flows

As a potent generative model, Normalizing Flows can be directly adopted as policy generators for tackling challenging tasks. In this regard, recent works in off-policy RL have demonstrated that NFs can be used

Algorithm	CFIL	IL-flOw	SOIL-TDM	SLIL	GPRIL	Flow DAC	FlowPlan
Flow	MAF	NSF	Real NVP	DCNF	MAF	Real NVP	NAF
Flow Type	AR	CP	CP	ODE	AR	CP	AR
Flow Usage	DE ($\rho_E(s,a)$, $\rho_\pi(s,a)$)	DE ($P_E(s'\|s)$)	DE ($P_E(s'\|s)$, $\mathcal{T}_\pi(s'\|s,a)$, $\pi'(a\|s',s)$)	DE ($P_E(s)$)	DE $\mathcal{B}_\pi(s'',a''\|s)$	G (Policy Network)	G (Traj Planner)
Objective Type	KL	KL	KL	LIL	LIL	AIL	KL
Evaluation Task	MuJoCo	MuJoCo	MuJoCo	MuJoCo	Robotic Insertion	High-D & MuJoCo	HES-4D

Table 6: Summary of NF-based IL algorithms. AR, CP, and ODE represent autoregressive, coupling, and ODE-based continuous flows, respectively. DE and G represent the two manners that NFs can be used, corresponding to the density estimator and generator, respectively. For DE, we specifically point out the densities estimated, for which the definitions are available in Section 5.1.1. Regarding the types of IL objectives, KL, LIL, and AIL denote the KL divergence, Likelihood-based IL, and Adversarial IL, respectively. Examples for AIL include GAIL and AIRL, which are introduced in Section 4.1.1. For the benchmarks, MuJoCo (Todorov et al. (2012)) provides a series of robotic locomotion tasks; Robotic Insertion (Vecerík et al. (2017)) is a specific type of robotic manipulation task built on the MuJoCo engine; High-D (Krajewski et al. (2018)) and HES-4D (Meyer et al. (2019)) are two real-word driving dataset.

to model continuous policies (Haarnoja et al. (2018); Ward et al. (2019); Mazoure et al. (2019)), which can lead to faster convergence and higher rewards by enhancing exploration and supporting multi-modal action distributions. Compared with commonly employed diagonal Gaussian policies, where each action dimension is independent of the others, those based on NFs offer greater expressiveness. In the context of IL, **Flow DAC** (Boborzi et al. (2021a)) extends DAC (an off-policy IL algorithm Kostrikov et al. (2019)) by adopting a conditional version of Real NVP as the policy network. Specifically, the action a at state s is generated by: $z \sim P_Z(\cdot),\ a = G(z|s)$ where G denotes the NF generator and s is the conditioner. The stochasticity of this policy comes from the latent distribution $P_Z(\cdot)$, and the action output of G can be in any complex distribution. Similarly, **FlowPlan** (Agarwal et al. (2020)) adopts NFs as a trajectory generator through sequentially predicting the next state embedding based on historical states. Specifically, NAF is adopted as the generative model, which is trained by minimizing the KL divergence between the expert's and generated trajectories.

In Table 6, we provide a summary of NF-based IL algorithms. For each algorithm, we provide key information including what type of and how the NF is utilized, its underlying IL framework, and evaluation tasks.

5.2 Reinforcement Learning with Offline Data

As mentioned in the beginning of Section 5, we broaden the scope of RL-related works to include both offline RL (Section 5.2.1) and online RL with offline data (Section 5.2.2). Similar with NF-based IL methods, algorithms in Section 5.2.1 and 5.2.2 can be categorized based on the usage of NFs, i.e., working as either a density estimator or function generator.

5.2.1 Adopting Normalizing Flows in Offline Reinforcement Learning

Offline reinforcement learning aims to train a policy on a pre-recorded dataset, collected by the behavior policy $\mu(a|s)$, without any additional environment interactions. As introduced in Section 3.1.1, major challenges in this setting include (1) extrapolation error caused by approximating the value of state-action pairs not well-covered by the training data and (2) distributional shift between behavior and inference policies. The common practice to tackle these problems is to induce conservatism, through either keeping the learned policies closer to the behavioral ones or constructing pessimistic value functions. However, this can lead to over-conservative, yet sub-optimal policies. By introducing Normalizing Flows, an agent can more effectively

utilize offline data and circumvent out-of-distribution (OOD) actions through its generative (Akimov et al. (2022); Yang et al. (2023d)) or density estimation capacity (Zhang et al. (2023)).

CNF (Akimov et al. (2022)) and LPD (Yang et al. (2023d)) employ a similar algorithm idea – using NFs to extract latent variables underlying primitive actions in the offline dataset. Specifically, they train a Normalizing Flow G conditioned on s to model the mapping from z to a, following $z \sim P_Z(\cdot),\ a = G(z|s)$, through supervised learning (i.e., Eq. (19)). After training, G can work as an action decoder to convert a latent variable z (following a simple base distribution) to its corresponding action. In this case, only a high-level policy $z \sim \pi_{\text{high}}(\cdot|s)$ needs to be learned with offline RL, and the function composition $G \circ \pi_{\text{high}}$ can work as a hierarchical policy mapping from s to a. In particular, CNF and LPD are driven by different motivations. **CNF** pretrains a Real NVP conditioned on s as the action decoder. To avoid OOD actions caused by the long tail effect, the latent space (i.e., the support of $P_Z(\cdot)$), which is also the output space of the high-level policy, is designed to be bounded, specifically an n-dim interval $(-1, 1)^n$. As a result, the actor model (i.e., $G \circ \pi_{\text{high}}$) should be unable to generate OOD actions, even without clipping the high-level policy's output (as in PLAS introduced in Section 3.1.3), which avoids possible sub-optimality. **LPD**, instead, focuses on improving the offline RL performance in challenging, long-horizon tasks, by adopting NFs to model the transformation from z to a fixed-length sequence of actions starting from s, i.e., a skill. Provable benefits can be gained when the learned skills are expressive enough to recover the original policy space (Yang et al. (2023d)), and Normalizing Flows can facilitate the learning of such skills. With this pretrained transformation, the dataset can be relabeled in terms of skills as $D_{\text{high}} = [(s_0^i, z^i, \sum_{t=0}^{h-1} \gamma^t r_t^i, s_h^i)]_{i=1}^N$, where h is the skill length and z^i can be acquired as $G^{-1}(a_{0:h-1}^i|s_0^i) = F(a_{0:h-1}^i|s_0^i)$ (i.e., via the normalizing direction of the NF). Then, offline RL can be adopted to learn $\pi_{\text{high}(z|s)}$ from D_{high}.

APAC (Zhang et al. (2023)) adopts NFs (specifically Flow-GAN (Grover et al. (2018))) as density estimators, rather than action decoders as in aforementioned algorithms, to filter out OOD actions while avoiding being over-conservative. To be specific, the density of the point (s, a) can be approximated as $P_Z(G^{-1}(a|s))$, where G is the NF: $a = G(z|s)$. Points with higher density are more likely to be generated by the behavior policy and so can be viewed as "safe" in-distribution points for training use. To be specific, they modify the policy improvement step in Eq. (32) as:

$$\pi_{k+1} = \arg\max_{\pi} \mathbb{E}_{s\sim D_\mu} \left[\mathbb{E}_{a\sim\pi(\cdot|s)} Q_{k+1}^{\pi}(s, a)\right] \ \ s.t.\ P_Z(G^{-1}(a|s)) > \epsilon(s, a). \tag{81}$$

where $\epsilon(s, a)$ is a prefixed threshold. In this way, samples for updating the policy are restricted within the safe area, which could contain both observed and unobserved points in the offline dataset. Thus, the policy can potentially perform exploration out of the given dataset and avoid visiting OOD actions, simultaneously. Note that this constraint on π is more relaxed and practical compared with the one of BEAR (introduced in Section 3.1.1): $\pi \in \{\pi' : \mathcal{S} \times \mathcal{A} \to [0, 1] \mid \pi'(a|s) = 0 \text{ whenever } \mu(a|s) < \epsilon\}$, to avoid being over-conservative.

5.2.2 Adopting Normalizing Flows in Online Reinforcement Learning with Offline Data

To deepen the understanding of applying NFs for RL, we incorporate another line of work that merges online RL with offline data. Still, these works can be categorized as utilizing NFs as potent generators (Mazoure et al. (2019); Yan et al. (2022); Slack et al. (2022)) or density estimators (Wu et al. (2021)). From another perspective, these studies either extract useful information from the offline data and subsequently apply online RL atop it (Yan et al. (2022); Slack et al. (2022); Wu et al. (2021)), or they alternate between these two processes till the end of training (e.g., conducting off-policy RL) (Mazoure et al. (2019)).

With the same insights as Flow DAC (introduced in Section 5.1), **SAC-NF** (Mazoure et al. (2019)) extends SAC, an off-policy RL algorithm (Haarnoja et al. (2018)), by adopting NFs (IAF (Kingma et al. (2016))) as the policy network, which could potentially improve exploration and support multi-modal action distributions. On the other hand, CEIP (Yan et al. (2022)) and SAFER (Slack et al. (2022)) leverage the offline data by first learning a transformation from latent variables z to actions a using NFs as an action decoder and then training a high-level policy $\pi_{\text{high}}(z|s)$ atop the transformation function with (online) RL, akin to CNF. Yet, in comparison to CNF, they extend the action decoder learning from different perspectives. In **CEIP**, the generator is conditioned on a concatenation of the current and next states, i.e., $u = [s, s']$, instead of the state alone, which can better inform the agent of the state it should try to achieve with its current action.

Algorithm	CNF	LPD	APAC	SAC-NF	CEIP	SAFER	NF Shaping
Flow	Real NVP	Real NVP	Flow-GAN	IAF	Real NVP	Real NVP	MAF
Flow Type	CP	CP	CP	AR	CP	CP	AR
Flow Usage	G (Action Decoder)	G (Skill Decoder)	DE ($P_G(s,a)$)	G (Policy Network)	G (Action Decoder)	G (Action Decoder)	DE ($P_G(s,a)$)
Evaluation Task	D4RL (L, M)	D4RL (M, A, K)	D4RL (L, M)	MuJoCo	Kitchen, Office, FetchReach	Operation	Robotic Insertion, Pick Place

Table 7: Summary of NF-based (Offline) RL algorithms. AR and CP represent autoregressive and coupling flows, respectively. DE and G represent the two manners that NFs can be used, corresponding to the density estimator and generator, respectively. Specifically, $P_G(s,a)$ denotes the state-action pair distribution in the offline dataset. For the benchmarks, all the evaluation tasks shown in this table are built on the MuJoCo (Todorov et al. (2012)) engine; D4RL (Fu et al. (2020)) provides a bunch of challenging (robotic) tasks specifically for offline RL, including Locomotion (L), AntMaze (M), Adroit (A), Kitchen (K); Office (Pertsch et al. (2021)), FetchReach (Plappert et al. (2018)), Kitchen (from D4RL), Robotic Insertion, Pick Place (Vecerík et al. (2017)), and Operation (Slack et al. (2022)) all involve the manipulation of a robot arm.

Moreover, they propose a manner to utilize data from various yet related tasks, which are more accessible than task-specific ones. Specifically, they first train a flow for each task i with corresponding demonstrations. The generator is defined as $a = G_i(z|u) = \exp\{c_i(u)\} \odot z + d_i(u)$ where c_i and d_i are trainable deep nets, $\odot$ refers to the Hadamard product. This structure design follows Real NVP (Dinh et al. (2017)). Subsequently, they train a combination flow on demonstrations of the target task, with the generator defined as $G(z|u) = (\sum_{i=1}^{n} \mu_i(u) \exp\{c_i(u)\}) \odot z + (\sum_{i=1}^{n} \lambda_i(u) d_i(u))$. At this stage, they fix c_i and d_i $(i = 1, \cdots, n)$ and train the weighting functions μ_i and λ_i to optimize the combination flow for the designated task via supervised learning (i.e., Eq. (19)). In this way, they efficiently utilize demonstrations from related tasks. While, **SAFER** emphasizes the safety aspect of the learned transformation. Specifically, the transformation should prevent selecting unsafe actions a_{unsafe} in the environment, which are labeled in the training dataset. To achieve this, the authors propose conditioning the flow on both the state s and a safety context c. It's important to note that c is not provided directly but must be inferred from the information available in the environment. Thus, SAFER simultaneously learns (1) an inference network $P_\phi(c|\Lambda)$ to determine the current safety context c based on a sliding window of states Λ and (2) a generator $a = G_\theta(z|s,c)$ (Real NVP) conditioned on s and c, with the following objective:

$$\max_{\theta,\phi} \mathbb{E}_{s,a,a_{\text{unsafe}} \sim D_\mu,\ c \sim P_\phi(\cdot|\Lambda)} \left[\log P_\theta(a|s,c) - \lambda \log P_\theta(a_{\text{unsafe}}|s,c)\right] - D_{KL}(P_\phi(c|\Lambda)||P_C(c)) \tag{82}$$

Here, D_μ is the training dataset, $P_\theta(a|s,c) = P_Z(G_\theta^{-1}(a|s,c))$, $P_C(c)$ denotes the assumed prior distribution of c. Intuitively, the first two terms encourage safe actions while deterring unsafe ones, and, in conjunction with the final term, the variable c is compelled to encapsulate useful information regarding safety. This algorithm serves as an illustration of how NFs and VAEs can be integrated. In this setup, P_ϕ and P_θ function as the encoder and decoder of the VAE, respectively, with P_θ being implemented as a Normalizing Flow.

Unlike SAC-NF, CEIP, and SAFER, **NF Shaping** (Wu et al. (2021)) adopts NFs as density estimators. This is a method that combines (online) reinforcement and imitation learning by shaping the reward function with a state-and-action-dependent potential learned from demonstrations. To be specific, they first train an NF (specifically MAF Papamakarios et al. (2017)) to estimate the density of state-action pairs in the demonstration dataset, i.e., $P_G(s,a) = P_Z(G^{-1}(a|s))$. Then, they shape the reward function as $\widetilde{r}_t = r(s_t, a_t, s_{t+1}) + \gamma\Phi(s_{t+1}, a_{t+1}) - \Phi(s_t, a_t)$, where $\Phi(s,a) = \beta \log(P_G(s,a) + \epsilon)$, $\beta > 0$ adjusts the weight, and $\epsilon > 0$ is a small constant to prevent numerical issues. According to (Ng et al. (1999); Wiewiora (2003)), reward shaping can intensify the reward and greatly improve the learning efficiency. Intuitively, this potential

term highlights regions where the demonstrated policy visits more frequently, signaling areas that should be explored more.

To sum up, it's noteworthy that among all the aforementioned works, the algorithms proposed in (Akimov et al. (2022); Yang et al. (2023d); Yan et al. (2022); Slack et al. (2022)) adopt similar ideas. They first learn an NF-based transformation from a latent space to the real action space based on the offline data. Subsequently, they train a high-level policy on the latent variables, rather than primitive actions, with online or offline RL. The prelearned transformation constitutes a mapping from a simpler, more controllable distribution to the target distribution, which is usually complex and unknown. Moreover, we can see that Normalizing Flows are primarily used as exact density estimators in IL (Section 5.1), while mainly functioning as expressive generators in (Offline) RL (Section 5.2). We further provide Table 6 and 7 as summaries for NF-based IL and RL algorithms. It can be observed that most works adopt autoregressive or coupling flows, which is probably due to their computation efficiency. While almost all algorithms are evaluated on robotic benchmarks such as MuJoCo or D4RL, there is a notable absence of comparative analysis among these algorithms. Given the diverse perspectives from which these algorithms are developed, it is challenging to compare them at the algorithmic level, thus comprehensive and fair empirical evaluations are essential for practical applications.

6 Transformers in Offline Policy Learning

Transformers can be used for offline RL (Section 6.1) or IL (Section 6.2) by modeling them as a problem of predicting the next token based on historical data. Specifically, most works in this section follow a similar algorithm design with Decision Transformer – a seminal work of trajectory-optimization-based offline RL. Thus, we start with an introduction of the background on trajectory-optimization-based offline RL, and then provide a comprehensive review on transformer-based offline RL and IL algorithms.

6.1 Offline Reinforcement Learning

The content of this section is arranged as follows. First, we highlight pioneering studies on transformer-based offline RL in Section 6.1.1, along with a series of follow-up works for improvements (i.e., Section 6.1.2 and 6.1.3). Subsequently, we explore the use of transformers in broader problem scenarios in Section 6.1.4, such as multi-agent and multi-task RL. Specifically, for multi-task settings, we focus on the development of generalist agents based on pretraining and fine-tuning. Last, we reflect on existing problems in this field and discuss potential future research directions in Section 6.1.5.

6.1.1 Background on Trajectory-Optimization-based Offline Reinforcement Learning

Inspired by the great success of high-capacity sequence generation models (such as the transformer) in natural language processing (NLP), Chen et al. (2021b) proposes to view offline RL as a sequence modeling problem and solve it with a **Decision Transformer** (DT). This algorithm exemplifies trajectory-optimization-based offline RL, so we provide a detailed introduction of it, along with two other seminal works, as a brief tutorial on this particular branch of offline RL methods. In particular, given offline trajectories $\{\tau = (s_0, a_0, R_0, \cdots, s_T, a_T, R_T)\}$, where $R_t = \sum_{i=t}^{T} r_i$ denotes the return-to-go (RTG), the DT is trained to predict the next action based on the previous $k+1$ transitions:

$$\min_{\pi} \mathbb{E}_{\tau} \left[\sum_{t=0}^{T} (a_t - \pi(\tau_{t-k:t}))^2 \right], \text{ or } \min_{\pi} \mathbb{E}_{\tau} \left[\sum_{t=1}^{T} -\log \pi(a_t | \tau_{t-k:t}) \right] \tag{83}$$

where $\tau_{t-k:t} = (s_j, a_j, R_j, \cdots, s_t, R_t)$ $(j = \min(t-k, 0))$ is the input sequence; the two terms above are for tasks with continuous and discrete actions, respectively. DT adopts a GPT-like architecture (Radford et al. (2018)), which is a decoder-only transformer as introduced in Section 2.4. During evaluation rollouts, an initial target return R_0 must be specified, which can be the highest achievable return for the task. The inference trajectory is then generated autoregressively using the DT as follows: $s_0 \sim \rho_0(\cdot)$, $a_0 \sim \pi(\cdot|s_0, R_0)$, $s_1 \sim \mathcal{T}(\cdot|s_0, a_0)$, $r_0 = r(s_0, a_0, s_1)$, $\cdots$, $R_t = R_{t-1} - r_{t-1}$, $a_t \sim \pi(\cdot|\tau_{t-k:t})$, $\cdots$, where $(\rho_0, \mathcal{T}, r)$ are components of the MDP. DT greatly simplifies offline RL by eliminating the necessity to fit value

functions through dynamic programming or to compute policy gradients as detailed in Section 3.1.1. Using such a (supervised-learning based) sequence modeling objective makes it less prone to selecting OOD actions, because multiple state and action anchors throughout the trajectory prevent the learned policy from deviating too far from the behavior policy $\mu(a|s)$. Additionally, as a high-capacity model, the transformer has the potential to enhance both the scalability and robustness of the learned policy, similar to its applications in NLP. Per Chen et al. (2021b), DT shows competitive performance compared with prior offline RL methods (such as Conservative Q-Learning (CQL, Kumar et al. (2020))) especially for tasks with sparse and delayed reward functions. However, Emmons et al. (2022) investigate what is essential for offline RL via supervised learning (RvS) through extensive experiments. Their findings indicate that a two-layer MLP model, utilizing a simpler input format (i.e., (s_t, R_t) instead of $\tau_{t-k:t}$) and the same objective, exhibits competitive, and in some cases superior, performance compared to DT, and DT underperform prior offline RL algorithms on most benchmark tasks. This raises the questions whether it is necessary to adopt such a high-capacity model, i.e., the transformer, as the policy network, and under what scenarios RvS methods might outperform dynamic-programming-based offline RL methods.

Trajectory Transformer (TT, Janner et al. (2021)) follows DT but utilizes more techniques from NLP, including tokenization, discretization, and beam search. In particular, they treat each dimension of the state and action as a token and discretize them independently. Suppose the state and action have N and M dimensions respectively, the objective is $\min_\pi \mathbb{E}_\tau \left[\mathcal{L}(\tau)\right]$, where $\mathcal{L}(\tau)$ is defined as follows:

$$\sum_{t=0}^{T}\left[\sum_{i=1}^{N}\log\pi(s_t^i|s_t^{<i},\tau_{<t})+\sum_{j=1}^{M}\log\pi(a_t^j|a_t^{<j},s_t,\tau_{<t})+\log\pi(r_t|a_t,s_t,\tau_{<t})+\log\pi(R_t|r_t,a_t,s_t,\tau_{<t})\right] \tag{84}$$

This objective involves supervision on each dimension of the state/action, reward, and return-to-go. As for the inference process, a beam search technique (Freitag & Al-Onaizan (2017)) is utilized. Specifically, B most-likely samples are kept when sampling each of a_t^j, R_t sequentially. Then, samples $(a_t^{1:M}, R_t)$ with the highest cumulative reward plus return-to-go (i.e, the estimated trajectory return $\sum_{i=0}^{t-1} r_i + R_t$) is selected for execution. Note that, during the evaluation, $s_t^{1:N}$ and r_t can be acquired from the simulator. TT shows superior performance than DT in some benchmarks as reported in (Janner et al. (2021)), but treating each dimension separately would introduce learning and sample inefficiencies, especially for high-dimensional tasks.

Instead of modeling the policy, **Q-Transformer** (Chebotar et al. (2023)) proposes to learn a transformer-based Q-network. Similar with TT, each dimension of the action is discretized and treated as a separate time step. When training, they update the Q-function in a temporal difference (TD) manner, i.e., minimizing the disagreement between the predicted Q-value $Q(s_{t-k:t}, a_t^{1:i})$ and target Q-value $\widehat{Q}(s_{t-k:t}, a_t^{1:i})$. If $i = M$ (i.e., the action dimension), $\widehat{Q}(s_{t-k:t}, a_t^{1:i}) = r_t + \max_{a_{t+1}^1} Q(s_{t-k+1:t+1}, a_{t+1}^1)$; otherwise, it is $\max_{a_t^{i+1}} Q(s_{t-k:t}, a_t^{1:i}, a_t^{i+1})$. Note that for the Bellman optimality (Puterman (2014)) of this per-dimension updating rule to hold, it requires the assumption that the choice of $a_t^{1:i}$ does not influence $\max_{a_t^{i+1}} Q(s_{t-k:t}, a_t^{1:i}, a_t^{i+1})$. However, this is probably not true since dimensions of an action are likely to be correlated. During evaluation, the action is also generated dimension by dimension, based on the trained Q-function.

So far, we have introduced some fundamental algorithm designs to cast offline RL as sequence modelling problems based on transformers. Next, we will present follow-up improvements of these methods. As illustrated in (Emmons et al. (2022)), **carefully aligning the model structure/capacity with the training data to prevent overfitting or underfitting** and **choosing which information to condition the policy on** are critical for RvS performance. Thus, we will categorize the following works based on these two aspects.

6.1.2 Balancing Model Capacity with Training Data

To better align the capacity of transformer-based models with the amount of training data, a series of studies have been proposed focusing on augmenting the offline dataset to avoid overfitting. These algorithms provide data augmentation strategies for different task scenarios. (1) Based on TT, **Bootstrapped Transformer**

(Wang et al. (2022a)) proposes to generate trajectories from π, i.e., the model being learned, and adopt them as additional training data to expand the amount and coverage of the offline dataset. The self-generated trajectories are filtered by their log probability under the policy π, which indicates the quality and reliability of the training data. (2) **SS-DT** (Zheng et al. (2023)) introduces a data augmentation method for semi-supervised settings, where most trajectories lack action labels and are in the format $(s_0, r_0, \cdots, s_T, r_T)$. Their approach simply involves training an inverse dynamics model, i.e., $\mathcal{T}_{\text{inv}}(a_t|s_t, s_{t+1})$, on trajectories with action labels and then applying this model to predict actions for the unlabeled trajectories. (3) Given only sub-optimal trajectories, the trajectory-level supervised learning would fail. In this case, the agent needs to learn to stitch segments from different trajectories for an optimal policy. Value-based RL does not have the same issue as it pools information for each state across trajectories through the Bellman backup. In this case, **QDT** (Yamagata et al. (2023)) suggests learning a Q-function via CQL and replacing the RTG values (i.e., R_t) in the offline dataset with the learned Q-values for DT training. (4) **CDT** (Liu et al. (2023b)) proposes a data augmentation method for safe RL. Specifically, in a Constrained MDP (Altman (1998)), the DT conditioned on both $R(\tau)$ and $C(\tau) = \sum_{i=0}^{T} c_t$ (i.e., the constraint-violation cost of the trajectory) is expected to achieve the target trajectory return while ensuring that the accumulated cost remains lower than $C(\tau)$. However, during inference, unachievable $(R(\tau), C(\tau))$ pairs may be given as conditions, which are not represented in the offline dataset. Thus, as an augmentation, they suggest using the trajectories from the offline dataset that achieve the highest return without violating $C(\tau)$ as the corresponding trajectories of $(R(\tau), C(\tau))$ for offline training. (5) For tasks with sparse and delayed rewards, DT suffers from model degradation, since the RTG does not change within a trajectory. **DTRD** (Zhu et al. (2023a)) proposes to learn a reward shaping function $r_\phi(s, a)$ to redistribute the delayed reward to each time step. This is achieved by solving a bi-level optimization problem as below:

$$\min_{\phi} \mathcal{L}_{\text{val}}(\theta^*(\phi), \phi) \ s.t. \ R(\tau) = \sum_{t=0}^{T} r_\phi(s_t, a_t), \ \forall \tau, \ \text{and} \ \theta^*(\phi) = \arg\min_{\theta} \mathcal{L}_{\text{train}}(\theta, \phi) \tag{85}$$

Here, θ is the parameter of the policy π; $\mathcal{L}_{\text{train}}(\theta, \phi)$ denotes the DT objective on the training dataset, which is augmented by replacing the original sparse rewards r_t with $r_\phi(s_t, a_t)$; $\mathcal{L}_{\text{val}}(\theta^*(\phi), \phi)$ is the DT objective on the augmented validation dataset. Intuitively, r_ϕ is updated so that the policy learned from the dataset augmented with the dense rewards is optimal. They propose a practical alternative training framework for θ and ϕ, which however lacks convergence guarantee in theory.

Another line of works in this category focus on modifying the DT model to explicitly make use of the structural patterns within the training trajectories. As mentioned in Section 2.4, introducing strutual assumptions/priors to the input data can greatly improve the learning efficiency and mitigate the overfitting issue of learning on small-scale datasets. (1) Based on the observation that each trajectory is a sequence of state-action-reward triplets, **StARformer** (Shang et al. (2022)) proposes to first extract representations z_t from each (r_{t-1}, a_{t-1}, s_t), and then apply DT on $(z_1, \cdots, z_t)$ to predict a_t. Note that they adopt r_t rather than R_t, which is a counterintuitive design, as RL decision-making typically requires information on the future return. (2) **GDT** (Hu et al. (2023b)) follows the same motivation as StARformer, recognizing that naively attending to all previous tokens, as in DT, can overlook the causal relationships among certain types of tokens and thus hurt the performance. In particular, they introduce the relation embeddings to the compatibility calculation (i.e., Eq. (20)) for each pair of inputs (x_i, x_j). With this modification, the compatibility between the query Q_i and key K_j can be calculated as $\langle Q_i + re_{i\to j}, K_j + re_{j\to i}\rangle$, where re is an embedding of the adjacency matrix that represents the causal relationships among elements in the input sequence. For instance, a_t is directly influenced by s_t and R_t, so there should be edges from s_t to a_t and from R_t to a_t in the casual graph. In this way, they incorporate the Markovian relationship into the DT model. (3) **DTd** (Wang et al. (2023c)) views the state, action, and RTG as distinct modalities. By analyzing attention values from a trained DT, they rank the importance of token interactions (for decision-making) within or cross modalities. Specifically, $s - s$, $a - a$, $R - R < s - R$, $a - R < s - a$, where $s - s$ denotes interactions (i.e., attending via the MHA) between states, and '$<$' denotes being less important. Consequently, they suggest a hierarchical DT structure, processing less crucial interactions before more significant ones to prevent important interactions from being distracted. The resulting structure is large in scale and outperforms DT, but its overall performance is close to traditional offline RL methods like CQL.

6.1.3 Mitigating Impacts from Environmental Stochasticity

Another category of research works propose to change the conditional information of the DT to enhance its performance in stochastic environments. (1) In the absence of determinism, a high-return offline trajectory could be the outcome of uncontrollable environmental randomness, rather than the result of the agent's actions. Thus, goals that are independent from the environmental stochasticity are the only conditions that the learned agent can reliably achieve. **ESPER** (Paster et al. (2022)) and **DOC** (Yang et al. (2023c)) propose methods to learn such conditions automatically from the offline dataset. They share a common intuition: to ensure the conditional variable to contain sufficient information on action predictions but no information regarding the environment dynamics (e.g., on predicting future rewards or state transitions). Both algorithms use a contrastive learning framework, resulting in similar objectives. However, these methods require to learn at least five networks (so we choose not to show the objectives here), which is more complicated than traditional offline RL approaches. (2) **SPLT** (Villaflor et al. (2022)) proposes to model the policy as $\pi(\hat{a}_t|(s_{t-k}, a_{t-k}, \cdots, s_t), z_t^\pi)$, where the condition z_t^π is sampled from an encoder that takes $(s_{t-k}, a_{t-k}, \cdots, s_t, a_t)$ as input. Both the encoder and π have DT-like architectures and are trained jointly in a CVAE framework, where π works as the decoder, $(s_{t-k}, a_{t-k}, \cdots, s_t)$ and a_t work as the condition c and data point x respectively. z_t^π is a d_π-dim discrete vector, each dimension of which has c categories. Thus, extracted by the CVAE, each specific z_t^π can be viewed as a mode that is contained in the offline data and can be assigned to π as a generation condition. In the same manner, they learn a prediction model $\omega(\hat{r}_t, \hat{s}_{t+1}, \widehat{R}_{t+1}|(s_{t-k}, a_{t-k}, \cdots, s_t, a_t), z_t^\omega)$. During inference, with (π, ω) and by enumerating (z_t^π, z_t^ω), $c^{d_\pi \times d_\omega}$ predictions on future h-length trajectories $\hat{\tau}_t^h$ can be obtained, and the next action is selected from the mode: $\arg\max_{z_t^\pi} \min_{z_t^\omega} \widehat{R}(\hat{\tau}_t^h)$ for robustness, where $\widehat{R}(\hat{\tau}_t^h) = \sum_{i=0}^{h-1} \hat{r}_{t+i} + \widehat{R}_{t+h}$. Through enumeration, the influence brought by the environmental randomness can be mitigated. (3) **CGDT** (Wang et al. (2023d)) suggests training an additional Q-network to guide the learning of DT. The rationale behind this method is that the Q-value, representing the expected return for each state-action pair, can help mitigate the impact of environmental stochasticity that might be captured by single-trajectory RTG values.

6.1.4 Transformers in Extended Offline Reinforcement Learning Setups

DT has been extended to various offline RL setups, including model-based, hierarchical, multi-agent, and multi-task offline RL. Unlike the previous three subsections, extensions in this part primarily expand on the problem setup rather than the algorithmic aspect with respect to DT. Thus, this part is not our primary focus and we only provide a taxonomy and brief introduction of the related works, serving as a reference for readers.

Model-based/Hierarchical/Multi-agent Offline RL: (1) Wang et al. (2023b) propose **Environment Transformer** to model the transition dynamics and reward function $P(s_{t+1}, r_t|s_t, a_t)$ from the offline dataset, which can be viewed as simply replacing the output of DT, i.e., a_t, with (s_{t+1}, r_t) for the learning process. The learned environment model can then be utilized as a simulator for policy learning with any RL algorithm. **TransDreamer** (Chen et al. (2022)) suggests replacing the RNN module within Dreamer (Hafner et al. (2020)), which is a state-of-the-art (SOTA) model-based RL algorithm, with a transformer, for improved performance on tasks requiring modeling long-term temporal dependency. (2) **HDT** (Correia & Alexandre (2022)) employs two DTs for hierarchical decision making. The high-level DT models the distribution $\pi_{\text{high}}(g_t|s_{t-k}, g_{t-k}, \cdots, s_t)$ for selecting a subgoal, while the low-level DT captures the corresponding action distribution $\pi_{\text{low}}(a_t|s_{t-k}, g_{t-k}, a_{t-k}, \cdots, s_t, g_t)$. Moreover, they propose a heuristic approach for extracting subgoals $g_{1:T}$ from the offline trajectories, when these subgoals are not labeled. **Skill DT** (Sudhakaran & Risi (2023)) adopts a similar hierarchical framework, but proposes to use a VQ-VAE (introduced in Section 2.1) as the high-level policy to extract the skill choices for the low-level policy to condition on. (3) **MADT+Distillation** (Tseng et al. (2022)) is proposed to reformulate offline MARL as a sequence modelling problem. First, a teacher (joint) policy $\pi(a_t^{1:n}|o_{t-k}^{1:n}, R_{t-k}^{1:n}, a_{t-k}^{1:n}, \cdots, o_t^{1:n}, R_t^{1:n})$ is learned, as a manner of centralized training. The learning process is the same as DT, viewing the concatenation of observations (RTGs/actions) from n agents as a single joint observation (RTG/action). Then, π is distilled to n student (individual) policies $\pi^i(a_t^i|o_{t-k}^i, R_{t-k}^i, a_{t-k}^i, \cdots, o_t^i, R_t^i)$, for decentralized execution. The policy distillation process is designed for $\pi^{1:n}$ to imitate π while maintaining the structural relation among these agents as in the joint policy π, which though does not rely on transformers. There are some other explo-

rations for the multi-agent scenario: **MADT** (Meng et al. (2021)) investigates combining offline pretraining using DT and online adaptation with gradient-based MARL algorithms; **SCT** (Li et al. (2023a)) proposes approaches for handling non-cooperative MARL scenarios. However, these two works are still in early stages of development.

Multi-task Offline RL: As a foundation model, the transformer has demonstrated exceptional generalization capabilities in NLP and CV tasks. Thus, there is a branch of research works on enhancing DT to enable policies pretrained on source tasks to be effectively adapted to target tasks through fine-tuning. The target task may be the same as the source task, differ but still fall within the same task distribution with the source task, or belong to entirely different modalities from the source task. We provide a brief review of these three categories as follows, each progressively demanding greater generalization capabilities. (1) Further adaption on the same task may be required when the provided offline data is highly sub-optimal or only covers a limited part of the state space, for which **ODT** (Zheng et al. (2022)) introduces a technique to fine-tune the pretrained DT through further online interactions with the environment. Another possible scenario is when the high-quality and labelled offline data is scarce while there are abundant unlabeled (i.e., reward-free) and sub-optimal trajectories. In this case, **PDT** (independently proposed by Cang et al. (2022) and Xie et al. (2023)) can be used for unsupervised pretraining on the unlabeled data, followed by fine-tuning using the limited high-quality data. (2) Adaptation to unseen tasks within the same task distribution is a primary focus in multi-task/meta (offline) RL. For extending DT in this realm, some studies suggest conditioning the DT on task-specific information $z \sim P_Z(\cdot)$ and training the DT across a range of tasks, each associated with unique embeddings $z_{\text{train}} \sim P_Z(\cdot)$. Consequently, when encountering new tasks sampled from $P_Z(\cdot)$ and conditioning on the corresponding z_{test}, the policy is expected to be effective in these previously unseen tasks after few/zero-shot fine-tuning. z can be a task id (Lin et al. (2022a)), segment of a task trajectory (Xu et al. (2022b)), or trajectory embedding from an encoder (Lin et al. (2022b)). Alternatively, Boustati et al. (2021) suggests running the source policy in similar but counterfactual environments to gather augmented data for DT training, to enhance the robustness of the policy on unseen tasks. (3) So far, the transformer has been successfully adopted in NLP, CV, and RL, which makes it possible to build a transformer-based generalist agent across these three modalities. **Gato** (Reed et al. (2022)) shows that a single transformer with the same set of weights can handle 604 distinct tasks with varying modalities. Considering that texts, images, and decision trajectories can all be tokenized and embedded, the transformer can learn to generate all modalities within a unified training framework – predicting the next token based on previously generated ones. Specifically, the training objective aligns with Eq. (83), but substitutes the training data with sequences of words for text generation and sequences of image patches for image understanding. During training, each batch of training data incorporates sequences from various modalities and each sequence is concatenated with a demonstration for the same task, serving as a prompt to assist the agent in differentiating between modalities. Gato utilizes a decoder-only transformer with 1.2 billion parameters and is trained on a dataset containing 1.76 trillion tokens. The empirical results show that Gato achieves performance exceeding 50% of the expert score threshold in 450 of the 604 evaluation tasks. Gato represents a significant attempt in developing generalist agents, yet its efficacy heavily depends on the quantity and quality of the training data. Especially, when learning control policies, it doesn't utilize reward signals, so its performance would be capped by the provided demonstrations. **Multi-Game DT** (Lee et al. (2022)) adopts a similar protocol with Gato and suggests how to utilize reward signals in both the training and inference process. Another critical question regrading multi-modal learning is whether the learning in distinct modalities can enhance each other. Reid et al. (2022) empirically show that pretrained language models can be effectively adapted to offline RL tasks with boosted performance. Following this work, Takagi (2022) provides an excellent in-depth empirical study on the effect of cross-modality pretraining for DT. They find that parameters of the language-pretrained model do not change that much as a randomly-initialized model after the fine-tuning, and these stable parameters preserves context-equivalent information such that the agent can make decisions even in the absence of contexts (i.e., without using the previous k transitions as input). Further, the way to efficiently utilize these context-equivalent information is also preserved by those stable parameters. As a result, they conclude that pretrained context-like information could help the DT training by enabling the model to predict action more accurately. In contrast, a transformer pretrained on images performs significantly worse than a standard DT, partly due to the significant differences in data characteristics.

Algorithm	Key Novelty	Evaluation Task
DT	Solving offline RL as sequence modeling	Atari, D4RL (L)
TT	Tokenization, discretization and beam search	D4RL (L, M)
Q-Transformer	Transformer-based Q learning	Real Robot
Boot Transformer	Data augmentation with self-generated data	D4RL (L, A)
SS-DT	Data augmentation via an inverse dynamic model	D4RL (L, M2d)
QDT	Replacing RTGs with Q-values to enable stitching	D4RL (L, M2d)
CDT	Data augmentation for safe RL in constrained MDP	Bullet-safety-gym
DTRD	Data augmentation for sparse, delayed reward setups	Atari, MiniGrid, D4RL (L, K, M2d)
StARformer	Processing (r_{t-1}, a_{t-1}, s_t) as a group	Atari, dm_control
GDT	Embedding the causal relation among s, a, R	Atari, D4RL (L)
DTd	Processing s, a, R as three distinct modalities	D4RL (L, M)
ESPER	Replacing RTGs with a stochasticity-free conditioner	Stochastic Benchmark
DOC	Replacing RTGs with a stochasticity-free conditioner	MuJoCo, D4RL (M), FrozenLake
SPLT	Enumerating future trajs to mitigate stochasticity	CARLA
CGDT	Critic-guided DT training	D4RL (L, M)
Env Trans (MB)	Modeling the dynamic and reward functions	D4RL (L)
TransDreamer (MB)	Integrating Dreamer with a transformer architecture	Hidden Order Discovery, dm_control, Atari
HDT (HRL)	Subgoal-conditioned decision-making	D4RL (L, A, K)
Skill DT (HRL)	Skill extraction via a VQ-VAE	D4RL (L, M)
MADT+Dist (MA)	A centralized training with decentralized execution (CTDE) framework for MARL based on policy distillation	Fill-In, Equal Space, SMAC, Grid-World, Highway
MADT (MA)	Applying a shared DT to each agent's sequence	SMAC
SCT (MA)	A DT-based method for non-cooperative MARL	simple-tag, simple-world
ODT (PT)	An online fine-tuning method for DT	D4RL (L, M)
PDT (PT)	Pretraining on large-scale reward-free trajectories	D4RL (L)
MG DT (MT)	A single transformer agent for 46 Atari games	Atari
Gato (MT)	A generalist agent for 604 cross-modality tasks	See Reed et al. (2022)

Table 8: Summary of transformer-based offline RL algorithms. In Column 1, we list representative (but not all) algorithms in this section, where Boot Transformer, Env Trans, MADT+Dist, and MG DT correspond to Bootstrapped Transformer, Environment Transformer, MADT+Distillation, and Multi-Game DT, respectively. These algorithms are grouped by their categories, with abbreviations MB, HRL, MA, PT, and MT denoting model-based, hierarchical, multi-agent, pretraining-based, and multi-task offline RL, respectively. The evaluation tasks are listed in Column 3. Most works are evaluated on D4RL (Fu et al. (2020)), which provides offline datasets for various tasks, including Locomotion (L), AntMaze (M), Adroit (A), Kitchen (K), Maze2d (M2d). Regarding the other benchmarks, we provide their references here: Atari (Bellemare et al. (2013)), Real Robot (Chebotar et al. (2023)), Bullet-safety-gym (Gronauer (2022)), MiniGrid (Chevalier-Boisvert et al. (2018)), dm_control (Tassa et al. (2018)), Stochastic Benchmark (Paster et al. (2022)), MuJoCo (Todorov et al. (2012)), FrozenLake (Foundation (2023)), CARLA (Dosovitskiy et al. (2017)), Hidden Order Discovery (Chen et al. (2022)), SMAC (Samvelyan et al. (2019)), Fill-In & Equal Space & Grid-World & Highway (Meng et al. (2021)), simple-tag & simple-world (Li et al. (2023a)).

6.1.5 Reflections on Transformer-based Offline Reinforcement Learning

We notice that there is a series of works on applying transformers to **online** partially-observable RL (Yuan et al. (2023a)). They adopt the transformer as the policy network in gradient-based or actor-critic RL algorithms, with the hope to harness its ability to process long-horizon historical information for decision making. These works focus on architectural modifications of the standard transformer, which are specially tailored for RL. For example, **GTrXL** (Parisotto et al. (2020)) and **Catformer** (Davis et al. (2021)) suggest adjustments to the MHA module to facilitate a more stable RL training process; **ALD** (Parisotto & Salakhutdinov (2021)) adopts model distillation to improve the computation efficiency in transformer-based distributed RL; **STT** (Yang et al. (2022f)) and **WMG** (Loynd et al. (2020)) propose adaptions for the transformer to process spatiotemporal coupling observarions and factored observations, respectively, for enhanced sample efficiency. These architectural modifications, or potentially new ones, could be integrated with policy-gradient-based offline RL algorithms or DT-like return-conditioned supervised learning (RCSL) algorithms for performance improvement. Conducting an (empirical) comparison between these two categories (i.e., RCSL and policy gradient offline RL), both utilizing the same transformer architecture, would be an intriguing study. There is also a growing body of research on using the transformer as the policy/value network in other online RL settings. For multi-agent RL, notable examples include **MAT** (Wen et al. (2022)), **UPDET** (Hu et al. (2021)), **ATM** (Yang et al. (2022e)), and **TransMix** (Khan et al. (2022)); while in multi-task RL, there is **DCRL** (Dance et al. (2021)). These advancements can be potentially adapted to offline settings.

Finally, we reflect on these DT-like RCSL methods. Although a series of improvements have been made, there are still fundamental problems or limitations regarding these algorithms. According to (Brandfonbrener et al. (2022)), RCSL returns near-optimal policy under a set of assumptions that are stronger than those needed for traditional RL algorithms, and RCSL alone is unlikely to be a general solution for offline RL problems. In particular, RCSL offers guarantees only when the environment dynamics (including the state transition and reward functions) are nearly deterministic, a priori knowledge of the optimal conditioning function (i.e., the RTG values) is available, and the return distribution of the provided offline trajectories can cover the possible values of the conditioning function. These findings inspire several directions for future research. First, adapting RCSL algorithms to stochastic environments, ideally backed by theoretical optimality guarantees, is a clear necessity. Second, developing effective strategies for selecting RTG values as the conditions during inference, or alternatively, exploring new conditioning functions, is crucial. Last, a significant challenge lies in addressing out-of-distribution scenarios in case that the offline dataset lacks adequate coverage of the task scenarios. Another fundamental problem regarding RCSL is whether it is necessary to learn low-return behaviors from the offline dataset and to require strong alignment between the target return (i.e., the condition of the DT) and realized return. As indicated in Eq. (83), the policy training involves imitating trajectories across a range of returns. However, only high-return policy is required during inference. This raises the possibility of developing a more efficient mechanism that strategically utilizes low-return samples to enhance the learning of a high-return policy.

6.2 Imitation Learning

Similarly with DT, transformer-based IL utilizes a supervised learning paradigm (see Section 6.2.1), where the transformer is adopted as the policy backbone (see Section 6.2.2). We differentiate works for IL and offline RL simply by if the reward or return is used as a condition of the policy. A significant advantage of the transformer is its capability to process large quantities of training data across multiple modalities, which enables the development of generalist agents, as shown in Section 6.2.3.

6.2.1 A Paradigm of Transformer-based Imitation Learning

Given expert demonstrations $D_E = \{\tau_E = (s_0, a_0, \cdots, s_T, a_T)\}$, transformer-based IL algorithms are designed to learn a policy π to replicate expert behaviors. The objective function is typically formulated as follows:

$$\min_{\pi} \mathbb{E}_{D_E} \left[(a_t - \log \pi(s_t, x_{t-1} \cdots, x_{t-k}))^2 \right], \text{ or } \min_{\pi} \mathbb{E}_{D_E} \left[-\log \pi(a_t | s_t, x_{t-1}, \cdots, x_{t-k}) \right] \tag{86}$$

Here, $x_t \triangleq (s_t, a_t)$ or s_t, and π is implemented as a decoder-only transformer (as introduced in Section 2.4). This objective is similar in form with the one of DT (i.e., Eq. (83)) but replaces (s_t, a_t, R_t) with x_t. IL algorithms do not require reward signals but place an emphasis on the quality of demonstrations, which ideally should come from experts, as the learning process relies solely on imitation. Also, to make full use of demonstrations, auxiliary supervision objectives, such as prediction errors on the next state (i.e., the forward model loss) or the intermediate action between two consecutive states (i.e., the inverse model loss), are often employed. These objectives complement the action prediction error (i.e., Eq. (86)) to aid the policy learning process. As a representative, **Behavior Transformer** (**BeT**, Shafiullah et al. (2022)) empirically shows that a standard transformer architecture (specifically minGPT Brown et al. (2020)) can significantly outperform commonly-used policy networks, like MLP and LSTM, in learning from large-scale, human-generated demonstrations, which typically exhibit high variance and multiple modalities. In particular, x_t is defined as s_t. To cover the multiple modes in expert behaviors, the authors suggest dividing the action a into two components: its corresponding action center $\lfloor a \rfloor$ and the residual action $\langle a \rangle$, such that $a = \lfloor a \rfloor + \langle a \rangle$. The set of action centers can be acquired by applying K-means clustering to the expert actions. Correspondingly, they apply a policy network π with two prediction heads, one for the action center and the other for the residual action. Explicitly employing clustering to identify the various modes in expert actions and utilizing dual-head predictions to reason the mode of each instance significantly aids in modelling multi-modal actions. However, this approach does not model the multi-modality that may exist in the joint distribution of (s, a).

6.2.2 Adopting Transformers as the Policy Backbone for Imitation Learning

A series of studies (Kim et al. (2021); Pan et al. (2022); Kim et al. (2022); Zhu et al. (2022); Chen et al. (2023a); Kim et al. (2023); Liang et al. (2023a)) have adopted transformers as the policy backbone for imitation learning in complex control tasks, such as vision-based robotic manipulation and end-to-end self-driving. As introduced in Section 2.4, the transformer has various advantages over CNNs and RNNs. Firstly, the transformer is adept at processing time-series data (Kim et al. (2022)) by capturing the long-term temporal dependencies between inputs across different time steps. By using the current state as the query and historical data as keys and values, the transformer-based agent can pinpoint vital information in the sequence for the current decision-making through the attention mechanism. Secondly, the transformer can concurrently process various types of input data, such as texts and images (Kamath et al. (2023)), texts and voxels (Shridhar et al. (2022)), point clouds (Pan et al. (2022)), enabling it to be the backbone of an end-to-end deep learning agent. Each type of data can be embedded to vectors by (pretrained) domain-specific neural networks. Then, instead of simply concatenating all these embeddings for subsequent processing, the transformer treats each embedding as distinct tokens. As detailed in Section 2.4, each token possesses its own query, key, and value, and can attend to the other tokens for more informative aggregation. Thirdly, the transformer is efficient in processing input that contains multiple entities by modeling their interrelations. For example, **TSE** (Liang et al. (2023a)) takes the state of the ego vehicle, the status of surrounding vehicles, and lane information as input, explicitly reasoning the relationship between the ego vehicle and its surrounding environment for self-driving decision-making; **Silver-Bullet-3D** (Pan et al. (2022)) models the relationship of embeddings corresponding to different parts of the manipulated objects and robotic arms through the transformer for complex manipulation tasks; **VIOLA** (Zhu et al. (2022)) extracts a series of object-centric representations from the visual observation, introduces an extra action token (whose corresponding output is the action prediction), and applies a transformer on top of these tokens, so that the action token can learn to attend to and focus on task-relevant objects for improved performance in action prediction.

6.2.3 Developing Generalist Imitation Learning Agents with Transformers

Another research focus in this field is language-conditioned IL, aiming at training (robot) agents to follow human instructions. A language instruction, comprising a sequence of words, can be embedded into a sequence of tokens $(l_1, \cdots, l_m)$ through a pretrained language model or a predefined embedding table. (1) A straightforward method for language-conditioned IL, as shown in **TDT** (Putterman et al. (2022)), is to incorporate language tokens into the policy input, i.e., $\pi(a_t | s_t, x_{t-1}, \cdots, x_{t-k}, l_1, \cdots, l_m)$. Still, π is implemented as a decoder-only transformer, which, as previously mentioned, is capable of processing multiple types of input concurrently. **Perceiver-Actor** (Shridhar et al. (2022)) adopts a similar design, but suggests using the Perceiver Transformer (Jaegle et al. (2022)) as the policy backbone to manage extra long sequence of input

(e.g., a sequence of image/voxel patches from the vision input and word tokens from the language input). (2) **MARVAL** (Kamath et al. (2023)) uses an encoder-only transformer to process inputs comprising four modalities: instruction texts $(l_1, \cdots, l_m)$, historical states and actions $(x_{t-k}, \cdots, x_{t-1})$, the current state s_t, and the current action candidates $\mathcal{A}_t$. As discussed in Section 2.4, without the Masked MHA component as in the transformer decoder, each input token can attend to every other token for more informative aggregation. However, each forward pass predicts only a single action a_t, making it less efficient in training than the decoder-only transformer. In decoder-only transformers, the output token corresponding to the state input s_i is used to predict a_i $(i = 0, \cdots, t)$. In contrast, encoder-only transformers require a special action token, i.e., CLS, as an input to capture the fused representation of the entire sequence via the attention mechanism, and its corresponding output token is utilized to predict the current action a_t. Additionally, MARVAL introduces auxiliary tasks, including predicting the masked language tokens and predicting the proportion of the trajectory that has been completed, to increase the amount of supervision for more efficient use of the demonstrations. (3) Instead of using instruction texts as conditions, **Lang** (Hejna et al. (2023)) proposes to predict corresponding instructions from the state sequence as an auxiliary task, to realize language-guided IL. Specifically, each demonstration trajectory is divided into m segments, with each segment $(s_{T_i}, \cdots, s_{T_{t+1}-1})$ associated with a subtask instruction $l^{(i)} = (l_1^{(i)}, \cdots, l_{b_i}^{(i)})$. A transformer encoder is applied to extract representations $(z_1, \cdots, z_t)$ from the state sequence $(s_1, \cdots, s_t)$. These representations are expected to encompass information essential for predicting both actions and instructions, achieved by minimizing the following equation: $-\sum_{t=1}^{T} \log \pi(a_t|z_1, \cdots, z_t) - \lambda \sum_{i=1}^{m} \sum_{j=1}^{b_i} \log P(l_j^{(i)}|l_1^{(i)}, \cdots, l_{j-1}^{(i)}, z_1, \cdots, z_{T_i-1})$. This approach offers an alternative way to incorporate language instructions into action predictions and has proven effective when training with a limited amount of demonstrations.

Language-conditioned IL can be viewed as an instance of multi-task IL, where language texts serve as task contexts. (1) Generally speaking, $(l_1, \cdots, l_m)$ could be substituted with any form of task context (Furuta et al. (2022)). For example, Dasari & Gupta (2020) suggest using demonstration videos from human operators, denoted as v, as contexts for corresponding tasks. They train the policy $\pi(a_t|s_t, \cdots, s_{t-k}, v)$ using Eq. (86), supplemented by an inverse model auxiliary loss term. (2) **Transformer Adapter** (Liang et al. (2022)) presents an alternative approach for multi-task IL through pretraining and fine-tuning. Initially, a transformer policy $\pi(a_t|s_{t-k}, a_{t-k}, \cdots, s_{t-1}, a_{t-1}, s_t)$, without task contexts, is pretrained on extensive multi-task demonstrations using Eq. (86). It is then fine-tuned with a limited amount of task-specific demonstrations before application. For efficient fine-tuning, the pretrained model's parameters are kept unchanged. Instead, lightweight adapters (Houlsby et al. (2019)) are introduced between the pretrained model's layers, with only these adapters being updated using the task-specific demonstrations. The structure of the adapter can be $\text{Adapter}(X) = X + W_2^A(\text{GeLU}(W_1^A(X)))$, where GeLU (Hendrycks & Gimpel (2023)) is the activation function and $W_{1,2}^A$ are the weight matrices of the adapter, and it is inserted between the point-wise FFN layer and Add & Normalization layer of the transformer (as shown in Fig. (1)). The intuition behind this paradigm is that agents can acquire a diverse set of behavioral priors through large-scale task-agnostic pretraining, which then enables them to be efficiently fine-tuned for specific tasks. (3) As introduced in Section 6.1, the target of multi-task learning is a generalist agent, i.e., one model with a single set of weights that can be directly applied to a wide range of tasks. Different from Gato, which is directly trained on batches of prompt-conditioned demonstrations, **DualMind** (Wei et al. (2023)) introduces a dual-phase method. Specifically, in Phase I, the transformer policy $\pi(a_t|s_{t-k}, a_{t-k}, \cdots, s_{t-1}, a_{t-1}, s_t)$ is trained with self-supervised learning objectives to capture generic information of state-action transitions, where the self-supervision involves predicting the next state, predicting the current action, and reconstructing masked actions based on the other elements. In Phase II, a prompt p, which can be either language or image tokens, is added as a condition to the policy, i.e., $\pi(a_t|p, s_{t-k}, a_{t-k}, \cdots, s_{t-1}, a_{t-1}, s_t)$. To achieve this, extra Cross Attention layers are incorporated into the transformer decoder, enabling state/action tokens to attend to the prompt tokens. A small fraction of the transformer, including the Cross Attention layers, would then be trained via the prompt-conditioned IL, which is similar with TDT, using expert trajectories with associated prompts. This method emulates how humans learn to act in the world, i.e., acquiring skills in a task-agnostic manner and then learning specific tasks based on the acquired knowledge, and achieves superior performance in a series of robotic manipulation and navigation tasks. Abramson et al. (2021) propose **MIA**, a multi-modal interactive agent that can naturally interact and communicate with humans. The agent can be simply trained by imitation learning of human-human interactions and self-supervised learning through an auxiliary

Algorithm	Key Novelty	Evaluation Task
BeT	Dual-head predictions for the action center and residual action, seperately.	CARLA, Block Push, Franka Kitchen
TSE	A transformer-based policy for end-to-end self-driving.	SMARTS
Silver-Bullet -3D	A transformer-based control policy for complex manipulation skills with a robotic arm.	ManiSkill
VIOLA	Adopting the transformer to identify task-relevant objects in a multi-object environment.	Sorting, Stacking, BUDS-Kitchen, real-world tasks
TDT	Language-conditioned IL with the transformer.	Atari Frostbite
Perceiver-Actor	Applying the Perceiver Transformer to manage long input sequences in Language-conditioned IL.	RLBench, real-world tasks
MARVAL	Segmenting the input into 4 modalities and applying various auxiliary tasks for more efficient use of the demonstrations.	Matterport, Gibson
Lang	Improving long-horizon imitation by representation learning based on instruction predictions.	BabyAI, Crafting, ALFREAD
Transformer Adapter	Introducing Adapters to pretrained transformers for lightweight task-specific fine-tuning.	MetaWorld
DualMind	A dual-phase training framework for generalist agents.	MetaWorld, Habitat
MIA	Training an interactive agent by imitation of human-human interactions and self-supervision via modality matching.	3D Playhouse

Table 9: Summary of transformer-based IL algorithms. Representative (but not all) algorithms in this section with their key novelties and evaluation tasks are listed in this table. These algorithms are all grounded in the Behavioral Cloning framework, hence the algorithmic and theoretical advancements in this section are relatively modest. However, the learned transformer-based agents are evaluated on much more diverse, realistic, and challenging tasks. First, there are some commonly-used benchmarks. CARLA (Dosovitskiy et al. (2017)) is a simulated environment for self-driving tasks. Block Push (Florence et al. (2021)), Franka Kitchen (Gupta et al. (2019a)), RLBench (James et al. (2020)), MetaWorld (Yu et al. (2019c)) provide a range of robotic manipulation tasks, featuring various types of robots and input modalities. Habitat (Ramakrishnan et al. (2021)) provides navigation tasks for embodied AI in large scale 3D environments. BabyAI (Chevalier-Boisvert et al. (2019)), Crafting (Chen et al. (2021c)), ALFREAD (Shridhar et al. (2020)) offer instruction-conditioned tasks and datasets. Second, some algorithms have shown superior performance on competitions. In the table, SMARTS refers to the NeurIPS 2022 Driving SMARTS Competition (Rasouli et al. (2022)), and ManiSkill refers to SAPIEN ManiSkill Challenge 2021 (Mu et al. (2021)). Third, in the table, VIOLA, TDT, MARVAL, and MIA each develop their own environments or create large-scale training datasets tailored to their specific purposes. These efforts can be regarded as significant contributions alongside their algorithm designs. Readers are encouraged to read the respective papers for details.

task. Specifically, a multi-modal transformer is used to extract representations from the vision and language input tokens (i.e., s_t^V, s_t^L) and is trained through the following objective:

$$\max_{\pi,f,D} \mathbb{E}_{D_E}\left[\sum_{t=0}^{T} \log \pi(a_t|f(s_t^V, s_t^L), \cdots, f(s_0^V, s_0^L)) + \lambda \sum_{t=0}^{T}\left[\log D(f(s_t^V, s_t^L)) + \log(1 - D(f(s_t^V, \tilde{s}_t^L)))\right]\right] \quad (87)$$

Here, f denotes the transformer to extract representations, π is the overall policy which comprises multiple components besides f, D is a discriminator (as in GANs) which is introduced to encourage f to generate distinct representations for matched vision and text data (i.e., (s_t^V, s_t^L)) and unmatched ones (i.e., $(s_t^V, \tilde{s}_t^L)$). This modality matching auxiliary task, also used in (Mees et al. (2022a)), has shown to significantly improve the agent's performance beyond imitation learning alone.

We summarize the representative algorithms discussed in this section in Table 9, highlighting their key novelties and evaluation tasks. As mentioned in the beginning of this section, transformer-based IL algorithms fundamentally rely on the straightforward BC framework. However, these algorithms have demonstrated promising outcomes in complex robotic manipulation tasks, both simulated and real-world. This leads to an inspiring paradigm for robust robotic learning, that is, using a potent foundation model trained by imitation learning from extensive, high-quality demonstrations. Future research directions may include developing methods to synthesize high-quality training data at lower costs or enhancing/replacing the foundational algorithm BC with more advanced alternatives.

7 Diffusion Models in Offline Policy Learning

In this section, we present applications of Diffusion Models (DM) in IL (i.e., Section 7.1) and offline RL (i.e., Section 7.2). In particular, there is an emerging body of researches on DM-based offline RL algorithms, while more extensions/explorations could be made for DM-based IL.

7.1 Imitation Learning

Most works regarding applying Diffusion Models in IL are based on the Behavioral Cloning (BC) framework (Pomerleau (1991)). To be specific, the objective of BC is to train a policy π_θ with which the likelihood of the expert demonstrations can be maximized:

$$\max_\theta \mathbb{E}_{(s,a)\sim D_E} \left[\log \pi_\theta(a|s)\right] \tag{88}$$

As mentioned in Section 2.5, diffusion models have shown superior performance in modeling and generating data following a certain distribution, i.e., $P_X(x)$. Thus, many recent works have proposed to improve BC by implementing the policy network as a diffusion model to model the conditional distribution $P_{A|S}(a|s)$ within the expert data D_E. Further, as shown in Section 2.5, the objective for training DM (i.e., Eq. (27)) provides an upper bound for the negative log-likelihood, which naturally connects DM with BC. Next, we introduce these works in details, which are designed to solve drawbacks of the original BC algorithm from multiple perspectives.

7.1.1 Improving Policy Expressiveness in Imitation Learning with Diffusion Models

The first group of works (Pearce et al. (2023); Chi et al. (2023); Reuss et al. (2023)) try to improve the expressiveness of the learned policy. Through minimizing the Mean Square Error (MSE) shown as Eq. (88), the BC policy π_θ is trained to give out point estimates [17], which precludes it from capturing the multi-modality of the state-action pairs in D_E. Moreover, π_θ is encouraged to learn an average distribution, as the objective is to maximize an expectation, which would result in bias towards more frequently occurring actions. Additionally, $\pi_\theta(a|s)$ is usually implemented as a diagonal Gaussian policy, thus the prediction of each action dimension is independent, potentially leading to uncoordinated behaviours in high-dimensional action spaces. On the other hand, DM has shown great potential in generating high-dimensional samples that adhere to complex, multi-modal distributions, while ensuring the precision and diversity. In this case, **Diffusion BC** (Pearce et al. (2023)) is proposed to utilize the denoising (score) function ϵ_θ in DDPM (Ho et al. (2020)) to generate actions a at given states s. Similarly with Eq. (28), the IL objective is as follows: (Please refer to Section 2.5 for notation definitions.)

$$\min_\theta \mathbb{E}_{t\sim\mathcal{U}[1,T],(s,a)\sim D_E,\epsilon\sim\mathcal{N}(0,I)} \left[||\epsilon - \epsilon_\theta(a_t = \sqrt{\alpha_t}a + \sqrt{1-\alpha_t}\epsilon, t; s)||^2\right] \tag{89}$$

Note that s is the conditioner which is not interrupted in the diffusion process. With the learned ϵ_θ, the estimated expert action $a = a_0$ can be generated following the denoising process in DDPM:

$$a_{t-1} = \frac{1}{\sqrt{1-\beta_t}}(a_t - \frac{\beta_t}{\sqrt{1-\alpha_t}}\epsilon_\theta(a_t, t; s)) + \sqrt{\beta_t}\epsilon,\ t = T, \cdots, 1,\ a_T \sim \mathcal{N}(0, I) \tag{90}$$

[17] Each state-action pair (s, a) is a data point.

Further, **Diffusion Policy** (Chi et al. (2023)) is proposed to utilize DDPM for closed-loop action-sequence prediction. In particular, it models the distribution $P_{\vec{A}|\vec{S}}(\vec{a}|\vec{s})$ in D_E, where $\vec{s}$ and $\vec{a}$ denote the previous T_s states and future T_p actions, respectively. T_a out of the T_p actions are executed without replanning. This framework allows long-horizon planning, encourages temporal consistency of the action sequence, and remains responsive to the changing environment through receding horizon planning. In order to learn the joint distribution of the T_p actions conditioned on the historical states – a task that is inherently high-dimensional – Chi et al. (2023) suggest modeling it as $\epsilon_\theta(\vec{a}_t, t|\vec{s}_t)$, which is trained and sampled with a DDPM framework as delineated in Eq. (89) and (90).

Last, Reuss et al. (2023) propose **BESO** for goal-conditioned IL. Specifically, one or more future states within the same trajectory as (s, a) are used as the goal g. The objective is now to get a goal-conditioned policy $\pi_\theta(a|s, g)$, which is learned as a conditional score function $S_\theta(a_t, t; s, g)$ in a Score SDE framework (Karras et al. (2022)). With $S_\theta(a_t, t; s, g)$, the action at s targeting g can be generated with a Probability Flow ODE, as introduced in Section 2.5. Goal-conditioned policies distill useful, goal-oriented behaviors, which can be integrated with a high-level planner for various downstream tasks, as in Hierarchical RL. However, incorporating the goal conditioner amplifies the multimodal nature of the demonstrations, since the same goal might be achieved via various distinct trajectories, underscoring the necessity of employing DM. It's worthy noting that all three works suggest using transformers as the denoising function (i.e., $\epsilon_\theta, S_\theta$) for sample quality, rather than the commonly-used U-Nets (Ronneberger et al. (2015)) for DM.

7.1.2 Addressing Common Issues of Imitation Learning with Diffusion Models

Beyond enhancing policy expressiveness, numerous studies have explored the use of DM to address other challenges in IL, including spurious correlations (Saxena et al. (2023)) and noisy (suboptimal) demonstrations (Wang et al. (2023e); Yuan et al. (2023b)). To be specific, due to spurious correlations, expressive models, such as DM, may focus on distractors that are irrelevant to action prediction and thus fragile in real-world deployment, which resembles the causal misidentification issue introduced in Section 3.2.5. Thus, Saxena et al. (2023) propose **C3DM** to improve the denoising process of Diffusion BC as follows:

$$s_t = C(s; \text{pos}(a_t), t),\ a_{t-1} = \frac{1}{\sqrt{1-\beta_t}}(a_t - \frac{\beta_t}{\sqrt{1-\alpha_t}}\epsilon_\theta(a_t, t; s_t)) + \sqrt{\beta_t}\epsilon,\ t = T, \cdots, 1,\ a_T \sim \mathcal{N}(0, I) \quad (91)$$

Compared with Eq. (90), the only difference is to replace the conditioner s with s_t which is updated with the denoising process. In particular, at each denosing iteration t, the image state s is zoomed into the region around the intermediate action, i.e., $\text{pos}(a_t)$, to acquire more details for decision-making while ignoring distractors in other regions. Note that this work assume the access to a transformation between the action and state spaces to determine $\text{pos}(a_t)$. Accordingly, they modify the training process in Eq. (89) by replacing s with $C(s; \text{pos}(a), t)$. Further, considering that expert demonstrations in real-world scenarios are often noisy, Wang et al. (2023e) propose **DP-IL** to adopt DM for purifying/denoising the demonstrations. Sequentially, any IL algorithm can be applied on these purified data. To be specific, based on the DDPM framework, they view (s, a) as the data point x (in Eq. (28)) and learn a denoising function $\epsilon_\theta(x_t, t)$ to recover the original state-action demonstrations (i.e., x_0) from samples interrupted with Gaussian noise (i.e., x_t). Note that this training process is based on a set of "clean" demonstartions. Then, for imperfect data points $\tilde{x}$, the learned DM can be used to purify them by first adding random noise to $\tilde{x}$ to get $\tilde{x}_t$ (i.e., via the forward process) and then using ϵ_θ in the reverse denoising process to get the purified data $\tilde{x}_0$. Theoretically, they prove that $\tilde{x}_t$ and x_t can be arbitrarily closed in distribution as t increases, and so ϵ_θ trained on x_t can be used to convert $\tilde{x}_t$ into purified demonstrations as well. Different from the two-stage framework in DP-IL, **SMILE** (Yuan et al. (2023b)) is proposed to jointly perform the automatic filtering of noisy demonstrations and learning of the expert policy. It is based on Diffusion BC (i.e., Eq. (89) and (90)), but changes the forward diffusion process of DDPM as follows:

$$a_t \sim \pi^t(\cdot|s),\ \pi^t(a_t|s) = \int \pi^0(a_0|s)\mathcal{N}(a_t|a_0, \sigma_t^2 I)\ da_0,\ \sigma_t^2 = \sum_{k=1}^{t} \beta_k^2 \quad (92)$$

Here, π^0 denotes the underlying policy of the provided demonstrations. Through this equation, the diffusion process of SMILE is conducted on a policy level rather than on data points, and so the learned denoising

Algorithm	Diffusion BC	Diffusion Policy	BESO	C3DM	DP-IL	SMILE
DM Type	DDPM	DDPM	Score SDE	DDPM	DDPM	DDPM
DM Usage	Policy Generator	Policy Generator	Policy Generator	Policy Generator	Data Denoiser	Policy Generator
IL Framework	BC	BC	BC	BC	Not Limited	BC
Targeted IL Issues	Multimodal distribution	Multimodal distribution & HD data	Multimodal distribution	Spurious correlation	Noisy data	Noisy data
Evaluation Task	Kitchen, CSGO	Kitchen, Push-T, Block-Push, Robomimic	Kitchen, Block-Push, CALVIN	Autodesk, Real Robot	MuJoCo	MuJoCo

Table 10: Summary of DM-based IL algorithms. Specifically, "HD" is short for "high-dimensional". Regarding the evaluation tasks, Kitchen (Gupta et al., 2019b), Block-Push & Push-T (Florence et al., 2022), Robomimic (Mandlekar et al., 2021b), CALVIN (Mees et al., 2022b) are robotic manipulation tasks in different scenarios; CSGO (Pearce & Zhu, 2022) is a 3D First-person Shooter video game; Autodesk (Koga et al., 2022) and Real Robot (Saxena et al., 2023) represent robotic manipulation tasks built on the Autodesk simulator and real robot platforms, respectively; MuJoCo (Todorov et al. (2012)) provides a series of robotic locomotion tasks.

function ϵ_θ can be used to compare the suboptimality among behavior policies underlying different trajectories (i.e., with Eq. (13) in (Yuan et al. (2023b))). Trajectories generated using policies noisier than the currently learned one are then filtered out from the training dataset.

While not exclusively designed for DM-based IL, the studies by Shi et al. (2023) and Sridhar et al. (2023) introduce techniques — namely, **AWE** and **MCNN** — that further enhance the performance of Diffusion Policy and Diffusion BC, respectively. Both techniques focus on mitigating the compounding errors of IL, i.e., prediction errors compounded over the decision horizon. AWE can be applied to automatically extract waypoints within an expert trajectory. The waypoint sequences are notably shorter in horizon and can then be used for waypoint-only imitation. On the other hand, MCNN doesn't modify the training data but enhances the policy for reduced errors. During evaluation, it identifies the nearest neighbor state of the current state in the expert dataset, and then blends the corresponding expert action with the output of the learned policy network to formulate an error-constrained policy.

In Table 10, we present a summary of DM-based IL methods. This includes their base IL algorithms, the specific IL challenges they aim to address, and how DM is used in resolving these issues. There are several promising future research directions in this field. Firstly, while most current works rely on DDPM for its robust performance, future studies could explore more advanced DM, particularly those with efficient sampling schemes which are crucial for sequential decision-making [18]. Secondly, given that these works target various IL issues, the development of a unified (DM-based) algorithm capable of simultaneously resolving multiple issues is also a promising direction. Finally, integrating DM with more advanced IL frameworks, as listed in Table 6, could offer solutions to fundamental issues in BC.

7.2 Offline Reinforcement Learning

Recently, there is an emerging body of advancements in applying Diffusion Models to offline RL (Zhu et al. (2023c)). In particular, Diffusion Models can be adopted as the policy, planner, or data synthesizer in the context of offline RL, as introduced in Section 7.2.1 - 7.2.3. Additionally, we present the applications of DM

[18] At each time step, to sample $a \sim \pi_\theta(\cdot|s)$, the entire denoising process (with T iterations) shown as Eq. (90) needs to be executed, thus the sampling efficiency of DM is essential.

for extended offline RL setups in Section 7.2.4. For each category, we introduce the seminal works in details as a tutorial on its paradigm, followed by a brief review of the extensions with a focus on their key novelties.

7.2.1 Diffusion Models as Policies

As introduced in Section 3.1.1, in order to alleviate the value overestimation issue caused by OOD actions, four offline RL schemes are developed. Among them, DM-based offline RL usually follows the policy constraint method, that is, constraining the learned policy π_θ to the behavior policy μ while maximizing the Q-function:

$$\max_\theta \mathbb{E}_{s\sim D_\mu}\left[\mathbb{E}_{a\sim\pi_\theta(\cdot|s)}Q_\phi(s,a) - \lambda D_{KL}(\pi_\theta(\cdot|s)||\mu(\cdot|s))\right] \tag{93}$$

where Q_ϕ is a learned Q-function for the current policy π_θ, and $\lambda > 0$ is the Lagrangian multiplier [19]. Such an optimization problem has a closed-form solution, i.e., $\pi^*(a|s) = \frac{1}{Z(s)}\mu(a|s)\exp(\frac{1}{\lambda}Q_\phi(s,a))$, where $Z(s)$ is the partition function for normalization. Suppose that π^* can be represented as a parametric function, then the optimal policy can be learned through weighted regression (Wang et al. (2020)) as below:

$$\max_\theta \mathbb{E}_{(s,a)\sim D_\mu}\left[\frac{1}{Z(s)}\log\pi_\theta(a|s)\exp(\frac{1}{\lambda}Q_\phi(s,a))\right] \tag{94}$$

Therefore, the parametric policy π_θ should be expressive enough to recover the optimal policy.

In this case, DM can be employed to model the policy π_θ. (1) **SfBC** (Chen et al. (2023b)) provides a straightforward manner to realize this. It first imitates the behavior policy $\mu(a|s)$ with a DM $\pi_\theta(a|s)$ (specifically, Score SDE) in an IL scheme as introduced in Section 7.1.1. Then, for any state s, N actions are sampled with $\pi_\theta(\cdot|s)$ as candidates, and one action is resampled from these candidates with $\exp(\frac{1}{\lambda}Q_\phi(s,a))$ being the sampling weights. In this way, $a \sim \pi^*(\cdot|s)$ is approximated via importance sampling. Note that $Q_\phi(s,a)$ can be learned with any offline RL protocol. **IDQL** (Hansen-Estruch et al. (2023)) adopts the same resampling scheme but imitates $\mu(a|s)$ with DDPM. Additionally, rather than using $\exp(\frac{1}{\lambda}Q_\phi(s,a))$, they design a sampling weight based on the Implicit Q-Learning framework (Kostrikov et al. (2022)), which is a SOTA offline RL algorithm. (2) Alternatively, the Q-function $Q_\phi(s,a)$ can be directly involved in training the DM policy $\pi_\theta(a|s)$. In particular, **Diffusion-QL** (Wang et al. (2023f)) learns a DDPM-based policy through the following objective:

$$\min_\theta \mathcal{L}_{DM}(\theta) - \frac{\eta}{\mathbb{E}_{(s,a)\sim D_\mu}\left[|Q_\phi(s,a)|\right]}\mathbb{E}_{s\sim D_\mu, a_0\sim\pi_\theta(\cdot|s)}\left[Q_\phi(s,a_0)\right] \tag{95}$$

Here, $\mathcal{L}_{DM}(\theta)$ is defined as Eq. (89) (i.e., an IL objective) and can be replaced by the corresponding training objective if a different DM is employed, π_θ is implied by the denoising function ϵ_θ, a_0 is the action sample after being denoised for T iterations (with Eq. (90)), $\mathbb{E}_{(s,a)\sim D_\mu}\left[|Q_\phi(s,a)|\right]$ is incorporated for adaption to Q-functions with different scales. Intuitively, the Q-function acts as guidance in the reverse generation process of the DM. Also, Eq. (95) mirrors Eq. (93), since both equations encourage the learned policy to maximize Q-values while being closed to the behavior policy, and it's noteworthy that DiffCPS (He et al. (2023b)) provides a theoretical connection between Eq. (95) and Eq. (93).

Following Diffusion-QL, several algorithms adopting a similar objective design with Eq. (95) have been proposed, including SRDP (Ada et al. (2023)), EDP (Kang et al. (2023)), and Consistency-AC (Ding & Jin (2023)). To be specific, **SRDP** additionally introduces a state-reconstruction loss term in Eq. (95) to enable generalization for OOD states through self-supervised learning (Liu et al. (2023a)). **EDP** improves the sampling efficiency of Diffusion-QL by modifying the sampling process $a_0 \sim \pi_\theta(\cdot|s)$ in Eq. (93). Instead of iterative sampling with Eq. (90), it first samples a_t via the forward process and then approximates a_0 as $\frac{1}{\sqrt{\alpha_t}}a_t - \frac{\sqrt{1-\alpha_t}}{\sqrt{\alpha_t}}\epsilon_\theta(a_t,t;s)$, since $a_t = \sqrt{\alpha_t}a_0 + \sqrt{1-\alpha_t}\epsilon$ and ϵ_θ is trained to estimate ϵ. Similarly, as a new variant of DM, Consistency Models (Song et al. (2023)) aims to learn a consistency function f_θ that can map the noisy sample at any iteration t to its original sample in just one iteration. **Consistency-AC** thus replaces DDPM in Diffusion-QL with a Consistency Model to improve the sampling efficiency.

[19] As a common practice, λ can be fine-tuned as a hyperparameter, controlling the tradeoff between the two objective terms.

At last, there are two works: QGPO (Lu et al. (2023)) and CPQL (Chen et al. (2023e)) aiming to directly learn the score function of the optimal policy: (This is derived from the definition of π^*, where $\alpha = 1/\lambda$.)

$$\nabla_{a_t} \log \pi^*(a_t|s) \propto \nabla_{a_t} \log \mu(a_t|s) + \nabla_{a_t} \alpha Q_\phi(s, a_t) \tag{96}$$

As mentioned in Section 2.5, with the score function $\nabla_{a_t} \log \pi^*(a_t|s)$, samples $a_t \sim \pi^*(\cdot|s)$ can be generated via various efficient score-based sampling schemes [20]. Here, the score function $\nabla_{a_t} \log \mu(a_t|s)$ can be learned with Score-based DM from D_μ, as introduced in Section 2.5, but $\nabla_{a_t} \alpha Q_\phi(s, a_t)$ relies on the Q-functions over intermediate samples a_t, which is intractable. As potential solutions, **QGPO** propose a contrastive learning framework to estimate $\alpha Q_\phi(s, a_t)$, $\forall t$. While, **CPQL** employs Consistency Models as the policy, reframes the score function estimation in Eq. (96) into an objective similar to Eq. (95), and theoretically establishes their equivalence when the weights for the two terms in Eq. (95) are properly assigned.

In Table 11, we provide a summary of these algorithms. All the algorithms in this category have been evaluated on the D4RL benchmark. Readers can refer to corresponding papers for the numeric evaluation results to compare their performance. In particular, we notice that three schemes of using diffusion models as policies for offline RL have been developed: SfBC & IDQL, QGPO & CPQL, and the other works that follow Diffusion-QL. Among them, QGPO & CPQL choose to directly learn the score function for the policy, which is a quite challenging but promising direction for future works.

7.2.2 Diffusion Models as Planners

For model-based offline RL, a dynamic function $\mathcal{T}_\psi(s^{k+1}|s^k, a^k)$ needs to be approximated from the dataset first, and then planning over the optimal action sequence $(a_*^1, \cdots, a_*^K)$ can be done by maximizing the return while avoiding OOD actions: (For clarity, we use superscript k to indicate the time step and subscript t to denote the iteration of the diffusion process.)

$$\max_{a^{1:K}} \sum_{k=1}^{K} r(s^k, a^k) - \lambda d_\mu(s^k, a^k) \ s.t. \ s^{k+1} = \mathcal{T}_{\psi^*}(s^k, a^k) \tag{97}$$

Here, $\psi^* = \arg\min_\psi \mathbb{E}_{D_\mu} \left[||s^{k+1} - \mathcal{T}_\psi(s^k, a^k)||^2 \right]$, $d_\mu(s^k, a^k)$ represents the uncertainty assessing whether the data point (s^k, a^k) conforms to the data distribution in D_μ. **SGP** (Suh et al. (2023)) proposes to implement $d_\mu(s, a)$ as the negative log-likelihood of (s, a) under a perturbed distribution, i.e., $-\log P_\sigma((s, a); D_\mu)$ where $P_\sigma(x; D_\mu) = \frac{1}{|D_\mu|} \sum_{x_i \in D_\mu} \mathcal{N}(x; x_i, \sigma^2 I)$. Intuitively, this likelihood measures the distance of (s, a) to the dataset D_μ and a large distance indicates a high uncertainty of the point (s, a) as it may be OOD. Then, to optimize Eq. (97) for trajectory planning, the score function $\nabla_a \log P_\sigma((s, a); D_\mu)$ needs to be estimated. As detailed in (Suh et al. (2023)), this estimation can be obtained using a denoising function in DM (specifically, SGM).

A more widely-adopted manner for planning with DM, which is firstly proposed in **Diffuser** (Janner et al. (2022)), is to fold the two processes mentioned above: transition dynamic modeling and trajectory optimization regarding $a^{1:K}$, as a trajectory modeling process using DM. Viewing trajectories $\tau = ((s^1, a^1), \cdots, (s^K, a^K))$ as data points (i.e., x in Eq. (28)), DDPM is used to model the distribution of τ in D_μ, through Eq. (28) where a denoising function for trajectory generation $\epsilon_\theta(\tau_t, t)$ is learned. Then, the planning can be done by sampling trajectories starting from the current state using the learned DM. The sampling process is similar with Eq. (90). However, for optimality, this process is guided by a (separately-trained) return function of the trajectory samples, i.e., $J_\phi(\hat{\tau})$ [21]: (β_t, α_t, and Σ_t are hyperparameters and defined in Section 2.5.)

$$\tau_{t-1} \sim G_\theta(\cdot|\tau_t, g) = \mathcal{N}(\mu_t + \Sigma_t g, \Sigma_t), \ \mu_t = \frac{1}{\sqrt{1-\beta_t}}(\tau_t - \frac{\beta_t}{\sqrt{1-\alpha_t}}\epsilon_\theta(\tau_t, t)), \ g = \nabla_{\hat{\tau}} J_\phi(\hat{\tau})|_{\hat{\tau}=\mu_t} \tag{98}$$

This process is also known as classifier-guided sampling (CG (Dhariwal & Nichol (2021))), which is widely adopted for conditional generations with diffusion models. Intuitively, the generation is guided by the

[20] Note that a_t represents the sample at the t-th diffusion iteration rather than the action at time step t.

[21] $J_\phi(\hat{\tau})$ is trained to estimate the return of the original trajectory, i.e., $J(\tau) = \sum_{k=1}^{K} r(s^k, a^k)$, where $\hat{\tau}$ can be the trajectory sample at any diffusion iteration, i.e., τ_t.

gradient $\nabla_\tau J(\tau)$ along which the expected return $J(\tau)$ would be maximized, aligning it with RL. In (Janner et al. (2022)), the authors connect this guided sampling design with the control-as-inference framework of RL (Levine (2018)) and claim that trajectories from such a generation process follows the distribution $P(\tau|\mathcal{O}_{1:K} = 1)$, where $\mathcal{O}_k = 1$ indicates the optimality of the time step k. During evaluation, the learned DM can applied as follows: ($\mathcal{T}$ is the real dynamic.)

$$[\tau_t(s^1) \leftarrow s^k,\ \tau_{t-1} \sim G_\theta(\cdot|\tau_t, g)]_{t=T}^1,\ a^k \leftarrow \tau_0(a^1),\ s^{k+1} \sim \mathcal{T}(\cdot|s^k, a^k),\ k = 1, \cdots, K \tag{99}$$

To determine a^k, trajectory samples at each iteration are forced to start with the current state, i.e., $\tau_t(s^1) \leftarrow s^k$ $(t = 1, \cdots, T)$. This follows the idea for solving inpainting problems (Sohl-Dickstein et al. (2015)), where the generation for the unobserved part is in a manner consistent with the observed constraints. Moreover, only the first action in the generated plan, i.e., $\tau_0(a^1)$, is executed without replanning, which aligns with the receding horizon control (Mayne & Michalska (1988)). **Decision Diffuser** (Ajay et al. (2023)) adopts similar designs with two key modifications. First, instead of training a return function for classifier-guided sampling, they adopt classifier-free guided sampling (CFG (Ho & Salimans (2022))), for which a conditional and an unconditional denoising function, i.e., $\epsilon_\theta(\tau_t, t; J(\tau))$ and $\epsilon_\theta(\tau_t, t; \emptyset)$, are jointly trained (with Eq. (28)) by randomly dropping out the condition $J(\tau)$. The trajectory generation process is the same as Eq. (90), but replaces the standard denoising function $\epsilon_\theta(\tau_t, t)$ with $\omega\epsilon_\theta(\tau_t, t; J(\tau)) + (1-\omega)\epsilon_\theta(\tau_t, t; \emptyset)$. Increasing the value of ω would decrease the diversity of samples but aligns the trajectory distribution more closely with $P(\tau|\mathcal{O}_{1:K} = 1)$. Notably, both CG and CFG can be utilized for generating samples that satisfy specific conditions y. In the context of RL, y can be the desired return $J(\tau)$, constraints to obey, task-specific information (for multi-task RL), subgoals/subtasks (for hierarchical RL), and so on. Second, only state sequences are modelled and predicted with the DM, i.e, $\tau = (s^1, \cdots, s^K)$ and actions are predicted with a separate inverse dynamic model, i.e., $a^k = \mathcal{T}_{\text{inv}}(s^k, s^{k+1})$. This is because sequences over actions tend to be more high-frequency and less smooth, making them much harder to predict and model.

Following Diffuser and Decision Diffuser, improvements have been made in multiple aspects such as the sampling process (SafeDiffuser, Discrete Diffuser), network structure (EDGI), training objective (PlanCP), and conditioners (TCD). We present a brief overview of these advancements in comparison to Diffuser and Decision Diffuser as follows. Notably, only TCP follows Decision Diffuser and the others follow Diffuser. **SafeDiffuser** (Xiao et al. (2023)) aims to ensure the safe generation of data in diffusion. For each iteration t, the diffusion dynamic $u_t = \frac{\tau_{t-1} - \tau_t}{\Delta t}$ is re-optimized to satisfy certain safety constraints and the resulting dynamic u_t^* is used to update τ_{t-1} as $\tau_t + \Delta t * u_t^*$. Δt is the diffusion time interval which should be small enough. They theoretically show that τ_0 generated in this manner fulfills the safety constraints with probability almost 1. **Discrete Diffuser** (Coleman et al. (2023)) proposes three diffusion-guidance sampling techniques for generation in discrete state and action spaces, where Gaussian-based DM cannot be applied. These guided sampling methods can work with discrete DM such as D3PM (Austin et al. (2021a)). **EDGI** (Brehmer et al. (2023)) proposes an equivariant network architecture for the scenario where an embodied agent operates n objects in a 3D environment. This network design takes geometric structures into account and ensures equal likelihood of a trajectory and its counterpart for which specific spatial/temporal translations or permutations over objects are applied. Better generalization across scenarios, where such translations or permutations happen, can thus be realized. **PlanCP** (Sun et al. (2023)) proposes to quantify the uncertainty of DM using Conformal Prediction (Vovk et al. (2005)). In particular, M trajectories are generated from DM corresponding to M trajectories in D_μ, each pair of which has a prediction error e_i. The conformity among $\{e_i\}$ inversely reflects the uncertainty of the DM. Introducing this conformity term to the DDPM training objective (i.e., Eq. (28)) as an auxiliary term can potentially reduce the uncertainty of sampling with DM. Compared with Decision Diffuser, **TCD** (Hu et al. (2023a)) utilizes more temporal information as the conditioner of the denoising function ϵ_θ to guide the sampling process. Specifically, following the insight of Decision Transformer (introduced in Section 6.1.1), the return-to-go and reward at the current time step are involved as the prospective and immediate conditions, respectively, to reason about the sampling progress while focusing more closely on the current generation step.

7.2.3 Diffusion Models as Data Synthesizers

The performance of offline RL is limited by the provided static dataset D_μ. Once trained with D_μ, the DM can potentially generate a variety of high-quality trajectory data. This newly generated data can then

be employed to augment D_μ, thereby creating a feedback loop to further improve the DM. Moreover, in an unseen but related task, the DM's inherent generality allows for generation of well-performing trajectories for fine-tuning the model in this novel environment. Several works have been developed in this direction following either Diffuser (Hwang et al. (2023); Liang et al. (2023b)) or Decision Diffuser (He et al. (2023a)). Specifically, **AdaptDiffuser** (Liang et al. (2023b)) suggests a rule-based method for filtering and enhancing generated trajectories $\tau = ((s^1, a^1), \cdots, (s^K, a^K))$ from Diffuser, based on the return values and dynamic consistency. Starting with $k = 1$, a revised action $\tilde{a}^k$ is determined using a well-trained or defined inverse dynamic model $\mathcal{T}_{\text{inv}}(\tilde{s}^k, s^{k+1})$ (with $\tilde{s}^1 = s^1$). Subsequently, the next state is adjusted according to the (learned) environment dynamic function as $\tilde{s}^{k+1} = \mathcal{T}(\tilde{s}^k, \tilde{a}^k)$. Trajectories with states s^k significantly deviating from their counterparts $\tilde{s}^k$ are filtered out. The remaining trajectories $\tilde{\tau}$ are further filtered based on their returns $J_\phi(\tilde{\tau}) = \sum_{k=1}^K r_\phi(s^k, a^k)$. Finally, the chosen trajectories are of high quality and can be used for effective data augmentation. In a more straightforward approach, **MTDiff** (He et al. (2023a)) models trajectories $\tau = ((s^1, a^1, r^1), \cdots, (s^K, a^K, r^K))$ conditioned on expert demonstrations from the same environment, denoted as y. Then, trajectory samples from the learned conditional denoising function $\epsilon_\theta(\tau_t, t; y)$ are directly used for data enhancement. For unseen tasks, a small amount of demonstrations can be used as prompts, i.e., y, for $\epsilon_\theta(\tau_t, t; y)$ to generate high-quality training data. These data can then be employed to adapt the DM policy to novel tasks.

7.2.4 Diffusion Models in Extended Offline Reinforcement Learning Setups

In addition to standard offline RL, diffusion models have been applied in multi-task, multi-agent, and hierarchical offline RL setups. Still, these methods are built on the foundational algorithms mentioned above, such as Diffusion-QL, Diffuser, and Decision Diffuser. **MTDiff** (He et al. (2023a)) and **MetaDiffuser** (Ni et al. (2023)) aim to learn task-conditioned planners to solve a distribution of tasks. They utilize offline data categorized for each task, i.e., $\cup_i D_{\mu_i}$, where μ_i denotes the behavior policy corresponding to task i. Following Decision Diffuser, MTDiff incorporates an expert trajectory from task i, denoted as y_i, as an extra condition for the planner specific to that task, represented as $\epsilon_\theta(\tau_t, t; J(\tau), y_i)$. Through training, the agent is expected to implicitly capture the transition model and reward function stored in the prompt trajectory, and perform task-specific planning based on these internalized knowledge. When being evaluated in a new but related task, the denoising function conditioned on a corresponding demonstration y_i can be used for planning. In contrast, MetaDiffuser uses an explicit approach by learning an encoder, denoted as E_η, to encode trajectories into compact representations through self-supervision on the reward and dynamic functions (Zintgraf et al. (2020)), resembling BoReL introduced in Section 3.1.5:

$$\max_{\eta,\psi,\phi} \mathbb{E}_{\tau\sim\cup_i D_{\mu_i}, y=E_\eta(\tau), (s^k,a^k,r^k,s^{k+1})\sim\tau} \left[\log \mathcal{T}_\psi(s^{k+1}|s^k, a^k, y) + \log r_\phi(r^k|s^k, a^k, y)\right] \tag{100}$$

When planning for a specific task i, the representation $y = E_\eta(\tau_i)$, $\tau_i \sim D_{\mu_i}$ can be used as an extra condition of the planner. MetaDiffuser is based on Diffuser and it adopts the learned reward and dynamic model to define the sampling guidance g in Eq. (98) to enhance the dynamics consistency of the generated trajectories while encouraging a high return, detailed as Eq. (7) in (Ni et al. (2023)).

DOM2 (Li et al. (2023c)) and **MADiff** (Zhu et al. (2023b)) target at fully cooperative, offline multi-agent RL. Built upon Diffusion-QL, DOM2 learns a Q-function and DM-based policy for each agent. This policy is tailored to map the individual observation of each agent to its own action, which is trained with Eq. (95). Following Decision Diffuser, MADiff is developed for joint trajectory planning of all agents. Each agent i has a separate denoising function ϵ_θ^i for planning its corresponding trajectory segment. To encourage global information interchange for better coordination, the denoising function contains an attention layer to aggregate trajectory embeddings from other agents. Clearly, more extensions can be developed regarding DM-based MARL, such as MARL algorithms for fully competitive or mixed (partially cooperative/competitive) task scenarios, and integration of DM with SOTA CTDE MARL methods, etc.

LDCQ (Venkatraman et al. (2023)) and **HDMI** (Li et al. (2023b)) are proposed to learn a hierarchical policy/planner from an offline dataset, which can be especially beneficial for long-horizon decision-making. LDCQ learns a high-level policy $\pi_{\text{high}}(z|s^1)$ to map an initial state to a skill z, and low-level policies for each skill $\pi_{\text{low}}(a|s, z)$. In particular, they first employ a β-VAE: (This objective is the same as the one for OPAL

Algorithm	DM Type	DM Usage	Evaluation Task
SfBC	Score SDE	Policy	D4RL (L, M, K)
IDQL	DDPM	Policy	D4RL (L, M)
Diffusion-QL	DDPM	Policy	D4RL (L, M, A, K)
SRDP	DDPM	Policy	D4RL (L, M)
DiffCPS	DDPM	Policy	D4RL (L, M)
EDP	DDPM	Policy	D4RL (L, M, A, K)
Consistency-AC	Consistency Model	Policy	D4RL (L, M, A, K)
QGPO	Score-SDE	Policy	D4RL (L, M)
CPQL	Consistency Model	Policy	D4RL (L, A), dm_control
DOM2 (MARL)	Score-SDE	Policy	MPE, MAMuJoCO
LDCQ (HRL)	DDPM	Policy	D4RL (L, M, A, K, C)
SGP	SGM	Planner	CartPole, D4RL (L), Pixel-Based Single Integrator, Box-Pushing
Diffuser	DDPM	Planner	D4RL (L, M), Kuka Robot
Decision Diffuser	DDPM	Planner	D4RL (L, K), Kuka Robot, Unitree-go-running
SafeDiffuser	DDPM	Planner (D)	D4RL (L, M)
Discrete Diffuser	D3PM	Planner (D)	D4RL (L)
EDGI	DDPM	Planner (D)	Kuka Robot
PlanCP	DDPM	Planner (D)	D4RL (L, M)
TCD	DDPM	Planner (DD)	D4RL (L)
MetaDiffuser (MTRL)	DDPM	Planner (D)	Multi-task MuJoCo
MADiff (MARL)	DDPM	Planner (DD)	MPE, SMAC, MATP
HDMI (HRL)	DDPM	Planner (DD)	D4RL (L, M), NeoRL
AdaptDiffuser	DDPM	Planner & Synthesizer (D)	D4RL (L, M), Kuka Robot
MTDiff (MTRL)	DDPM	Planner & Synthesizer (DD)	Meta-World-V2

Table 11: Summary of DM-based offline RL algorithms. Some algorithms in this table can be categorized as multi-agent RL (MARL), multi-task RL (MTRL), or hierarchical RL (HRL). When DM are used as planners, most algorithms can be viewed as extensions of Diffuser (D) or Decision Diffuser (DD). Regarding the benchmarks, nearly all algorithms in this category have been evaluated on D4RL (Fu et al. (2020)), which provides offline datasets for various data-driven RL tasks, including Locomotion (L), AntMaze (M), Adroit (A), Kitchen (K), and CARLA Autonomous Driving (C). dm_control (Tassa et al. (2018)), Kuka Robot (Janner et al. (2022)), Unitree-go-running Margolis & Agrawal (2022), CartPole (Tedrake (2023)), Box-Pushing (Manuelli et al. (2020)) are a series of continuous (robotic) control tasks. Pixel-Based Single Integrator (Chou & Tedrake (2023)) requires dynamic learning and control over the pixel space. NeoRL (Qin et al. (2022)) is an industrial benchmark on financial decision making. Lastly, Multi-task MuJoCo (Mitchell et al. (2021)) and Meta-World-V2 (Yu et al. (2019c)) are widely-used benchmarks for multi-task/meta RL. MPE (2D control Lowe et al. (2017)), MAMuJoCo (robotic locomotion Peng et al. (2021)), SMAC (video gaming Samvelyan et al. (2019)), and MATP (trajectory prediction Alcorn & Nguyen (2021)) provide diverse evaluation tasks for multi-agent RL.

introduced in Section 3.1.5.)

$$\max_{\phi,\theta} \mathbb{E}_{\tau\sim D_\mu, z\sim P_\phi(\cdot|\tau)} \left[\sum_{k=1}^{K} \log P_\theta(a^k|s^k, z) - \beta D_{KL}(P_\phi(z|\tau)||\text{prior}(z|s^1)) \right] \tag{101}$$

Similar with OPAL, after training, P_θ is used as π_{low} and P_ϕ is adopted to create (s, z) pairs for training π_{high}. π_{high} is modeled as DM and trained in a similar manner with SfBC (introduced in Section 7.2.1). Alternatively, HDMI extracts the skill list corresponding to a trajectory as a series of subgoals within it,

following a heuristic method (Eysenbach et al. (2019)). Then, based on Decision Diffuser, HDMI learns a high-level planner to generate subgoal list τ_z guided by the trajectory return, i.e., $\epsilon_{\text{high}}(\tau_{z,t}, t; J(\tau))$, and a low-level planner to give out the state sequence corresponding to each certain subgoal z, i.e., $\epsilon_{\text{low}}(\tau_{s,t}, t; z)$.

It's worthy noting that fast sampling is essential for the application of DM for offline RL or IL. Besides adopting Consistency Models, for DDPM-based methods, they usually limit the number of iterations for the reverse generation process to a relatively small value and adopt a carefully-designed variance schedule, i.e., $\beta_{0:T}$, as proposed in (Xiao et al. (2022)). For SDE-based methods, they would solve a probability flow ODE for the reverse generation process (as introduced in Section 2.5) with a fast solver: DPM-solver (Lu et al. (2022)). All algorithms mentioned in this section have been summarized in Table 11 and categorized based on the DM type and usage. When applying DM as planners, most algorithms are built upon DDPM and follow the design of either Diffuser (D) or Decision Diffuser (DD). Also, applying DM for offline RL has been an emerging research field and multiple extensions, including the multi-task, multi-agent, and hierarchical setups, have been explored.

8 Discussions and Open Problems

In this section, we provide in-depth discussions on deep generative models (DGMs) in offline policy learning and our perspectives on future research directions of this area, based on the main text in Section 3 - 7. The discussions are centered around how DGMs have been used in offline policy learning, which provide a comprehensive summary of this paper and insightful ideas for future works. Note that, for simplicity, we use abbreviations of the DGMs: VAE - Variational Auto-Encoder, GAN - Generative Adversarial Network, NF - Normalizing Flow, DM - Diffusion Model.

8.1 Discussions on Deep Generative Models and Offline Policy Learning

A common usage of DGMs in offline policy learning: All DGMs can be utilized as policy functions in offline policy learning. In the context of IL, they can be the student policy learned by imitating the expert, while, in offline RL, they can either be the approximated behavior policy or the RL policy. To be specific, we list their mathematical forms as follows, in the order they were introduced [22]:

$$\begin{gathered} z \sim P_\theta(\cdot|s),\ a \sim P_\theta(\cdot|s,z);\ z \sim P_Z(\cdot),\ a = G(z|s);\ z \sim P_Z(\cdot),\ a = G(z|s),\ G = G_1 \circ \cdots \circ G_N; \\ a_t \sim \pi(\cdot|\tau_{t-k:t});\ a_T \sim \mathcal{N}(0, I),\ a_{t-1} \sim G_\theta(\cdot|a_t, s),\ (t = T, \cdots, 1),\ a = a_0. \end{gathered} \tag{102}$$

All these DGM-based policies show superior expressiveness compared with the one using only feed-forward neural networks, and each of them has unique advantages/disadvantages: (1) VAEs might be less expressive than the others, but offers a lightweight model choice and relatively stable training process; (2) As mentioned in Section 4.1.4, GAN-based polices can generate sharp data samples but may suffer from the mode collapse issue, meaning that they may not be able to cover the multiple modes in the (s, a) distribution of the dataset like the other DGMs; (3) With its special architecture (e.g., the attention mechanism), the transformer can process time series or data encompassing multiple entities, as mentioned in Section 6.2.2; (4) As for NF and DM, they excel in modelling/generating high-dimensional and complex behaviors, due to their multi-component or multi-iteration designs shown as Eq. (102). As a spotlight, we note that both VAE- and transformer-based policies have been used to make decisions on multi-modal input (e.g., information from different sensors or in different formats like images and languages), but they adopt different strategies. In particular, VAEs try to embed input from different modalities into a unified latent space, and then a single latent policy (coupled with encoders for each modality) can be used to predict actions based on multiple types of input, as introduced in Section 3.2.3. Transformers, as a universal foundation model, do not make assumptions on the structure of the input data, and so can be used in various task scenarios such as CV and NLP, as introduced in Section 2.4. Thus, a transformer can directly take a data sequence containing

[22] $P_\theta(z|s)$ and $P_\theta(a|s,z)$ denote the prior and decoder of the VAE, respectively. $P_Z(z)$ is the assumed prior distribution of the latent variable z. $G(z|s)$ denotes the generator in the GAN or NF, and it is composed of a series of invertible and differentiable functions, i.e, $G_1 \circ \cdots \circ G_N$, in the NF. $\pi(\cdot|\tau_{t-k:t})$ represents a transformer-based policy, where $\tau_{t-k:t}$ can be $(s_{t-k}, a_{t-k}, \cdots, s_t)$ in IL and $(s_{t-k}, a_{t-k}, R_{t-k}, \cdots, s_t, R_t)$ in offline RL. $G_\theta(a_{t-1}|a_t, s)$ represents the denosing process of DM, and the subscript t denotes the denoising iteration.

different modalities as input, treat each modality as a separate token, and integrate them via the attention mechanism, as shown in Section 6.2.2.

The unique usages of each DGM for offline policy learning: We notice that each DGM has its own unique usage for offline policy learning. (1) VAEs can learn **latent representations** of the data samples. These representations, which are potentially disentangled, can be used as data transformation for learning efficiency (Section 3.1.4), task or subtask representations for multi-task or hierarchical learning (Section 3.1.5), similarity measure of data samples for data augmentation (Section 3.2.2), unified representations of multi-modal input (Section 3.2.3), or disentangled representations of the states for mitigating causal confusion (Section 3.2.5), etc. (2) GANs utilize an adversarial learning framework to practically realize **distribution matching**. Specifically, GANs can be used to minimize the discrepancy between the learned policy and expert policy, i.e., $d(\rho_\pi(s,a)||\rho_{\pi_E}(s,a))$, for IL, or the discrepancy between the learned policy and behavior policy, i.e., $d(\rho_\pi(s,a)||\rho_\mu(s,a))$, to mitigate the OOD issue for offline RL, as introduced in Section 4.1.1 and 4.2.2, respectively. (3) NFs can provide **exact density estimation** due to its special architecture design (i.e., invertiable and differentiable components), enabling them to be incorporated with various advanced IL frameworks, as detailed in Section 5.1.1. We highlight that whenever there is a requirement for exact density estimation, NFs can be utilized. For example, SOPT, as introduced in Section 3.1.3, proposes to approximate the behavior policy's density function, i.e., $\mu(a|s)$, using a VAE to apply support-constraint offline RL. However, the NF is a better choice for this purpose since it can provide more exact estimations. (4) Due to its ability for **sequence modelling**, transformers enable trajectory-optimization-based offline RL/IL, as introduced in Section 6.1.1 and 6.2.1. Also, as shown in Section 6.2.3, owing to its **high capacity and generalization ability**, it can be used as the core component of a generalist agent to handle a range of tasks with a single set of parameters, and it allows for pretraining and fine-tuning as in CV and NLP. (5) Finally, DM can be used to **purify noisy training data** with its special denoising process, as illustrated in Section 7.1.2, and solve model-based offline RL as **trajectory modelling**, as shown in Section 7.2.2, due to its efficiency in generating high-dimensional data and its special conditional sampling mechanisms (i.e., classifier guided or classifier-free guided sampling).

Integrated use of different DGMs for offline policy learning: The unique usages/advantages of each DGM form the basis of an integrated use of different DGMs in offline policy learning, and there are already some works exploring in this direction. Here, we list some (but not all) examples introduced in this paper. (1) In Section 4.1.4, we present a spotlight on integrating VAEs and GANs for IL to synthesize their advantages, i.e., to mitigate the mode collapse issue of GANs and the blurry sample issue of VAEs. (2) In Section 5.2, APAC adopts a Flow-GAN to model the distribution of (s,a) in D_μ, which can be viewed as an integration of NFs and GANs; SAFER adopts a VAE to extract the safety context from the state sequence, which is then used as a condition of an NF-based policy for safe generation. (3) In Section 6.1.3, SPLT shows a coherent use of VAEs and transformers, where the VAE is used to capture the multiple modes/possibilities within the data as latent variables, which are then used as conditioners of a Decision Transformer to mitigate the impact from environmental stochasticity. (4) MIA, as introduced in Section 6.2.3, adopts a GAN-based auxiliary loss term to improve the data usage in transformer-based IL. (5) In Section 7.1.1, all three DM-based IL works implement their denoising functions as transformers, rather than commonly-used U-nets, for sample quality and policy expressiveness.

A summary of the base IL/offline RL algorithms for each DGM: We provide this summary as Table 12. (1) Regarding IL, most DGMs, including VAEs, GANs, and DMs, select BC as the base algorithm, of which the objective is simply to maximize a log likelihood as shown in Eq. (88). However, there are differences in the realization. Specifically, as introduced in Section 3.2.1, VAE-based IL algorithms either adopt a VAE ELBO, which is a lower bound of the BC objective, or a VIB-based framework, which is closed in form with the ELBO. For transformer-based Il, besides the BC term, to make full use of demonstrations, auxiliary supervision objectives, such as prediction errors on the next state (i.e., the forward model loss) or the intermediate action between two consecutive states (i.e., the inverse model loss), are often employed. As for DM-based IL, the objective for training DM (i.e., Eq. (27)) provides a lower bound of the log-likelihood, which naturally connects DM with BC, as mentioned in the beginning of Section 7.1. On the other hand, GANs and NFs are integrated with more advanced IL frameworks. In particular, as introduced in Section 4.1.1, the fundamental GAN-based Il algorithms are derived from MaxEntIRL and practically implemented

DGM	VAE	GAN	Normalizing Flow	Transformer	Diffusion Model
IL	BC (ELBO, VIB)	MaxEntIRL (AIL)	KL, LIL, AIL	BC (self-supervision)	BC
Offline RL	DP-based offline RL	Model-based offline RL	DP-based offline RL	Trajectory optimization	DP/Model-based offline RL, Trajectory modelling

Table 12: A summary of the base offline RL/IL algorithms for DGM-based offline policy learning. MaxEntIRL (Section 4.1.1) is short for maximum causal entropy inverse RL. KL, LIL, and AIL (Section 5.1.1) denote the KL-divergence-based, Likelihood-based, and Adversarial IL framework, respectively. DP-based offline RL (Section 3.1.1) refers to the Dynamic-Programming-based offline RL.

as Adversarial IL (AIL) frameworks; NFs, as exact density estimators, have the flexibility to be adopted in various IL frameworks such as KL, LIL, and AIL, as illustrated in Section 5.1.1. (2) As for offline RL, we have introduced multiple categories within it throughout this paper, including dynamic-programming-based, model-based, and trajectory-optimization-based offline RL, as shown in Section 3.1.1, 4.2.1, and 6.1.1, respectively. The corresponding categories for each DGM are listed in Table 12. More specifically, we note that VAE-based offline RL mainly follows policy penalty, support constraint, and pessimistic value methods, which are subcategories of dynamic-programming-based offline RL, as introduced in Section 3.1.3; while, DM-based offline RL mainly follows another subcategory of dynamic-programming-based offline RL – policy constraint methods.

Seminal works of DGM-based offline policy learning: Regarding the applications in offline policy learning, developments for different DGMs are quite unbalanced, and even for the same type of DGM, the applications in IL may be significantly more than the ones in offline RL, or vice versa. One main factor is whether there are seminal works in that category, since many research works would follow the seminal ones for extensions. Here, we highlight the seminal works introduced in this paper: VAE - offline RL - BCQ (Fujimoto et al. (2019)), GAN - IL - GAIL (Ho & Ermon (2016)) and AIRL (Fu et al. (2017)), Transformer - offline RL - Decision Transformer (Chen et al. (2021b)) and Trajectory Transformer (Janner et al. (2021)), Diffusion Model - offline RL - Diffuser (Janner et al. (2022)) and Decision Diffuser (Ajay et al. (2023)). There are still no seminal works for NF-based offline policy learning, which explains why there are relatively fewer works in Section 5. Notably, some seminal works pioneer new paradigms for offline policy learning. For example, GAIL converts IL/IRL to a distribution matching problem [23]; Decision Transformer realizes offline RL via trajectory optimization, which eliminates the necessity to fit value functions through dynamic programming or to compute policy gradients; Diffuser folds the two processes in model-based offline RL: transition dynamic modeling and trajectory optimization, into a trajectory modeling process. These paradigm shifts are closely related to corresponding DGMs and make full use of their unique advantages, which open up promising directions for offline policy learning. On the other hand, simply using DGMs as function estimators in traditional offline RL or IL methods can be less attractive, unless the applications of DGMs brings superior scalability or generalization ability.

A summary of the issues and extensions of offline policy learning that have been targeted by the DGMs: In Table 13, we enumerate the IL/offline RL issues that each DGM has tried to solve, as well as the extended IL/offline RL setups that have been explored by each DGM. Specifically, there are in total six setup extensions, including multi-task (MT), multi-agent (MA), hierarchical (Hier), model-based (MB) learning, policy safety, and policy generalization. Readers can easily find the research works targeting at specific issues/extensions in corresponding sections. However, we note that the listed issues/extensions should not be considered as completely resolved by the DGMs, and future works can focus on the unsolved or under-explored issues/extensions as detailed in Section 8.2.4. Here, we provide some remarks on this

[23] Although GAIL- or AIRL-based algorithms are used for imitation learning from offline expert data, these algorithms also rely on simulators in their learning process, because there is an inner (online) RL process in their algorithm designs. Similarly, most algorithms within Section 5.1.1 require simulators, as they also realize imitation learning via distribution matching (like GAIL and AIRL), i.e., $\min_\pi d(\rho_\pi(s,a)||\rho_{\pi_E}(s,a))$, and RL is a natural choice for optimization regarding the occupancy measure of the policy, i.e., $\rho_\pi(s,a)$.

DGM	VAE	GAN	Normalizing Flow	Transformer	Diffusion Model
IL issues	Insufficient demonstrations, Causal confusion, Multi-modal input	Insufficient demonstrations, Compounding error, Multi-modal demonstrations	Exact density estimation, Learning from observations, Policy expressiveness	Sequential/ multi-modal/ multi-entity input, Multi-modal actions, Insufficient demonstrations	High-dim/ multi-modal state-action, Spurious correlations, Insufficient/ low-quality demonstrations, Compounding error
IL extensions	Hier	MT, MA, Hier, MB, Safety	N/A	MT, Generalization	Hier
Offline RL issues	OOD actions, Low-quality training data, High-dim states, Continuous actions	OOD actions, (Vision-based) world model estimation, Segment stitching	OOD actions, Over conservatism, Insufficient training data, Sparse reward	OOD actions, Learning difficulty, Insufficient training data, Segment stitching, Sparse reward, Partially observable	OOD actions, Insufficient training data
Offline RL extensions	MT, Hier	Hier, MB	Hier, Safety	MT, MA, Hier, MB, Safety, Generalization	MT, MA, Hier, MB, Safety

Table 13: A summary of the issues and extensions of offline policy learning targeted by the DGMs. MT, MA, Hier, MB represents multi-task, multi-agent, hierarchical, model-based learning, respectively. Safety and generalization refer to if the learned policy can be safely applied to risky environments or be generalizable to unseen environments.

table. (1) Low-quality training data is characterized by its limited coverage of the state-action space, a lack of diversity in behavior patterns, or the inclusion of suboptimal/noisy demonstrations. (2) Multi-modal demonstrations/actions refer to demonstrations/actions containing multiple distributional modes, while by multi-modal input, we mean input from multiple sensors or in various formats (e.g., images and texts). (3) Learning from observations refer to imitating from sequences of states only, which is notably more challenging than usual imitation learning. (4) Compared with BC, GAN-based IL can mitigate the issues of insufficient demonstrations and compounding errors. This is because GAN-based IL methods do more than just mimicking observed behaviors – they reason about the underlying reward function from demonstrations and utilizes it for further RL training, which complements the static demonstrations and enables the agent to act reasonably at unseen states. However, GAN-based IL methods rely on simulators for RL training and suffer from issues regarding sampling efficiency and training stability, as introduced in Section 4.1.2. (5) Decision Transformer has lower learning difficulty and can avoid OOD actions for offline RL, because it is based on trajectory optimization, which eliminates the necessity to fit value functions or compute policy gradients, and multiple state and action anchors throughout the trajectory prevent the learned policy from deviating too far from the behavior policy. However, there are still pending issues for Decision Transformer, such as the impacts from environmental stochasticity (Section 6.1.3) and its theoretical shortcomings as listed in Section 6.1.5.

Foundation model & Algorithm & Data: Among all the applications of DGMs, transformer-based IL/offline RL have shown some of the most promising and exciting evaluation results: (1) As listed in

Table 9, most algorithms have seen success in challenging robotic simulators, real-world tasks, or large scale competitions; (2) As shown in Section 6.2.3, the use of transformer enables the process of input encompassing (extra) long time sequences or multiple modalities/entities, and (robotic) agents that can follow language instructions or interact with humans can be developed solely by imitation and self-supervision; (3) As introduced in Section 6.1.4, Gato (Reed et al. (2022)), as a single transformer with the same set of weights, can handle 604 distinct tasks with varying modalities (i.e., images, texts, robotic control, and video gaming); further, Reid et al. (2022) and Takagi (2022) explore pretraining the transformer on language tasks and fine-tuning it on RL tasks, and demonstrate promising cross-modality pretraining effects. All these advancements are based on simple supervised learning objectives and are not related to any theoretical breakthrough. However, they do rely on a high-capacity and computation-efficient foundation model – transformer, and a large amount of diverse training data from multiple modalities. This leads to an inspiring paradigm for developing generalist agents, that is, using a potent foundation model trained by (self-) supervised learning from extensive, high-quality demonstrations. On the other hand, it also raises the question whether the future development should be data-driven or algorithm-driven, but there is no doubt that the development of new foundation models or algorithms should put more emphasis on the scalability and computation efficiency, like the transformer.

8.2 Perspectives on Future Directions

Based on the discussions above and the main content in Section 3 - 7, we present some perspectives on future research directions here, and we categorize the content in this section as four aspects: data, benchmarking, theories, and algorithms. We believe more open problems can be gleaned from the detailed introductions in the main content, and we have included comments on future works specific to certain DGMs in corresponding sections, including the last paragraphs of Section 3, 5, 6.2, 7.1, 7.2.1, and Section 6.1.5.

8.2.1 Future Works on Data-centric Research

How would the offline policy learning agent evolve with the quality and quantity of the training data? The performance of offline policy learning is closely related to the quality and quantity of the provided offline data. Therefore, one potential research direction would be investigating how the dataset's characteristics would impact the learned policy, as instructions for building datasets. (1) First, the static dataset may contain noise (i.e., disturbed or misleading information) or suboptimal behaviors [24]. In this case, open questions include how to measure the noise or suboptimality of the provided data and how robust can the policy learning be to these data imperfections. The answers to these questions would vary with the used algorithms, DGMs, or evaluation tasks, but the imperfection measure and robustness evaluation protocol can be general and beneficial for algorithm development. These questions are important because perfect datasets are costly to build in scale and the tolerance for imperfection can greatly reduce the burden for data collection and possessing. (2) Second, the performance of an offline policy learning agent on evaluation tasks relies heavily on the coverage and diversity of the training data. An effective set of behaviors for policy learning should cover the possible task scenarios and provide various behavioral patterns/skills for the agent to learn. How to measure the coverage and diversity of the dataset and how these properties would influence the generalization of the learned policy on evaluation tasks would be interesting questions. (3) One key factor contributing to the success of certain DGMs in CV and NLP is their ability to leverage extensive training datasets. Notably, their training performance would continue to improve as the quantity of the training data increases. Thus, for each variant of DGM-based offline policy learning, it is essential to study their scalability, that is, how the learned agent would evolve with the quantity of the training data. Algorithms with superior scalability would be more promising in challenging, real-life applications.

How to construct a training dataset for effective offline policy learning? With efforts for the open problems mentioned above, we could establish measurements for noise, suboptimality, diversity, and coverage of the dataset and get some insights on the relationship between these measurements and the performance of

[24] This would be an issue for IL, since IL requires expert-level demonstartions. However, for offline RL, the dataset could contain suboptimal behaviors as long as their rewards are correctly labeled. If there are only suboptimal trajectories in the dataset for offline RL, the learning difficulty would be high, since the agent needs to learn to stitch segments from various trajectories to form an optimal strategy.

the learned policy, which can guide the construction of training datasets for effective offline policy learning. However, there are some other problems that need to be explored. First, the original state and action spaces may be high-dimensional and continuous, which would require exponentially more data for policy learning. Utilizing compact representations, which can be obtained from DGMs like VAEs and encoder-only transformers, or discretization could help improve the learning efficiency, but also would introduce inaccuracy. Second, for offline RL datasets, sparse rewards can bring training difficulty but dense rewards are costly to annotate. Thus, a tradeoff needs to be achieved between them and strategically annotating part of the dataset with rewards could be a promising direction. Similarly, although there are algorithms for learning multi-task, hierarchical, or safe policies from data without the task, skill, or safe action labels, having these labels either fully or partially annotated can significantly aid in the policy learning process. However, given that real-life datasets can be enormous in scale, the labeling should be only for critical points or regions in the state-action space, which requires techniques for identification.

Data Augmentation & Data Synthesis. VAEs, transformers, and DMs have been used for data augmentation or synthesis, as shown in Section 3.1.4, 6.1.2, and 7.2.3, respectively, of which the purpose is simply to involve more data for training. The data used for augmentation may already exist but require transformation or supplementation to be effectively utilized, or could be synthesized using DGMs. DGMs exhibit remarkable capability in synthesizing new data that shares statistical properties with the real data. Thus, this approach has the potential to bridge the gap between the demand for large datasets and the feasibility of acquiring them. Multiple research directions in this domain could be developed. First, based on the coverage or diversity indicators of the dataset, targeted data synthesis to supplement the under-covered area or to avoid repeated behavioral patterns for better diversity could be developed. Second, the synthesized data usually cannot be directly employed without filtering. In this case, necessary quality measure, such as the similarity of the synthesized data with the real (optimal) data, should be established. Also, ideally, there should be (theoretical) study on the relationship of the suboptimality of the learned policy with the quality/quantity of the synthesized data. All in all, it would be quite exciting to see the creation of a positive feedback loop: enhanced policies emerging from newly synthesized data, which in turn can be leveraged to generate even higher quality data for training.

8.2.2 Future Works on Benchmarking

Development of more realistic, challenging benchmarks. We notice that most DGM-based offline RL algorithms are evaluated on D4RL, as shown in the tables of Section 3 - 7, which is a standard benchmark for offline RL. However, widely-used benchmarks like D4RL, cannot fully show or evaluate the advantages of DGM-based offline policy learning algorithms, as we have seen agents, which are implemented as two-layer neural networks and trained with a moderate amount of data, can already achieve excellent performance on these benchmarks. To fully explore the potential and guide the development of DGM-based offline policy learning, more challenging benchmarks are required. (1) First, the benchmark dataset should be large in size to evaluate the scalability of the DGM-based algorithms. This includes evaluating the trend of performance improvement relative to the volume of training data and determining whether DGM-based algorithms can significantly outperform the others when provided with extensive training data. (2) Second, the dataset should contain multiple modalities. For example, state inputs could be collected from various sources, such as language instructions, visual information from different sensors, or even videos; moreover, the state-action space should feature multiple distributional modes, such as containing distinct trajectories for achieving the same goal. DGM-based algorithms are expected to effectively harness information from diverse modalities and learn policies that cover the multiple modes within the policy space. Further, benchmarks should not be limited to control or decision-making tasks but also include assignments from other modalities, such as CV and NLP. These cross-modal tasks could serve as auxiliary tasks or be utilized to evaluate the capabilities of generalist agents. (3) The task scenarios should be more realistic. A main reason that CV and NLP techniques, which are usually DGM-based, can be widely adopted in real life is that these algorithms are directly evaluated on real-life tasks/datasets rather than simplified simulators. Thus, realistic offline dataset in a large scale could greatly advance the development of offline policy learning and showcase the superiority of DGM-based algorithms. (4) The benchmark should evaluate more than just the policy return. It should also assess aspects such as the generalization, safety of the learned policy and the robustness of policy learning in noisy or sparse-reward environments.

Comparisons among different DGMs. Although there are numerous offline RL or IL algorithms for each type of DGMs and they have shared benchmarks, comparisons among them are quite rare. It would be insightful to see fair and thorough comparisons among different DGMs with the same usage (e.g., as policy backbones) on the same set of tasks. Also, as task complexity or dataset size escalates, analyzing the trends in policy performance and computational cost across different DGMs can provide useful insights. Such comparisons provide suggestions on the choice of DGMs, conditioning on the task difficulty and dataset scale. Moreover, as mentioned in the main text of this paper, algorithms that fall in the same category, such as NF-based offline RL algorithms, are also rarely compared with each other. Comparisons within the same category can be valuable, as they can indicate which usage of a certain DGM is more effective.

8.2.3 Future Works on Theories

Most works on applying DGMs in offline policy learning focus on algorithm designs rather than theoretical analysis, so more theoretical research works could be done for this field. One promising direction is derivations of the convergence rate or performance guarantee for the seminal works in DGM-based offline policy learning, such as (Zhang et al. (2020b)) for GAIL and (Brandfonbrener et al. (2022)) for return-conditioned supervised learning like Decision Transformer, based on the theoretical results from either DGMs or offline RL/IL. Moreover, we notice that there have been efforts on theoretically unifying the objectives of different DGMs for a deeper understanding of the relationship between DGMs and improved learning performance, such as (Nielsen et al. (2020); Kingma & Gao (2023)). This group of works can greatly inspire development of new DGM-based offline policy learning algorithms or unified analysis of existing ones.

Next, we outline some specific theoretical problems in this field. (1) First, regarding GAN-based IL (i.e., Section 4.1), so far, no approach has been developed that is both computationally efficient and can theoretically guarantee the recovery of the reward function. Also, many works propose to replace the on-policy RL within GAIL/AIRL (i.e., TRPO) with off-policy RL algorithms (e.g., DDPG) for improved sample efficiency. However, this improvement lacks theoretical backup. With off-policy RL, the policy training at each iteration is based on samples from multiple past iterations, during which the reward function keeps changing. As a result, the RL training is conducted in an unstationary MDP where typical RL algorithms would theoretically fail. (2) Second, as mentioned in Section 6.1.5, return-conditioned supervised learning (e.g., Decision Transformer) alone is unlikely to be a general solution for offline RL problems, and it offers guarantees only when the environment dynamics are nearly deterministic. Thus, adapting these algorithms to stochastic environments, ideally backed by theoretical optimality guarantees, is a clear necessity. Also, Decision Transformer would imitate both high-return and low-return trajectories, and claims that the learning performance in this manner is better than imitating high-return trajectories only. A theoretical explanation on how the low-return behavior learning would benefit the overall performance can be insightful. (3) Third, as introduced in Section 7.2.2, the algorithm design of Diffuser is mainly based on intuitions from similar problems, such as the inpainting problem and receding horizon control, but lacks theoretical support. To be specific, in Eq. (99), to decide on the action choice a at state s, the trajectory generation is hardcoded to start with s, and then the action $\hat{a}$ that is right after s in the generated trajectory is adopted as a. The problem here is how to ensure the causal relationship between s and a, which is crucial for (RL) sequential decision-making, and whether it is necessary to generate a trajectory segment in case that only the first action prediction is utilized.

8.2.4 Future Works on Algorithm Designs

From the discussions in Section 8.1 and the main content in Section 3 - 7, we can identify many potential future directions regarding the algorithm design. Here, we list some of them as examples.

Under-explored categories in the main text. For existing categories of algorithms, some of them are still under-explored, such as GAN-based IL algorithms that do not rely on simulators (Section 4.1), NF-based IL where the NF works as the policy (Section 5.1.2), NF-based offline RL algorithms (Section 5.2.1), efficient algorithms on mitigating impacts from environmental stochasticity for transformer-based offline RL (Section 6.1.3), transformer-based offline RL which integrates traditional offline RL methods with transformer architectures (Section 6.1.5), DM-based offline policy learning where DMs work as data synthesizers (Section 7.2.3), and so on.

Integrated use of various DGMs for offline policy learning. As mentioned in Section 8.1, each DGM has distinct usages due to their special design and there have been a few algorithms managing to integrate two DGMs together for improved offline policy learning performance. More in-depth exploration can be done in this direction, especially for involving more DGMs in a unified offline policy learning framework. For example, we observe from Table 12 that most DGM-based IL algorithms are based on BC, which is a relatively basic IL algorithm and has fundamental issues [25], while NFs are integrated with various advanced IL frameworks due to its ability for exact density estimations. In this case, NFs can be integrated with transformer-based DMs, where NFs extend the base IL framework and transformer-based DMs work as a core component of a generalist agent that can deal with multi-modal input and high-dimensional generations. Further, they can be integrated with VAEs, which can be used to extract task or subtask representations for multi-task or hierarchical learning, as introduced in Section 3.1.5.

Unsolved issues and extensions of DGM-based offline policy learning. Table 13 provides a summary of the issues and extensions of IL and offline RL that have been explored by DGM-based algorithms, which provides indications for future works. (1) By checking the outlined issues, we can pinpoint unresolved or inadequately addressed issues by existing methods as future directions. For example, although there have been GAN-based or DM-based algorithms targeting at the compounding error issue, the GAN-based ones rely on simulators and DM-based ones (i.e., AWE and MCNN in Section 7.1.2) are still in the early stages of development. Similarly, in offline RL, reward sparsity is a significant issue, for which the explorations made by NFs (i.e., NF Shaping in Section 5.2.2) and transformers (i.e., DTRD in Section 6.1.2) have tried reward shaping and reward function learning, which are both interesting directions awaiting further development. (2) Regarding the extensions, there can be in total six (or more) setup extensions: multi-task, multi-agent, hierarchical, model-based, safety, and generalization. Table 13 illustrates the extensions that are awaiting exploration for each DGM. Further, we note that the extension method can be potentially transferred among DGMs. For instance, as shown in Section 7.2.4, DM-based multi-task and hierarchical offline RL algorithms adopt the same algorithm ideas as BOReL and OPAL (i.e., the VAE-based methods introduced in Section 3.1.5). In particular, we note that multi-agent extensions for DGM-based offline policy learning require further development, and existing explorations (such as MAGAIL, MA-AIRL in Section 4.1 and DOM2, MADiff in Section 7.2.4) are still quite immature. Specifically, developments of MARL algorithms for fully competitive or mixed (partially cooperative/competitive) task scenarios based on game theory, and integrations of DGMs with state-of-the-art CTDE [26] MARL methods are essential future directions.

Development of generalist agents. One of the most exciting future directions for DGM-based offline policy learning is developing a decision-making agent that can continually evolve with the amount of training data and the size of the DGM-based policy network and can handle a range of tasks, including unseen ones. CV and NLP have made great progress in this direction, owing to the use of DGMs. To realize this for offline policy learning, several things should be done. (1) First, the base IL or offline RL algorithm should be compatible with deep and broad neural networks, so that its performance can grow with the size of the foundation model. This is also the reason why mainstream transformer-based and DM-based offline policy learning methods (e.g., Decision Transformer and Diffuser) are based on supervised learning as in CV and NLP. Future works can work on developing deep foundation models that are compatible with policy-gradient methods or dynamic programming. (2) Second, besides constructing large-scale, high-quality training datasets as mentioned in Section 8.2.1, some algorithm-driven efforts can be done. For example, algorithms that are robust to suboptimal training data or capable of processing multi-modal inputs should be developed. Specifically, learning from demonstration videos (in third-person views) is a quite challenging but promising research direction, as large-scale video datasets are more accessible and videos usually contain more learnable information than images or vectorized data. Agents capable of learning from videos have the

[25] BC is implemented as supervised learning, of which the objective is shown as Eq. (88). However, predictions made by π, which is learned with BC and used for sequential decision-making, can impact future observations, thus breaching a fundamental assumption of supervised learning (Ross & Bagnell (2010)): training inputs should be drawn from an independent and identically distributed population. Consequently, errors and deviations from the demonstrated behavior tend to accumulate over time, as minor mistakes lead the agent into areas of the observation space that the expert has not ventured into, known as the compounding error. Additionally, BC learns policies merely through imitation, without engaging in reasoning, which restricts the generalization capability of the learned policy. In this case, extending the base IL framework for transformer- or DM-based IL can be essential future directions.

[26] CTDE refers to a scheme of multi-agent RL (MARL) that employs centralized training and decentralized execution.

potential to continuously evolve by observing their surrounding environments during deployment. (3) Third, to enhance generalization, employing advanced meta-learning or multi-task learning techniques is advisable. Further, adopting the "pretraining + fine-tuning" approach, similar to that used in large language and vision models, is also promising, since it enables the accumulation of training efforts. Notably, the more significant the difference between the source and target tasks, the more challenging it becomes to make pretraining effective, yet the more data can be utilized for training the agent.

Future works in related areas. Finally, there are some related areas that can be used as future research directions. First, reviews on the applications of DGMs in Inverse Reinforcement Learning (IRL) or (Online) Reinforcement Learning have not yet been developed. IRL and RL are important approaches for sequential decision-making, but they both require online interactions with the environment. Second, as shown in Table 12, integrations with dynamic-programming-based, model-based, and trajectory-optimization-based offline RL have been explored. There are some other branches in offline RL (Levine et al. (2020)), such as importance-sampling-based and uncertainty-estimation-based offline RL, which have the potential to be enhanced with DGMs. Third, we notice that new foundation models and DGMs are continually emerging, such as Mamba (Gu & Dao (2023)) and Poisson Flows (Xu et al. (2022c; 2023)). Applying these SOTA models in offline policy learning is certainly a promising research direction.

9 Conclusion

In this paper, we show a systematic review on the applications of DGMs in offline policy learning. In Section 2, we provide necessary background on several mainstream DGMs, including Variational Auto-Encoders, Generative Adversarial Networks, Normalizing Flows, Transformers, and Diffusion Models. Then, in Section 3 - 7, we introduce the applications of each DGM in both offline RL and IL, i.e., the two primary branches of offline policy learning. Each section includes both a tutorial and a survey on the respective topic. Following these main content, we provide a summary on existing works and our perspectives on future research directions in Section 8. As the first review paper of this field, we wish this work to be a hands-on reference for better understanding the current research progress on DGMs in offline policy learning and help researchers to further improve DGM-based offline RL/IL algorithms.

References

Josh Abramson, Arun Ahuja, Arthur Brussee, Federico Carnevale, Mary Cassin, Felix Fischer, Petko Georgiev, Alex Goldin, Tim Harley, Felix Hill, Peter C. Humphreys, Alden Hung, Jessica Landon, Timothy P. Lillicrap, Hamza Merzic, Alistair Muldal, Adam Santoro, Guy Scully, Tamara von Glehn, Greg Wayne, Nathaniel Wong, Chen Yan, and Rui Zhu. Creating multimodal interactive agents with imitation and self-supervised learning. *CoRR*, abs/2112.03763, 2021.

Suzan Ece Ada, Erhan Öztop, and Emre Ugur. Diffusion policies for out-of-distribution generalization in offline reinforcement learning. *CoRR*, abs/2307.04726, 2023.

Shubhankar Agarwal, Harshit Sikchi, Cole Gulino, and Eric Wilkinson. Imitative planning using conditional normalizing flow. *CoRR*, abs/2007.16162, 2020.

Anurag Ajay, Aviral Kumar, Pulkit Agrawal, Sergey Levine, and Ofir Nachum. OPAL: offline primitive discovery for accelerating offline reinforcement learning. In *Proceedings of the 9th International Conference on Learning Representations*. OpenReview.net, 2021.

Anurag Ajay, Yilun Du, Abhi Gupta, Joshua B. Tenenbaum, Tommi S. Jaakkola, and Pulkit Agrawal. Is conditional generative modeling all you need for decision making? In *Proceedings of the 11th International Conference on Learning Representations*. OpenReview.net, 2023.

Dmitry Akimov, Vladislav Kurenkov, Alexander Nikulin, Denis Tarasov, and Sergey Kolesnikov. Let offline rl flow: Training conservative agents in the latent space of normalizing flows. In *NeurIPS Offline RL Workshop*, 2022.

Michael A. Alcorn and Anh Nguyen. baller2vec++: A look-ahead multi-entity transformer for modeling coordinated agents. *CoRR*, abs/2104.11980, 2021.

Alexander A. Alemi, Ian Fischer, Joshua V. Dillon, and Kevin Murphy. Deep variational information bottleneck. In *Proceedings of the 5th International Conference on Learning Representations*. OpenReview.net, 2017.

Eitan Altman. Constrained markov decision processes with total cost criteria: Lagrangian approach and dual linear program. *Mathematical methods of operations research*, 48(3):387–417, 1998.

Shun-ichi Amari. Backpropagation and stochastic gradient descent method. *Neurocomputing*, 5(4-5):185–196, 1993.

Tomer Amit, Tal Shaharbany, Eliya Nachmani, and Lior Wolf. Segdiff: Image segmentation with diffusion probabilistic models. *arXiv preprint arXiv:2112.00390*, 2021.

Brian DO Anderson. Reverse-time diffusion equation models. *Stochastic Processes and their Applications*, 12(3):313–326, 1982.

Martín Arjovsky, Soumith Chintala, and Léon Bottou. Wasserstein GAN. *CoRR*, abs/1701.07875, 2017.

Vladimir I Arnold. *Ordinary differential equations*. Springer Science & Business Media, 1992.

Jacob Austin, Daniel D. Johnson, Jonathan Ho, Daniel Tarlow, and Rianne van den Berg. Structured denoising diffusion models in discrete state-spaces. In *Advances in Neural Information Processing Systems 34*, 2021a.

Jacob Austin, Daniel D Johnson, Jonathan Ho, Daniel Tarlow, and Rianne Van Den Berg. Structured denoising diffusion models in discrete state-spaces. *Advances in Neural Information Processing Systems*, 34:17981–17993, 2021b.

Omri Avrahami, Dani Lischinski, and Ohad Fried. Blended diffusion for text-driven editing of natural images. In *Proceedings of the IEEE/CVF Conference on Computer Vision and Pattern Recognition*, pp. 18208–18218, 2022.

Lei Jimmy Ba, Jamie Ryan Kiros, and Geoffrey E. Hinton. Layer normalization. *CoRR*, abs/1607.06450, 2016.

Nir Baram, Oron Anschel, Itai Caspi, and Shie Mannor. End-to-end differentiable adversarial imitation learning. In *Proceedings of the 34th International Conference on Machine Learning*, volume 70, pp. 390–399, 2017.

Dmitry Baranchuk, Ivan Rubachev, Andrey Voynov, Valentin Khrulkov, and Artem Babenko. Label-efficient semantic segmentation with diffusion models. *arXiv preprint arXiv:2112.03126*, 2021.

Jens Behrmann, Will Grathwohl, Ricky T. Q. Chen, David Duvenaud, and Jörn-Henrik Jacobsen. Invertible residual networks. In *Proceedings of the 36th International Conference on Machine Learning*, volume 97 of *Proceedings of Machine Learning Research*, pp. 573–582. PMLR, 2019.

Marc G. Bellemare, Yavar Naddaf, Joel Veness, and Michael Bowling. The arcade learning environment: An evaluation platform for general agents. *Journal of Artificial Intelligence Research*, 47:253–279, 2013.

Xihan Bian, Oscar Mendez Maldonado, and Simon Hadfield. SKILL-IL: disentangling skill and knowledge in multitask imitation learning. In *IEEE/RSJ International Conference on Intelligent Robots and Systems*, pp. 7060–7065. IEEE, 2022.

Lionel Blondé and Alexandros Kalousis. Sample-efficient imitation learning via generative adversarial nets. In *Proceedings of the 22nd International Conference on Artificial Intelligence and Statistics*, volume 89, pp. 3138–3148, 2019.

Damian Boborzi, Christoph-Nikolas Straehle, Jens S. Buchner, and Lars Mikelsons. Learning normalizing flow policies based on highway demonstrations. In *Proceedings of the 24th IEEE International Intelligent Transportation Systems Conference*, pp. 22–29. IEEE, 2021a.

Damian Boborzi, Christoph-Nikolas Straehle, Jens Stefan Buchner, and Lars Mikelsons. State-only imitation learning by trajectory distribution matching. In *Submission to the 10th International Conference on Learning Representations*, 2021b.

Damian Boborzi, Christoph-Nikolas Straehle, Jens S. Buchner, and Lars Mikelsons. Imitation learning by state-only distribution matching. *CoRR*, abs/2202.04332, 2022.

Rogerio Bonatti, Ratnesh Madaan, Vibhav Vineet, Sebastian A. Scherer, and Ashish Kapoor. Learning visuomotor policies for aerial navigation using cross-modal representations. In *IEEE/RSJ International Conference on Intelligent Robots and Systems*, pp. 1637–1644. IEEE, 2020.

Ayman Boustati, Hana Chockler, and Daniel C. McNamee. Transfer learning with causal counterfactual reasoning in decision transformers. *CoRR*, abs/2110.14355, 2021.

David Brandfonbrener, Alberto Bietti, Jacob Buckman, Romain Laroche, and Joan Bruna. When does return-conditioned supervised learning work for offline reinforcement learning? In *Advances in Neural Information Processing Systems 35*, 2022.

Johann Brehmer, Joey Bose, Pim de Haan, and Taco Cohen. EDGI: equivariant diffusion for planning with embodied agents. *CoRR*, abs/2303.12410, 2023.

Greg Brockman, Vicki Cheung, Ludwig Pettersson, Jonas Schneider, John Schulman, Jie Tang, and Wojciech Zaremba. Openai gym, 2016.

Tim Brooks, Bill Peebles, Connor Homes, Will DePue, Yufei Guo, Li Jing, David Schnurr, Joe Taylor, Troy Luhman, Eric Luhman, Clarence Wing Yin Ng, Ricky Wang, and Aditya Ramesh. Video generation models as world simulators, 2024. URL `https://openai.com/research/video-generation-models-as-world-simulators`.

Tom B. Brown, Benjamin Mann, Nick Ryder, Melanie Subbiah, Jared Kaplan, Prafulla Dhariwal, Arvind Neelakantan, Pranav Shyam, Girish Sastry, Amanda Askell, Sandhini Agarwal, Ariel Herbert-Voss, Gretchen Krueger, Tom Henighan, Rewon Child, Aditya Ramesh, Daniel M. Ziegler, Jeffrey Wu, Clemens Winter, Christopher Hesse, Mark Chen, Eric Sigler, Mateusz Litwin, Scott Gray, Benjamin Chess, Jack Clark, Christopher Berner, Sam McCandlish, Alec Radford, Ilya Sutskever, and Dario Amodei. Language models are few-shot learners. In *Advances in Neural Information Processing Systems 33*, 2020.

Catherine Cang, Kourosh Hakhamaneshi, Ryan Rudes, Igor Mordatch, Aravind Rajeswaran, Pieter Abbeel, and Michael Laskin. Semi-supervised offline reinforcement learning with pre-trained decision transformers, 2022. URL `https://openreview.net/forum?id=fwJWhOxuzV9`.

Bo Chang, Lili Meng, Eldad Haber, Lars Ruthotto, David Begert, and Elliot Holtham. Reversible architectures for arbitrarily deep residual neural networks. In *Proceedings of the 32nd AAAI Conference on Artificial Intelligence*, pp. 2811–2818. AAAI Press, 2018.

Wei-Di Chang, Juan Camilo Gamboa Higuera, Scott Fujimoto, David Meger, and Gregory Dudek. Il-flow: Imitation learning from observation using normalizing flows. *arXiv preprint arXiv:2205.09251*, 2022.

Yevgen Chebotar, Quan Vuong, Karol Hausman, Fei Xia, Yao Lu, Alex Irpan, Aviral Kumar, Tianhe Yu, Alexander Herzog, Karl Pertsch, et al. Q-transformer: Scalable offline reinforcement learning via autoregressive q-functions. In *Conference on Robot Learning*, pp. 3909–3928. PMLR, 2023.

Chang Chen, Yi-Fu Wu, Jaesik Yoon, and Sungjin Ahn. Transdreamer: Reinforcement learning with transformer world models. *CoRR*, abs/2202.09481, 2022.

Changyou Chen, Chunyuan Li, Liquan Chen, Wenlin Wang, Yunchen Pu, and Lawrence Carin. Continuous-time flows for efficient inference and density estimation. In *Proceedings of the 35th International Conference on Machine Learning*, volume 80, pp. 823–832. PMLR, 2018a.

Cynthia Chen, Xin Chen, Sam Toyer, Cody Wild, Scott Emmons, Ian Fischer, Kuang-Huei Lee, Neel Alex, Steven H. Wang, Ping Luo, Stuart Russell, Pieter Abbeel, and Rohin Shah. An empirical investigation of representation learning for imitation. In *Proceedings of the Neural Information Processing Systems Track on Datasets and Benchmarks 1*, 2021a.

Daoming Chen, Ning Wang, Feng Chen, and Tony Pipe. Detrive: Imitation learning with transformer detection for end-to-end autonomous driving. *CoRR*, abs/2310.14224, 2023a.

Huayu Chen, Cheng Lu, Chengyang Ying, Hang Su, and Jun Zhu. Offline reinforcement learning via high-fidelity generative behavior modeling. In *Proceedings of the 11th International Conference on Learning Representations*. OpenReview.net, 2023b.

Jiayu Chen, Tian Lan, and Vaneet Aggarwal. Hierarchical adversarial inverse reinforcement learning. *IEEE Transactions on Neural Networks and Learning Systems*, 2023c.

Jiayu Chen, Dipesh Tamboli, Tian Lan, and Vaneet Aggarwal. Multi-task hierarchical adversarial inverse reinforcement learning. In *Proceedings of the 40th International Conference on Machine Learning*, volume 202, pp. 4895–4920, 2023d.

Lili Chen, Kevin Lu, Aravind Rajeswaran, Kimin Lee, Aditya Grover, Misha Laskin, Pieter Abbeel, Aravind Srinivas, and Igor Mordatch. Decision transformer: Reinforcement learning via sequence modeling. *Advances in neural information processing systems*, 34:15084–15097, 2021b.

Tian Qi Chen, Yulia Rubanova, Jesse Bettencourt, and David Duvenaud. Neural ordinary differential equations. In *Advances in Neural Information Processing Systems 31*, pp. 6572–6583, 2018b.

Tian Qi Chen, Jens Behrmann, David Duvenaud, and Jörn-Henrik Jacobsen. Residual flows for invertible generative modeling. In *Advances in Neural Information Processing Systems 32*, pp. 9913–9923, 2019.

Valerie Chen, Abhinav Gupta, and Kenneth Marino. Ask your humans: Using human instructions to improve generalization in reinforcement learning. In *Proceedings of the 9th International Conference on Learning Representations*, 2021c.

Xi Chen, Yan Duan, Rein Houthooft, John Schulman, Ilya Sutskever, and Pieter Abbeel. Infogan: Interpretable representation learning by information maximizing generative adversarial nets. *Advances in neural information processing systems*, 29, 2016.

Yuhui Chen, Haoran Li, and Dongbin Zhao. Boosting continuous control with consistency policy. *CoRR*, abs/2310.06343, 2023e.

Maxime Chevalier-Boisvert, Lucas Willems, and Suman Pal. Minimalistic gridworld environment for openai gym. `https://github.com/maximecb/gym-minigrid`, 2018.

Maxime Chevalier-Boisvert, Dzmitry Bahdanau, Salem Lahlou, Lucas Willems, Chitwan Saharia, Thien Huu Nguyen, and Yoshua Bengio. Babyai: First steps towards grounded language learning with a human in the loop. In *International Conference on Learning Representations*, volume 105, 2019.

Cheng Chi, Siyuan Feng, Yilun Du, Zhenjia Xu, Eric Cousineau, Benjamin Burchfiel, and Shuran Song. Diffusion policy: Visuomotor policy learning via action diffusion. In *Robotics: Science and Systems*, 2023.

Rewon Child, Scott Gray, Alec Radford, and Ilya Sutskever. Generating long sequences with sparse transformers. *CoRR*, abs/1904.10509, 2019.

Daesol Cho, Dongseok Shim, and H. Jin Kim. S2P: state-conditioned image synthesis for data augmentation in offline reinforcement learning. In *Advances in Neural Information Processing Systems 35*, 2022.

Glen Chou and Russ Tedrake. Synthesizing stable reduced-order visuomotor policies for nonlinear systems via sums-of-squares optimization. *CoRR*, abs/2304.12405, 2023.

Junyoung Chung, Kyle Kastner, Laurent Dinh, Kratarth Goel, Aaron C. Courville, and Yoshua Bengio. A recurrent latent variable model for sequential data. In *Advances in Neural Information Processing Systems 28*, pp. 2980–2988, 2015.

Karl Cobbe, Christopher Hesse, Jacob Hilton, and John Schulman. Leveraging procedural generation to benchmark reinforcement learning. In *Proceedings of the 37th International Conference on Machine Learning*, volume 119, pp. 2048–2056, 2020.

Matthew Coleman, Olga Russakovsky, Christine Allen-Blanchette, and Ye Zhu. Discrete diffusion reward guidance methods for offline reinforcement learning. In *ICML 2023 Workshop: Sampling and Optimization in Discrete Space*, 2023.

Robert Cornish, Anthony L. Caterini, George Deligiannidis, and Arnaud Doucet. Relaxing bijectivity constraints with continuously indexed normalising flows. In *Proceedings of the 37th International Conference on Machine Learning*, volume 119, pp. 2133–2143. PMLR, 2020.

André Correia and Luís A. Alexandre. Hierarchical decision transformer. *CoRR*, abs/2209.10447, 2022.

Erwin Coumans and Yunfei Bai. Pybullet, a python module for physics simulation for games, robotics and machine learning. `http://pybullet.org`, 2016–2021.

Imre Csiszár and Paul C. Shields. Information theory and statistics: A tutorial. *Foundations and Trends in Communications and Information Theory*, 1(4), 2004.

Christopher R. Dance, Julien Perez, and Théo Cachet. Demonstration-conditioned reinforcement learning for few-shot imitation. In *Proceedings of the 38th International Conference on Machine Learning*, volume 139, pp. 2376–2387, 2021.

Sudeep Dasari and Abhinav Gupta. Transformers for one-shot visual imitation. In *Proceedings of the 4th Conference on Robot Learning*, volume 155, pp. 2071–2084, 2020.

Jared Quincy Davis, Albert Gu, Krzysztof Choromanski, Tri Dao, Christopher Ré, Chelsea Finn, and Percy Liang. Catformer: Designing stable transformers via sensitivity analysis. In *Proceedings of the 38th International Conference on Machine Learning*, volume 139, pp. 2489–2499, 2021.

Pim De Haan, Dinesh Jayaraman, and Sergey Levine. Causal confusion in imitation learning. *Advances in Neural Information Processing Systems*, 32, 2019.

Coline Devin. craftingworld. `https://github.com/cdevin/craftingworld`, 2024. Accessed: 2024-02-05.

Prafulla Dhariwal and Alexander Quinn Nichol. Diffusion models beat gans on image synthesis. In *Advances in Neural Information Processing Systems 34*, pp. 8780–8794, 2021.

Zihan Ding and Chi Jin. Consistency models as a rich and efficient policy class for reinforcement learning. *CoRR*, abs/2309.16984, 2023.

Laurent Dinh, David Krueger, and Yoshua Bengio. NICE: non-linear independent components estimation. In *3rd International Conference on Learning Representations, Workshop Track Proceedings*, 2015.

Laurent Dinh, Jascha Sohl-Dickstein, and Samy Bengio. Density estimation using real NVP. In *Proceedings of the 5th International Conference on Learning Representations*. OpenReview.net, 2017.

Wenbo Dong, Shaofan Liu, and Shiliang Sun. Safe batch constrained deep reinforcement learning with generative adversarial network. *Information Science*, 634:259–270, 2023.

Yihe Dong, Jean-Baptiste Cordonnier, and Andreas Loukas. Attention is not all you need: pure attention loses rank doubly exponentially with depth. In *Proceedings of the 38th International Conference on Machine Learning*, volume 139, pp. 2793–2803, 2021.

Monroe D Donsker and SR Srinivasa Varadhan. Asymptotic evaluation of certain markov process expectations for large time—iii. *Communications on pure and applied Mathematics*, 29(4):389–461, 1976.

Ron Dorfman, Idan Shenfeld, and Aviv Tamar. Offline meta reinforcement learning - identifiability challenges and effective data collection strategies. In *Advances in Neural Information Processing Systems 34*, pp. 4607–4618, 2021.

Alexey Dosovitskiy, Germán Ros, Felipe Codevilla, Antonio M. López, and Vladlen Koltun. CARLA: an open urban driving simulator. In *Proceedings of the 1st Annual Conference on Robot Learning*, volume 78, pp. 1–16, 2017.

Maximilian Du, Suraj Nair, Dorsa Sadigh, and Chelsea Finn. Behavior retrieval: Few-shot imitation learning by querying unlabeled datasets. In *Robotics: Science and Systems XIX*, 2023.

Yuqing Du, Daniel Ho, Alex Alemi, Eric Jang, and Mohi Khansari. Bayesian imitation learning for end-to-end mobile manipulation. In *Proceedings of the 39th International Conference on Machine Learning*, volume 162 of *Proceedings of Machine Learning Research*, pp. 5531–5546. PMLR, 2022.

Dheeru Dua, Casey Graff, et al. Uci machine learning repository, 2017. *URL http://archive. ics. uci. edu/ml*, 7(1), 2019.

Darrell Duffie and Jun Pan. An overview of value at risk. *Journal of derivatives*, 4(3):7–49, 1997.

Emilien Dupont, Arnaud Doucet, and Yee Whye Teh. Augmented neural odes. In *Advances in Neural Information Processing Systems 32*, pp. 3134–3144, 2019.

Conor Durkan, Artur Bekasov, Iain Murray, and George Papamakarios. Neural spline flows. *Advances in neural information processing systems*, 32, 2019.

Scott Emmons, Benjamin Eysenbach, Ilya Kostrikov, and Sergey Levine. Rvs: What is essential for offline RL via supervised learning? In *Proceedings of the 10th International Conference on Learning Representations*. OpenReview.net, 2022.

Ben Eysenbach, Ruslan Salakhutdinov, and Sergey Levine. Search on the replay buffer: Bridging planning and reinforcement learning. In *Advances in Neural Information Processing Systems 32*, pp. 15220–15231, 2019.

Kuan Fang, Patrick Yin, Ashvin Nair, Homer Walke, Gengchen Yan, and Sergey Levine. Generalization with lossy affordances: Leveraging broad offline data for learning visuomotor tasks. In *Conference on Robot Learning*, volume 205 of *Proceedings of Machine Learning Research*, pp. 106–117. PMLR, 2022.

Cong Fei, Bin Wang, Yuzheng Zhuang, Zongzhang Zhang, Jianye Hao, Hongbo Zhang, Xuewu Ji, and Wulong Liu. Triple-gail: A multi-modal imitation learning framework with generative adversarial nets. In *Proceedings of the 29th International Joint Conference on Artificial Intelligence*, pp. 2929–2935, 2020.

Panna Felsen, Patrick Lucey, and Sujoy Ganguly. Where will they go? predicting fine-grained adversarial multi-agent motion using conditional variational autoencoders. In *Proceedings of the 15th European Conference on Computer Vision*, volume 11215, pp. 761–776. Springer, 2018.

Pete Florence, Corey Lynch, Andy Zeng, Oscar A. Ramirez, Ayzaan Wahid, Laura Downs, Adrian Wong, Johnny Lee, Igor Mordatch, and Jonathan Tompson. Implicit behavioral cloning. In *Conference on Robot Learning*, volume 164, pp. 158–168, 2021.

Pete Florence, Corey Lynch, Andy Zeng, Oscar A Ramirez, Ayzaan Wahid, Laura Downs, Adrian Wong, Johnny Lee, Igor Mordatch, and Jonathan Tompson. Implicit behavioral cloning. In *Conference on Robot Learning*, pp. 158–168. PMLR, 2022.

Farama Foundation. Frozen lake environment. `https://gymnasium.farama.org/environments/toy_text/frozen_lake/`, 2023.

Katerina Fragkiadaki, Pulkit Agrawal, Sergey Levine, and Jitendra Malik. Learning visual predictive models of physics for playing billiards. In *proceedings of the 4th International Conference on Learning Representations*, 2016.

Markus Freitag and Yaser Al-Onaizan. Beam search strategies for neural machine translation. *arXiv preprint arXiv:1702.01806*, 2017.

Gideon Joseph Freund, Elad Sarafian, and Sarit Kraus. A coupled flow approach to imitation learning. In *Proceedings of the 40th International Conference on Machine Learning*, pp. 10357–10372. PMLR, 2023.

Huiqiao Fu, Kaiqiang Tang, Yuanyang Lu, Yiming Qi, Guizhou Deng, Flood Sung, and Chunlin Chen. Ess-infogail: Semi-supervised imitation learning from imbalanced demonstrations. In *Advances in Neural Information Processing Systems 36*, 2023.

Justin Fu, Katie Luo, and Sergey Levine. Learning robust rewards with adversarial inverse reinforcement learning. *CoRR*, abs/1710.11248, 2017.

Justin Fu, Aviral Kumar, Ofir Nachum, George Tucker, and Sergey Levine. D4RL: datasets for deep data-driven reinforcement learning. *CoRR*, abs/2004.07219, 2020.

Scott Fujimoto, David Meger, and Doina Precup. Off-policy deep reinforcement learning without exploration. In *Proceedings of the 36th International Conference on Machine Learning*, volume 97, pp. 2052–2062. PMLR, 2019.

Hiroki Furuta, Yutaka Matsuo, and Shixiang Shane Gu. Generalized decision transformer for offline hindsight information matching. In *Proceedings of the 10th International Conference on Learning Representations*. OpenReview.net, 2022.

Seyed Kamyar Seyed Ghasemipour, Shixiang Gu, and Richard S. Zemel. Smile: Scalable meta inverse reinforcement learning through context-conditional policies. In *Advances in Neural Information Processing Systems 32*, pp. 7879–7889, 2019a.

Seyed Kamyar Seyed Ghasemipour, Richard S. Zemel, and Shixiang Gu. A divergence minimization perspective on imitation learning methods. In *Proceedings of the 3rd Annual Conference on Robot Learning*, volume 100, pp. 1259–1277. PMLR, 2019b.

Aidan N. Gomez, Mengye Ren, Raquel Urtasun, and Roger B. Grosse. The reversible residual network: Backpropagation without storing activations. In *Advances in Neural Information Processing Systems 30*, pp. 2214–2224, 2017.

Ian Goodfellow. Nips 2016 tutorial: Generative adversarial networks, 2017.

Ian Goodfellow, Jean Pouget-Abadie, Mehdi Mirza, Bing Xu, David Warde-Farley, Sherjil Ozair, Aaron Courville, and Yoshua Bengio. Generative adversarial nets. *Advances in neural information processing systems*, 27, 2014a.

Ian J. Goodfellow, Jean Pouget-Abadie, Mehdi Mirza, Bing Xu, David Warde-Farley, Sherjil Ozair, Aaron C. Courville, and Yoshua Bengio. Generative adversarial nets. In *Advances in Neural Information Processing Systems 27*, pp. 2672–2680, 2014b.

Will Grathwohl, Ricky TQ Chen, Jesse Bettencourt, Ilya Sutskever, and David Duvenaud. Ffjord: Free-form continuous dynamics for scalable reversible generative models. *arXiv preprint arXiv:1810.01367*, 2018.

Arthur Gretton, Karsten M. Borgwardt, Malte J. Rasch, Bernhard Schölkopf, and Alexander J. Smola. A kernel two-sample test. *Journal of Machine Learning Research*, 13:723–773, 2012.

Sven Gronauer. Bullet-safety-gym: A framework for constrained reinforcement learning. Technical report, mediaTUM, 2022.

Aditya Grover, Manik Dhar, and Stefano Ermon. Flow-gan: Combining maximum likelihood and adversarial learning in generative models. In *Proceedings of the 32nd AAAI Conference on Artificial Intelligence*, pp. 3069–3076. AAAI Press, 2018.

Albert Gu and Tri Dao. Mamba: Linear-time sequence modeling with selective state spaces. *CoRR*, abs/2312.00752, 2023.

Jiayi Guan, Shangding Gu, Zhijun Li, Jing Hou, Yiqin Yang, Guang Chen, and Changjun Jiang. Uac: Offline reinforcement learning with uncertain action constraint. *IEEE Transactions on Cognitive and Developmental Systems*, 2023.

Abhishek Gupta, Vikash Kumar, Corey Lynch, Sergey Levine, and Karol Hausman. Relay policy learning: Solving long-horizon tasks via imitation and reinforcement learning. In *Conference on Robot Learning*, volume 100, pp. 1025–1037, 2019a.

Abhishek Gupta, Vikash Kumar, Corey Lynch, Sergey Levine, and Karol Hausman. Relay policy learning: Solving long-horizon tasks via imitation and reinforcement learning. *arXiv preprint arXiv:1910.11956*, 2019b.

William H. Guss, Brandon Houghton, Nicholay Topin, Phillip Wang, Cayden Codel, Manuela Veloso, and Ruslan Salakhutdinov. Minerl: A large-scale dataset of minecraft demonstrations. In *Proceedings of the 28th International Joint Conference on Artificial Intelligence*, pp. 2442–2448. ijcai.org, 2019.

Tuomas Haarnoja, Aurick Zhou, Pieter Abbeel, and Sergey Levine. Soft actor-critic: Off-policy maximum entropy deep reinforcement learning with a stochastic actor. In *Proceedings of the 35th International Conference on Machine Learning*, volume 80 of *Proceedings of Machine Learning Research*, pp. 1856–1865. PMLR, 2018.

Danijar Hafner, Timothy P. Lillicrap, Jimmy Ba, and Mohammad Norouzi. Dream to control: Learning behaviors by latent imagination. In *Proceedings of the 8th International Conference on Learning Representations*, 2020.

Jay Hambidge. *The elements of dynamic symmetry.* Courier Corporation, 1967.

Jungwoo Han and Jinwhan Kim. Selective data augmentation for improving the performance of offline reinforcement learning. In *International Conference on Control, Automation and Systems (ICCAS)*, pp. 222–226. IEEE, 2022.

Kai Han, Yunhe Wang, Hanting Chen, Xinghao Chen, Jianyuan Guo, Zhenhua Liu, Yehui Tang, An Xiao, Chunjing Xu, Yixing Xu, et al. A survey on vision transformer. *IEEE transactions on pattern analysis and machine intelligence*, 45(1):87–110, 2022.

Philippe Hansen-Estruch, Ilya Kostrikov, Michael Janner, Jakub Grudzien Kuba, and Sergey Levine. IDQL: implicit q-learning as an actor-critic method with diffusion policies. *CoRR*, abs/2304.10573, 2023.

Xiaotian Hao, Weixun Wang, Jianye Hao, and Yaodong Yang. Independent generative adversarial self-imitation learning in cooperative multiagent systems. In *Proceedings of the 18th International Conference on Autonomous Agents and MultiAgent Systems*, pp. 1315–1323, 2019.

Karol Hausman, Yevgen Chebotar, Stefan Schaal, Gaurav S. Sukhatme, and Joseph J. Lim. Multi-modal imitation learning from unstructured demonstrations using generative adversarial nets. In *Advances in Neural Information Processing Systems 30*, pp. 1235–1245, 2017.

Haoran He, Chenjia Bai, Kang Xu, Zhuoran Yang, Weinan Zhang, Dong Wang, Bin Zhao, and Xuelong Li. Diffusion model is an effective planner and data synthesizer for multi-task reinforcement learning. *CoRR*, abs/2305.18459, 2023a.

Kaiming He, Xiangyu Zhang, Shaoqing Ren, and Jian Sun. Deep residual learning for image recognition. In *2016 IEEE Conference on Computer Vision and Pattern Recognition*, pp. 770–778. IEEE Computer Society, 2016.

Longxiang He, Linrui Zhang, Junbo Tan, and Xueqian Wang. Diffcps: Diffusion model based constrained policy search for offline reinforcement learning. *CoRR*, abs/2310.05333, 2023b.

Joey Hejna, Pieter Abbeel, and Lerrel Pinto. Improving long-horizon imitation through instruction prediction. In *Proceedings of the 37th AAAI Conference on Artificial Intelligence*, pp. 7857–7865, 2023.

Dan Hendrycks and Kevin Gimpel. Gaussian error linear units (gelus), 2023.

Charles A. Hepburn and Giovanni Montana. Model-based trajectory stitching for improved offline reinforcement learning. *CoRR*, abs/2211.11603, 2022.

Irina Higgins, Loïc Matthey, Arka Pal, Christopher P. Burgess, Xavier Glorot, Matthew M. Botvinick, Shakir Mohamed, and Alexander Lerchner. beta-vae: Learning basic visual concepts with a constrained variational framework. In *Proceedings of the 5th International Conference on Learning Representations*. OpenReview.net, 2017.

Jean-Baptiste Hiriart-Urruty and Claude Lemaréchal. *Fundamentals of convex analysis*. Springer Science & Business Media, 2004.

Jonathan Ho and Stefano Ermon. Generative adversarial imitation learning. In *Advances in Neural Information Processing Systems 29*, pp. 4565–4573, 2016.

Jonathan Ho and Tim Salimans. Classifier-free diffusion guidance. *CoRR*, abs/2207.12598, 2022.

Jonathan Ho, Xi Chen, Aravind Srinivas, Yan Duan, and Pieter Abbeel. Flow++: Improving flow-based generative models with variational dequantization and architecture design. In *Proceedings of the 36th International Conference on Machine Learning*, volume 97, pp. 2722–2730. PMLR, 2019.

Jonathan Ho, Ajay Jain, and Pieter Abbeel. Denoising diffusion probabilistic models. *Advances in neural information processing systems*, 33:6840–6851, 2020.

Emiel Hoogeboom, Didrik Nielsen, Priyank Jaini, Patrick Forré, and Max Welling. Argmax flows and multinomial diffusion: Learning categorical distributions. *Advances in Neural Information Processing Systems*, 34:12454–12465, 2021.

Neil Houlsby, Andrei Giurgiu, Stanislaw Jastrzebski, Bruna Morrone, Quentin de Laroussilhe, Andrea Gesmundo, Mona Attariyan, and Sylvain Gelly. Parameter-efficient transfer learning for NLP. In *Proceedings of the 36th International Conference on Machine Learning*, volume 97, pp. 2790–2799, 2019.

Jifeng Hu, Yanchao Sun, Sili Huang, Siyuan Guo, Hechang Chen, Li Shen, Lichao Sun, Yi Chang, and Dacheng Tao. Instructed diffuser with temporal condition guidance for offline reinforcement learning. *CoRR*, abs/2306.04875, 2023a.

Shengchao Hu, Li Shen, Ya Zhang, and Dacheng Tao. Graph decision transformer. *CoRR*, abs/2303.03747, 2023b.

Siyi Hu, Fengda Zhu, Xiaojun Chang, and Xiaodan Liang. Updet: Universal multi-agent rl via policy decoupling with transformers. In *Proceedings of the 9th International Conference on Learning Representations*, 2021.

Chin-Wei Huang, David Krueger, Alexandre Lacoste, and Aaron C. Courville. Neural autoregressive flows. In *Proceedings of the 35th International Conference on Machine Learning*, volume 80 of *Proceedings of Machine Learning Research*, pp. 2083–2092. PMLR, 2018.

Dongyoon Hwang, Minho Park, and Jiyoung Lee. Sample generations for reinforcement learning via diffusion models. *OpenReview.net*, 2023.

Aapo Hyvärinen. Estimation of non-normalized statistical models by score matching. *Journal of Machine Learning Research*, 6:695–709, 2005.

Jörn-Henrik Jacobsen, Arnold W. M. Smeulders, and Edouard Oyallon. i-revnet: Deep invertible networks. In *Proceedings of the 6th International Conference on Learning Representations*, 2018.

Andrew Jaegle, Sebastian Borgeaud, Jean-Baptiste Alayrac, Carl Doersch, Catalin Ionescu, David Ding, Skanda Koppula, Daniel Zoran, Andrew Brock, Evan Shelhamer, Olivier J. Hénaff, Matthew M. Botvinick, Andrew Zisserman, Oriol Vinyals, and João Carreira. Perceiver IO: A general architecture for structured inputs & outputs. In *Proceedings of the 10th International Conference on Learning Representations*. OpenReview.net, 2022.

Stephen James, Zicong Ma, David Rovick Arrojo, and Andrew J. Davison. Rlbench: The robot learning benchmark & learning environment. *IEEE Robotics Automation Letters*, 5(2):3019–3026, 2020.

Michael Janner, Justin Fu, Marvin Zhang, and Sergey Levine. When to trust your model: Model-based policy optimization. In *Advances in Neural Information Processing Systems 32*, 2019.

Michael Janner, Qiyang Li, and Sergey Levine. Offline reinforcement learning as one big sequence modeling problem. In *Advances in Neural Information Processing Systems 34*, pp. 1273–1286, 2021.

Michael Janner, Yilun Du, Joshua B. Tenenbaum, and Sergey Levine. Planning with diffusion for flexible behavior synthesis. In *Proceedings of the 39th International Conference on Machine Learning*, volume 162, pp. 9902–9915. PMLR, 2022.

Wonseok Jeon, Seokin Seo, and Kee-Eung Kim. A bayesian approach to generative adversarial imitation learning. In *Advances in Neural Information Processing Systems 31*, pp. 7440–7450, 2018.

Mingxuan Jing, Wenbing Huang, Fuchun Sun, Xiaojian Ma, Tao Kong, Chuang Gan, and Lei Li. Adversarial option-aware hierarchical imitation learning. In *Proceedings of the 38th International Conference on Machine Learning*, volume 139, pp. 5097–5106. PMLR, 2021.

Alexia Jolicoeur-Martineau, Rémi Piché-Taillefer, Ioannis Mitliagkas, and Remi Tachet des Combes. Adversarial score matching and improved sampling for image generation. In *Proceedings of the 9th International Conference on Learning Representations*. OpenReview.net, 2021.

Katikapalli Subramanyam Kalyan, Ajit Rajasekharan, and Sivanesan Sangeetha. AMMUS : A survey of transformer-based pretrained models in natural language processing. *CoRR*, abs/2108.05542, 2021.

Aishwarya Kamath, Peter Anderson, Su Wang, Jing Yu Koh, Alexander Ku, Austin Waters, Yinfei Yang, Jason Baldridge, and Zarana Parekh. A new path: Scaling vision-and-language navigation with synthetic instructions and imitation learning. In *IEEE/CVF Conference on Computer Vision and Pattern Recognition*, pp. 10813–10823, 2023.

Bingyi Kang, Xiao Ma, Chao Du, Tianyu Pang, and Shuicheng Yan. Efficient diffusion policies for offline reinforcement learning. *CoRR*, abs/2305.20081, 2023.

Tero Karras, Miika Aittala, Timo Aila, and Samuli Laine. Elucidating the design space of diffusion-based generative models. In *Advances in neural information processing systems 35*, 2022.

Muhammad Junaid Khan, Syed Hammad Ahmed, and Gita Sukthankar. Transformer-based value function decomposition for cooperative multi-agent reinforcement learning in starcraft. In *Proceedings of the 18th AAAI Conference on Artificial Intelligence and Interactive Digital Entertainment*, pp. 113–119. AAAI Press, 2022.

Heecheol Kim, Yoshiyuki Ohmura, and Yasuo Kuniyoshi. Transformer-based deep imitation learning for dual-arm robot manipulation. In *IEEE/RSJ International Conference on Intelligent Robots and Systems*, pp. 8965–8972, 2021.

Heecheol Kim, Yoshiyuki Ohmura, and Yasuo Kuniyoshi. Memory-based gaze prediction in deep imitation learning for robot manipulation. In *International Conference on Robotics and Automation*, pp. 2427–2433. IEEE, 2022.

Heecheol Kim, Yoshiyuki Ohmura, Akihiko Nagakubo, and Yasuo Kuniyoshi. Training robots without robots: Deep imitation learning for master-to-robot policy transfer. *IEEE Robotics Automation Letters*, 8 (5):2906–2913, 2023.

Diederik Kingma and Ruiqi Gao. Understanding diffusion objectives as the elbo with simple data augmentation. *Advances in Neural Information Processing Systems 36*, 36, 2023.

Diederik P. Kingma and Prafulla Dhariwal. Glow: Generative flow with invertible 1x1 convolutions. In *Advances in Neural Information Processing Systems 31*, pp. 10236–10245, 2018.

Diederik P. Kingma and Max Welling. Auto-encoding variational bayes. In *Proceedings of the 2nd International Conference on Learning Representations*, 2014.

Diederik P. Kingma and Max Welling. An introduction to variational autoencoders. *Foundations and Trends® in Machine Learning*, 12(4):307–392, 2019.

Durk P Kingma, Tim Salimans, Rafal Jozefowicz, Xi Chen, Ilya Sutskever, and Max Welling. Improved variational inference with inverse autoregressive flow. *Advances in neural information processing systems*, 29, 2016.

Thomas Kipf, Yujia Li, Hanjun Dai, Vinícius Flores Zambaldi, Alvaro Sanchez-Gonzalez, Edward Grefenstette, Pushmeet Kohli, and Peter W. Battaglia. Compile: Compositional imitation learning and execution. In *Proceedings of the 36th International Conference on Machine Learning*, volume 97 of *Proceedings of Machine Learning Research*, pp. 3418–3428. PMLR, 2019.

Ivan Kobyzev, Simon J. D. Prince, and Marcus A. Brubaker. Normalizing flows: An introduction and review of current methods. *IEEE TRANSACTIONS ON PATTERN ANALYSIS AND MACHINE INTELLIGENCE*, 43(11):3964–3979, 2021.

Yotto Koga, Heather Kerrick, and Sachin Chitta. On CAD informed adaptive robotic assembly. In *IEEE/RSJ International Conference on Intelligent Robots and Systems*, pp. 10207–10214. IEEE, 2022.

Ilya Kostrikov, Kumar Krishna Agrawal, Debidatta Dwibedi, Sergey Levine, and Jonathan Tompson. Discriminator-actor-critic: Addressing sample inefficiency and reward bias in adversarial imitation learning. In *Proceedings of the 7th International Conference on Learning Representations*. OpenReview.net, 2019.

Ilya Kostrikov, Ashvin Nair, and Sergey Levine. Offline reinforcement learning with implicit q-learning. In *Proceedings of the 10th International Conference on Learning Representations*. OpenReview.net, 2022.

Robert Krajewski, Julian Bock, Laurent Kloeker, and Lutz Eckstein. The highd dataset: A drone dataset of naturalistic vehicle trajectories on german highways for validation of highly automated driving systems. In *Proceedings of the 21st International Conference on Intelligent Transportation Systems*, pp. 2118–2125. IEEE, 2018.

Alex Kuefler and Mykel J. Kochenderfer. Burn-in demonstrations for multi-modal imitation learning. In *Proceedings of the 17th International Conference on Autonomous Agents and MultiAgent Systems*, pp. 1071–1078, 2018.

Aviral Kumar, Justin Fu, Matthew Soh, George Tucker, and Sergey Levine. Stabilizing off-policy q-learning via bootstrapping error reduction. In *Advances in Neural Information Processing Systems 32*, pp. 11761–11771, 2019.

Aviral Kumar, Aurick Zhou, George Tucker, and Sergey Levine. Conservative q-learning for offline reinforcement learning. In *Advances in Neural Information Processing Systems 33*, 2020.

Jonathan Lacotte, Mohammad Ghavamzadeh, Yinlam Chow, and Marco Pavone. Risk-sensitive generative adversarial imitation learning. In *Proceedings of the 22nd International Conference on Artificial Intelligence and Statistics*, volume 89, pp. 2154–2163, 2019.

Kuang-Huei Lee, Ofir Nachum, Mengjiao Yang, Lisa Lee, Daniel Freeman, Sergio Guadarrama, Ian Fischer, Winnie Xu, Eric Jang, Henryk Michalewski, and Igor Mordatch. Multi-game decision transformers. In *Advances in Neural Information Processing Systems 35*, 2022.

Su-Jin Lee, Tae Yoon Chun, Hyoung Woo Lim, and Sang-Ho Lee. Path tracking control using imitation learning with variational auto-encoder. In *Proceedings of the 19th International Conference on Control, Automation and Systems*, pp. 501–505. IEEE, 2019.

Sergey Levine. Reinforcement learning and control as probabilistic inference: Tutorial and review. *arXiv preprint arXiv:1805.00909*, 2018.

Sergey Levine, Aviral Kumar, George Tucker, and Justin Fu. Offline reinforcement learning: Tutorial, review, and perspectives on open problems. *CoRR*, abs/2005.01643, 2020.

Chongxuan Li, Taufik Xu, Jun Zhu, and Bo Zhang. Triple generative adversarial nets. In *Advances in Neural Information Processing Systems 30*, pp. 4088–4098, 2017a.

Jinning Li, Chen Tang, Masayoshi Tomizuka, and Wei Zhan. Hierarchical planning through goal-conditioned offline reinforcement learning. *IEEE Robotics Automation Letters*, 7(4):10216–10223, 2022.

Tao Li, Juan Guevara, Xinghong Xie, and Quanyan Zhu. Self-confirming transformer for locally consistent online adaptation in multi-agent reinforcement learning. *CoRR*, abs/2310.04579, 2023a.

Wenhao Li, Xiangfeng Wang, Bo Jin, and Hongyuan Zha. Hierarchical diffusion for offline decision making. In *Proceedings of the 40th International Conference on Machine Learning*, volume 202, pp. 20035–20064, 2023b.

Yunzhu Li, Jiaming Song, and Stefano Ermon. Infogail: Interpretable imitation learning from visual demonstrations. In *Advances in Neural Information Processing Systems 30*, pp. 3812–3822, 2017b.

Zhuoran Li, Ling Pan, and Longbo Huang. Beyond conservatism: Diffusion policies in offline multi-agent reinforcement learning. *CoRR*, abs/2307.01472, 2023c.

Anthony Liang, Ishika Singh, Karl Pertsch, and Jesse Thomason. Transformer adapters for robot learning. In *CoRL 2022 Workshop on Pre-training Robot Learning*, 2022. URL `https://openreview.net/forum?id=H--wvRYBmF`.

Hebin Liang, Zibin Dong, Yi Ma, Xiaotian Hao, Yan Zheng, and Jianye Hao. A hierarchical imitation learning-based decision framework for autonomous driving. In *Proceedings of the 32nd ACM International Conference on Information and Knowledge Management*, pp. 4695–4701. ACM, 2023a.

Zhixuan Liang, Yao Mu, Mingyu Ding, Fei Ni, Masayoshi Tomizuka, and Ping Luo. Adaptdiffuser: Diffusion models as adaptive self-evolving planners. In *Proceedings of the 40th International Conference on Machine Learning*, volume 202, pp. 20725–20745, 2023b.

Timothy P. Lillicrap, Jonathan J. Hunt, Alexander Pritzel, Nicolas Heess, Tom Erez, Yuval Tassa, David Silver, and Daan Wierstra. Continuous control with deep reinforcement learning. In *Proceedings of the 4th International Conference on Learning Representations*, 2016.

Qinjie Lin, Han Liu, and Biswa Sengupta. Switch trajectory transformer with distributional value approximation for multi-task reinforcement learning. *CoRR*, abs/2203.07413, 2022a.

Runji Lin, Ye Li, Xidong Feng, Zhaowei Zhang, Xian Hong Wu Fung, Haifeng Zhang, Jun Wang, Yali Du, and Yaodong Yang. Contextual transformer for offline meta reinforcement learning. *CoRR*, abs/2211.08016, 2022b.

Tianyang Lin, Yuxin Wang, Xiangyang Liu, and Xipeng Qiu. A survey of transformers. *AI Open*, 2022c.

Fangchen Liu, Zhan Ling, Tongzhou Mu, and Hao Su. State alignment-based imitation learning. In *Proceedings of the 8th International Conference on Learning Representations*. OpenReview.net, 2020.

Xiao Liu, Fanjin Zhang, Zhenyu Hou, Li Mian, Zhaoyu Wang, Jing Zhang, and Jie Tang. Self-supervised learning: Generative or contrastive. *IEEE Transactions on Knowledge and Data Engineering*, 35(1): 857–876, 2023a.

Zuxin Liu, Zijian Guo, Yihang Yao, Zhepeng Cen, Wenhao Yu, Tingnan Zhang, and Ding Zhao. Constrained decision transformer for offline safe reinforcement learning. In *Proceedings of the 40th International Conference on Machine Learning*, volume 202, pp. 21611–21630, 2023b.

Francesco Locatello, Stefan Bauer, Mario Lucic, Gunnar Rätsch, Sylvain Gelly, Bernhard Schölkopf, and Olivier Bachem. Challenging common assumptions in the unsupervised learning of disentangled representations. In *Proceedings of the 36th International Conference on Machine Learning*, volume 97, pp. 4114–4124, 2019.

Ryan Lowe, Yi Wu, Aviv Tamar, Jean Harb, Pieter Abbeel, and Igor Mordatch. Multi-agent actor-critic for mixed cooperative-competitive environments. In *Advances in Neural Information Processing Systems 30*, pp. 6379–6390, 2017.

Ricky Loynd, Roland Fernandez, Asli Celikyilmaz, Adith Swaminathan, and Matthew J. Hausknecht. Working memory graphs. In *Proceedings of the 37th International Conference on Machine Learning*, volume 119, pp. 6404–6414, 2020.

Cheng Lu, Yuhao Zhou, Fan Bao, Jianfei Chen, Chongxuan Li, and Jun Zhu. Dpm-solver: A fast ODE solver for diffusion probabilistic model sampling in around 10 steps. In *Advances in Neural Information Processing Systems 35*, 2022.

Cheng Lu, Huayu Chen, Jianfei Chen, Hang Su, Chongxuan Li, and Jun Zhu. Contrastive energy prediction for exact energy-guided diffusion sampling in offline reinforcement learning. In *Proceedings of the 40th International Conference on Machine Learning*, volume 202, pp. 22825–22855. PMLR, 2023.

Xiaoyu Lu, Jan Stuehmer, and Katja Hofmann. Trajectory VAE for multi-modal imitation, 2019. URL `https://openreview.net/forum?id=Byx1VnR9K7`.

Yiren Lu and Jonathan Tompson. ADAIL: adaptive adversarial imitation learning. *CoRR*, abs/2008.12647, 2020.

Jianlan Luo, Perry Dong, Jeffrey Wu, Aviral Kumar, Xinyang Geng, and Sergey Levine. Action-quantized offline reinforcement learning for robotic skill learning. In *Conference on Robot Learning*, pp. 1348–1361. PMLR, 2023.

Corey Lynch and Pierre Sermanet. Language conditioned imitation learning over unstructured data. In *Robotics: Science and Systems XVII, Virtual Event, July 12-16, 2021*, 2021.

Corey Lynch, Mohi Khansari, Ted Xiao, Vikash Kumar, Jonathan Tompson, Sergey Levine, and Pierre Sermanet. Learning latent plans from play. In *Proceedings of the 3rd Annual Conference on Robot Learning*, volume 100, pp. 1113–1132, 2019.

Jiafei Lyu, Xiaoteng Ma, Xiu Li, and Zongqing Lu. Mildly conservative q-learning for offline reinforcement learning. In *Advances in Neural Information Processing Systems 35*, 2022.

Ajay Mandlekar, Danfei Xu, Josiah Wong, Soroush Nasiriany, Chen Wang, Rohun Kulkarni, Li Fei-Fei, Silvio Savarese, Yuke Zhu, and Roberto Martín-Martín. What matters in learning from offline human demonstrations for robot manipulation. In *Conference on Robot Learning*, volume 164, pp. 1678–1690, 2021a.

Ajay Mandlekar, Danfei Xu, Josiah Wong, Soroush Nasiriany, Chen Wang, Rohun Kulkarni, Li Fei-Fei, Silvio Savarese, Yuke Zhu, and Roberto Martín-Martín. What matters in learning from offline human demonstrations for robot manipulation. *arXiv preprint arXiv:2108.03298*, 2021b.

Lucas Manuelli, Yunzhu Li, Peter R. Florence, and Russ Tedrake. Keypoints into the future: Self-supervised correspondence in model-based reinforcement learning. In *Proceedings of the 4th Conference on Robot Learning*, volume 155, pp. 693–710, 2020.

Xudong Mao, Qing Li, Haoran Xie, Raymond Y. K. Lau, Zhen Wang, and Stephen Paul Smolley. Least squares generative adversarial networks. In *IEEE International Conference on Computer Vision*, 2017.

Gabriel Margolis and Pulkit Agrawal. Walk these ways: Gait-conditioned policies yield diversified quadrupedal agility. In *Conference on Robot Learning*, volume 1, pp. 2, 2022.

Saeed Masoudnia and Reza Ebrahimpour. Mixture of experts: a literature survey. *Artificial Intelligence Review*, 42:275–293, 2014.

James Massey et al. Causality, feedback and directed information. In *The International Symposium on Information Theory and Its Applications*, pp. 303–305, 1990.

David Q Mayne and Hannah Michalska. Receding horizon control of nonlinear systems. In *Proceedings of the 27th IEEE Conference on Decision and Control*, pp. 464–465. IEEE, 1988.

Bogdan Mazoure, Thang Doan, Audrey Durand, Joelle Pineau, and R. Devon Hjelm. Leveraging exploration in off-policy algorithms via normalizing flows. In *Proceedings of the 3rd Annual Conference on Robot Learning*, volume 100 of *Proceedings of Machine Learning Research*, pp. 430–444. PMLR, 2019.

Oier Mees, Lukás Hermann, and Wolfram Burgard. What matters in language conditioned robotic imitation learning over unstructured data. *IEEE Robotics Automation Letters*, 7(4):11205–11212, 2022a.

Oier Mees, Lukas Hermann, Erick Rosete-Beas, and Wolfram Burgard. Calvin: A benchmark for language-conditioned policy learning for long-horizon robot manipulation tasks. *IEEE Robotics and Automation Letters*, 7(3):7327–7334, 2022b.

ML Menéndez, JA Pardo, L Pardo, and MC Pardo. The jensen-shannon divergence. *Journal of the Franklin Institute*, 334(2):307–318, 1997.

Linghui Meng, Muning Wen, Yaodong Yang, Chenyang Le, Xiyun Li, Weinan Zhang, Ying Wen, Haifeng Zhang, Jun Wang, and Bo Xu. Offline pre-trained multi-agent decision transformer: One big sequence model tackles all SMAC tasks. *CoRR*, abs/2112.02845, 2021.

Gregory P Meyer, Ankit Laddha, Eric Kee, Carlos Vallespi-Gonzalez, and Carl K Wellington. Lasernet: An efficient probabilistic 3d object detector for autonomous driving. In *Proceedings of the IEEE/CVF conference on computer vision and pattern recognition*, pp. 12677–12686, 2019.

Mehdi Mirza and Simon Osindero. Conditional generative adversarial nets. *arXiv preprint arXiv:1411.1784*, 2014.

Eric Mitchell, Rafael Rafailov, Xue Bin Peng, Sergey Levine, and Chelsea Finn. Offline meta-reinforcement learning with advantage weighting. In *Proceedings of the 38th International Conference on Machine Learning*, volume 139, pp. 7780–7791, 2021.

Shakir Mohamed and Danilo Jimenez Rezende. Variational information maximisation for intrinsically motivated reinforcement learning. In *Advances in Neural Information Processing Systems 28*, pp. 2125–2133, 2015.

Tongzhou Mu, Zhan Ling, Fanbo Xiang, Derek Yang, Xuanlin Li, Stone Tao, Zhiao Huang, Zhiwei Jia, and Hao Su. Maniskill: Generalizable manipulation skill benchmark with large-scale demonstrations. In *Proceedings of the Neural Information Processing Systems Track on Datasets and Benchmarks 1*, 2021.

Ashvin Nair, Murtaza Dalal, Abhishek Gupta, and Sergey Levine. Accelerating online reinforcement learning with offline datasets. *CoRR*, abs/2006.09359, 2020.

Soroush Nasiriany, Tian Gao, Ajay Mandlekar, and Yuke Zhu. Learning and retrieval from prior data for skill-based imitation learning. In *Proceedings of the 6th Annual Conference on Robot Learning*, 2022.

Andrew Y. Ng, Daishi Harada, and Stuart Russell. Policy invariance under reward transformations: Theory and application to reward shaping. In *Proceedings of the 16th International Conference on Machine Learning*, pp. 278–287, 1999.

Fei Ni, Jianye Hao, Yao Mu, Yifu Yuan, Yan Zheng, Bin Wang, and Zhixuan Liang. Metadiffuser: Diffusion model as conditional planner for offline meta-rl. In *Proceedings of the 40th International Conference on Machine Learning*, volume 202, pp. 26087–26105, 2023.

Tianwei Ni, Harshit S. Sikchi, Yufei Wang, Tejus Gupta, Lisa Lee, and Ben Eysenbach. f-irl: Inverse reinforcement learning via state marginal matching. In *Proceedings of the 4th Conference on Robot Learning*, volume 155, pp. 529–551, 2020.

Alexander Quinn Nichol and Prafulla Dhariwal. Improved denoising diffusion probabilistic models. In *Proceedings of the 38th International Conference on Machine Learning*, volume 139, pp. 8162–8171. PMLR, 2021.

Didrik Nielsen, Priyank Jaini, Emiel Hoogeboom, Ole Winther, and Max Welling. Survae flows: Surjections to bridge the gap between vaes and flows. In *Advances in Neural Information Processing Systems 33*, 2020.

Michael D. Noseworthy, Rohan Paul, Subhro Roy, Daehyung Park, and Nicholas Roy. Task-conditioned variational autoencoders for learning movement primitives. In *Proceedings of the 3rd Annual Conference on Robot Learning*, volume 100 of *Proceedings of Machine Learning Research*, pp. 933–944. PMLR, 2019.

Sebastian Nowozin, Botond Cseke, and Ryota Tomioka. f-gan: Training generative neural samplers using variational divergence minimization. In *Advances in Neural Information Processing Systems 29*, pp. 271–279, 2016.

OpenAI. Gpt-4 technical report, 2023. URL `https://arxiv.org/pdf/2303.08774.pdf`.

Yingwei Pan, Yehao Li, Yiheng Zhang, Qi Cai, Fuchen Long, Zhaofan Qiu, Ting Yao, and Tao Mei. Silver-bullet-3d at maniskill 2021: Learning-from-demonstrations and heuristic rule-based methods for object manipulation. In *ICLR 2022 Workshop on Generalizable Policy Learning in Physical World*, 2022.

George Papamakarios, Iain Murray, and Theo Pavlakou. Masked autoregressive flow for density estimation. In *Advances in Neural Information Processing Systems 30*, pp. 2338–2347, 2017.

Emilio Parisotto and Ruslan Salakhutdinov. Efficient transformers in reinforcement learning using actor-learner distillation. In *Proceedings of the 9th International Conference on Learning Representations*. OpenReview.net, 2021.

Emilio Parisotto, H. Francis Song, Jack W. Rae, Razvan Pascanu, Çaglar Gülçehre, Siddhant M. Jayakumar, Max Jaderberg, Raphaël Lopez Kaufman, Aidan Clark, Seb Noury, Matthew M. Botvinick, Nicolas Heess, and Raia Hadsell. Stabilizing transformers for reinforcement learning. In *Proceedings of the 37th International Conference on Machine Learning*, volume 119, pp. 7487–7498. PMLR, 2020.

Jongjin Park, Younggyo Seo, Chang Liu, Li Zhao, Tao Qin, Jinwoo Shin, and Tie-Yan Liu. Object-aware regularization for addressing causal confusion in imitation learning. *Advances in Neural Information Processing Systems*, 34:3029–3042, 2021.

Keiran Paster, Sheila A. McIlraith, and Jimmy Ba. You can't count on luck: Why decision transformers and rvs fail in stochastic environments. In *Advances in Neural Information Processing Systems 35*, 2022.

Pranay Pasula. Complex skill acquisition through simple skill adversarial imitation learning. *CoRR*, abs/2007.10281, 2020.

Tim Pearce and Jun Zhu. Counter-strike deathmatch with large-scale behavioural cloning. In *2022 IEEE Conference on Games (CoG)*, pp. 104–111. IEEE, 2022.

Tim Pearce, Tabish Rashid, Anssi Kanervisto, David Bignell, Mingfei Sun, Raluca Georgescu, Sergio Valcarcel Macua, Shan Zheng Tan, Ida Momennejad, Katja Hofmann, and Sam Devlin. Imitating human behaviour with diffusion models. In *Proceedings of the 11th International Conference on Learning Representations*, 2023.

Bei Peng, Tabish Rashid, Christian Schröder de Witt, Pierre-Alexandre Kamienny, Philip H. S. Torr, Wendelin Boehmer, and Shimon Whiteson. FACMAC: factored multi-agent centralised policy gradients. In *Advances in Neural Information Processing Systems 34*, pp. 12208–12221, 2021.

Jian-Wei Peng, Min-Chun Hu, and Wei-Ta Chu. An imitation learning framework for generating multi-modal trajectories from unstructured demonstrations. *Neurocomputing*, 500:712–723, 2022.

Xue Bin Peng, Angjoo Kanazawa, Sam Toyer, Pieter Abbeel, and Sergey Levine. Variational discriminator bottleneck: Improving imitation learning, inverse rl, and gans by constraining information flow. In *Proceedings of the 7th International Conference on Learning Representations*, 2019a.

Xue Bin Peng, Aviral Kumar, Grace Zhang, and Sergey Levine. Advantage-weighted regression: Simple and scalable off-policy reinforcement learning. *CoRR*, abs/1910.00177, 2019b.

Karl Pertsch, Youngwoon Lee, Yue Wu, and Joseph J. Lim. Demonstration-guided reinforcement learning with learned skills. In *Conference on Robot Learning*, volume 164 of *Proceedings of Machine Learning Research*, pp. 729–739. PMLR, 2021.

Samuel Pfrommer, Yatong Bai, Hyunin Lee, and Somayeh Sojoudi. Initial state interventions for deconfounded imitation learning. In *Proceedings of the 62nd IEEE Conference on Decision and Control*, pp. 2312–2319. IEEE, 2023.

Matthias Plappert, Marcin Andrychowicz, Alex Ray, Bob McGrew, Bowen Baker, Glenn Powell, Jonas Schneider, Josh Tobin, Maciek Chociej, Peter Welinder, Vikash Kumar, and Wojciech Zaremba. Multi-goal reinforcement learning: Challenging robotics environments and request for research. *CoRR*, abs/1802.09464, 2018.

Bryan A. Plummer, Liwei Wang, Chris M. Cervantes, Juan C. Caicedo, Julia Hockenmaier, and Svetlana Lazebnik. Flickr30k entities: Collecting region-to-phrase correspondences for richer image-to-sentence models. *CoRR*, abs/1505.04870, 2015.

Dean Pomerleau. Efficient training of artificial neural networks for autonomous navigation. *Neural Computation*, 3(1):88–97, 1991.

Rafael Figueiredo Prudencio, Marcos ROA Maximo, and Esther Luna Colombini. A survey on offline reinforcement learning: Taxonomy, review, and open problems. *IEEE Transactions on Neural Networks and Learning Systems*, 2023.

Martin L Puterman. *Markov decision processes: discrete stochastic dynamic programming*. John Wiley & Sons, 2014.

Aaron L Putterman, Kevin Lu, Igor Mordatch, and Pieter Abbeel. Pretraining for language conditioned imitation with transformers, 2022. URL `https://openreview.net/forum?id=eCPCn25gat`.

Han Qi, Yi Su, Aviral Kumar, and Sergey Levine. Data-driven offline decision-making via invariant representation learning. In *Advances in Neural Information Processing Systems 35*, 2022.

Mengshi Qi, Jie Qin, Yu Wu, and Yi Yang. Imitative non-autoregressive modeling for trajectory forecasting and imputation. In *IEEE/CVF Conference on Computer Vision and Pattern Recognition*, pp. 12733–12742. Computer Vision Foundation / IEEE, 2020.

Rongjun Qin, Xingyuan Zhang, Songyi Gao, Xiong-Hui Chen, Zewen Li, Weinan Zhang, and Yang Yu. Neorl: A near real-world benchmark for offline reinforcement learning. In *Advances in Neural Information Processing Systems 35*, 2022.

Ahmed Hussain Qureshi, Byron Boots, and Michael C. Yip. Adversarial imitation via variational inverse reinforcement learning. In *Proceedings of the 7th International Conference on Learning Representations*. OpenReview.net, 2019.

Lawrence Rabiner and Biinghwang Juang. An introduction to hidden markov models. *IEEE ASSP Magazine*, 3(1):4–16, 1986.

Alec Radford, Karthik Narasimhan, Tim Salimans, Ilya Sutskever, et al. Improving language understanding by generative pre-training. *mikecaptain.com*, 2018.

Rafael Rafailov, Tianhe Yu, Aravind Rajeswaran, and Chelsea Finn. Offline reinforcement learning from images with latent space models. In *Proceedings of the 3rd Annual Conference on Learning for Dynamics and Control*, volume 144, pp. 1154–1168, 2021.

Rouhollah Rahmatizadeh, Pooya Abolghasemi, Ladislau Bölöni, and Sergey Levine. Vision-based multi-task manipulation for inexpensive robots using end-to-end learning from demonstration. In *IEEE International Conference on Robotics and Automation*, pp. 3758–3765. IEEE, 2018.

Santhosh Kumar Ramakrishnan, Aaron Gokaslan, Erik Wijmans, Oleksandr Maksymets, Alexander Clegg, John M. Turner, Eric Undersander, Wojciech Galuba, Andrew Westbury, Angel X. Chang, Manolis Savva, Yili Zhao, and Dhruv Batra. Habitat-matterport 3d dataset (HM3D): 1000 large-scale 3d environments for embodied AI. In *Proceedings of the Neural Information Processing Systems Track on Datasets and Benchmarks 1*, 2021.

Aditya Ramesh, Prafulla Dhariwal, Alex Nichol, Casey Chu, and Mark Chen. Hierarchical text-conditional image generation with clip latents. *arXiv preprint arXiv:2204.06125*, 2022.

Amir Rasouli, Randy Goebel, Matthew E. Taylor, Iuliia Kotseruba, Soheil Alizadeh, Tianpei Yang, Montgomery Alban, Florian Shkurti, Yuzheng Zhuang, Adam Scibior, Kasra Rezaee, Animesh Garg, David Meger, Jun Luo, Liam Paull, Weinan Zhang, Xinyu Wang, and Xi Chen. Neurips 2022 competition: Driving smarts, 2022.

Scott E. Reed, Konrad Zolna, Emilio Parisotto, Sergio Gómez Colmenarejo, Alexander Novikov, Gabriel Barth-Maron, Mai Gimenez, Yury Sulsky, Jackie Kay, Jost Tobias Springenberg, Tom Eccles, Jake Bruce, Ali Razavi, Ashley Edwards, Nicolas Heess, Yutian Chen, Raia Hadsell, Oriol Vinyals, Mahyar Bordbar, and Nando de Freitas. A generalist agent. *Transactions on Machine Learning Research*, 2022.

Machel Reid, Yutaro Yamada, and Shixiang Shane Gu. Can wikipedia help offline reinforcement learning? *CoRR*, abs/2201.12122, 2022.

Allen Z. Ren, Sushant Veer, and Anirudha Majumdar. Generalization guarantees for imitation learning. In *Proceedings of the 4th Conference on Robot Learning*, volume 155, pp. 1426–1442. PMLR, 2020.

Moritz Reuss, Maximilian Li, Xiaogang Jia, and Rudolf Lioutikov. Goal-conditioned imitation learning using score-based diffusion policies. In *Robotics: Science and Systems*, 2023.

Shideh Rezaeifar, Robert Dadashi, Nino Vieillard, Léonard Hussenot, Olivier Bachem, Olivier Pietquin, and Matthieu Geist. Offline reinforcement learning as anti-exploration. In *Thirty-Sixth AAAI Conference on Artificial Intelligence*, pp. 8106–8114. AAAI Press, 2022.

Danilo Jimenez Rezende and Shakir Mohamed. Variational inference with normalizing flows. In *Proceedings of the 32nd International Conference on Machine Learning*, volume 37, pp. 1530–1538, 2015.

Luigi M Ricciardi. On the transformation of diffusion processes into the wiener process. *Journal of Mathematical Analysis and Applications*, 54(1):185–199, 1976.

Robin Rombach, Andreas Blattmann, Dominik Lorenz, Patrick Esser, and Björn Ommer. High-resolution image synthesis with latent diffusion models. In *IEEE/CVF Conference on Computer Vision and Pattern Recognition*, pp. 10674–10685. IEEE, 2022.

Olaf Ronneberger, Philipp Fischer, and Thomas Brox. U-net: Convolutional networks for biomedical image segmentation. In *Medical Image Computing and Computer-Assisted Intervention–MICCAI 2015: 18th International Conference, Munich, Germany, October 5-9, 2015, Proceedings, Part III 18*, pp. 234–241. Springer, 2015.

Erick Rosete-Beas, Oier Mees, Gabriel Kalweit, Joschka Boedecker, and Wolfram Burgard. Latent plans for task-agnostic offline reinforcement learning. In *Conference on Robot Learning*, volume 205 of *Proceedings of Machine Learning Research*, pp. 1838–1849. PMLR, 2022.

Stéphane Ross and Drew Bagnell. Efficient reductions for imitation learning. In *Proceedings of the 13th International Conference on Artificial Intelligence and Statistics*, pp. 661–668. JMLR Workshop and Conference Proceedings, 2010.

Tim Salimans, Ian J. Goodfellow, Wojciech Zaremba, Vicki Cheung, Alec Radford, and Xi Chen. Improved techniques for training gans. In *Advances in Neural Information Processing Systems 29*, pp. 2226–2234, 2016.

Mikayel Samvelyan, Tabish Rashid, Christian Schröder de Witt, Gregory Farquhar, Nantas Nardelli, Tim G. J. Rudner, Chia-Man Hung, Philip H. S. Torr, Jakob N. Foerster, and Shimon Whiteson. The starcraft multi-agent challenge. *CoRR*, abs/1902.04043, 2019.

Vaibhav Saxena, Yotto Koga, and Danfei Xu. Constrained-context conditional diffusion models for imitation learning. *CoRR*, abs/2311.01419, 2023.

Yannick Schroecker and Charles L. Isbell Jr. Universal value density estimation for imitation learning and goal-conditioned reinforcement learning. *CoRR*, abs/2002.06473, 2020.

Yannick Schroecker, Mel Vecerík, and Jonathan Scholz. Generative predecessor models for sample-efficient imitation learning. In *Proceedings of the 7th International Conference on Learning Representations*. OpenReview.net, 2019.

John Schulman, Sergey Levine, Pieter Abbeel, Michael I. Jordan, and Philipp Moritz. Trust region policy optimization. In *Proceedings of the 32nd International Conference on Machine Learning*, volume 37, pp. 1889–1897, 2015.

Nur Muhammad Shafiullah, Zichen Jeff Cui, Ariuntuya Altanzaya, and Lerrel Pinto. Behavior transformers: Cloning k modes with one stone. In *Advances in Neural Information Processing Systems 35*, 2022.

Shital Shah, Debadeepta Dey, Chris Lovett, and Ashish Kapoor. Airsim: High-fidelity visual and physical simulation for autonomous vehicles. In *Field and Service Robotics, Results of the 11th International Conference*, volume 5 of *Springer Proceedings in Advanced Robotics*, pp. 621–635. Springer, 2017.

Ohad Shamir. Are resnets provably better than linear predictors? In *Advances in Neural Information Processing Systems 31*, pp. 505–514, 2018.

Jinghuan Shang and Michael S. Ryoo. Self-supervised disentangled representation learning for third-person imitation learning. In *IEEE/RSJ International Conference on Intelligent Robots and Systems*, pp. 214–221. IEEE, 2021.

Jinghuan Shang, Kumara Kahatapitiya, Xiang Li, and Michael S. Ryoo. Starformer: Transformer with state-action-reward representations for visual reinforcement learning. In *Proceedings of the 17th European Conference on Computer Vision*, volume 13699, pp. 462–479, 2022.

Pratyusha Sharma, Lekha Mohan, Lerrel Pinto, and Abhinav Gupta. Multiple interactions made easy (MIME): large scale demonstrations data for imitation. In *Proceedings of the 2nd Annual Conference on Robot Learning*, volume 87, pp. 906–915, 2018.

Lucy Xiaoyang Shi, Archit Sharma, Tony Z. Zhao, and Chelsea Finn. Waypoint-based imitation learning for robotic manipulation. *CoRR*, abs/2307.14326, 2023.

Mohit Shridhar, Jesse Thomason, Daniel Gordon, Yonatan Bisk, Winson Han, Roozbeh Mottaghi, Luke Zettlemoyer, and Dieter Fox. ALFRED: A benchmark for interpreting grounded instructions for everyday tasks. In *2020 IEEE/CVF Conference on Computer Vision and Pattern Recognition*, pp. 10737–10746, 2020.

Mohit Shridhar, Lucas Manuelli, and Dieter Fox. Perceiver-actor: A multi-task transformer for robotic manipulation. In *Conference on Robot Learning, CoRL 2022, 14-18 December 2022, Auckland, New Zealand*, volume 205 of *Proceedings of Machine Learning Research*, pp. 785–799. PMLR, 2022.

Dylan Z Slack, Yinlam Chow, Bo Dai, and Nevan Wichers. Safer: Data-efficient and safe reinforcement learning via skill acquisition. In *ICML Decision Awareness in Reinforcement Learning Workshop*, 2022.

Shagun Sodhani, Amy Zhang, and Joelle Pineau. Multi-task reinforcement learning with context-based representations. In *Proceedings of the 38th International Conference on Machine Learning*, volume 139 of *Proceedings of Machine Learning Research*, pp. 9767–9779. PMLR, 2021.

Jascha Sohl-Dickstein, Eric Weiss, Niru Maheswaranathan, and Surya Ganguli. Deep unsupervised learning using nonequilibrium thermodynamics. In *International conference on machine learning*, pp. 2256–2265. PMLR, 2015.

Jascha Sohl-Dickstein, Eric A. Weiss, Niru Maheswaranathan, and Surya Ganguli. Deep unsupervised learning using nonequilibrium thermodynamics. In *Proceedings of the 32nd International Conference on Machine Learning*, volume 37, pp. 2256–2265, 2015.

Kihyuk Sohn, Honglak Lee, and Xinchen Yan. Learning structured output representation using deep conditional generative models. In *Advances in Neural Information Processing Systems 28*, pp. 3483–3491, 2015.

Jiaming Song, Hongyu Ren, Dorsa Sadigh, and Stefano Ermon. Multi-agent generative adversarial imitation learning. In *Advances in Neural Information Processing Systems 31*, pp. 7472–7483, 2018.

Yang Song and Stefano Ermon. Generative modeling by estimating gradients of the data distribution. *Advances in neural information processing systems*, 32, 2019.

Yang Song and Stefano Ermon. Improved techniques for training score-based generative models. In *Advances in Neural Information Processing Systems 33*, 2020.

Yang Song, Sahaj Garg, Jiaxin Shi, and Stefano Ermon. Sliced score matching: A scalable approach to density and score estimation. In *Proceedings of the 35th Conference on Uncertainty in Artificial Intelligence*, volume 115, pp. 574–584, 2019.

Yang Song, Jascha Sohl-Dickstein, Diederik P Kingma, Abhishek Kumar, Stefano Ermon, and Ben Poole. Score-based generative modeling through stochastic differential equations. *arXiv preprint arXiv:2011.13456*, 2020.

Yang Song, Conor Durkan, Iain Murray, and Stefano Ermon. Maximum likelihood training of score-based diffusion models. In *Advances in Neural Information Processing Systems 34*, pp. 1415–1428, 2021.

Yang Song, Prafulla Dhariwal, Mark Chen, and Ilya Sutskever. Consistency models. In *Proceedings of the 40th International Conference on Machine Learning*, volume 202, pp. 32211–32252. PMLR, 2023.

Adrian Spurr, Jie Song, Seonwook Park, and Otmar Hilliges. Cross-modal deep variational hand pose estimation. In *IEEE Conference on Computer Vision and Pattern Recognition*, pp. 89–98. Computer Vision Foundation / IEEE Computer Society, 2018.

Kaustubh Sridhar, Souradeep Dutta, Dinesh Jayaraman, James Weimer, and Insup Lee. Memory-consistent neural networks for imitation learning. *CoRR*, abs/2310.06171, 2023.

Shyam Sudhakaran and Sebastian Risi. Skill decision transformer. *CoRR*, abs/2301.13573, 2023.

H.J. Terry Suh, Glen Chou, Hongkai Dai, Lujie Yang, Abhishek Gupta, and Russ Tedrake. Fighting uncertainty with gradients: Offline reinforcement learning via diffusion score matching. In *7th Annual Conference on Robot Learning*, 2023.

Jiankai Sun, Lantao Yu, Pinqian Dong, Bo Lu, and Bolei Zhou. Adversarial inverse reinforcement learning with self-attention dynamics model. *IEEE Robotics and Automation Letters*, 6(2):1880–1886, 2021.

Jiankai Sun, Yiqi Jiang, Jianing Qiu, Parth Talpur Nobel, Mykel Kochenderfer, and Mac Schwager. Conformal prediction for uncertainty-aware planning with diffusion dynamics model. In *Advances in Neural Information Processing Systems 36*, 2023.

Richard S Sutton and Andrew G Barto. *Reinforcement learning: An introduction*. MIT press, 2018.

Shiro Takagi. On the effect of pre-training for transformer in different modality on offline reinforcement learning. In *Advances in Neural Information Processing Systems 35*, 2022.

Yuval Tassa, Yotam Doron, Alistair Muldal, Tom Erez, Yazhe Li, Diego de Las Casas, David Budden, Abbas Abdolmaleki, Josh Merel, Andrew Lefrancq, Timothy P. Lillicrap, and Martin A. Riedmiller. Deepmind control suite. *CoRR*, abs/1801.00690, 2018.

Russ Tedrake. *Underactuated Robotics*. Course Notes for MIT 6.832, 2023. URL `https://underactuated.csail.mit.edu`.

Naftali Tishby and Noga Zaslavsky. Deep learning and the information bottleneck principle. In *IEEE Information Theory Workshop*, pp. 1–5. IEEE, 2015.

Emanuel Todorov, Tom Erez, and Yuval Tassa. Mujoco: A physics engine for model-based control. In *IEEE/RSJ International Conference on Intelligent Robots and Systems*, 2012.

Sam Toyer, Rohin Shah, Andrew Critch, and Stuart Russell. The MAGICAL benchmark for robust imitation. In *Advances in Neural Information Processing Systems 33*, 2020.

Brandon Trabucco, Xinyang Geng, Aviral Kumar, and Sergey Levine. Design-bench: Benchmarks for data-driven offline model-based optimization. In *Proceedings of the 39th International Conference on Machine Learning*, volume 162, pp. 21658–21676, 2022.

Wei-Cheng Tseng, Tsun-Hsuan Johnson Wang, Yen-Chen Lin, and Phillip Isola. Offline multi-agent reinforcement learning with knowledge distillation. In *Advances in Neural Information Processing Systems 35*, 2022.

Núria Armengol Urpí, Sebastian Curi, and Andreas Krause. Risk-averse offline reinforcement learning. In *Proceedings of the 9th International Conference on Learning Representations*. OpenReview.net, 2021.

Rianne van den Berg, Leonard Hasenclever, Jakub M. Tomczak, and Max Welling. Sylvester normalizing flows for variational inference. In *Proceedings of the 34th Conference on Uncertainty in Artificial*, pp. 393–402, 2018.

Aäron van den Oord, Oriol Vinyals, and Koray Kavukcuoglu. Neural discrete representation learning. In *Advances in Neural Information Processing Systems 30*, pp. 6306–6315, 2017.

Ashish Vaswani, Noam Shazeer, Niki Parmar, Jakob Uszkoreit, Llion Jones, Aidan N Gomez, Łukasz Kaiser, and Illia Polosukhin. Attention is all you need. *Advances in neural information processing systems*, 30, 2017.

Matej Vecerík, Todd Hester, Jonathan Scholz, Fumin Wang, Olivier Pietquin, Bilal Piot, Nicolas Heess, Thomas Rothörl, Thomas Lampe, and Martin A. Riedmiller. Leveraging demonstrations for deep reinforcement learning on robotics problems with sparse rewards. *CoRR*, abs/1707.08817, 2017.

Siddarth Venkatraman, Shivesh Khaitan, Ravi Tej Akella, John M. Dolan, Jeff G. Schneider, and Glen Berseth. Reasoning with latent diffusion in offline reinforcement learning. *CoRR*, abs/2309.06599, 2023.

David Venuto, Jhelum Chakravorty, Léonard Boussioux, Junhao Wang, Gavin McCracken, and Doina Precup. oirl: Robust adversarial inverse reinforcement learning with temporally extended actions. *CoRR*, abs/2002.09043, 2020.

Adam R. Villaflor, Zhe Huang, Swapnil Pande, John M. Dolan, and Jeff Schneider. Addressing optimism bias in sequence modeling for reinforcement learning. In *Proceedings of the 39th International Conference on Machine Learning*, volume 162, pp. 22270–22283, 2022.

Pascal Vincent. A connection between score matching and denoising autoencoders. *Neural Computation*, 23 (7):1661–1674, 2011.

Vladimir Vovk, Alexander Gammerman, and Glenn Shafer. *Algorithmic learning in a random world*, volume 29. Springer, 2005.

Matthew J. Vowels, Necati Cihan Camgöz, and Richard Bowden. Gated variational autoencoders: Incorporating weak supervision to encourage disentanglement. In *Proceedings of the 15th IEEE International Conference on Automatic Face and Gesture Recognition*, pp. 125–132. IEEE, 2020.

Quan Vuong, Aviral Kumar, Sergey Levine, and Yevgen Chebotar. DASCO: dual-generator adversarial support constrained offline reinforcement learning. In *Advances in Neural Information Processing Systems 35*, 2022.

Jianhao Wang, Wenzhe Li, Haozhe Jiang, Guangxiang Zhu, Siyuan Li, and Chongjie Zhang. Offline reinforcement learning with reverse model-based imagination. In *Advances in Neural Information Processing Systems 34*, pp. 29420–29432, 2021.

Kerong Wang, Hanye Zhao, Xufang Luo, Kan Ren, Weinan Zhang, and Dongsheng Li. Bootstrapped transformer for offline reinforcement learning. In *Advances in Neural Information Processing Systems 35*, 2022a.

Mianchu Wang, Rui Yang, Xi Chen, and Meng Fang. Goplan: Goal-conditioned offline reinforcement learning by planning with learned models. *CoRR*, abs/2310.20025, 2023a.

Pengqin Wang, Meixin Zhu, and Shaojie Shen. Environment transformer and policy optimization for model-based offline reinforcement learning, 2023b.

Tianyu Wang, Nikhil Karnwal, and Nikolay Atanasov. Latent policies for adversarial imitation learning. *CoRR*, abs/2206.11299, 2022b.

Yiqi Wang, Mengdi Xu, Laixi Shi, and Yuejie Chi. A trajectory is worth three sentences: multimodal transformer for offline reinforcement learning. In *Uncertainty in Artificial Intelligence*, volume 216, pp. 2226–2236, 2023c.

Yuanfu Wang, Chao Yang, Ying Wen, Yu Liu, and Yu Qiao. Critic-guided decision transformer for offline reinforcement learning. *arXiv preprint arXiv:2312.13716*, 2023d.

Yunke Wang, Minjing Dong, Bo Du, and Chang Xu. Imitation learning from purified demonstration. *arXiv preprint arXiv:2310.07143*, 2023e.

Zhendong Wang, Jonathan J. Hunt, and Mingyuan Zhou. Diffusion policies as an expressive policy class for offline reinforcement learning. In *Proceedings of the 11th International Conference on Learning Representations*. OpenReview.net, 2023f.

Ziyu Wang, Josh Merel, Scott E. Reed, Nando de Freitas, Gregory Wayne, and Nicolas Heess. Robust imitation of diverse behaviors. In *Advances in Neural Information Processing Systems 30, Long Beach, CA, USA*, pp. 5320–5329, 2017.

Ziyu Wang, Alexander Novikov, Konrad Zolna, Josh Merel, Jost Tobias Springenberg, Scott E. Reed, Bobak Shahriari, Noah Y. Siegel, Çaglar Gülçehre, Nicolas Heess, and Nando de Freitas. Critic regularized regression. In *Advances in Neural Information Processing Systems 33*, 2020.

Patrick Nadeem Ward, Ariella Smofsky, and Avishek Joey Bose. Improving exploration in soft-actor-critic with normalizing flows policies. *CoRR*, abs/1906.02771, 2019.

Hua Wei, Deheng Ye, Zhao Liu, Hao Wu, Bo Yuan, Qiang Fu, Wei Yang, and Zhenhui Li. Boosting offline reinforcement learning with residual generative modeling. In *Proceedings of the 30th International Joint Conference on Artificial Intelligence*, pp. 3574–3580. ijcai.org, 2021.

Yao Wei, Yanchao Sun, Ruijie Zheng, Sai Vemprala, Rogerio Bonatti, Shuhang Chen, Ratnesh Madaan, Zhongjie Ba, Ashish Kapoor, and Shuang Ma. Is imitation all you need? generalized decision-making with dual-phase training. In *IEEE/CVF International Conference on Computer Vision*, pp. 16221–16231, 2023.

Matthias Weissenbacher, Samarth Sinha, Animesh Garg, and Yoshinobu Kawahara. Koopman q-learning: Offline reinforcement learning via symmetries of dynamics. In *Proceedings of the 39th International Conference on Machine Learning*, volume 162, pp. 23645–23667, 2022.

Max Welling and Yee Whye Teh. Bayesian learning via stochastic gradient langevin dynamics. In *Proceedings of the 28th International Conference on Machine Learning*, pp. 681–688, 2011.

Muning Wen, Jakub Grudzien Kuba, Runji Lin, Weinan Zhang, Ying Wen, Jun Wang, and Yaodong Yang. Multi-agent reinforcement learning is a sequence modeling problem. In *Advances in Neural Information Processing Systems 35*, 2022.

Qingsong Wen, Tian Zhou, Chaoli Zhang, Weiqi Chen, Ziqing Ma, Junchi Yan, and Liang Sun. Transformers in time series: A survey. In *Proceedings of the 32nd International Joint Conference on Artificial Intelligence*, pp. 6778–6786, 2023.

Eric Wiewiora. Potential-based shaping and q-value initialization are equivalent. *Journal of Artificial Intelligence Research*, 19:205–208, 2003.

Jialong Wu, Haixu Wu, Zihan Qiu, Jianmin Wang, and Mingsheng Long. Supported policy optimization for offline reinforcement learning. In *Advances in Neural Information Processing Systems 35*, 2022.

Yifan Wu, George Tucker, and Ofir Nachum. Behavior regularized offline reinforcement learning. *CoRR*, abs/1911.11361, 2019.

Yuchen Wu, Melissa Mozifian, and Florian Shkurti. Shaping rewards for reinforcement learning with imperfect demonstrations using generative models. In *IEEE International Conference on Robotics and Automation*, pp. 6628–6634. IEEE, 2021.

Wei Xiao, Tsun-Hsuan Wang, Chuang Gan, and Daniela Rus. Safediffuser: Safe planning with diffusion probabilistic models. *CoRR*, abs/2306.00148, 2023.

Zhisheng Xiao, Karsten Kreis, and Arash Vahdat. Tackling the generative learning trilemma with denoising diffusion gans. In *Proceedings of the 10th International Conference on Learning Representations*, 2022.

Zhihui Xie, Zichuan Lin, Deheng Ye, Qiang Fu, Yang Wei, and Shuai Li. Future-conditioned unsupervised pretraining for decision transformer. In *Proceedings of the 40th International Conference on Machine Learning*, volume 202, pp. 38187–38203, 2023.

Haoran Xu, Xianyuan Zhan, and Xiangyu Zhu. Constraints penalized q-learning for safe offline reinforcement learning. In *Thirty-Sixth AAAI Conference on Artificial Intelligence*, pp. 8753–8760. AAAI Press, 2022a.

Mengdi Xu, Yikang Shen, Shun Zhang, Yuchen Lu, Ding Zhao, Joshua B. Tenenbaum, and Chuang Gan. Prompting decision transformer for few-shot policy generalization. In *Proceedings of the 39th International Conference on Machine Learning*, volume 162, pp. 24631–24645, 2022b.

Yilun Xu, Ziming Liu, Max Tegmark, and Tommi S. Jaakkola. Poisson flow generative models. In *Advances in Neural Information Processing Systems 35*, 2022c.

Yilun Xu, Ziming Liu, Yonglong Tian, Shangyuan Tong, Max Tegmark, and Tommi S. Jaakkola. PFGM++: unlocking the potential of physics-inspired generative models. In *proceedings of the 40th International Conference on Machine Learning*, volume 202 of *Proceedings of Machine Learning Research*, pp. 38566–38591. PMLR, 2023.

Taku Yamagata, Ahmed Khalil, and Raúl Santos-Rodríguez. Q-learning decision transformer: Leveraging dynamic programming for conditional sequence modelling in offline RL. In *Proceedings of the 40th International Conference on Machine Learning*, volume 202, pp. 38989–39007, 2023.

Kai Yan, Alexander G. Schwing, and Yu-Xiong Wang. CEIP: combining explicit and implicit priors for reinforcement learning with demonstrations. In *Advances in Neural Information Processing Systems 35*, 2022.

Junming Yang, Xingguo Chen, Shengyuan Wang, and Bolei Zhang. Model-based offline policy optimization with adversarial network. In *Proceedings of the 26th European Conference on Artificial Intelligence*, volume 372, pp. 2850–2857, 2023a.

Ling Yang, Zhilong Zhang, Yang Song, Shenda Hong, Runsheng Xu, Yue Zhao, Yingxia Shao, Wentao Zhang, Ming-Hsuan Yang, and Bin Cui. Diffusion models: A comprehensive survey of methods and applications. *CoRR*, abs/2209.00796, 2022a.

Rui Yang, Lin Yong, Xiaoteng Ma, Hao Hu, Chongjie Zhang, and Tong Zhang. What is essential for unseen goal generalization of offline goal-conditioned rl? In *Proceedings of the 40th International Conference on Machine Learning*, volume 202, pp. 39543–39571, 2023b.

Shentao Yang, Yihao Feng, Shujian Zhang, and Mingyuan Zhou. Regularizing a model-based policy stationary distribution to stabilize offline reinforcement learning. In *Proceedings of the 39th International Conference on Machine Learning*, volume 162, pp. 24980–25006, 2022b.

Shentao Yang, Zhendong Wang, Huangjie Zheng, Yihao Feng, and Mingyuan Zhou. A behavior regularized implicit policy for offline reinforcement learning. *arXiv preprint arXiv:2202.09673*, 2022c.

Shentao Yang, Shujian Zhang, Yihao Feng, and Mingyuan Zhou. A unified framework for alternating offline model training and policy learning. In *Advances in Neural Information Processing Systems 35*, 2022d.

Sherry Yang, Dale Schuurmans, Pieter Abbeel, and Ofir Nachum. Dichotomy of control: Separating what you can control from what you cannot. In *Proceedings of the 11th International Conference on Learning Representations*. OpenReview.net, 2023c.

Yaodong Yang, Guangyong Chen, Weixun Wang, Xiaotian Hao, Jianye Hao, and Pheng-Ann Heng. Transformer-based working memory for multiagent reinforcement learning with action parsing. In *Advances in Neural Information Processing Systems 35*, 2022e.

Yiming Yang, Dengpeng Xing, and Bo Xu. Efficient spatiotemporal transformer for robotic reinforcement learning. *IEEE Robotics Automation Letters*, 7(3):7982–7989, 2022f.

Yiqin Yang, Hao Hu, Wenzhe Li, Siyuan Li, Jun Yang, Qianchuan Zhao, and Chongjie Zhang. Flow to control: Offline reinforcement learning with lossless primitive discovery. In *Proceedings of the 37th AAAI Conference on Artificial Intelligence*, pp. 10843–10851. AAAI Press, 2023d.

Lantao Yu, Jiaming Song, and Stefano Ermon. Multi-agent adversarial inverse reinforcement learning. In *Proceedings of the 36th International Conference on Machine Learning*, volume 97, pp. 7194–7201, 2019a.

Lantao Yu, Tianhe Yu, Chelsea Finn, and Stefano Ermon. Meta-inverse reinforcement learning with probabilistic context variables. In *Advances in Neural Information Processing Systems 32*, pp. 11749–11760, 2019b.

Tianhe Yu, Deirdre Quillen, Zhanpeng He, Ryan Julian, Karol Hausman, Chelsea Finn, and Sergey Levine. Meta-world: A benchmark and evaluation for multi-task and meta reinforcement learning. In *Proceedings of the 3rd Annual Conference on Robot Learning*, volume 100, pp. 1094–1100, 2019c.

Tianhe Yu, Garrett Thomas, Lantao Yu, Stefano Ermon, James Y. Zou, Sergey Levine, Chelsea Finn, and Tengyu Ma. MOPO: model-based offline policy optimization. In *Advances in Neural Information Processing Systems 33*, 2020a.

Xingrui Yu, Yueming Lyu, and Ivor W. Tsang. Intrinsic reward driven imitation learning via generative model. In *Proceedings of the 37th International Conference on Machine Learning*, volume 119 of *Proceedings of Machine Learning Research*, pp. 10925–10935. PMLR, 2020b.

William Yuan, Jiaxing Chen, Shaofei Chen, Lina Lu, Zhenzhen Hu, Peng Li, Dawei Feng, Furong Liu, and Jing Chen. Transformer in reinforcement learning for decision-making: A survey. *TechRxiv*, 2023a.

Ye Yuan, Xin Li, Yong Heng, Leiji Zhang, and Mingzhong Wang. Good better best: Self-motivated imitation learning for noisy demonstrations. *CoRR*, abs/2310.15815, 2023b.

Chi Zhang, Sanmukh R. Kuppannagari, and Viktor K. Prasanna. BRAC+: improved behavior regularized actor critic for offline reinforcement learning. In *Asian Conference on Machine Learning*, volume 157 of *Proceedings of Machine Learning Research*, pp. 204–219. PMLR, 2021a.

Hongchang Zhang, Jianzhun Shao, Yuhang Jiang, Shuncheng He, Guanwen Zhang, and Xiangyang Ji. State deviation correction for offline reinforcement learning. In *Thirty-Sixth AAAI Conference on Artificial Intelligence*, pp. 9022–9030. AAAI Press, 2022.

Jing Zhang, Chi Zhang, Wenjia Wang, and Bing-Yi Jing. APAC: authorized probability-controlled actor-critic for offline reinforcement learning. *CoRR*, abs/2301.12130, 2023.

Xin Zhang, Yanhua Li, Xun Zhou, and Jun Luo. Unveiling taxi drivers' strategies via cgail: Conditional generative adversarial imitation learning. In *IEEE International Conference on Data Mining*, pp. 1480–1485. IEEE, 2019.

Xin Zhang, Yanhua Li, Ziming Zhang, and Zhi-Li Zhang. f-gail: Learning f-divergence for generative adversarial imitation learning. In *Advances in Neural Information Processing Systems 33*, 2020a.

Xin Zhang, Yanhua Li, Ziming Zhang, Christopher Brinton, Zhenming Liu, Zhi-Li Zhang, Hui Lu, and Zhihong Tian. Stabilized likelihood-based imitation learning via denoising continuous normalizing flow. In *Submission to the 10th International Conference on Learning Representations*, 2021b.

Yufeng Zhang, Qi Cai, Zhuoran Yang, and Zhaoran Wang. Generative adversarial imitation learning with neural network parameterization: Global optimality and convergence rate. In *Proceedings of the 40th International Conference on Machine Learning*, pp. 11044–11054. PMLR, 2020b.

Qinqing Zheng, Amy Zhang, and Aditya Grover. Online decision transformer. In *Proceedings of the 39th International Conference on Machine Learning*, volume 162, pp. 27042–27059, 2022.

Qinqing Zheng, Mikael Henaff, Brandon Amos, and Aditya Grover. Semi-supervised offline reinforcement learning with action-free trajectories. In *Proceedings of the 40th International Conference on Machine Learning*, volume 202, pp. 42339–42362, 2023.

Wenxuan Zhou, Sujay Bajracharya, and David Held. PLAS: latent action space for offline reinforcement learning. In *Proceedings of the 4th Conference on Robot Learning*, volume 155 of *Proceedings of Machine Learning Research*, pp. 1719–1735. PMLR, 2020.

Tianchen Zhu, Yue Qiu, Haoyi Zhou, and Jianxin Li. Towards long-delayed sparsity: Learning a better transformer through reward redistribution. In *Proceedings of the 32nd International Joint Conference on Artificial Intelligence*, pp. 4693–4701, 2023a.

Yifeng Zhu, Abhishek Joshi, Peter Stone, and Yuke Zhu. VIOLA: imitation learning for vision-based manipulation with object proposal priors. *CoRR*, abs/2210.11339, 2022.

Yuke Zhu, Josiah Wong, Ajay Mandlekar, and Roberto Martín-Martín. robosuite: A modular simulation framework and benchmark for robot learning. *CoRR*, abs/2009.12293, 2020.

Zhengbang Zhu, Minghuan Liu, Liyuan Mao, Bingyi Kang, Minkai Xu, Yong Yu, Stefano Ermon, and Weinan Zhang. Madiff: Offline multi-agent learning with diffusion models. *CoRR*, abs/2305.17330, 2023b.

Zhengbang Zhu, Hanye Zhao, Haoran He, Yichao Zhong, Shenyu Zhang, Yong Yu, and Weinan Zhang. Diffusion models for reinforcement learning: A survey. *CoRR*, abs/2311.01223, 2023c.

Brian D. Ziebart, J. Andrew Bagnell, and Anind K. Dey. Modeling interaction via the principle of maximum causal entropy. In *Proceedings of the 27th International Conference on Machine Learning*, pp. 1255–1262, 2010.

Luisa M. Zintgraf, Kyriacos Shiarlis, Maximilian Igl, Sebastian Schulze, Yarin Gal, Katja Hofmann, and Shimon Whiteson. Varibad: A very good method for bayes-adaptive deep RL via meta-learning. In *Proceedings of the 8th International Conference on Learning Representations*. OpenReview.net, 2020.

Konrad Zolna, Scott E. Reed, Alexander Novikov, Sergio Gómez Colmenarejo, David Budden, Serkan Cabi, Misha Denil, Nando de Freitas, and Ziyu Wang. Task-relevant adversarial imitation learning. In *Proceedings of the 4th Conference on Robot Learning*, volume 155, pp. 247–263. PMLR, 2020.

Guoyu Zuo, Kexin Chen, Jiahao Lu, and Xiangsheng Huang. Deterministic generative adversarial imitation learning. *Neurocomputing*, 388:60–69, 2020.